Generation of an Isoform-Specific Knockout Mouse to Study the Functions of Versican V2 in the Adult Central Nervous System

Dissertation

zur
Erlangung der naturwissenschaftlichen Doktorwürde
(Dr. sc. nat.)

vorgelegt der
Mathematisch-naturwissenschaftlichen Fakultät
der
Universität Zürich

von

María Teresa Zimmermann-Dours

von Döttingen (AG) und Argentinien

Promotionskomitee

Prof. Dr. Peter Sonderegger (Vorsitz)
Prof. Dr. Dieter Zimmermann (Leitung der Dissertation)
Prof. Dr. Esther Stöckli
Prof. Dr. Alex Hajnal

Zürich, 2009

Caminante, no hay camino,
se hace camino al andar.

Antonio Machado (Spanish poet, 1875–1939)

To my parents, who with their immense love taught me to follow my dreams....
....and to finish my job.

And to Dieter, who helped me along this part of the way.

1. Summary / Zusammenfassung

The neurons and glial cells of the central nervous system (CNS) are embedded in a specialized extracellular matrix (ECM), which mainly consists of hyaluronan, chondroitin sulfate proteoglycans (CSPGs) of the lectican family, link proteins and tenascins. Although this general composition is maintained in the course of development, the meshwork becomes tighter during CNS maturation as individual members of the three protein families are exchanged. Since particularly the CSPGs impede axonal growth in vitro, the strategic accumulation of this adult type of extracellular matrix along myelinated fiber tracts and in perineuronal nets is thought to limit structural plasticity and contribute to the stabilization of mature neuronal circuits. Moreover, the failure of axonal regeneration after CNS injury has been partly attributed to the resident and the newly formed glial scar matrix.

The V2 splice-variant of versican is one of the main constituents of the mature extracellular matrix. The initial expression of this large secreted lectican coincides with myelination. At this late phase of CNS development, versican V2 accumulates along the myelinated fiber tracts and is preferentially deposited around emerging nodes of Ranvier. In vitro it binds to tenascin-R, hyaluronan and link proteins and it is a potent inhibitor of axonal growth.

To further explore the putative functions of versican V2 in vivo, we have now generated a versican V2-deficient mouse strain using a novel isoform-specific gene targeting approach, which circumvents the early embryonic lethality of the complete versican gene knockout. The mutant mice are viable and fertile and display no overt morphological or behavioral phenotype. Our subsequent molecular and immunohistological analyses of the versican V2-null mice and the comparisons with other knockout strains provided however, strong evidence that versican V2 is required to orchestrate the assembly of the perinodal extracellular matrix around the CNS nodes of Ranvier. Additionally, we have demonstrated that the absence of this perinodal matrix does not, as previously postulated, affect the clustering of voltage-gated ion channels and the formation of paranodal and juxtaparanodal structures.

To address the participation of the CNS matrix in restraining regeneration after injury, we furthermore analyzed the distributions of distinct CSPGs in different lesion models. In rhizotomy experiments, we could observe a selective upregulation of neurocan and versican V1 in the dorsal root entry zone, while the levels of the resident versican V2 and brevican were little affected. A similar emergence of versican V1 expression was also detected in the newly formed glial scar after contusion lesion. These experiments indicate that the inhibitory properties of the extracellular matrix are even enhanced after lesion by the temporally increased incorporation of lecticans that are usually absent from the mature CNS tissues. Our findings form the basis for future experiments aiming at CNS regeneration in mice lacking main components of the resident and/or the reactive extracellular matrix.

Neuronen und Gliazellen des zentralen Nervensystem (ZNS) sind von einer spezialisierten extrazelluläre Matrix (ECM) umgeben, die mehrheitlich aus Hyaluronan, Chondroitinsulfat-Proteoglycanen (CSPG) der Lectican-Familie, Link Proteinen und Tenascinen besteht. Obwohl diese Zusammensetzung während der neuralen Entwicklung grundsätzlich erhalten bleibt, findet im Rahmen des Reifungsprozesses durch Austausch individueller Mitglieder der drei Proteinfamilien eine Verdichtung des extrazellulären Geflechtes statt. Da insbesondere die CSPGs das Axonwachstum in vitro unterbinden können, wird vermutet, dass die strategische Ansammlung der adulten Matrix entlang myelinisierter Fasern und in perineuronalen Netzen die strukturelle Plastizität begrenzt und somit zur Stabilisierung ausgereifter neuronaler Schaltkreise beiträgt. Auch das Ausbleiben der Axonregeneration nach ZNS-Verletzungen wird teilweise der ansässigen ECM und der neuformierten Matrix des glialen Narbengewebes zugeschrieben.

Die Versican-Spleissvariante V2 ist eine der Hauptkomponenten der reifen extrazellulären Matrix im ZNS. Der Beginn der Expression dieses grossen sezernierten Lecticans fällt zeitlich mit dem Myelinisierungsprozess zusammen. In dieser späten Entwicklungphase wird Versican V2 in myeliniserten Fasertrakten angelagert und sammelt sich insbesondere in Nähe der sich bildenden Ranvierschen Schnürknoten an. In vitro bindet es Tenascin-R, Hyaluronan und Link Proteine und funktioniert als potenter Hemmer des Axonwachstums.

Zur Erforschung mutmasslicher Versican V2-Funktionen in vivo, haben wir nun einen Versican V2-defizienten Mausstamm hergestellt, bei dem wir die frühe embryonale Letalität des kompletten Genknockouts mittels eines neuen Isoform-spezifischen Gentargeting-Ansatzes umgingen. Die mutanten Mäuse sind lebens- und fortpflanzungsfähig und lassen auf den ersten Blick keine Veränderungen der Morphologie oder des Verhaltens erkennen. Unsere molekularen und immunhistochemischen Analysen der Versican V2-Null Mäuse und Vergleiche mit anderen Knockout-Stämmen haben dann aber klare Indizien für eine zentrale Rolle von Versican V2 bei der Orchestrierung des perinodalen ECM-Aufbaus um die Ranvierschen Schnürknoten ergeben. Wir konnten allerdings auch aufzeigen, dass das Fehlen dieser perinodalen Matrix, entgegen früherer Postulate, die normale Ansammlung spannungsabhängiger Ionenkanäle und die Bildung paranodaler und juxtaparanodaler Strukturen unbeeinflusst lässt.

Zur Untersuchung der Matrixbeteiligung an der Einschränkung der Regeneration nach ZNS-Verletzungen, haben wir die Verteilung bestimmter CSPGs auch in verschiedenen Läsionsmodellen analysiert. In Rhizotomie-Experimenten konnten wir in der Eintrittszone der Rückenwurzelfasern eine selektive Hochregulation von Neurocan und Versican V1 beobachten, während die Anteile der normalerweise vorhandenen Versican V2 und Brevican keine grundlegenden Veränderungen erfuhren. Ein ähnliches Hervortreten von Versican V1 wurde auch in frischen glialen Narbengeweben nach Kontusionsläsionen nachgewiesen. Unsere Resultate deuten darauf hin, dass die hemmende Eigenschaft der ECM nach einer Läsion durch den temporären Einbau weiterer Lecticane zusätzlich verstärkt wird. Diese Befunde bilden die Basis für zukünftige Experimente mit Fokus auf das Regenerationsverhalten in Mäusen, denen mehrere Komponenten der regulär ansässigen und/oder reaktiven extrazellulären Matrix fehlen.

2. General Introduction

2.1. The extracellular matrix of the central nervous system

It was not until 1971 that the existence of an extracellular matrix (ECM) in the brain was acknowledged (Tani and Ametani, 1971). Then the predominant presence of hyaluronan and chondroitin sulfate proteoglycans (CSPG) in the central nervous system (CNS) (Margolis et al., 1975), and the virtual absence of otherwise frequent ECM molecules like fibronectin or collagens were described (Carbonetto, 1984; Rutka et al., 1988; Sanes, 1989). Today we know that this distinctive ECM is mainly composed of proteoglycans of the lectican/hyalectan family and their binding partners, hyaluronan, link proteins and tenascins (Ruoslahti, 1996) (reviewed by (Ruoslahti, 1996; Rauch, 1997; Bandtlow and Zimmermann, 2000; Novak and Kaye, 2000; Yamaguchi, 2000)). In the following, I will introduce the components of this extracellular meshwork in more detail.

2.1.1. Proteoglycans and Hyaluronan

Proteoglycans (PGs) are glycoproteins carrying in addition to variable numbers of N- and O-linked oligosaccharides, at least one glycosaminoglycan (GAG) side chain, which is covalently bound to the core protein via a partly conserved attachment site (consensus sequence motifs: Ser-Gly-X-Gly or (Asp/Glu)-X-Ser-Gly) (Bourdon et al., 1987)) and a short oligosacharide linker. The GAGs themselves are long unbranched polymers of repetitive disaccharide units consisting of an uronic acid (glucuronic or iduronic) or galactose and an amino sugar (N-acetylglucosamine or N-acetylgalactosamine). According to the combination of these sugars, the GAGs are subclassified in heparin/heparan-, keratan- or chondroitin/dermatan-sulfates (fig. 1) (Bandtlow and Zimmermann, 2000).

The GAG side chains are usually 20-200 disaccharide-repeats long and show complex modifications, mainly sulfation of hydroxyl groups and epimerization of the carboxyl group on C-5 position of D-glucuronic acid to yield L-iduronic acid. The binding of chondroitin/dermatan sulfate and heparin/heparan sulfate chains to the core protein is mediated by a serine residue and four sequentially added monosaccharides: xylose, two consecutive galactoses and glucuronic acid (Kjellén and Lindahl, 1991). In general, this tetrasaccharide-linker is common to the attachment region of these GAGs, but can sometimes be slightly altered, for example by phosphorylation of the xylose, or sulfation at various positions and epimerization of the glucuronic acid (Prydz and Dalen, 2000). Altogether, the numerous modifications of the GAGs lead to a high structural variability and open up countless possibilities for the modulation of proteoglycan functions (Bulow and Hobert, 2006). Most prominently, GAGs are strongly negatively charged due to their high content of acidic sugars and sulfate substitutions and therefore attract and bind water and cations (Prydz and Dalen, 2000).

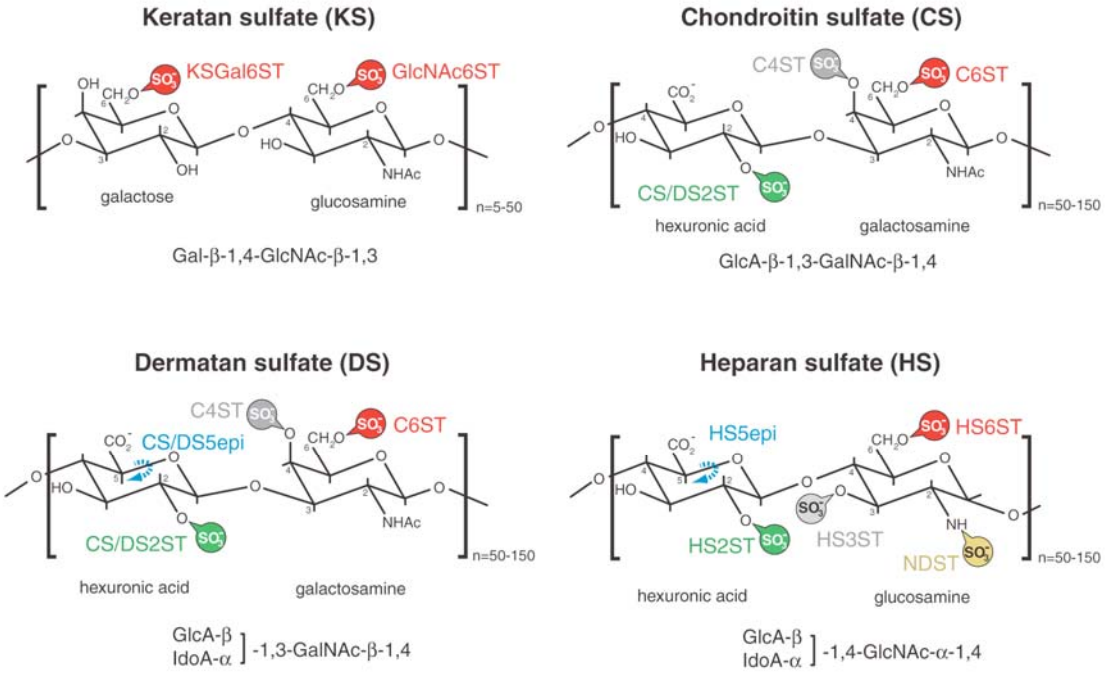

Figure 1: Disaccharide units of the GAGs: each modification is shown in different color and with the enzyme that catalyzes the reaction (from (Bulow and Hobert, 2006)). Abbreviations: *GlcA: glucuronic acid, IdoA: iduronic acid, epi: epimerase, ST: sulfotransferase, NDST: N-deacetylase-N-sulfotransferase*.

In contrast to the other glycosaminoglycans, hyaluronan, also known as hyaluronic acid (HA) or hyaluronate, is not covalently bound to any core protein, but is directly deposited in the extracellular matrix. It is a very large linear polymer built of repetitive disaccharides units that are composed of glucuronic acid and N-acetylglucosamine [-β(1,4)-GlcA- β(1,3)-GlcNAc-]$_n$ (fig. 2). Hyaluronan reaches up to 10^7 Da in size and extends over lengths of 2-25 µm. Unlike the other GAGs, it is not sulfated and the glucuronic acid units are not epimerized (reviewed by (Toole, 2000, 2004)).

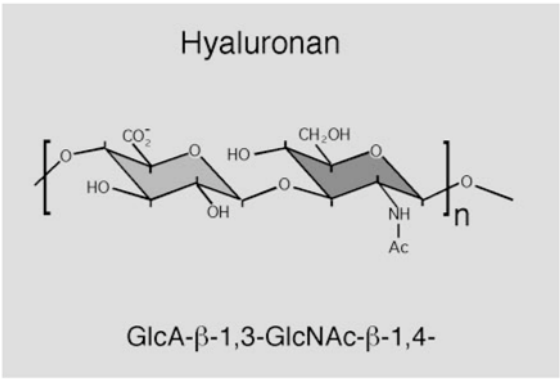

Figure 2: Disaccharide units of HA (from (Bandtlow and Zimmermann, 2000)).

HA is synthesized by specific glycosyltransferases called hyaluronan synthases (HAS). Three vertebrate HAS genes have been identified, *HAS1*, *HAS2*, and *HAS3* (reviewed by

(Weigel et al., 1997; Spicer and McDonald, 1998; DeAngelis, 1999)). HAS are in many senses unique glycosyltransferases, as they 1) are able to catalyze the incorporation of two different monosaccharides into the nascent string, and hence, oppose the dogma “single enzyme, single sugar”, 2) elongate the hyaluronan chain through its reducing end and 3) are not present in the endoplasmic reticulum or Golgi apparatus like most other glycosyltransferases. HAS are in fact positioned at the inner face of the cell membrane from where the growing HA is directly extruded into the pericellular space while being still attached to the enzyme (Weigel et al., 1997; Spicer and Tien, 2004) (fig. 3).

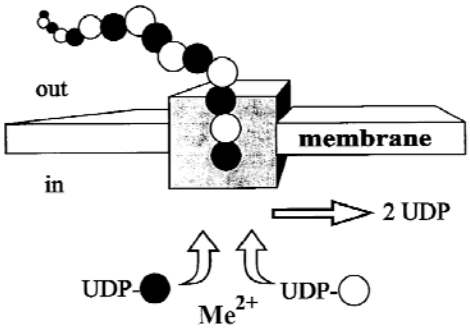

Figure 3: Model of HA biosynthesis (from (DeAngelis, 1999)).
(Gray cube: HAS, white and black circles: sugars from UDP-sugars; Me^{2+}: Mn^{2+} or Mg^{2+})

Hyaluronan turnover is regulated by endocytic uptake and through its degrading enzymes, the hyaluronidases (Fraser et al., 1997; Tammi et al., 2002). Five human hyaluronidases are known, *HYAL1-4* and *PH-20*. Each of them displays different substrate specificities (Csoka et al., 1999; Csoka et al., 2001).

HA is indispensable for normal embryogenesis, as targeted inactivation of *HAS2* results in severe aberrations in heart development and causes intra-uterine death of E10.5 mice. (Camenisch et al., 2000). The crucial steps affected by the HAS2-deficiency are matrix expansion and initiation of cell migration during heart formation (McDonald and Camenisch, 2002). In contrast, mice lacking HAS1 or HAS3 expression are viable and fertile (Spicer et al., 2002), indicating that HAS2 is the key enzyme during embryogenesis.

Hyaluronan is also abundantly present during brain development being however, reduced to one fourth of its maximal content during tissue maturation (Margolis et al., 1975). In the adult CNS it is diffusely distributed within the neuropil (Costa et al., 2007) and along the myelinated fiber tracts (Bignami and Asher, 1992; Girard et al., 1992). It also accumulates in perineuronal nets (PNNs), where it builds specialized meshworks with lecticans and tenascins. PNNs wrap some highly active neurons and are thought to block the establishment of new synaptic contacts (Celio and Blumcke, 1994; Yasuhara et al., 1994). During cerebellar development, HA is expressed in the prospective white matter. There it might support neural migration by forming arrays of extracellular fibers that are structurally rather different from the PNN lattices (Baier et al., 2007).

Recent observations point to diverse functional roles of different size species of HA (Sherman et al., 2002). Deposits of high molecular weight HA have been found in chronically demyelinated lesions of multiple sclerosis patients. Since this form of the carbohydrate inhibits maturation of oligodendrocyte precursor cells, it has been suggested that high molecular hyaluronan hinders remyelination (Back et al., 2005).

In spite of being a rather simple unbranched polysaccharide, hyaluronan not only acts as a structural component that fills the interstitial space, it is also able to signal through cell surface receptors. Moreover, it provides the backbone for the assembly of highly hydrated matrices that form protective pericellular coats, down-regulate cellular adhesion and allow cells to divide and to migrate. Most of these functions are not exerted by hyaluronan alone, but rather in concert with its numerous binding-partners of which link proteins and proteoglycans of the lectican/hyalectan family are the best characterized (Toole, 2001; Day and Prestwich, 2002).

2.1.1.1. Lecticans/Hyalectans

The structurally closely related extracellular matrix chondroitin sulfate proteoglycans (CSPGs) that aggregate with hyaluronan to form high molecular complexes have been named hyalectans (Iozzo and Murdoch, 1996) or lecticans (Ruoslahti, 1996) in reference to their N-terminal hyaluronan-binding region (Johansson et al., 1985; LeBaron et al., 1992) and to the presence of a C-type lectin-like element near their C-terminus (fig. 4). Members of this CSPG-family are aggrecan (Doege et al., 1987), versican (or PG-M) (Zimmermann and Ruoslahti, 1989; Shinomura et al., 1993), neurocan (Rauch et al., 1992) and brevican (Yamada et al., 1994; Rauch et al., 1997b) (reviewed by (Ruoslahti, 1996; Bandtlow and Zimmermann, 2000; Yamaguchi, 2000; Rauch, 2004)).

The N-terminal hyaluronan-binding domain of all lecticans/hyalectans (G1 domain) consists of an immunoglobulin (Ig)-like loop and two link-protein-like tandem repeats (“link modules” or proteoglycan tandem repeats, PTR). The Ig-like loop and each tandem repeat contain two respectively four conserved cysteine residues that form intra-chain disulfide bridges and consequently ensure the proper folding of the domain. The G1 domain is essential for interactions with hyaluronan and link proteins that stabilize the ternary complex by binding to both, lectican and hyaluronan.

The C-terminal portion (G3 domain) of the lectican core proteins contains the lectin-like element, which is flanked by one or two EGF-repeats and a complement regulatory protein-like (CRP)/sushi domain, respectively. Recombinantly expressed G3 domains and/or the C-type lectin element alone bind *in vitro* simple carbohydrates and heparin or heparan sulfate (Ujita et al., 1994), fibulins -1 and -2 (Aspberg et al., 1999; Olin et al., 2001), fibrillin-1 (Isogai et al., 2002), sulfoglycolipids (Miura et al., 1999) and the tenascins Tn-C and Tn-R (Aspberg et al., 1995; Aspberg et al., 1997; Rauch et al., 1997a).

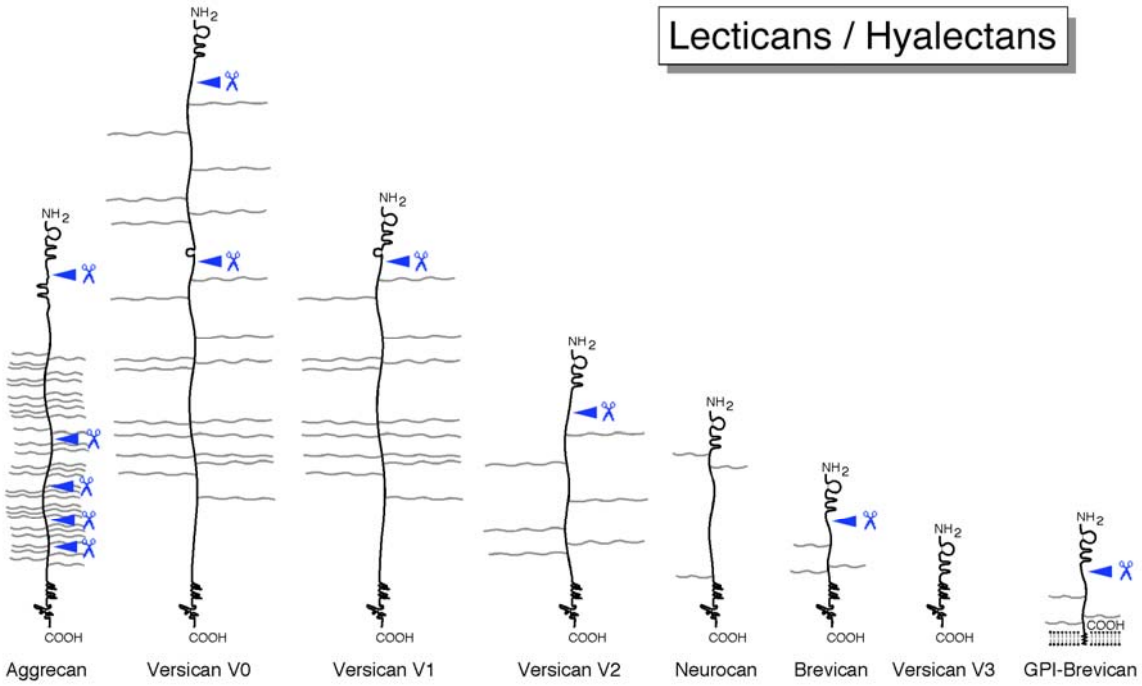

Figure 4: Structural models of lecticans/hyalectans (modified from (Bandtlow and Zimmermann, 2000).
(Wavy lines represent CS chains and arrowheads ADAMTS cleavage sites; GPI: glycosyl-phosphatidyl-inositol)

The G1 as well as the G3 domains are highly homologous among lecticans and appear in rotary shadowing electron microscopy as compact globular structures at either end of an extended central region that carries all GAG side chains. This middle part of the core protein, which is in versican subjected to alternative splicing, is poorly sequence-conserved among the different lectican family members. It also greatly varies in size and numbers of carbohydrate attachment sites. In aggrecan, for example, the central region extends over an average distance of 200 nm (Mörgelin et al., 1994) and potentially harbors over 100 GAG side chains, whereas it hosts in neurocan only a few GAGs and reaches maximally a length of 90 nm (Retzler et al., 1996). As a result, the distinct lecticans and their splice-variants form an almost perfect array of modular proteins that seem functionally closely related but differ extensively in size (Bandtlow and Zimmermann, 2000) (fig. 4).

Several CSPGs negatively modulate cell-cell and cell-matrix interactions and hence, are thought to inhibit growth of axons during nervous system development and maturation. Inhibitory activity on neurite outgrowth *in vitro* has been described for all lecticans (Snow et al., 1991; Friedlander et al., 1994; Yamada et al., 1997; Schmalfeldt et al., 2000), and all of them are expressed in the central nervous system at certain stages of development or in adulthood (Milev et al., 1998). Consequently, CSPGs and particularly lecticans have lately received special attention in regard to their potential role in obstructing CNS regeneration after injuries.

The expression and turnover of lecticans is during development highly dynamic. As a result, core proteins are in adult tissues often encountered in a fragmented form. Several characteristic products result from cleavage with specific ADAMTS proteases (fig. 4). ADAMTSs (**a d**isintegrin

and **m**etalloproteinase with **t**hrombo**s**pondin motifs) are a group of secreted multi-domain metalloenzymes containing as main features a zinc-binding-catalytic domain, a disintegrin module and thrombospondin type I repeat(s), some of which are able to interact with glycosaminoglycans (Apte, 2004; Porter et al., 2005; Flannery, 2006) (fig. 5). Cleavage activity towards aggrecan, versican and/or brevican has been mainly attributed to ADAMTS-1, ADAMTS-4, ADAMTS-5 and ADAMTS-9. Neurocan has not yet been identified as substrate of these metalloenzymes.

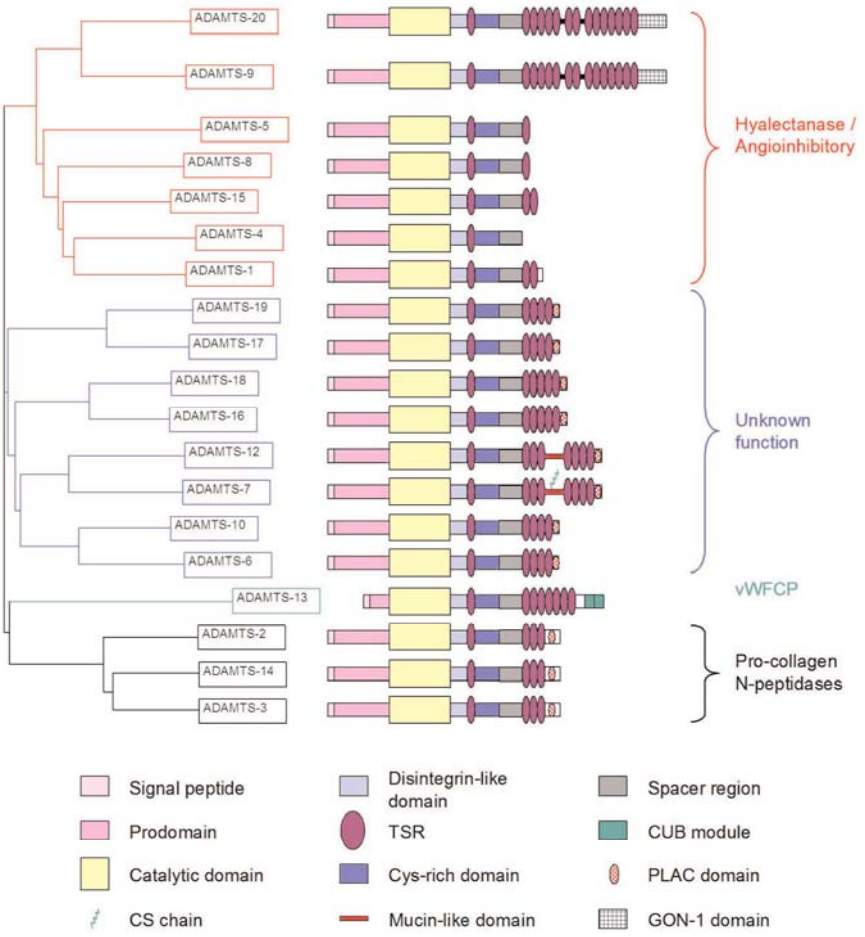

Figure 5: Structure and evolutionary relationship of human ADAMTS (from (Jones and Riley, 2005)).

Based on sequence alignments of the known ADAMTS cleavage sites in aggrecan and brevican a rather loose consensus recognition sequence {pt(V/I)XX(V/I)(t/d)XXlvEXvtpXXXXeXE*Xrg} has been proposed (where the asterisk represents the scissile bond, uppercase residues are 100 % conserved, lowercase residues are about 50 % conserved and X represents non conserved residues) (Sandy et al., 2001). The selective cleavage of lecticans by ADAMTSs is thought to modulate the functions of these proteoglycans by limited proteolysis and/or initiate complete degradation in combination with the action of various matrix metalloproteinases (MMPs).

2.1.1.1.1. Aggrecan

Aggrecan is the first characterized and thus most studied lectican. It is a main ECM component of cartilage, where it accumulates to very high concentrations by forming large aggregates with hyaluronan and cartilage link protein (Hascall and Heinegard, 1974; Franzen et al., 1981). Up to one hundred 1:1-complexes of aggrecan and link protein can associate with one single HA chain resulting in a high molecular lampbrush-like structure (10^8-10^9 Da). This large aggregate is strongly hydrated and consequently confers the resilience to cartilaginous tissues (Maroudas et al., 1969) (fig. 6). Although primarily expressed in cartilage, aggrecan is also present in other extracellular matrices (e.g. in brain).

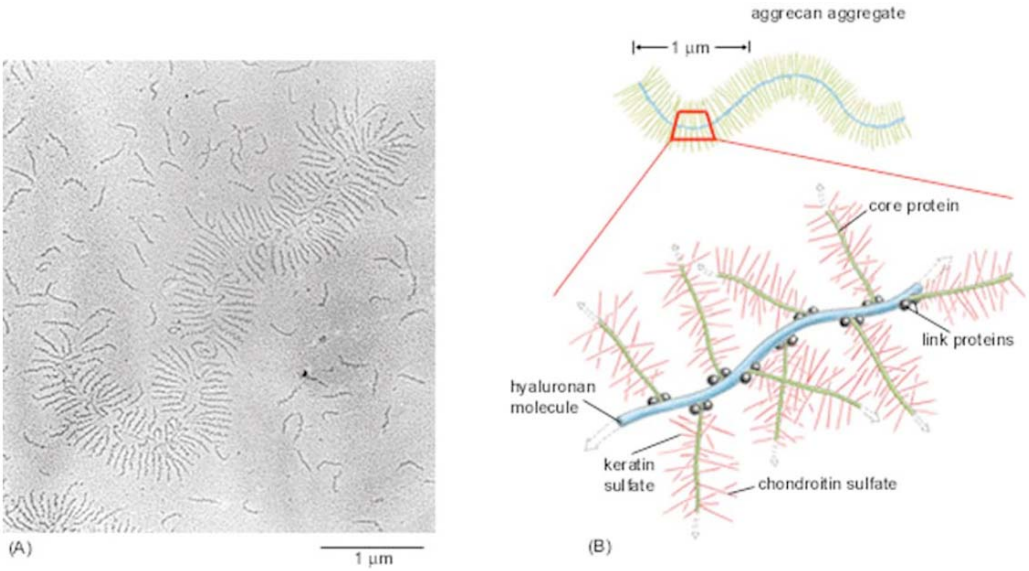

Figure 6: Aggregates of hyaluronan, aggrecan and link protein in cartilage (from (Alberts et al., 2002)).
(A: rotary shadowing EM picture and B: cartoon describing the molecular composition)

Some unique structural features characterize aggrecan and distinguish it to some extend from the other lecticans. This includes the presence of an additional globular domain (G2), a considerably higher density of GAG-attachment sites and the incorporation of a keratan sulfate (KS) bearing subdomain into the core protein (Antonsson et al., 1989). The G2 globule of aggrecan is located C-terminally to the G1 domain being separated by an about 130 amino acids-long interglobular domain (IGD). Similar to G1, the aggrecan G2 domain consists of two link modules, but lacks the Ig-like loop and does not bind to hyaluronan. Alternative splicing gives rise to distinct isoforms containing variable numbers of EGF-like elements (0 to 2) and/or lack the C-terminal sushi domain (Doege et al., 1987; Baldwin et al., 1989; Fülöp et al., 1993).

Around 120 potential GAG-attachment sites are present in aggrecan, largely outnumbering the corresponding sites in versican (~ 20 in the largest isoform), neurocan or brevican (7 and 3 respectively). With an average size of around 20 kDa per CS chain, the 225 kDa core protein of cartilage aggrecan accounts for only 10-20% of the total molecular weight of about 2’500 kDa

(Hardingham and Fosang, 1992; Dudhia, 2005). Noticeably, number, size and composition of GAGs may greatly vary according to the tissue origin of a particular lectican. For instance, the aggrecan core protein carries around 100 CS and 30 KS side chains in cartilage, while it is substituted with significantly fewer and shorter CS side chains and probably lacks KS in the central nervous system (Schwartz et al., 1996).

In rat brain, aggrecan deposition starts around embryonic day E14 and increases steadily until it reaches plateau at an almost 20-fold higher level around postnatal day P150 (Milev et al., 1998). Nevertheless, due to its restricted accumulation in perineuronal nets the total tissue content of aggrecan remains also in adult brain rather low in comparison to other lecticans.

Spontaneous mutations of the aggrecan gene have been described in mice (the cartilage matrix deficient *cmd* strain (Watanabe et al., 1994) and *cmd-Bc* strain (Krueger et al., 1999)), as well as in chicken (nanomelia (*nm*) (Li et al., 1993)). These mutations provoke in homozygous animals severe abnormalities in skeletal development and cause perinatal death probably due to respiratory failure. A similar frame-shift mutation in the aggrecan gene has also been identified in connection with a heritable human disease (Gleghorn et al., 2005). Similar to the animal model strains, only patients heterozygous for this mutation survive. These individuals suffer from a relatively mild variant of chondrodysplasia characterized by shortening of the trunk and the limbs and a premature degenerative arthropathy (spondyloepiphyseal dysplasia type Kimberley; SEDK).

Due to the lethal character of the homozygous mutations, the role of aggrecan in the postnatal maturation of the CNS could so far not be explored.

2.1.1.1.2. Neurocan

The prevalent lectican in the developing brain is neurocan. It is solely present in the nervous system and mainly expressed by neurons (Oohira et al., 1994; Zhou et al., 2001). The core protein with a predicted molecular weight of 130 kDa carries, apart from 5 N- and up to 40 O-linked oligosaccharides, three chondroitin sulfate chains. There are no alternative splice variants known for neurocan, but a developmentally regulated proteolytic cleavage in the middle of the GAG attachment domain renders two well-defined polypeptides with molecular weights of 130 kDa (N-terminal fragment) and 150 kDa (C-terminal fragment). Each of these fragments carries a globular domain, G1 or G3, respectively (Matsui et al., 1994). In addition, the size and sulfation of the chondroitin sulfate chains of neurocan change postnatally (Rauch et al., 1991).

Neurocan mRNA is first detected in embryonic mouse brain at E10, being slightly downregulated between E14.5 to E15.5 and then reaching maximal expression around birth (Zhou et al., 2001). On protein level, neurocan decreases significantly during the first month after birth (Milev et al., 1998), and becomes confined to specific perineuronal nets in adult brain tissues.

Despite its dominant presence during development, the lack of neurocan in mutant mice is not lethal and the animals do not develop immediately obvious deficits. Brain anatomy, morphology and ultrastructure are normal, and the perineuronal nets do not appear affected. Yet, some disturbances of synaptic plasticity in the mutants have been reported. The fact that it is dispensable for brain development suggests however that neurocan fulfills only a minor role in the control of synaptic function (Zhou et al., 2001).

2.1.1.1.3. Brevican

Brevican, the smallest CSPG of the lectican family, is like neurocan exclusively expressed in the CNS. Its core protein has a predicted molecular weight of 99.5 kDa. Following selective degradation of the CS-chains with chondroitinase ABC, it migrates in non-reducing SDS-PAGE as a 145 kDa glycoprotein (Yamaguchi, 1996). A second membrane-bound variant arises from alternative transcription termination (Seidenbecher et al., 1995). In this isoform the C-terminal globular domain (G3) is replaced by a short peptide module carrying a GPI-anchor. Brevican is, like other lecticans proteolytically cleaved by ADAMTS proteases giving rise to a 50 kDa N-terminal and a 90 kDa C-terminal product. In adult bovine and rat brain, brevican does not carry any GAG side chains. It is therefore considered to be a part-time proteoglycan.

Brevican mRNA has been detected in astrocytes and oligodendrocytes in culture. In situ hybridization (ISH) experiments localized the transcript of the secreted variant in neurons of cerebellar and cerebral cortex, hippocampus and thalamic nuclei, and the mRNA of the GPI-linked isoform in glial cells (Seidenbecher et al., 1998). Unlike the mostly embryonically expressed neurocan, brevican immunoreactivity is first noticed after birth in the prospective cerebellar white matter (around P21) and reaches in the granular cell layer only a significant level at P28, when the migration of these neurons has been completed. After this time point the expression steadily increases and maintains its level in the mature brain (Yamada et al., 1997). Consequently, brevican evolves to one of the main components of adult extracellular matrix in the CNS being mainly associated with myelinated fibers, with neuroglial sheaths of cerebellar glomeruli and with PNNs that include the matrix around the axon initial segment (AIS) (Yamada et al., 1997; Hagihara et al., 1999; Niederöst et al., 1999; Bruckner et al., 2000; Hedstrom et al., 2007).

Brevican null mice are viable, fertile and have a normal lifespan. Anatomically they are indistinguishable from wild type littermates (Brakebusch et al., 2002). Although they show significant deficits in the maintenance of hippocampal long-term potentiation (LTP; an indicator of memory formation in neuronal circuits), brevican mutants display no impairment of synaptic transmission and no statistically significant deficits in memory and learning experiments.

2.1.1.1.4. Versican

Versican is the most versatile lectican in regard to core protein size variability and expression pattern. The alternative usage of exons VII and VIII of the *VCAN* gene generates at least four splice variants including the largest and the smallest core proteins of the lectican family. These exons encode the central glycosaminoglycan attachment domains, GAG-α and GAG-β, respectively (Dours-Zimmermann and Zimmermann, 1994) (fig. 7). Both of these GAG-carrying core protein portions are present in the V0 splice-variant, which has a predicted molecular weight of 370 kDa. The smaller V1 (262 kDa) and V2 (180kDa) isoforms either contain only the GAG-β or the GAG-α domain, whereas the fourth and shortest versican splice-variant V3 (71 kDa) is devoid of both modules, being most probably not a proteoglycan (Zako et al., 1995).

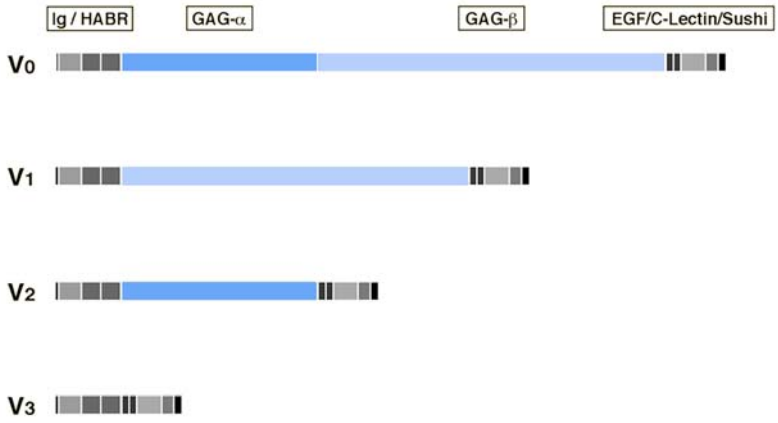

Figure 7: Versican splice variants.

Due to the substitution with various carbohydrates, intact versican proteoglycans are very large, reaching relative molecular masses between 5 x 10^5 and 1.5 x 10^6. The numbers of putative GAG-attachment sites amount to 17-23 in the isoform V0, 12-15 in V1 and 5-8 in the V2-variant (Dours-Zimmermann and Zimmermann, 1994). After removal of the chondroitin sulfate side chains by digestion with chondroitinase ABC, versican V0, V1 and V2 migrate on SDS-polyacrylamide gels at about 550, 500 and 400 kDa (Schmalfeldt et al., 1998). The discrepancy to the core protein sizes predicted from the amino acid sequences can be attributed to the presence of a few N- and numerous O-linked oligosaccharides (i.e. 9 and more than 80, respectively in versican V2) and to the high content of acidic amino acid residues (pIs around 4.5), which influences the gel migration properties.

The versican gene *(VCAN/CSPG2)* spans over 90-100 kb on chromosome 13 of the mouse (Naso et al., 1995; Shinomura et al., 1995) and on chromosome 5 (5q14.3) of the human genome (Naso et al., 1994). The arrangement of its 15 exons shows a remarkable concordance of the exon-intron architecture and the modular structure of the core protein (fig. 8).

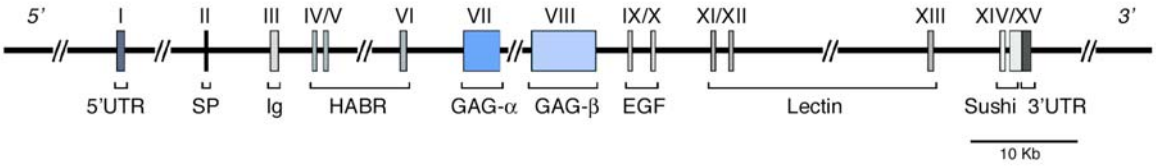

Figure 8: Versican genomic structure of the Versican gene (*VCAN*).

The translational start codon is located in exon II, preceded by a 5'-untranslated region (UTR) covered by exon I and parts of exon II. The Ig-like loop is encoded by exon III, while the tandem repeats responsible for binding to hyaluronan are located in exons IV, V and VI. Downstream of the CS attachment coding exons VII and VIII, exons IX and X cover the two EGF-like tandem repeats, while exons XI, XII, and XIII give rise to the C-type lectin like motif. Exon XIV generates the sushi element and exon XV contains the remaining sequence including the C-terminus and the entire 3'-untranslated region.

Like all lecticans, the proteoglycan isoforms of versican V0-V2 (and presumably also the V3 glycoprotein) bind to hyaluronan with a K_D in the lower nanomolar range (Kimata et al., 1986; LeBaron et al., 1992; Schmalfeldt et al., 1998). The interaction is mediated by the typical link-protein-like tandem repeat in the N-terminal globular domain. Similar to other lecticans, the C-type lectin module in the G3 domain of versican binds tenascin-R in the fibronectin type III domains 3-5 (K_D $15x10^{-9}$ M). This binding is calcium-dependent and occurs through a protein-protein interaction without involvement of carbohydrates (Aspberg et al., 1997). Likewise, the C-type lectin domain of versicans also binds *in vitro* to the sulfated cell surface glycolipid, sulfatide. This interaction may be physiologically significant for lectican-mediated adhesion of neural cells expressing sulfated glycolipids on their surface (Miura et al., 1999).

The large versican isoforms V0 and V1 are highly expressed in morphogenetically active regions during embryogenesis and in particular in condensing mesenchyme prior to cartilage formation (Shinomura et al., 1990) as well as in tissues that impede neural crest cell migration and sensory and motor axons extension (Landolt et al., 1995). This first evidence for a putative involvement of versican in guidance processes e.g. during innervation of the limbs prompted *in vitro* experiments, in which the potentially inhibitory properties of these versican isoforms were tested. Using stripe-choice assays Dutt et al. could indeed demonstrate that versican V0/V1 inhibits neural crest stem cell migration (Dutt et al., 2006), as well as neurite outgrowth from chick retinal ganglion cell explants and DRGs (Dutt, S. and Zimmermann, D.R., unpublished observations).

The relatively high levels of versican V0/V1 expression during embryonic development are in general greatly reduced in mature extracellular matrices of healthy individuals. Exceptions are large blood vessels and the loose connective tissues of some internal organs, where versican V0/V1 or its proteolytic fragments are retained throughout adulthood (Bode-Lesniewska et al., 1996). Versican V0/V1 is also present in the basal layer of the epidermis positively correlating

with cell proliferation - an observation that could be confirmed in cultures of primary keratinocytes and skin fibroblasts (Zimmermann et al., 1994).

Using a slot blotting radioimmunoassay with antibodies against versican GAG-attachment domains Milev et al. have shown that the isoforms V0/V1 are in rat brain extracts predominantly present during embryogenesis and at very early postnatal stages mostly disappearing upon CNS maturation (Milev et al., 1998). On the contrary, the extent of the GAG-α immunoreactivity (V0 or V2 isoforms) steadily increases from 2 weeks to 3 months after birth, subsequently persisting at a constantly high level in adult brain. By RT-PCR, biochemical and immunohistochemical studies we have obtained strong indications that this increase is associated with the expression of versican V2, an isoform which is exclusively present in the mature CNS (Dours-Zimmermann and Zimmermann, 1994; Schmalfeldt et al., 1998). By in situ hybridization we have identified cells of oligodendrocytic lineage as main source of versican V2 expression (Schmalfeldt et al., 2000). Our immunohistochemical analyses of mouse CNS tissues show versican V2 staining primarily along myelinated fibers with particularly high levels of versican deposition at the nodes of Ranvier (Schmalfeldt et al., 2000; Oohashi et al., 2002). In line with these observations, versican V2 has been detected in one of the neurite growth inhibitory fractions of CNS myelin preparations (Niederöst et al., 1999) and we have demonstrated that isolated versican V2 isoform indeed exerts a potent inhibitory activity towards neurite outgrowth *in vitro* (Schmalfeldt et al., 2000). All these findings have provided further support for the hypothesis that versican V2 enriched matrices suppress axonal growth also *in vivo* and consequently restrict structural plasticity and regenerative capacity of the adult CNS.

While the formation of versican-rich matrices during tissue development is highly dynamic, establishing an efficient and selective cleavage of versicans may be crucial for its functional attenuation. Like other lecticans, versicans are specifically recognized by ADAMTS proteases as revealed *in vitro* and by neo-epitope immunostaining *in vivo* (Sandy et al., 2001; Westling et al., 2004). ADAMTS-1 and -4 digest versican V1 at the Glu^{441}-Ala^{442} bond within the sequence DPEAAE^{441}-A^{442}RRGQ and liberate a 70 kDa product corresponding to the G1 domain of versican. Analogously a 220 kDa fragment is generated, when V0 is cleaved at this site. Both products have been identified in aortic and skin extracts supporting the physiological character of the process. Similarly, a 64 kDa product, abundant in human brain white matter, results from ADAMTS-4 cleavage of versican V0 or V2 at the Glu^{405}–Gln^{406} that follows the sequence NIVSFE^{405} (Westling et al., 2004). This fragment has previously been regarded as independent hyaluronan-binding protein and has been named hyaluronectin or GHAP (Delpech and Halavent, 1981; Perides et al., 1989). Apart from ADAMTS-1 and -4, ADAMTS-5 and -9 have been considered to function as "versicanases" (Somerville et al., 2003). Cleavage of versican (probably mediated by ADAMTS-1) seems to be essential for cumulus-oocyte-complex expansion and ovulation (Russell et al., 2003), whereas its putative role in regulating axon growth inhibiting properties of ECMs in the nervous system is currently only speculative.

Constitutive abolition of versican expression by random transgene integration into the *CSPG2 (VCAN)* gene on chromosome 13 (Yamamura et al., 1997) leads to intrauterine death of homozygous *hdf* (heart defect) mice at E10.5 (Mjaatvedt et al., 1998). The mutant embryos, lacking all known versican variants, exhibit aberrations along the anterior-posterior cardiac axis, fail to form the future right ventricle and conus/truncus of the single heart tube and lack the endocardial cushions in the atrioventricular and conus/truncus regions. Remarkably, *hdf* and the *HAS2* null mice show very similar phenotypes, implying that both versican and hyaluronan are required for the stabilization of the ECM in the developing heart. While the early recessive lethality of the *CSPG2*-null mutants proves the necessity of versican for heart development, it unfortunately prevents the elucidation of other functional aspects, for example during CNS development.

The importance of versican gene expression is also underscored by the existence of a heritable human disease. The Wagner Syndrome is an autosomal dominant vitreoretinopathy linked to specific mutations in the human versican gene (Miyamoto et al., 2005; Kloeckener-Gruissem et al., 2006; Mukhopadhyay et al., 2006). Similar to the *hdf* mice only heterozygous Wagner patients survive. Although they do not suffer from systemic abnormalities, they present with an optically empty vitreous cavity with fibrillary condensations, avascular preretinal membrane and other deteriorations causing severe visual impairments already early in adulthood. The mutations of the versican gene in the originally described Swiss family and in subsequently identified Japanese and Dutch families involve the highly conserved splice donor or acceptor sites in the introns 8 and 7, respectively. They all interfere with the correct splicing of exon VIII consequently reducing the expression of versican V1, the main isoform in the vitreous humor. It seems therefore conceivable that the compensatory up-regulation of the smaller V2 and V3 variants perturbs the normal formation of large aggregates of hyaluronan, versican V1 and fibrillin-1 and weakens the mechanical stability of this delicate gel-like structure.

2.1.1.2. Phosphacan

Apart from the lectican family members, phosphacan, a secreted CSPG-isoform of the receptor-type protein-tyrosine phosphatase β (RPTPβ), plays a prominent role in the brain ECM (Levy et al., 1993; Barnea et al., 1994; Maurel et al., 1994). Arising from alternative mRNA splicing, it contains like the other isoforms of RPTPβ a carbonic anhydrase domain (CAH), a FN type III repeat and a spacer element (S), but lacks the transmembrane domain and the cytoplasmic tyrosine phosphatase modules (fig. 9).

Phosphacan and the largest membranous variant (~2300 amino acids) of RPTPβ include an additional 860 residues long insert, which carries the chondroitin sulfate side chains. The core glycoprotein of phosphacan migrates on SDS-PAGE in the range of the 400 kDa standard.

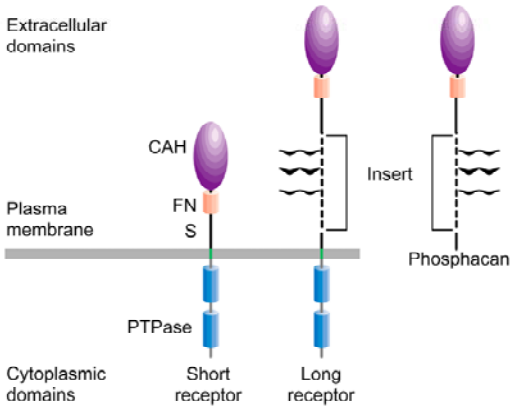

Figure 9: Isoforms of RPTPβ (from (Peles et al., 1998)).

The expression of all RPTPβ isoforms is restricted to CNS tissues (Shintani et al., 1998) and is mostly associated with glial cells and also some neurons. During development RPTPβ/phosphacan is present along radial glial fibers and on astrocytes, in a pattern suggesting an involvement in neuronal migration (Canoll et al., 1993; Maeda et al., 1995). Glial progenitor cells located in the subventricular zone express predominantly the transmembrane isoforms, while more mature glial cells synthesize the secreted phosphacan (Canoll et al., 1996). In adult mice transcripts are limited to the olfactory bulb, cerebral cortex, hippocampus and cerebellum (Canoll et al., 1996; Shintani et al., 1998), whereas immuno-staining is mainly observed at the nodes of Ranvier (Xiao et al., 1997), molecular layer of the cerebellum and in PNNs (Maeda et al., 1995; Haunso et al., 1999; Bruckner et al., 2000).

RPTPβ/phosphacan has been shown to interact *in vitro* with various cell adhesion molecules like N-CAM, Ng-CAM, Nr-CAM (Milev et al., 1994; Sakurai et al., 1997). Also contactin (F3/F11), another Ig-CAM, which is expressed on primary tectal neurons, acts as cellular receptor for glial-derived RPTPβ. The binding, which involves the carbonic anhydrase (CAH) domain of RPTPβ, mediates neuronal adhesion and neurite outgrowth (Peles et al., 1995) possibly by inducing receptor-dimerization (Peles et al., 1998). The abnormal distribution of RPTPβ/phosphacan in the hippocampi of contactin null mice underlines the physiological relevance of this interaction (Murai et al., 2002). Moreover, tenascin-R, a neural ECM protein, binds to phosphacan through its EGF-like repeats in a Ca^{2+} dependent manner (Xiao et al., 1997) (fig. 10).

Finally, the CAH domain of RPTPβ/phosphacan participates in interactions with the extracellular region of sodium channels and the first intracellular phosphatase domain of the receptor isoforms appears to bind to both (α and β) subunits of sodium channels (Ratcliffe et al., 2000). It has therefore been speculated that these contacts would be needed for recruiting and/or clustering of sodium channels.

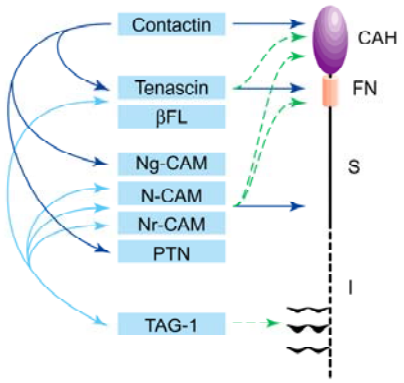

Figure 10: Extracellular binding partners of RPTPβ /phosphacan (from (Peles et al., 1998)).
(Blue arrows represent protein-protein interactions; green arrows, carbohydrate-mediated interactions)

In spite of the multitude of proposed functions of RPTPβ/phosphacan in neurite outgrowth, axon guidance and gliogenesis, mice deficient in all three isoforms are viable, fertile and show no gross anatomical alteration in the nervous system. The migratory patterns of neurons in the null animals are normal and the ultrastructures of nodal and paranodal regions are not modified. Even the number and clustering of Na_vCh are unaltered and the nerve conduction velocity is not significantly reduced in RPTPβ$^{-/-}$ mutants. Only a certain tendency for an increased myelin fragmentation has been noted on electron microscopical level, although the sheath organization appeared normal (Harroch et al., 2000). Further analysis subsequently revealed that these mice display an impaired recuperation from EAE (experimental autoimmune encephalomyelitis), an experimental model of multiple sclerosis. After being challenged by MOG peptide-injection (myelin oligodendrocyte glycoprotein) the mutants remained paralyzed for at least 2 months. In analogy, an up-regulation of RPTPβ was also found in lesions from multiple sclerosis patients, further fueling speculations about a role for RPTPβ in oligodendrocyte survival and recovery from demyelinating disease (Harroch et al., 2002).

Similarly, another knockout strain, in which all isoforms of RPTPβ were abrogated by insertion of the LacZ gene (Shintani et al., 1998), showed first no obvious abnormalities. However, animals older than thirteen weeks developed subsequently an age-dependent impairment of spatial learning and an enhanced LTP in the CA1 region of hippocampal slices. The defect in memory formation has been attributed to the lack of modulation of RhoGTPase activity in the mutants (Niisato et al., 2005; Tamura et al., 2006).

2.1.2. Link proteins

The interaction between HA and lecticans is strengthened by small link proteins recently summarized under the term HAPLNs (hyaluronan and proteoglycan binding link proteins) (Spicer et al., 2003). This family of ancillary glycoproteins consists of four members, including the classical cartilage link protein (HAPLN1=Crtl1) discovered more than three decades ago. In the meantime, it has been noted that Crtl1/HAPLN1 expression is not limited to cartilage tissues

alone, but is also present in placenta, the gastrointestinal tract and in the CNS, while Lp3/HAPLN3 is even more widely distributed being produced by smooth muscle cells (Spicer et al., 2003; Ogawa et al., 2004). The remaining two family members, the brain link proteins-1 and -2 (Bral1/HAPLN2 and Bral2/HPLN4), are restricted to the CNS (Hirakawa et al., 2000; Bekku et al., 2003). In fact, all link proteins, except for the vessel associated Lp3/HAPLN3, are at some point expressed in the brain parenchyma (Ogawa et al., 2004). While Crtl1 is predominantly observed during embryogenesis, Bral1 and Bral2 are almost exclusively found in adult brain, where they are secreted by neurons (Oohashi et al., 2002; Bekku et al., 2003).

Being built-up of an Ig-fold and a hyaluronan-binding tandem repeat, the link protein structure strongly resembles the G1 domain of lecticans. This close relationship is also reflected in their genomic organization and location. Intriguingly, each of the link protein genes is paired up with one of the lectican genes: *HAPLN1* with *VCAN, HAPLN2* with *BCAN, HAPLN3* with *AGC* and *HAPLN4* with *NCAN.* Whereas three of these pairs are joined in a tail-to-tail fashion, only *HAPLN2* and *BCAN* follow the same genomic orientation. Despite this particularity, the expression of link protein and lecticans seems to be uncoupled from their genomic setup. For instance, the HAPLN1/Crtl1 protein is co-expressed with aggrecan in cartilage and versicans V0 and V1 are synthesized together with Lp3/HAPLN3 by smooth muscle cells, while they possibly team up with HAPLN1/Crtl1 during neural development. The Bral1/HAPLN2 protein co-localizes with versican V2 along the myelinated fiber tracts and, with accentuation, at the CNS nodes of Ranvier (Oohashi et al., 2002). Finally, Bral2/HAPLN4 associates with brevican in the perineuronal nets of the adult brain, being mostly lost upon elimination of brevican in the knockout mouse strain (Bekku et al., 2003).

2.1.3. Tenascins

Apart from HA, lecticans and link proteins, tenascins represent the fourth class of molecules that form the basic constituents of the brain ECM. Tenascins are very large multimeric glycoproteins that are well conserved among vertebrates (reviewed by (Jones and Jones, 2000; Joester and Faissner, 2001; Chiquet-Ehrismann and Chiquet, 2003; Hsia and Schwarzbauer, 2005)). In mammals, the family includes four members: tenascin-C, -R, -X and -W (-N), (fig. 11). The macromolecular structures of the different tenascin monomers are highly alike as they follow the same modular arrangement. They consist of an amino-terminal cysteine-rich oligomerization region composed of three to four α-helical heptad repeats, EGF-like elements, fibronectin type III-repeats (FN III) and a carboxyl-terminal fibrinogen-like globular domain.

The heptad domains allow an N-terminal association of the individual subunits that primarily form homotrimers. In the case of tenascin-C and tenascin-W, an additional cysteine residue in this region permits that these trimers then further assemble into a hexameric quarternary structure. Although this cysteine is also present in tenascin-R, only trimers of this ECM molecule have been observed so far.

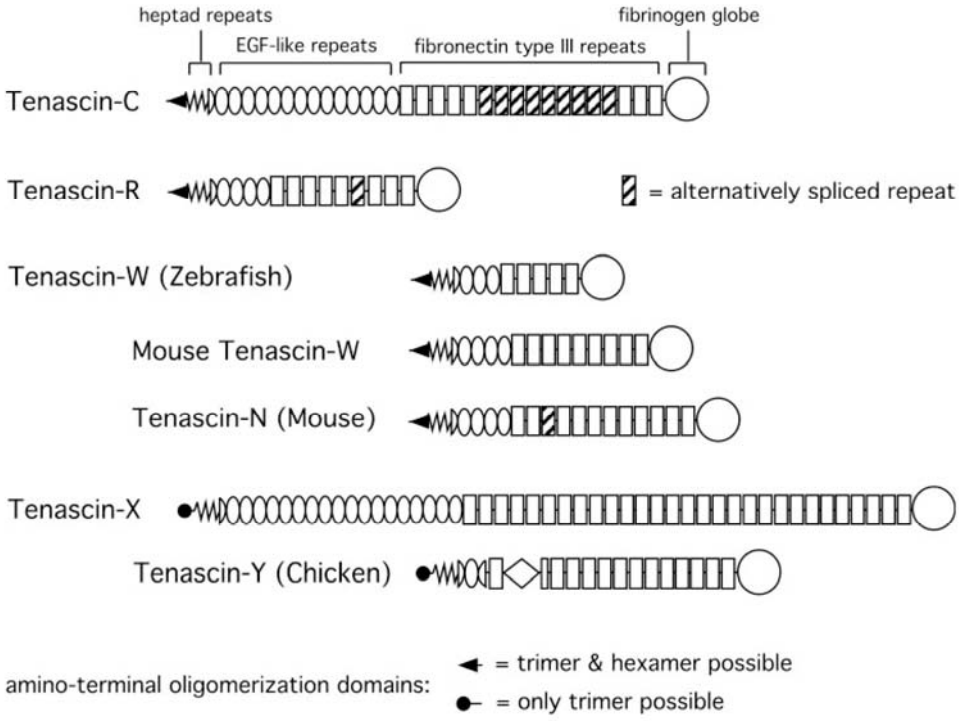

Figure 11: Structures of the tenascins (from (Hsia and Schwarzbauer, 2005)).

While the number of EGF-like repeats vary only between the different tenascins, some of the FN III domains are also subjected to alternative splicing. Since different combinations of these variable FNIII repeats are possible, several isoforms of the individual tenascin exist (Norenberg et al., 1992; Ikuta et al., 1998). For instance, the tenascin-C monomers bear 14.5 EGF-repeats plus 17 FN III repeats, 9 of which can be alternative spliced. As a result, up to 27 different tenascin-C transcripts are expressed during mouse brain development (Joester and Faissner, 1999), each subunit comprising molecular weights in the range of 180-300 kDa. In contrast, tenascin-R, which includes 4.5 EGF and 9 FN III repeats, gives only rise to two splice variants of 180 an 160 kDa per subunit. This difference depends on the presence or absence of the sixth FN III repeat. There is evidence that alternative splicing of FN III repeats also occurs in Tn-W/-N (monomer 170-180 kDa) and the biggest family member, tenascin-X (monomer around 450-500 kDa).

Tenascin-C (Tn-C) is expressed already during gastrulation and somite formation in the chick embryo (Crossin et al., 1986) and then all along the development of neural, skeletal and vascular tissues. In the CNS, glia-derived Tn-C particularly accumulates around the fibers of radial and Bergmann glial cells that direct the migration of neuronal precursors during cortical and cerebellar development, respectively. Finally upon maturation, the expression of Tn-C is being reduced to tendon-associated ECMs, but it strongly returns when remodeling processes, such as wound repair, neovascularization, inflammation and tumorigenesis take place.

In contrast to Tn-C, the CNS-specific Tn-R is mainly present in mature tissues, where it is produced by oligodendrocytes and by small subsets of motor- and interneurons (Pesheva and

Probstmeier, 2000). The beginning of Tn-R expression coincides with the onset of myelination. Tn-R is first deposited along the presumptive white matter and concentrates later in adult animals around the nodes of Ranvier. Moreover, it forms part of the ECM of the granular cell layer of the cerebellum and associates with perineuronal nets covering the cell bodies of large neurons in selected nuclei.

In vitro, tenascins support cell adhesion only weakly or they display under certain conditions even anti-adhesive properties. For this reason, tenascins have been considered to act as adhesion-modulating ECM proteins. For instance, Tn-C is permissive for axonal growth, if offered as unique substrate, but growth cones turn away from Tn-C, as soon as neurite promoting molecules, like laminin-1, are offered as alternative. The axon growth inhibitory capacity of Tn-R is a matter of debate (Rathjen et al., 1991; Pesheva et al., 1993). The effect of Tn-C on neurite growth seems to depend partly on the neuronal origin, as it supports axon elongation of rat hippocampal neurons, while it restricts neurite outgrowth from retinal ganglion cells. This apparent inconsistency in behavior is possibly linked to the partly opposing effects of interactions between distinctive tenascin domains and their highly diverse sets of cellular receptors (fig. 12) and thus, may rather reflect specific differences in the integral of all of these interactions.

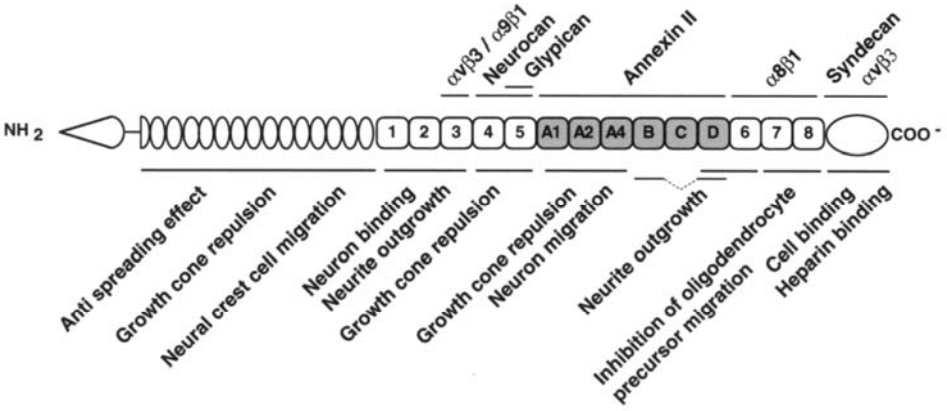

Figure 12: Binding partners and different functions of Tn-C (from (Joester and Faissner, 2001).

Most cell membrane receptors for Tn-C and Tn-R belong to the integrins or to the cell adhesion molecules of the immunoglobulin superfamily (Ig-CAMs contactin/F11/F3, axonin/TAG-1 and neurofascin). Other cell surface binding partners are annexin II and the receptor protein tyrosine phosphatase (RPTP-ζ/β). Albeit of uncertain physiological relevance, a low affinity of the EGF-like repeats of Tn-C for EGF-receptors has also been reported. Finally heparin/heparan sulfate (proteoglycans), fibronectin, phosphacan and lecticans are included among the ECM binding partners of tenascins.

The key partner for Tn-R on the neuronal cell surface appears to be the GPI (glycosyl-phosphatidylinositol)-anchored protein contactin (Brummendorf et al., 1993; Pesheva et al., 1993; Xiao et al., 1996), which may mediate the inhibitory effect of Tn-R on the attachment and

neurite outgrowth of various CNS neurons *in vitro* (Pesheva et al., 1993). Under certain conditions, the association of Tn-R and contactin could also lead to increased neurite fasciculation due to a reduced substrate adhesion (Pesheva et al., 1993).

In the mature CNS, Tn-R, lecticans and hyaluronan are the main components of the perineuronal nets that surround the cell bodies and the associated synapses of large motor- and interneurons (Celio et al., 1998). Since the lecticans and possibly also Tn-R impede axonal growth and neuronal interactions *in vitro*, one might hypothesize that these ECM components build a molecular barrier, which prevents the establishment of new synaptic connections. The fact that the formation of perineuronal nets coincides with the completion of the experience-dependent plasticity further supports this notion. Moreover, the ability of Tn-R to bind to the β-subunits of voltage-gated sodium channels (Na_vCh) *in vitro* (Srinivasan et al., 1998; Xiao et al., 1999) suggests a potential role for the oligodendrocyte derived Tn-R in clustering or activity modulation of sodium channels at the CNS nodes of Ranvier, while the interaction of Tn-R with sulfoglycolipid sulfatide *in vitro* points towards a regulatory function in the adhesion and differentiation of oligodendrocytes (Pesheva et al., 1997).

Considering this profusion of interactions, it is quite surprising that Tn-C and Tn-R null mice are viable, fertile and display grossly normal phenotypes (Saga et al., 1992; Forsberg et al., 1996; Weber et al., 1999). A more detailed analysis (Mackie and Tucker, 1999) of the Tn-C mice subsequently revealed subtle deficits in motor coordination and in exploratory behavior (Fukamauchi et al., 1996; Fukamauchi et al., 1997; Kiernan et al., 1999). Defects in wound healing (Forsberg et al., 1996) and impairments in the recovery from an experimental glomerulonephritis (Nakao et al., 1998) have also been described. Similarly mild deficiencies were reported for Tn-R null mice. This includes a decrease in axonal conduction velocity in the CNS as well as less developed perineuronal nets and a reduced and diffuse deposition of phosphacan at the nodes of Ranvier (Weber et al., 1999). In addition, an aberrant migration behavior of neuroblasts in the mature olfactory bulb has been observed (Saghatelyan et al., 2004). In behavioral tests Tn-R mice displayed lessened motor coordination, deficit in associative learning, differences in the exploratory behavior, and in general an impairment of functions that involve the cerebellum and the hippocampus (Freitag et al., 2003; Montag-Sallaz and Montag, 2003).

The only tenascin family member that could be linked to a heritable disease in humans so far is Tn-X (Burch et al., 1997). Defects in the tenascin-X gene cause an autosomal recessive form of the Ehlers-Danlos Syndrome, a disorder presenting with hyperelastic skin, hypermobile joints and increased connective tissue fragility. Because Tn-X seems not to reach significant levels in the central nervous system (Matsumoto et al., 1994) and because the neural expression of the only recently described mammalian Tn-W/Tn-N is currently still unclear (Neidhardt et al., 2003; Scherberich et al., 2004), these two other tenascins are not discussed in more detail here.

2.1.4. Supramolecular organization of the neural extracellular matrix

The ability of the brain ECM-components to selectively aggregate, allows them to establish large, relatively loose and flexible meshworks, where hyaluronan acts as backbone. The filamentous HA-molecules associate with the G1 domains of multiple lecticans and with link proteins that stabilize the complex. At the other end of the lectican core protein the G3 domains engage in an interaction with one of the arms of the tenascin oligomers. This way tenascins may cross-link up to three (Tn-R) or up to six lecticans (Tn-C) and consequently bridge neighboring HA-lectican-link protein-complexes to complete the extracellular network ((Norenberg et al., 1992; Ruoslahti, 1996; Rauch, 1997; Yamaguchi, 2000)) (fig. 13). Although this model of the supramolecular assembly has mainly been postulated on single interactions *in vitro*, it has recently been supported by rotary shadowing electron micrographs displaying such large complexes (Lundell et al., 2004).

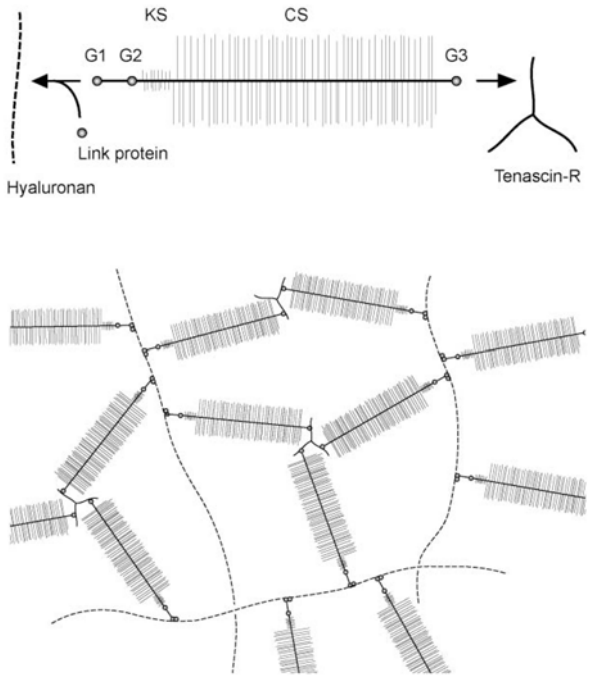

Figure 13: Putative assembly of aggregates of HA, link proteins, lecticans and Tn-R (from (Lundell et al., 2004)).

Because of the high proportion of negatively charged carbohydrates these supramolecular complexes attract large amounts of water and cations and consequently form gel-like structures that occupy the large extracellular spaces within the central nervous system. Estimates of the extracellular space reach in adults values of about 20% of the total tissue volume being even double as high in the developing brain (Nicholson and Sykova, 1998). Concomitant with this significant volume reduction during tissue morphogenesis, the expression of lecticans and tenascins changes from the larger ECM-family members and splice-forms (versican V0, V1, neurocan and Tn-C) to their smaller relatives (versican V2, brevican and Tn-R). The altered expression together with a selective enzymatic cleavage of the components of the juvenile matrix

(Tortorella et al., 1999; Matthews et al., 2000; Westling et al., 2004) transforms the brain ECM to a much tighter and less hydrophilic network (Rauch, 1997; Bandtlow and Zimmermann, 2000). This transition terminates the highly dynamic periods of cell and axonal migrations and the establishment of a functional neuronal circuitry and it heralds the phase of attenuated plasticity and structural maintenance of the mature central nervous system.

Despite this clear correlation between ECM reorganization and nervous tissue maturation a quadruple knockout approach abrogating the expression of neurocan, brevican, tenascin-C and tenascin-R has recently led to viable and fertile mice that display an unexpectedly mild phenotype (Rauch et al., 2005). Due to the compensatory up-regulation of the fibulins-1 and -2 and the perpetuation of the versican expression, a structurally similar ECM can still form in the brain despite its altered composition. It has therefore been hypothesized that the brain ECM can withstand major changes as long as the basic rules for assembling of the meshwork are kept, i.e. the formation of hyaluronan-lectican aggregates and the cross-linking and stabilization by lectican-binding and hence, tenascin substituting fibulin-dimers.

2.2. Myelin and myelinated nerve fibers

2.2.1. Myelinated nerve fibers

Rapid conduction of nerve impulses became a priority in the course of evolution. Yet, the fast transmission of an action potential in a metabolically efficient way and under space constraints is difficult, given the long distances that often separate the neuronal cell bodies from their axonal targets. Accelerating the conduction velocity can be reached in two ways: 1) by creating giant axons and 2) by developing an envelope that insulates the nerve fibers.

Axons that are several times larger in diameter than the average, the so-called giant axons, have lower interior resistance. They form part of fast neuronal circuits in many lower organisms, from worms to squids and from lobsters to fruit flies (Hartline and Colman, 2007). Giant axons, although effective, occupy much space. For instance, in order to achieve a comparable transmission speed (25 m/sec) the giant squid axon requires 5000 times more energy and occupies 1500 times more space than a myelinated nerve fiber of 12 μm diameter in the frog.

Insulating the nerve fiber with a lipid-rich multilayered coat, the myelin sheath, represents the second option to improve transmission. Myelin confers high resistance and low capacitance to the axonal membrane and consequently increases the conduction velocity. However, specific interruptions in the insulation are required for a rapid exchange of ions propagating the nerve impulses en route. These periodic gaps are called nodes of Ranvier. At these myelin-free axonal

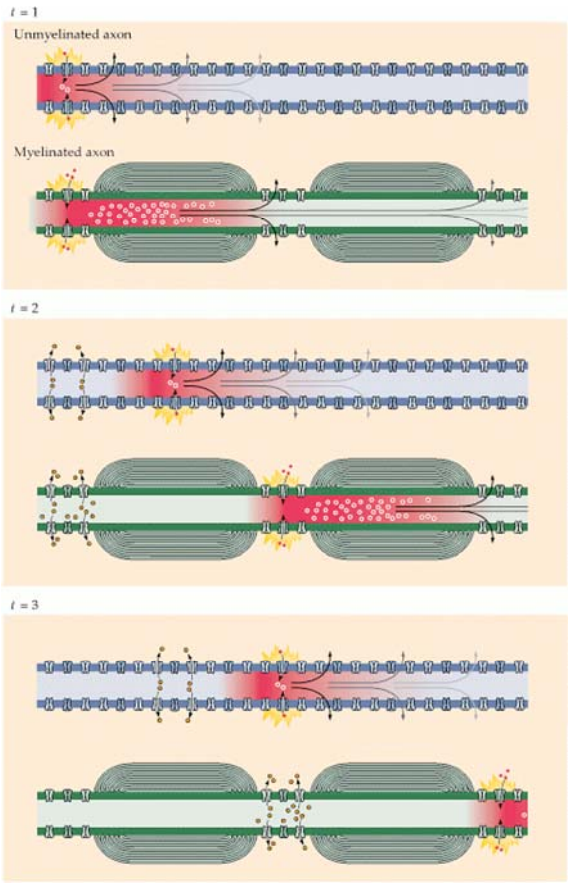

Figure 14: Action potential conduction along unmyelinated and myelinated axons: the inputs depolarize the axonal membrane, triggering the opening of local Na_v channels and the generation of an action potential at this point (t=1). The originated current flows passively along the axon, depolarizing the adjacent region in unmyelinated axons (t=2, t=3). Current flows much farther in the myelinated axon due to the insulation properties of myelin, which prevents leaking and thus accelerates the current transmission (from (Purves et al., 2001)).

zones, voltage-dependent sodium channels (Na_v) cluster to very high densities (~2000/μm^2) (Rasband and Trimmer, 2001). The periodicity of the intervals between the nodes of Ranvier corresponds to about 100 times the axonal diameter. Because the axon is exposed only at the nodes, depolarization occurs exclusively there and the generated action potential must jump from one node to the next, greatly accelerating transmission by this “saltatory” conduction (from Latin *saltare,* to jump). On the contrary, in unmyelinated fibers the voltage-dependent channels are distributed all along the axon and the action potential travels lengthwise by successive depolarization of neighboring patches (fig. 14).

Myelination proves to be very efficient as the conduction velocities of action potentials in rat optic nerve, for example, change from less than 0.2 m/sec in premyelinated axons to 10 m/sec after myelination and nodes of Ranvier formation (Rasband and Trimmer, 2001). Myelin sheaths of similar architecture and apparently identical function enwrap specific axons in most vertebrates (from sharks to humans) and in some invertebrates (Hartline and Colman, 2007).

2.2.1.1. Structure of myelinated fibers

The multilamellar myelin coat is in fact the extremely extended cytoplasm of a myelinating cell that spirals around the axon. The cells producing myelin are the Schwann cells in the peripheral nervous system (PNS) and the oligodendrocytes in the CNS, both belonging to the “neural glue”, the glia (fig. 15). Although both function similarly, PNS and CNS myelin differ from each other not only in their origins. Also their cellular morphology and parts of their molecular components are distinct (reviewed by (Fields and Stevens-Graham, 2002; Poliak and Peles, 2003; Salzer, 2003; Sherman and Brophy, 2005; Simons and Trajkovic, 2006)).

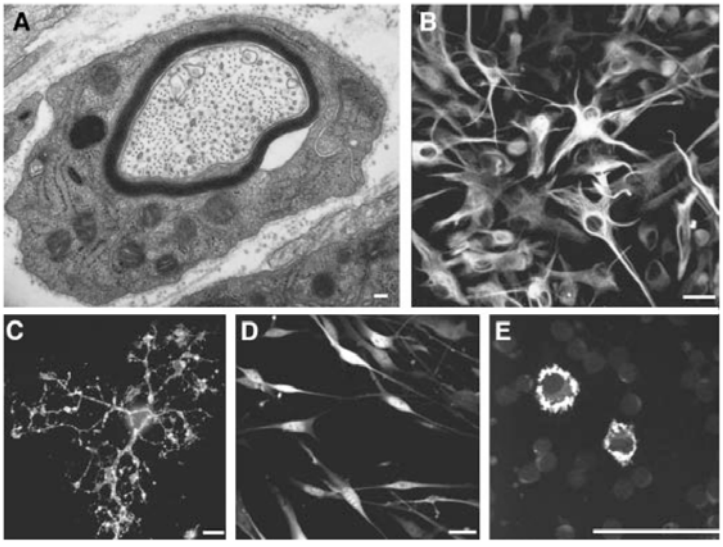

Figure 15: Glial cells in the nervous system. A) Electron micrograph of a Schwann cell myelinating an axon; dark laminas represent the myelin sheath. B) to E) Pictures from cells grown in culture and labeled by immunofluorescence with the antibodies indicated between brackets: B) Astrocytes [GFAP-Ab], C) Oligodendrocytes [O4-Ab], D) Schwann cells [S-100 Ab] and E) Microglia [OX-42 Ab] (from (Fields and Stevens-Graham, 2002)).

In the PNS each Schwann cell myelinates only one single segment of a single axon. The nucleus of the myelinating cell is located on the outside of the sheath, and a ring of cytoplasm persists both on the outer layer (the abaxonal compartment, also called outer mesaxon) and

adjacent to the axon (the adaxonal compartment or inner mesaxon). There is a periaxonal space between the axon and the inner glial membrane. Within the myelin sheath, cytoplasmic channels wind around the axon. They are called the Schmidt-Lanterman clefts or incisures. They form a conduit between the inner and outer cytoplasmic compartments. The lateral edges of the outermost membrane layer of the Schwann cells extends microvilli that cover the nodes of Ranvier, while their outside surface is completely engulfed in a basal lamina (figs. 16 and 17).

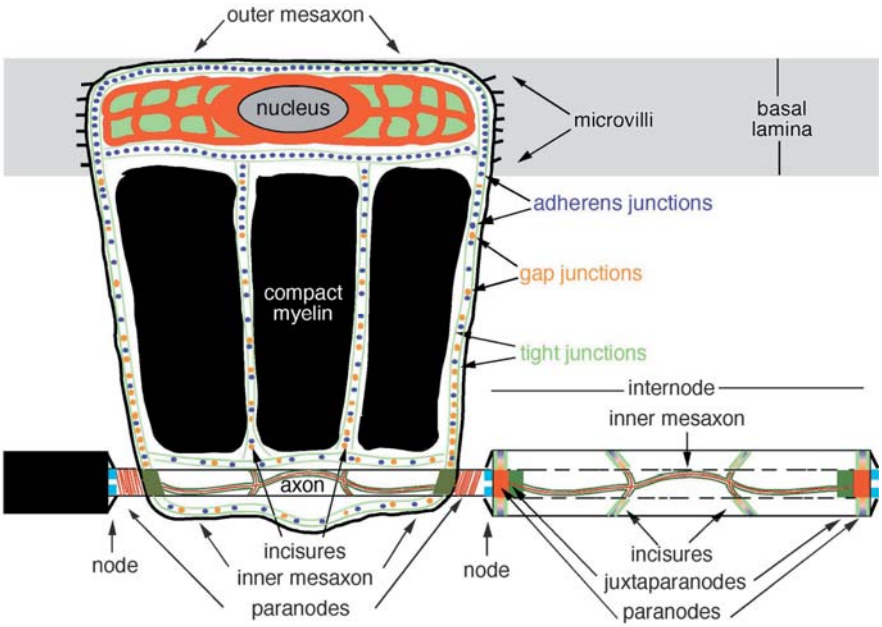

Figure 16: Schematic drawing of an “unrolled” myelinating Schwann cell. Tight junctions are depicted as green continuous lines; gap junctions and adherens junctions are shown as little ovals, orange and purple respectively. A “rolled-up” myelinating cell is shown in the second segment (from (Scherer and Arroyo, 2002)).

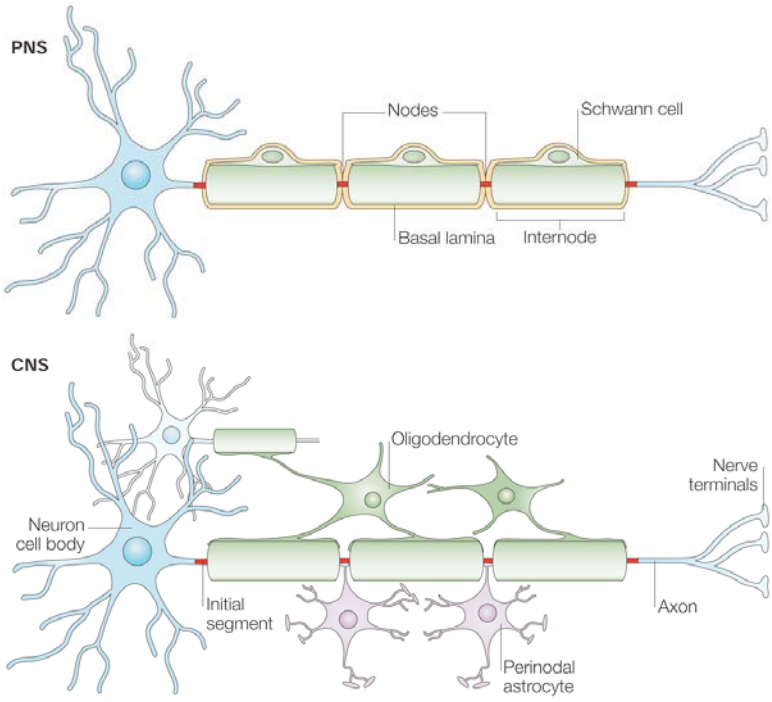

Figure 17: In the PNS, each Schwann cell builds a single myelin segment, while in the CNS an oligodendrocyte myelinates more than one axon (from (Poliak and Peles, 2003)).

Oligodendrocytes, the counterpart of Schwann cells in the CNS, are neither covered by a basal lamina nor do they develop microvilli that contact the nodes. Moreover, one oligodendrocyte may enwrap segments of up to forty separate axons (fig. 17). This translates into up to 5000 μm^2 of myelin sheath, which may be generated in approximately one day (Hudson, 2001). To achieve such a high level of production, some of the myelin components are synthesized far from the cell body. For this purpose, RNA-granules and ribosomes are transported by a microtubular system to the corresponding assembly sites (fig. 18).

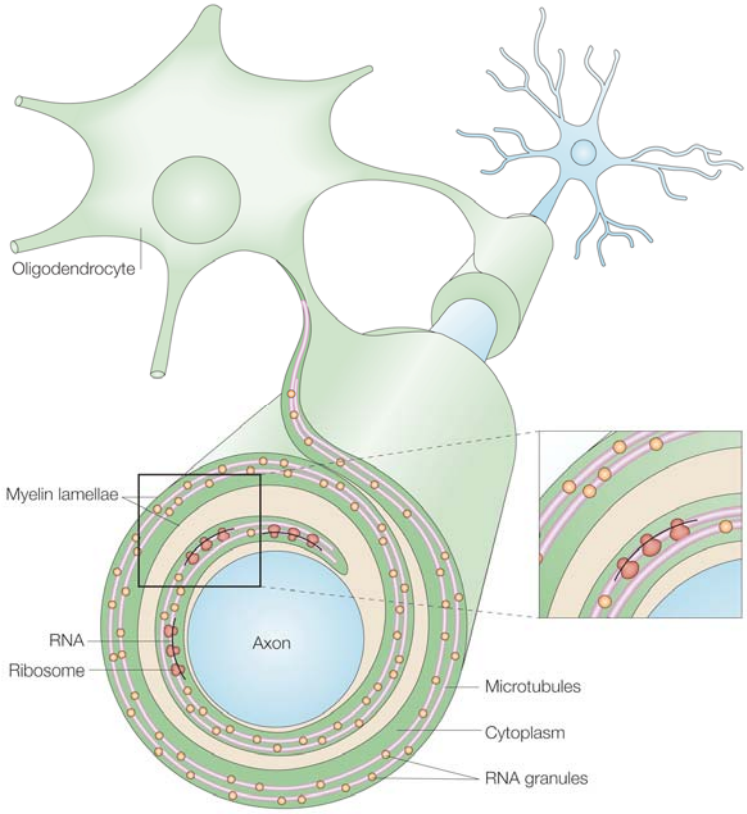

Figure 18: Ensheathment of an axon by an oligodendrocyte: some myelin proteins are synthesized at sites distal from the cell body (from (Sherman and Brophy, 2005)).

After contacting an axon, an oligodendrocytic process rolls multiple times around the axon. The newly formed membranous stack is subsequently depleted of most of the cytoplasm rendering a compact myelin sheath. In analogy to the Schwann cells in the PNS, each process of the CNS-specific oligodendrocytes gives rise to a myelin segment (named internode), which is delimited by two bare spaces (the nodes of Ranvier).

The axon communicates with the extracellular environment at the nodes. Whereas microvilli of the Schwann cells contact the nodal axolemma in the peripheral nervous system, processes of specialized perinodal astrocytes touch the axonal cell surface at the CNS-nodes of Ranvier (Black and Waxman, 1988; Butt et al., 2002) (fig. 17). Lateral to the nodes the compact layers of the Schwann cell or the oligodendrocytic processes fan out and the edge of each lamina apposes the axon, forming a structure called the paranodes. These highly organized regions

serve as diffusion barriers to solutes and membrane proteins. In longitudinal nerve sections, the paranodes appear as a series of cytoplasm-filled loops (up to 40 paranodal loops) with the outermost loop closest to the node of Ranvier (fig. 19). The paranodes are the sites of the tightest contacts between the myelinating cell and the axon (3-5 nm versus approximately 15 nm in the internodes). Ultra-structural analysis reveals several septate-like junctions between each loop and the axolemma. These transverse bands are a characteristic attribute of mature junctions, as they only develop after all contacts between paranodal loops and axon have been established. They separate the nodal sodium and potassium channels from the juxtaparanodal potassium channels. Apart from their interaction with the axon, the paranodal loops bind firmly to each other in both, the PNS and CNS. In the PNS, tight-, adherens- (desmosome-like) and gap-junctions stabilize the region (fig. 16). The paranodal gap junctions are the largest known continuous intercellular contacts, reaching a surface of 1 mm^2 in large fibers (Salzer, 2003). Unlike in the internode, the paranodal region of the myelin sheath is not compacted.

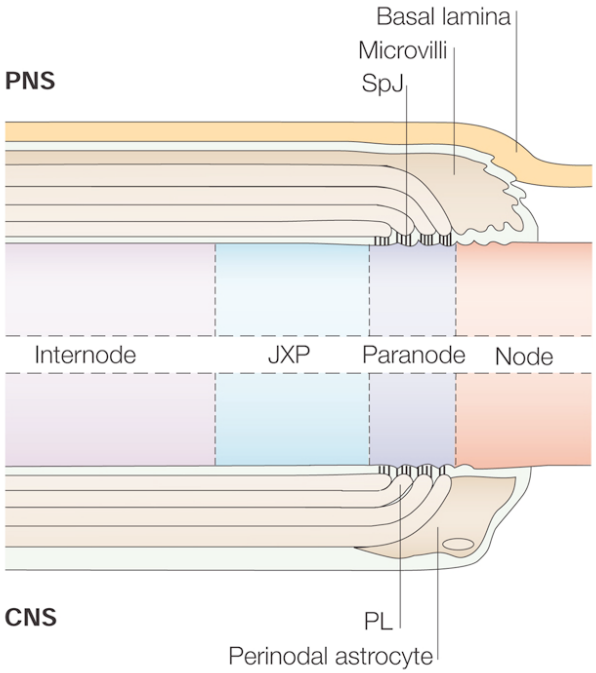

Figure 19: Cartoon of a longitudinally cut myelinated axon demonstrating the differences between PNS (up) and CNS (low) at the axoglial junction (from (Poliak and Peles, 2003)). *Abbreviations: SpJ: septate-like junctions (transverse bands), JXP: juxtaparanode, PL: paranodal loop.*

The axonal domain adjacent to the paranode, the juxtaparanode, lays under a compact myelin sheath. In this area the delayed rectifier K^+ channels $K_v1.1$ and $K_v1.2$ (with their β-subunits) concentrate near the paranodes, disseminating gradually towards the internodes. These K^+ channels stabilize conduction and help to maintain resting potential in the internodes (fig. 20).

The internode is the region where the most uniform and extended interaction between the myelinating glia and the axon occurs. The distance between the axon and the inner glial membrane keeps constant (15 nm). There are no specialized structures in the internodes and ion-channels are not clustered, but diffusely distributed at low density.

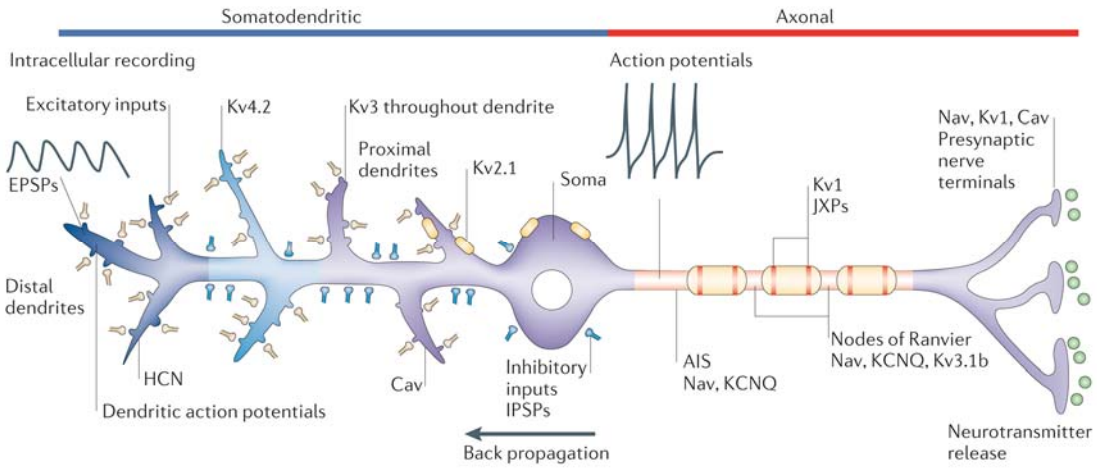

Figure 20: Localization of ion channels in a model neuron from myelinated tracts (from (Lai and Jan, 2006)). Na_v channels are found in the axon initial segment (AIS), the nodes of Ranvier and the presynaptic terminals, $K_v1.2$ channels in the juxtaparanodes and $K_v3.1b$ and KCNQ channels in the nodes of Ranvier. Excitatory and inhibitory inputs (EPSPs and IPSPs) diffuse to the AIS, where action potentials are generated by depolarization and reach the presynaptic terminals via saltatory conduction. Ca_v channels become activated in the terminals, increase intracellular Ca levels and trigger neurotransmitters release.

2.2.1.2. Molecular composition of axonal regions

The analyses of the molecular assembly of the distinct axonal regions emphasizes the importance of the communication between axons and glia. In fact, the signal that induces Schwann cells to myelinate fibers of >1 µm diameter is emitted by the contacted axons themselves. The axon also dictates the number of myelin layers, which are in general proportional to the fiber diameter. In turn, glial signals affect the axonal cytoskeleton, promote the polarization of the neuron and induce the clustering of voltage-gated channels.

A common feature of all axonal regions are specific complexes between cell adhesion molecules (CAMs) and ion-channels that bind to membrane ligands exposed on the surface of adjacent glial processes. These complexes are in addition linked to cytoskeletal proteins that stabilize the structures. In the PNS, the assembly starts at the nodes and proceeds subsequently to the paranodes and juxtaparanodes. In the following, I will describe these specific protein accumulations in more detail.

2.2.1.2.1. Nodes of Ranvier

The most remarkable attribute of the nodes is the presence of highly clustered voltage-gated sodium channels (Na_v). They are heterotrimeric aggregates of a pore forming α-subunit (molecular mass around 260 kDa) and two β-subunits (30-35 kDa) that regulate the kinetics of the channel and its surface expression (Catterall, 2000). In mammals, there exist ten Na_v α- and four β-subunits. The α-subunits consist of four domains, each of which has six transmembrane segments. The loop between segments 5 and 6 (S-5 and S-6) forms the pore, through which the sodium ions flow (fig. 21). At the node of Ranvier, the expression of the α-subunit alters upon

compact myelin formation changing from the $Na_v1.2$ to $Na_v1.6$ channel in both, PNS and CNS (Boiko et al., 2001). As the two channels differ in their activation kinetics, this developmentally regulated adjustment may be linked to an acceleration of the conduction velocity in the course of network maturation.

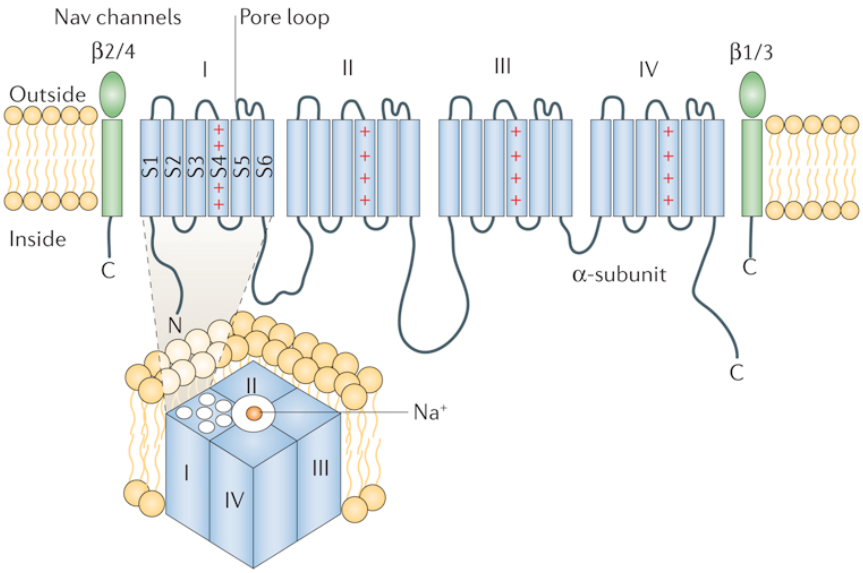

Figure 21: Structural topology of voltage-gated sodium channels showing the α-chain and the corresponding β-subunits (from (Lai and Jan, 2006)).

Each α-chain of the Na_v channel associates with one disulfide-linked and one non-covalently bound β-subunit (fig. 22). The β-subunits belong to the Ig-superfamily of cell surface proteins. They are transmembrane CAMs with short cytoplasmic tails (Malhotra et al., 2000). They promote interactions with other CAMs. For instance, β1 binds to the axonal members of the L1-subfamily, NrCAM (NgCAM-related-CAM) and Nfasc186 (neurofascin-186), as well as to contactin. On the cytoplasmatic side, Nfasc186 and NrCAM attach to ankyrin-G, which in turn interacts with βIV spectrin. This way they link the β-subunits with the actin cytoskeleton. Furthermore, the α-subunits contribute to the assembly by binding to ankyrin-G through a highly conserved linker motif in the loop II-III. Also the mostly glial-derived ECM proteins tenascin-C, tenascin-R and phosphacan, have been reported to associate with the β-subunits of sodium channels.

The α-subunit of voltage-gated potassium (K_v) channels (K_v1 to K_v12) are divided into twelve distinct families. In mammals they are encoded by around 40 genes. The α-subunits form homo- or heterotetrameric channels. Some of these K_v channels, like KCNQ (or K_v7) and $K_v3.1b$, are localized at selected nodes of Ranvier in the CNS and PNS. These nodal potassium channels are slow delayed rectifiers that activate at sub-threshold levels and reduce excitability.

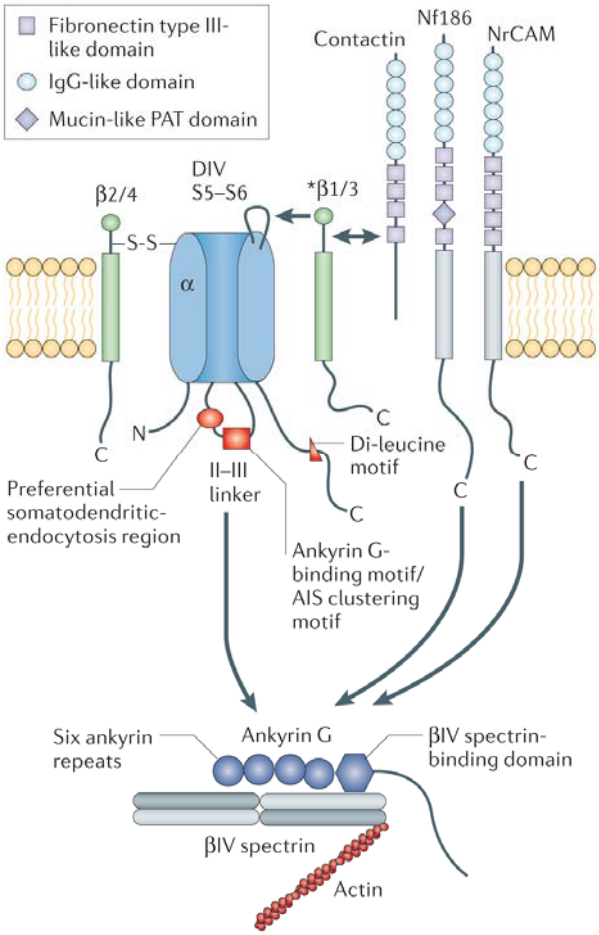

Figure 22: Complex formation of the voltage-gated sodium channels: the CAMs contactin, Nfasc186 and NrCAM interact with the β1-subunit (*), which binds to the S5-S6 loop in domain IV (DIV) of the α-subunit. Connections to the cytoskeleton are also shown (from (Lai and Jan, 2006)).
AIS: axon initial segment, PAT: domain rich in proline alanine and threonine.

The prominent Ig-CAM in the nodal axolemma is the neurofascin isoform 186 (Nfasc186), while its glial variant, Nfasc155, accumulates at the paranodes. Mice deficient in both isoforms display at first sight only mild defects in myelination, but nevertheless die a few days after birth (around P7), when the transition to saltatory conduction should occur. The cause is most likely a failure in the clustering of NrCAM (PNS), ankyrin-G, βIV spectrin and Na_v channels at the nodes, and the lack of recruitment of contactin and Caspr to the paranodes. Transgenic expression of Nfasc155 in the myelinating glia of Nfasc-/- mutants rescues the paranodal phenotype, but the Na_v channels remain diffusely distributed along the axon (Sherman et al., 2005). Conversely, when Nfasc186 is expressed in the Nfasc-/- background the nodal complex is rescued, allowing the transgenic animals to survive longer (Zonta et al., 2008). These observations provide evidence that Nfasc186 pioneers the assembly of the nodal structures, whereas Nfasc155 directs the formation of the paranodal junctions. Although NrCAM is detected at the PNS nodes as early as Nfasc186 expression, NrCAM null mice are viable and display, apart from a slightly retarded Na_v channel clustering, no nodal phenotype (Custer et al., 2003). In conclusion, only Nfasc186, but not NrCAM is a key regulator of node formation in the PNS (reviewed by (Schafer and Rasband, 2006)).

The initial signal for the node formation in the PNS seems to originate from the Schwann cells. Likely mediator is gliomedin, a transmembrane protein, which is shed by proteolytic cleavage and bound to the surface of the Schwann cell in a heparan sulfate-dependent manner. After oligomerization, gliomedin

facilitates axonodal clustering of Nfasc186 and NrCAM (Eshed et al., 2005; Eshed et al., 2007), which apparently induce the docking of ankyrin-G, the subsequent accumulation of Na_v and K_v channels and the retention of βIV spectrin (fig. 23) (reviewed by (Schafer and Rasband, 2006). While cell-cell contact seems to be needed for node induction in the PNS it has been suggested that a diffusible, but not yet closely characterized factor produced by oligodendrocytes is sufficient to cause clustering of Na_v channels in culture of retinal ganglion cells (Kaplan et al., 1997).

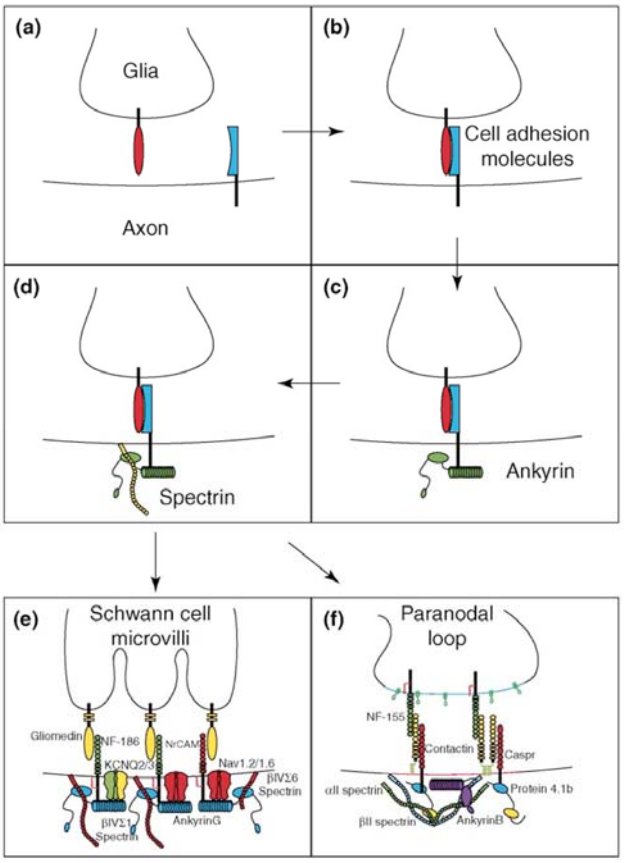

Figure 23: Formation of axoglial junctions. a) to c) display sequence of the initial steps of the assembly, which finally lead to the supramolecular complexes in PNS nodes (e) and paranodes (f) (from (Schafer and Rasband, 2006)).

The initial steps of node formation are followed by structural stabilization. Microvillar processes of Schwann cells extending into the nodel gap in the PNS express the cytoskeleton linkers, ezrin, radixin and moesin, the ezrin binding protein EBP50 and the Rho-A GTPase (reviewed by (Poliak and Peles, 2003). Also the heparan sulfate proteoglycan syndecan-3 is highly enriched at the PNS nodes of Ranvier (Melendez-Vasquez et al., 2005). Tenascin-C, versican V1 and the NG2 proteoglycan accumulate between the axon and the basal lamina, and last but not least, dystroglycan abundantly expressed on the abaxonal surface of Schwann cells is also present at the nodal gap. In contrast, the nodes of the CNS, which lack the microvillar component, show major deposits of the ECM proteins tenascin-R, phosphacan, versican V2 and the neuronal link protein Bral1 instead. Perinodal astrocytes synthesize NG2, but not common astrocytic markers like glial fibrillary acidic protein (GFAP) and vimentin.

Several of the molecules of the nodal zone are also associated with another myelin-free portion of the axon, which emerges from the soma. This area, called the axon initial segment (AIS), generates the action potentials. Sodium channel $Na_v1.2$ subunits and Nfasc186 are clustered here by the action of ankyrin-G, which also connects to βIV spectrin. Suppression of ankyrin-G prevents the recruitment of all the other proteins to the AIS suggesting an inside out sequence of the protein complex assembly. This mechanism contrasts the formation of the nodal structure, where the initial signal seems to emanate from outside and Nfasc186 precedes the ankyrin-G accumulation (Dzhashiashvili et al., 2007). Moreover, ion channel clustering at the AIS does not require Nfasc186 and NrCAM, but Nfasc186 is needed for the incorporation of brevican into the ECM that surrounds the AIS (Hedstrom et al., 2007).

2.2.1.2.2. Paranodes

Highly concerted axo-glial interactions form the basis for the assembly of the paranodes (fig. 24). It initiates with the binding of the glial isoform of neurofascin (Nfasc 155) to the axonal GPI-linked CAM contactin, which in turn associates in *cis* with the transmembrane protein Caspr (contactin associated protein or paranodin). Caspr subsequently anchors the complex to the cytoskeleton through the 4.1B protein (Rios et al., 2000; Charles et al., 2002; Gollan et al., 2002; Gollan et al., 2003) (reviewed by (Simons and Trajkovic, 2006)).

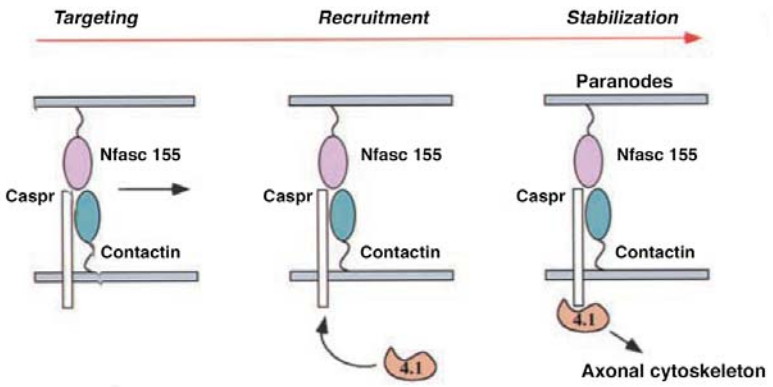

Figure 24: Molecular assembly of the paranode (modified from (Gollan et al., 2002)).

Gene inactivation experiments in mice confirm the key role of Nfasc 155 in the building of the paranodes (Sherman et al., 2005) and the reciprocal requirement of contactin and Caspr, as the lack of one causes the loss of the other in these structures (Bhat et al., 2001; Boyle et al., 2001). In all three mutants the transverse bands that connect the paranodal loops with the axolemma are missing and anomalous displacements of K_v channels and Caspr-2 from juxtaparanodes into the paranodal region is observed (Bhat et al., 2001; Boyle et al., 2001; Zonta et al., 2008).

The paranodes are not only disrupted in mice devoid of Nfasc 155, contactin or Caspr. An unexpected high number of gene knockouts targeting myelin components lead to paranodal aberrations. This includes animals deficient in the synthesis of myelin glycolipids (galactosylceramide and/or

sulfatide) or lacking the expression of myelin and lymphocyte protein (MAL) and the 2',3'-cyclic nucleotide 3'-phosphodiesterase (CNP) (reviewed by (Poliak and Peles, 2003; Salzer, 2003; Simons and Trajkovic, 2006)). These molecules are all involved in membrane sorting or cytoskeletal connection (table 1).

2.2.1.2.3. Juxtaparanodes

The formation of the juxtaparanodal region starts with the homophilic interaction between axonal and glial TAG-1 molecules in *trans*, followed by their association with the axonal Caspr-2 (fig. 25). TAG-1 (called axonin-1 in chick) is a GPI-linked CAM belonging to the Ig-superfamily. It is structurally closely related to contactin. Conversely, Caspr-2, the transmembrane binding-partner of TAG-1, displays sequence similarities with the paranodal Caspr. In mice lacking TAG-1 or Caspr-2 the clustering of $K_v1.1$ and $K_v1.2$ is impaired, strongly indicating that these molecules are needed to maintain the delayed rectifier potassium channels in the juxtaparanodal region (Poliak et al., 2003; Traka et al., 2003). Since both, Caspr-2 and K_v1 channels include at their C-terminus a PDZ-binding motif, they may be linked by a currently unidentified PDZ-domain scaffolding protein. Moreover, the anchoring of the complex to the cytoskeleton seems also to be mediated by the cytoplasmic domain of Caspr-2, which binds to the intacellular protein 4.1B.

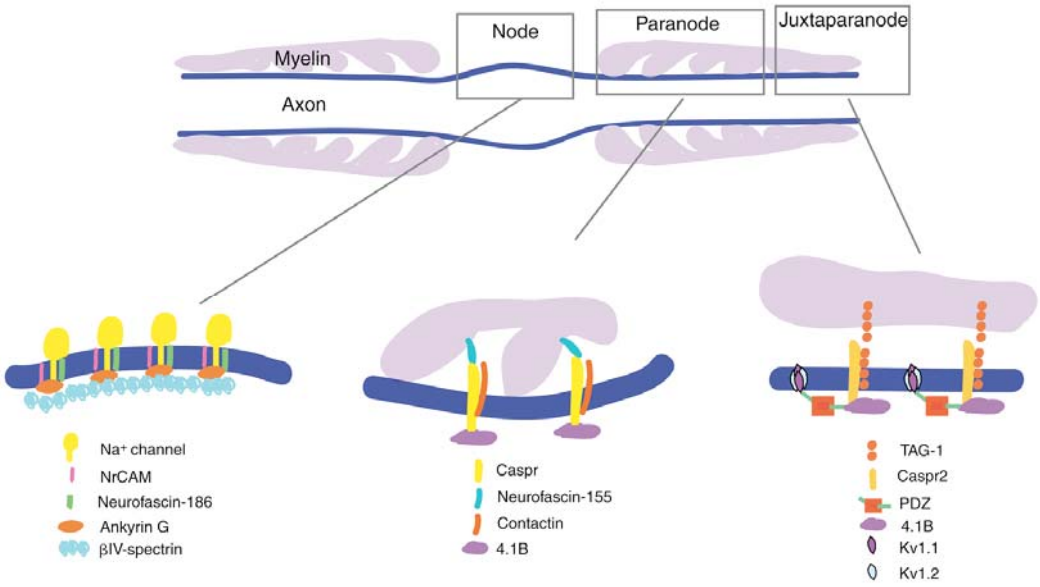

Figure 25: Molecular composition of different substructures of the nodal region (from (Simons and Trajkovic, 2006)).

2.2.1.2.4. Internodes

The molecules participating in axo-glial interactions in the internodes are currently little known. L1 and MAG (myelin associated glycoprotein), two internodal Ig-CAMs initially thought to be essential for myelination, turned out to be functionally redundant in single knockout mouse models. Other candidates for interactions are nectin-like proteins (Nectl). They have recently been identified in a screen for surface molecules expressed at the onset of myelination. Nectl proteins are also transmembrane Ig-CAMs with

a short cytoplasmic tail, through which they bind protein 4.1B. They are differentially expressed by neurons and glia and can interact homophilically as well as heterophilically. Necl-1 and Necl-2 are present on axons along the internode, while Necl-4 (also known as SynCAM4) is localized on the surface of myelinating Schwann cells. The Necl-1 and the Necl-4 are both early detected at axoglial contact sites (Maurel et al., 2007; Spiegel et al., 2007) and are known to interact with each other.

2.2.2. Myelin components

In relation to most biological membranes, myelin contains a significantly higher proportion of lipids (70-85% of its dry weight) in comparison to proteins (15-30%). This applies for both CNS and PNS myelin. There are no lipids exclusively associated with the myelin, but the most typical components are galactocerebroside (GalC) and its sulfated form, sulfatide. Other lipids present are cholesterol, lecithin, sphingomyelin and gangliosides (Siegel et al., 1999).

To study the functions of GalC and sulfatides, the genes coding for the enzymes that catalyze the last steps of their biosynthesis have been targeted. By ablating UDP-galactose ceramide galactosyltransferase (CGT) in mice, the synthesis of both, GalC and sulfatide has been completely disrupted. Yet, structurally closely related glucocerebroside-surrogates replace at least in part these major lipids. As a result, the mutants are still able to form myelin. The nerve sheaths are, however, thinner and more fragile. Consequently, the insulation capacity is greatly reduced leading to severe tremor and early death of the mutants. Ceramide sulfotransferase (CST)-knockout mice, lacking only sulfatide, show a milder phenotype, but their myelinated fiber tracts similarly degenerate with age. In conclusion, these knockout experiments indicate that GalC is essential for proper myelin formation, while sulfatides are required for its maintenance (Bosio et al., 1996; Coetzee et al., 1996; Honke et al., 2002; Marcus et al., 2006) (table 1).

Some proteins are constituents of both CNS and PNS myelin, but their proportion varies. For example, the Myelin Basic Protein (MBP) accounts for up to 30% of the whole protein in the CNS, whereas it reaches only levels of 5-18% in the PNS. Several isoforms of MBP with molecular masses between 14 and 21 kDa arise from alternative splicing. By being localized on the cytoplasmic side of the myelin membranes, where myelin compaction takes place, MBP influences the apposition of the myelin layers.

Another well-studied component of both, CNS and PNS myelin, is MAG (Myelin Associated Glycoprotein), a relatively large (100 kDa), but not very abundant glycoprotein. MAG is composed of five extracellular Ig-like domains, a transmembrane region and cytoplasmic portion, which changes in the course of development (from L-MAG to S-MAG). MAG interacts with the axonal surface and is not present in compact myelin, but enriched at the inner glial membrane. The fact that it belongs to the Ig-CAM family suggests that it participates in adhesion and signaling between the glia and the axolemma and is involved in myelin formation and stabilization.

The most prominent protein in compact myelin of the CNS is the Proteolipid Protein (PLP) with an isoform lacking 35 amino acids called DM-20. PLP and MBP represent together up to 80% of the total protein in CNS myelin preparations. PLP has several membrane-spanning domains reaching a

molecular weight of approximately 30 kDa. PLP plays a structural role in myelin and is needed for oligodendrocyte differentiation.

The Myelin Oligodendrocyte Glycoprotein (MOG) is an additional myelin component that is exclusively expressed in the CNS myelin. MOG, a transmembrane protein with one Ig-like domain, is like MAG absent from the compact laminas and consequently represents a rather minor myelin constituent. Of note, MOG is concentrated in the abaxonal membrane of the myelin sheath. Finally, Oligodendrocyte Myelin Glycoprotein (OMgp), a GPI-linked membrane protein, has been localized to the glial-axonal interface. In contrast to the other myelin components in the CNS, it is not solely expressed by oligodendrocytes, but also by diverse groups of neurons.

PNS myelin differs from CNS myelin by the presence of P_0, a 30 kDa transmembrane protein with one Ig-like domain. P_0 accounts for more than half of the total protein of the nerve sheath and is involved in cell-cell interactions. It is able to form tetramers through homophilic binding of its extracellular domain. P_0 plays a significant structural role. Also PMP-22, a 22 kDa protein with four transmembrane domains is exclusively present in PNS myelin.

Similarly to the CNS, some proteins, like ECM receptors, are only present in the outer lamina (abaxonal membrane) of PNS myelin, while adhesion molecules, such as MAG, are enriched in the adaxonal membrane and interact with the axon.

Several spontaneous mutations in mice have been helpful to study the functions of the numerous myelin components (reviewed in (Nave, 1994)). For example, *jimpy* mice suffering from severe hypomyelination in the CNS carry a frame-shifting deletion in the PLP gene. A milder form of this phenotype has also been observed in the *rumpshaker* strain, which contain a missense mutation that affects only PLP, but not its alternative splice variant DM-20. A natural knockout of the MBP gene, which leads to an almost total lack of CNS myelin, gives rise to the *shiverer* strain and a point mutation in the the first transmembrane domain of PMP-22 is responsible for the severe PNS hypomyelination phenotype in the *trembler* mouse.

Although essential for the structural formation of myelination *per se*, some myelin components may also be responsible for the regeneration-suppressing properties of CNS white matter that inhibits re-growth of axons after lesion.

Table 1: Mouse mutants affecting nodal structures

Mutant / Gene	Node	Paranodes	Juxtaparanodes	References
***Cgt* null (paranodal)**	CNS: elongated nodes, abnormal shape; heminodes; some clusters do not surround the full circumference. PNS: minor expansion of Na^+ channel clusters and ankyrin-G. Age-dependent decrease in number and intensity of $Na_v1.6$ clusters; increased nodal length.	Absence of transverse bands. Caspr and contactin almost completely absent from paranodes; diffuse staining of Caspr adjacent to narrow labeling of paranodal K^+ channels; reduced paranodal labeling of Nfasc155. Reduced accumulation of paranodal 4.1B.	K^+ channels, Caspr2 and TAG-1 are mislocated to paranodes in PNS and are diffused along the internode in CNS; some paranodal concentration of K^+ channels is observed in spinal cord.	(Dupree et al., 1999), (Poliak et al., 2001), (Dupree et al., 1998), (Rosenbluth et al., 2003), (Rasband et al., 2003)
***Contactin* null (paranodal)**	PNS: normal appearance of Na^+ channels. CNS: fewer and elongated Na^+ channel-labeled nodes.	Absence of transverse bands. Absence of Caspr from paranodes (found in soma); reduced paranodal Nfasc155. Protein 4.1B is diffusely distributed along the axon.	PNS: K^+ channels and Caspr2 are found in paranodes.	(Kazarinova-Noyes and Shrager, 2002), (Boyle et al., 2001), (Gollan et al., 2002), (Poliak et al., 2001)
***Caspr* null (paranodal)**	Elongated nodes (labeled with Na^+ channels, NrCAM and spectrin βIV); CNS nodes progressively disperse; normal ERM positive microvilli. Aberrant Na^+ channel isoform-switch in CNS; switch is delayed in PNS. Increased contactin in CNS nodes.	Absence of transverse bands. Absence of contactin and Nfasc155 from paranodes. Progressive detachment of paranodal loops in CNS.	K^+ channels and Caspr2 are found in paranodes; more diffuse in CNS than in PNS. $K_v1.1$ clusters are lost over time in CNS. Increased juxta-incisural lines along internodes.	(Gollan et al., 2003), (Bhat et al., 2001), (Rios et al., 2003)
***Cst* null (paranodal)**	CNS: elongated nodes, abnormal shape and intensity; binary clusters. Decreased clustering with age (12% at 22 weeks).	Disrupted axoglial junction. Caspr diffusely distributed along the axon.	CNS and PNS: diffuse K^+ channels with some concentration at paranodes. Decreased clustering with age (8% at 22 weeks).	(Honke et al., 2002), (Ishibashi et al., 2002)
***Caspr2* null (juxtaparanodal)**	Normal appearance.	Normal appearance.	Reduced K^+ channels clustering. Absence of TAG-1. Intense juxtamesaxonal labeling of K^+ channels.	(Poliak et al., 2003)
***TAG-1* null (juxtaparanodal)**	Normal appearance.	Normal appearance.	Reduced K^+ channels clustering. Absence of Caspr2. Small decrease in juxtaparanodal labeling of 4.1B.	(Traka et al., 2003), (Poliak et al., 2003)
Dystroglycan (nodal)	Reduced Na^+ channels clustering (90%); channels dispersed along a broader region (7%): Normal distribution of ankyrin-G, moesin and Nfasc186. Abnormal microvilli morphology.	Normal localization of Nfasc155	Normal localization of K^+ channels and Caspr2.	(Saito et al., 2003)

Mutant / Gene	Node	Paranodes	Juxtaparanodes	References
***quivering* Spectrin βIV (nodal)**	ND	ND	K_v1.1 is upregulated and redistributed along the length of the axon.	(Parkinson et al., 2001)
Spectrin βIV-genetrap (nodal)	55% reduction in number of nodes as measured by Na_v1.6 immuno-reactivity. Reduced intensity of Na^+ channels compared with WT.	ND	ND	(Komada and Soriano, 2002)
***NrCAM* null (nodal)**	Delayed Na^+ channel and ankyrin-G clustering in PNS.	Normal Caspr localization.	ND	(Custer et al., 2003)
***Na^+ channel β2* null (nodal)**	Normal appearance; Na_v1.6 appears within a normal time course. Reduced Na^+ current in optic nerve; CAP data consistent with loss of nodal Na^+ channels.	Normal Caspr localization.	ND	(Chen et al., 2002)
***Na^+ channel β1* null (nodal)**	PNS: normal axonal conduction. CNS: altered CAP in optic nerve, deficit in rapidly conducting fibers. Number of nodes reduced in optic nerve. Na_v1.6 normally localized.	In ~20-30% of axons: absence of transverse bands adjacent to nodal gaps. Normal contactin and Caspr localization.	Normal localization of K^+ channels and Caspr2.	(Chen et al., 2004)
Neurofascins (nodal and paranodal)	Absence of Nfasc186: Na^+ channels, NrCAM, ankyrin-G and βIVSpectrin are not concentrated at the nodes.	Absence of Nfasc155: no contactin or Caspr in paranodes. Loss of septate junctions and wider junctional gap.	ND	(Sherman et al., 2005)
MAL	Normal number and clustering of Na^+ channels.	CNS: reduced Caspr and Nfasc155 expression (~70-90%). Normal formation but impaired maintenance of paranodes (everted paranodal loops and irregular transverse bands).	CNS: reduced K_v1.2 expression (~70%) but no translocation to the paranodes.	(Schaeren-Wiemers et al., 2004)
CNP	Initial normal clustering of Na^+ channels, become progressively disorganized and decrease with age.	Progressively aberrant localization of Caspr with age. Number of Caspr positive paranodes gets reduced.	ND	(Lappe-Siefke et al., 2003), (Rasband et al., 2005)

ND: not described, CAP: compound action potential, MAL: myelin and lymphocyte protein, CNP: cyclic nucleotide phosphodiesterase (modified from Poliak and Peles, 2003).

2.2.3. Inhibitors of axonal regeneration

In the CNS, the ability of late embryonic and early postnatal axons to regenerate is virtually lost in the course of glial cell maturation and the onset of myelination. This change also coincides with a decrease in expression of growth-associated proteins. Although a limited intrinsic growth capability is upheld in adult CNS neurons, enabling them to extend short sprouts after a lesion, the full program required for robust axon elongation cannot be activated and/or maintained anymore.

In addition, the CNS environment has a significant inhibitory effect on axonal regeneration, as underscored by two fundamental observations: 1) peripheral neurons, which extend their axons well in their own milieu, show limited growth, when transplanted into adult brain or spinal cord; and 2) adult CNS axons are able to cross after a lesion over bridges of peripheral nerve grafts, but fail to continue their advance as soon as they encounter central nervous tissue (Richardson et al., 1980; David and Aguayo, 1981).

The main inhibitory activity is associated with the CNS myelin itself (Caroni and Schwab, 1988b; Bandtlow et al., 1990) being inherent to its proteins and not to its lipids. Several myelin components act as potent inhibitors of axonal growth (fig. 26). This includes the afore-mentioned MAG and OMgp as well as Nogo-A, ephrin-B3 and semaphorin 4D (for recent reviews, see (Schweigreiter et al., 2006; Viapiano and Matthews, 2006; Yiu and He, 2006; Zheng et al., 2006; Zurn and Bandtlow, 2006; Gonzenbach and Schwab, 2008; Xie and Zheng, 2008).

During earlier developmental stages, MAG may also exert some growth-promoting property, as demonstrated in neurite outgrowth experiments with embryonic neurons in vitro. MAG becomes however, a non-permissive substrate, when older neurons are tested in these assays. Also the GPI-anchored OMgp exerts an inhibitory activity in vitro. In vivo it has been localized to the nodal area, where it is believed to prevent collateral sprouting (Huang et al., 2005).

The most extensively studied inhibitor of axonal growth is Nogo (fig. 26). Nogo has been identified as the antigen of the monoclonal antibody IN-1, which exhibits neutralizing activity towards myelin-derived inhibition (Caroni and Schwab, 1988a; Chen et al., 2000; GrandPre et al., 2000). Three isoforms of Nogo arise from alternative splicing (A and B) or alternative promoter usage (C). Nogo is a member of the reticulon (RTN) family of proteins, which carry an ER-retention motif. In consequence, it is at least partly associated with the ER and possibly involved in membrane trafficking and/or sorting. The C-terminal domain of 188 amino acids length (the reticulon-homology domain) holds two long hydrophobic regions and is shared by all Nogo isoforms. Between these transmembrane domains, a stretch of 66 amino acids (aa) forms a loop called Nogo-66. It inhibits neurite outgrowth and provokes growth cone collapse *in vitro*. Also an 800 aa long portion, termed NiG or central inhibitory domain, interferes with axonal growth and cell spreading. This domain is unique to Nogo-A. Since there is evidence that cell surface Nogo-A can adopt two different topologies, NiG may either face the extracellular space or the cytoplasma. Finally the N-terminal region shared by Nogo-A and -B constitutes an additional active site impeding fibroblast spreading and stimulating endothelial cell migration.

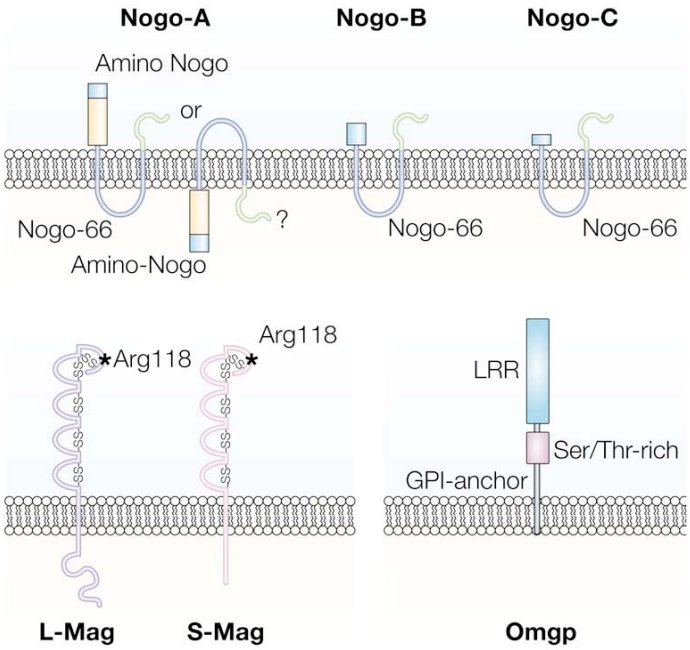

Figure 26: Structure and membrane topology of myelin-derived axonal growth inhibitors (from (Filbin, 2003)).

Apart from these cell surface associated components, the CSPGs brevican and versican V2, localized in between the myelin sheaths, strongly impede axonal growth in vitro (Yamada et al., 1997; Schmalfeldt et al., 2000). Both proteoglycans are co-purified from myelin preparations revealing an inhibitory activity comparable to the Nogo-A containing fraction (Niederöst et al., 1999).

The inhibitors so far described are normal constituents of mature myelin and its surrounding extracellular matrix. They are up-regulated late in development reaching constant levels only at time points when fully myelinated fiber tracts have been established and axonal growth is mostly terminated. Their properties contribute to the limitation of structural plasticity and the consequent stabilization of the CNS network. Apart from this, they are also responsible for the lack of regeneration in the CNS. After a lesion, they are released into the environment as myelin debris, being the first inhibitory molecules encountered by the damaged axons. Since most CNS injuries disrupt the blood brain barrier, a strong inflammatory response with migration of neutrophils, macrophages and meningeal cells usually follows. Moreover, reactive microglia and astrocytes are recruited to the site. They form within a few days an astroglial scar tissue that contains additional inhibitors of nerve elongation including the CSPGs NG2, versican V1, neurocan and phosphacan. Hence, lesioned axons are after injury confronted with the resident myelin inhibitors and the impenetrable barriers that the scar tissues impose. It is therefore not surprising that the initial axon sprouting is in the CNS fast aborted.

In order to exert their function, most inhibitory proteins depend on neuronal receptors (fig. 27). The first receptor described is NgR (now NgR1). It binds with very high affinity to the Nogo-66 domain of Nogo. As NgR1 is a GPI-linked molecule, it needs a transmembrane co-receptor for

signaling. The co-receptors so far identified are the neurotrophin receptor $p75^{NTR}$ and LINGO-1, a CNS specific protein with a short cytoplasmic domain. A $p75^{NTR}$ homologue called TROY can replace the neurotrophin receptor in the complex with NgR/LINGO-1. Unlike $p75^{NTR}$, TROY is widely expressed in the adult CNS. Surprisingly, MAG and OMgp, two structurally completely unrelated molecules, interact also strongly with NgR. In contrast, the neuronal receptors for NiG (amino-Nogo) and for the various CSPGs have not been identified yet. Other axonal receptors that are likely to mediate the inhibitory signal emanating from the injury site are EphA4, a receptor tyrosine kinase that binds B-class ephrins and thus ephrin-B3, and Plexin-B1 that induces growth cone collapse when associated to its ligand Sema4D.

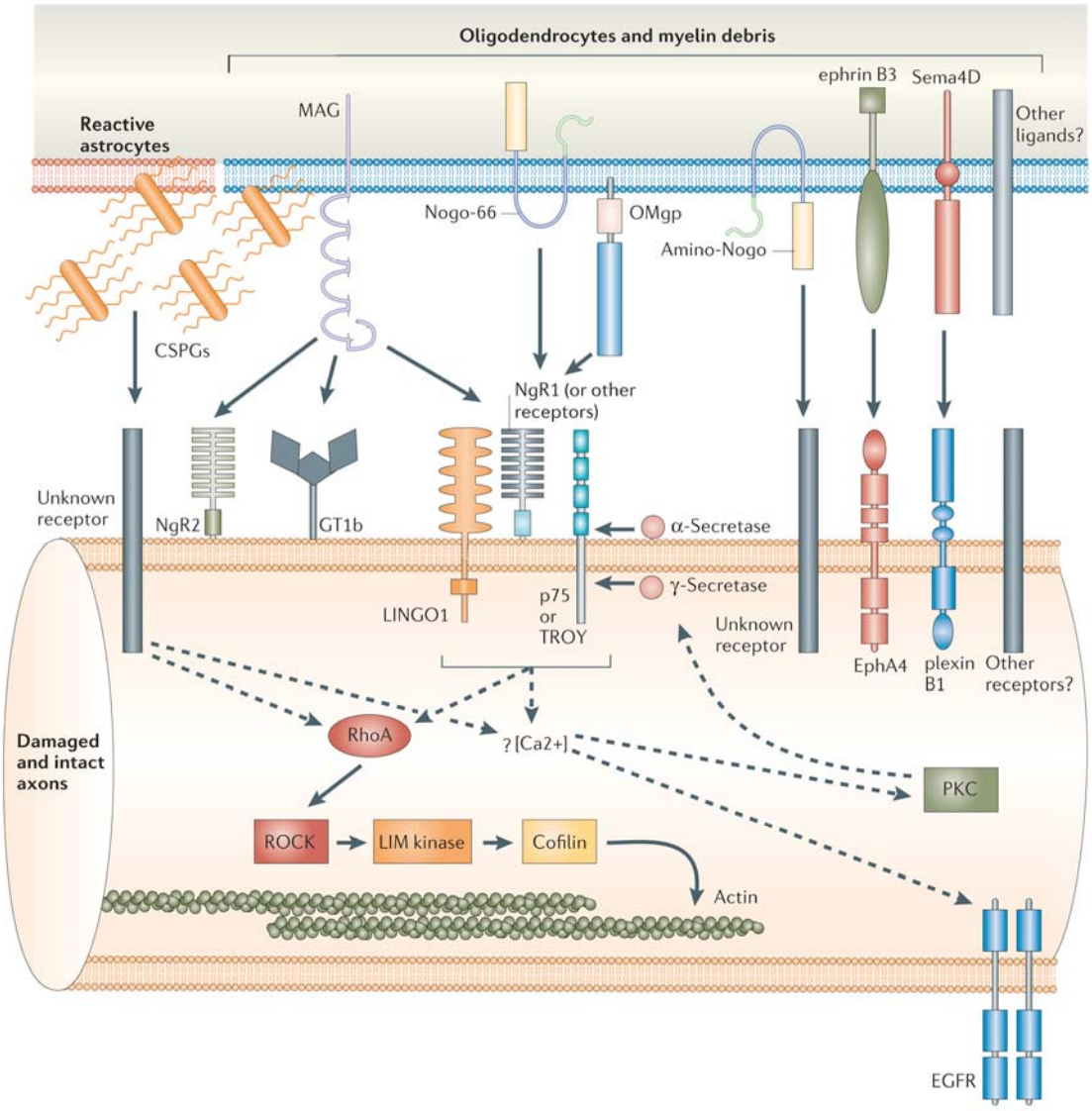

Figure 27: Glial inhibitors and their signaling mechanisms (modified from (Yiu and He, 2006)).

For most of these receptors, intracellular signaling appears to converge in RhoA. RhoA belongs to the Rho family of small GTPases that comprises Rho, Rac and Cdc42. These GTPases regulate cytoskeletal rearrangements by cycling between an inactive GDP-bound form

and an active GTP-bound state. Rho-activation induces growth cone collapse. Rho mediates this way repulsive signals from guidance cues that direct axonal growth during development. Amino-Nogo-A, Nogo-66, MAG and versican V2 activate RhoA, which in turn activates ROCK (Rho associated kinase). This results in the phosphorylation of several other effectors that control actin polymerization (fig. 27). Additional intracellular signal mediators for CSPGs and myelin inhibitors are protein kinase-C (PKC) as well as regulators of neuronal Ca^{2+} and cAMP levels.

2.2.3.1. Models to study nerve injuries in the CNS and at the PNS/CNS interface

Common traumas to the CNS range from minor contusions to open injuries of diverse severity. Different types of lesions deploy distinctive cellular and molecular reactions and consequently vary in their perspectives for a partial recovery. Numerous paradigms have been applied to study the CNS responses to injury. These include simple nerve crush, transection and contusion lesions, stab injuries or stroke-simulations to optic nerve, spinal cord, dorsal roots and brain tissues, respectively (recent reviews: (Silver and Miller, 2004; Maier and Schwab, 2006; Scott et al., 2006; Yiu and He, 2006; Zurn and Bandtlow, 2006). Analogous to the clinical situation, these lesion models differ from each other in the extent that they affect nervous tissue structures. If the blood-brain barrier (BBB) and/or the meninges are disrupted, for instance, the damage caused reaches generally a much higher dimension (fig. 28).

Some cellular processes, like reactive gliosis, astrocyte-hypertrophy and Wallerian degeneration are common to most lesions. Gliosis implies proliferation of astrocytes, oligodendrocyte precursor cells (OPC) and microglia (or macrophages). Astrocytes become hypertrophic by enhancing their production of intermediate filaments with high levels of GFAP and vimentin (Silver and Miller, 2004). Wallerian degeneration denotes the deterioration of the axon segment and nerve terminals distal to the lesion; the proximal part of the axon and the neuron itself may survive, if the insult occurs far from the cell body. Wallerian degeneration is induced immediately after injury by the release of activated proteases that initiate the degradation of myelin sheaths and the axonal cytoskeleton. This in turn leads to activation of microglia and cytokine secretion that attract and engage other cells in the process.

2.2.3.1.1. Spinal cord lesions

Spinal cord injuries cause frequently a disruption of the BBB, ischemia and edema. They result in significant neuronal cell death, degeneration of axons, astrocyte proliferation, and infiltration of immune cells and/or fibroblasts in their acute phase. The primary lesion is over time magnified by a secondary damage caused by reactive gliosis, inflammation and the development of cystic cavities and glial scars (fig. 28).

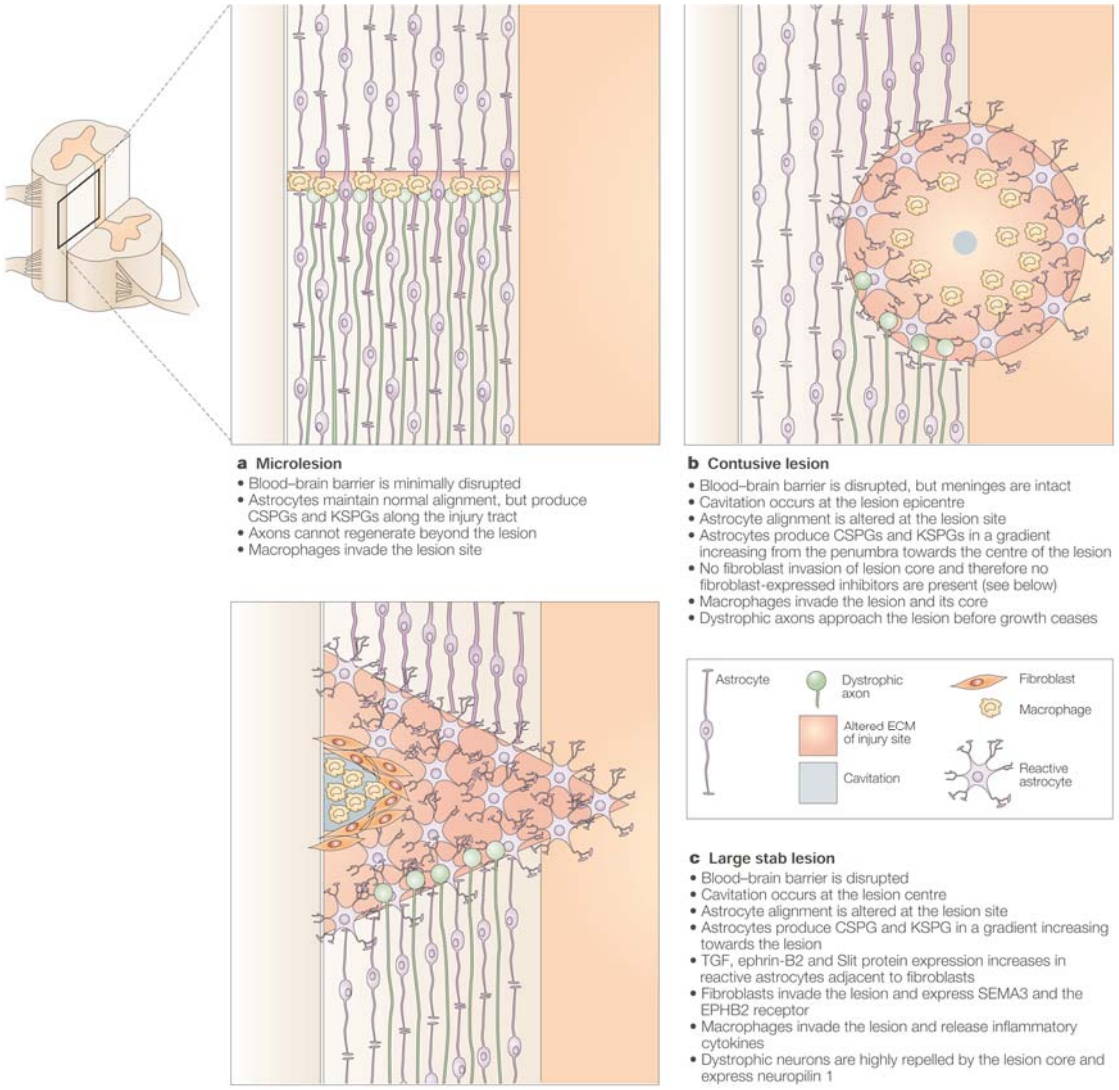

Figure 28: Three stereotypical spinal cord lesions and sequence of the damage processes (from (Silver and Miller, 2004)).

The glial scars are formed mostly by reactive astrocytes that up-regulate their production of cell surface and ECM molecules, in particular CSPGs and tenascin-C. The role of the glial scar is not completely clarified yet. On one hand, the astrocytic reaction may partly protect neuronal function (Faulkner et al., 2004) and contribute to repair the BBB (Bush et al., 1999), as long as the meninges are not contacted by the wound. On the other hand, a large infiltration of fibroblasts might take place in more severe cases, augmenting the secretion of ECM molecules and transforming the scar into a sturdy physical barrier. Activated microglia and invading macrophages (after BBB breakdown) releasing cytokines finally trigger the recruitment of OPC to the lesion site and consequently further promote the CSPG deposition.

2.2.3.1.2. Dorsal root lesions

Another model of CNS lesion targets the sensory neurons of the dorsal root ganglia (fig. 29). These neural crest cell-derived neurons extend a single axon that bifurcates into a peripheral and a CNS projecting branch. The sensory afferents enter during development the spinal cord at the

DREZ (Dorsal Root Entry Zone, also called transitional zone), which constitutes an interface between CNS and PNS. If the sensory nerve of an adult animal is transected at the dorsal root the cut fibers start to sprout, but are blocked from crossing into the DREZ. Thus, the sensory axons fail to restore the connections with the dorsal horn of the spinal cord (reviewed by (Ramer et al., 2001; Scott et al., 2006)).

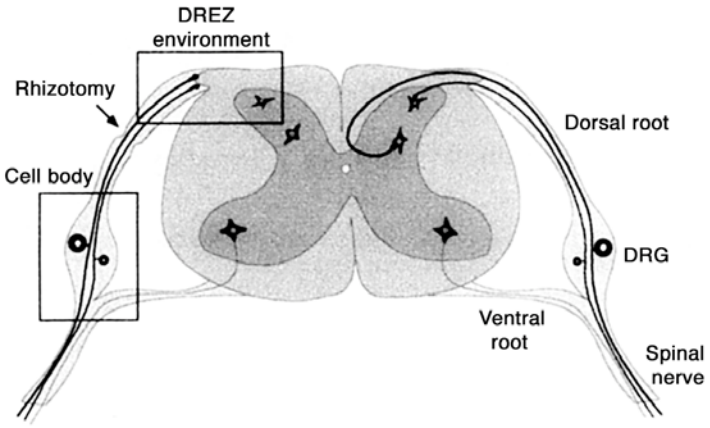

Figure 29: Model of DREZ lesion (modified from (Ramer et al., 2001)).

This type of lesion is in the context of e.g. motorcycle accident or complications during child's birth of clinical relevance and is in the experimental setting emulated by the dorsal rhizotomy model. In this paradigm, the centrally projecting branches are carefully cut between the cell bodies and the DREZ without affecting the meninges. Rhizotomy induces gliosis and Wallerian degeneration, but avoids the scar formation in the CNS. Consequently, studies of the axonal growth inhibition are in this model focused onto the CNS-resident factors and exclude the molecular impediments associated with the secondary scar tissue. Furthermore, the contra-lateral dorsal root area provides a convenient control for experimental attempts to neutralize the growth inhibition potentially allowing axonal regeneration in the central nervous system.

2.3. References

Alberts B, Johnson A, Lewis J, Raff M, Roberts K, Walter P (2002) Molecular Biology of the Cell, 4th Edition. New York: Garland Science.

Antonsson P, Heinegard D, Oldberg A (1989) The keratan sulfate-enriched region of bovine cartilage proteoglycan consists of a consecutively repeated hexapeptide motif. J Biol Chem 264:16170-16173.

Apte SS (2004) A disintegrin-like and metalloprotease (reprolysin type) with thrombospondin type 1 motifs: the ADAMTS family. Int J Biochem Cell Biol 36:981-985.

Aspberg A, Binkert C, Ruoslahti E (1995) The versican C-type lectin domain recognizes the adhesion protein tenascin-R. Proc Natl Acad Sci USA 92:10590-10594.

Aspberg A, Adam S, Kostka G, Timpl R, Heinegard D (1999) Fibulin-1 is a ligand for the C-type lectin domains of aggrecan and versican. J Biol Chem 274:20444-20449.

Aspberg A, Miura R, Bourdoulous S, Shimonaka M, Heinegård D, Schachner M, Ruoslahti E, Yamaguchi Y (1997) The C-type lectin domains of lecticans, a family of aggregating chondroitin sulfate proteoglycans, bind tenascin-R by protein-protein interactions independent of carbohydrate moiety. Proc Natl Acad Sci USA 94:10116-10121.

Back SA, Tuohy TM, Chen H, Wallingford N, Craig A, Struve J, Luo NL, Banine F, Liu Y, Chang A, Trapp BD, Bebo BF, Jr., Rao MS, Sherman LS (2005) Hyaluronan accumulates in demyelinated lesions and inhibits oligodendrocyte progenitor maturation. Nat Med 11:966-972.

Baier C, Baader SL, Jankowski J, Gieselmann V, Schilling K, Rauch U, Kappler J (2007) Hyaluronan is organized into fiber-like structures along migratory pathways in the developing mouse cerebellum. Matrix Biol 26:348-358.

Baldwin CT, Reginato AM, Prockop DJ (1989) A new epidermal growth factor-like domain in the human core protein for the large cartilage-specific proteoglycan. J Biol Chem 264:15747-15750.

Bandtlow C, Zachleder T, Schwab ME (1990) Oligodendrocytes arrest neurite growth by contact inhibition. J Neurosci 10:3837-3848.

Bandtlow CE, Zimmermann DR (2000) Proteoglycans in the developing brain - new conceptual insights for old proteins. Physiol Rev 80:1267-1290.

Barnea G, Grumet M, Milev P, Silvennoinen O, Levy JB, Sap J, Schlessinger J (1994) Receptor tyrosine phosphatase beta is expressed in the form of proteoglycan and binds to the extracellular matrix protein tenascin. J Biol Chem 269:14349-14352.

Bekku Y, Su WD, Hirakawa S, Fassler R, Ohtsuka A, Kang JS, Sanders J, Murakami T, Ninomiya Y, Oohashi T (2003) Molecular cloning of Bral2, a novel brain-specific link protein, and immunohistochemical colocalization with brevican in perineuronal nets. Mol Cell Neurosci 24:148-159.

Bhat MA, Rios JC, Lu Y, Garcia-Fresco GP, Ching W, St Martin M, Li J, Einheber S, Chesler M, Rosenbluth J, Salzer JL, Bellen HJ (2001) Axon-glia interactions and the domain organization of myelinated axons requires neurexin IV/Caspr/Paranodin. Neuron 30:369-383.

Bignami A, Asher R (1992) Some observations on the localization of hyaluronic acid in adult, newborn and embryonal rat brain. Int J Dev Neurosci 10:45-57.

Black JA, Waxman SG (1988) The perinodal astrocyte. Glia 1:169-183.

Bode-Lesniewska B, Dours-Zimmermann MT, Odermatt BF, Briner J, Heitz PU, Zimmermann DR (1996) Distribution of the large aggregating proteoglycan versican in adult human tissues. J Histochem Cytochem 44:303-312.

Boiko T, Rasband MN, Levinson SR, Caldwell JH, Mandel G, Trimmer JS, Matthews G (2001) Compact myelin dictates the differential targeting of two sodium channel isoforms in the same axon. Neuron 30:91-104.

Bosio A, Binczek E, Stoffel W (1996) Functional breakdown of the lipid bilayer of the myelin membrane in central and peripheral nervous system by disrupted galactocerebroside synthesis. Proc Natl Acad Sci U S A 93:13280-13285.

Bourdon MA, Krusius T, Campbell S, Schwartz NB, Ruoslahti E (1987) Identification and synthesis of a recognition signal for the attachment of glycosaminoglycans to proteins. Proc Natl Acad Sci U S A 84:3194-3198.

Boyle ME, Berglund EO, Murai KK, Weber L, Peles E, Ranscht B (2001) Contactin orchestrates assembly of the septate-like junctions at the paranode in myelinated peripheral nerve. Neuron 30:385-397.

Brakebusch C, Seidenbecher CI, Asztely F, Rauch U, Matthies H, Meyer H, Krug M, Bockers TM, Zhou X, Kreutz MR, Montag D, Gundelfinger ED, Fassler R (2002) Brevican-deficient mice display impaired hippocampal CA1 long-term potentiation but show no obvious deficits in learning and memory. Mol Cell Biol 22:7417-7427.

Bruckner G, Grosche J, Schmidt S, Hartig W, Margolis RU, Delpech B, Seidenbecher CI, Czaniera R, Schachner M (2000) Postnatal development of perineuronal nets in wild-type mice and in a mutant deficient in tenascin-R. J Comp Neurol 428:616-629.

Brummendorf T, Hubert M, Treubert U, Leuschner R, Tarnok A, Rathjen FG (1993) The axonal recognition molecule F11 is a multifunctional protein: specific domains mediate interactions with Ng-CAM and restrictin. Neuron 10:711-727.

Bulow HE, Hobert O (2006) The molecular diversity of glycosaminoglycans shapes animal development. Annu Rev Cell Dev Biol 22:375-407.

Burch GH, Gong Y, Liu W, Dettman RW, Curry CJ, Smith L, Miller WL, Bristow J (1997) Tenascin-X deficiency is associated with Ehlers-Danlos syndrome. Nat Genet 17:104-108.

Bush TG, Puvanachandra N, Horner CH, Polito A, Ostenfeld T, Svendsen CN, Mucke L, Johnson MH, Sofroniew MV (1999) Leukocyte infiltration, neuronal degeneration, and neurite outgrowth after ablation of scar-forming, reactive astrocytes in adult transgenic mice. Neuron 23:297-308.

Butt AM, Kiff J, Hubbard P, Berry M (2002) Synantocytes: new functions for novel NG2 expressing glia. J Neurocytol 31:551-565.

Camenisch TD, Spicer AP, Brehm-Gibson T, Biesterfeldt J, Augustine ML, Calabro A, Jr., Kubalak S, Klewer SE, McDonald JA (2000) Disruption of hyaluronan synthase-2 abrogates normal cardiac morphogenesis and hyaluronan-mediated transformation of epithelium to mesenchyme. J Clin Invest 106:349-360.

Canoll PD, Petanceska S, Schlessinger J, Musacchio JM (1996) Three forms of RPTP-beta are differentially expressed during gliogenesis in the developing rat brain and during glial cell differentiation in culture. Journal of Neuroscience Research 44:199-215.

Canoll PD, Barnea G, Levy JB, Sap J, Ehrlich M, Silvennoinen O, Schlessinger J, Musacchio JM (1993) The expression of a novel receptor-type tyrosine phosphatase suggests a role in morphogenesis and plasticity of the nervous system. Brain Research Developmental Brain Research 75:293-298.

Carbonetto S (1984) The extracellular matrix of the nervous system. Trends in Neuroscience:382-387.

Caroni P, Schwab ME (1988a) Antibody against myelin-associated inhibitor of neurite growth neutralizes nonpermissive substrate properties of CNS white matter. Neuron 1:85-96.

Caroni P, Schwab ME (1988b) Two membrane protein fractions from rat central myelin with inhibitory properties for neurite growth and fibroblast spreading. J Cell Biol 106:1281-1288.

Catterall WA (2000) From ionic currents to molecular mechanisms: the structure and function of voltage-gated sodium channels. Neuron 26:13-25.

Celio MR, Blumcke I (1994) Perineuronal nets--a specialized form of extracellular matrix in the adult nervous system. Brain Res Brain Res Rev 19:128-145.

Celio MR, Spreafico R, De Biasi S, Vitellaro-Zuccarello L (1998) Perineuronal nets: past and present. Trends Neurosci 21:510-515.

Charles P, Tait S, Faivre-Sarrailh C, Barbin G, Gunn-Moore F, Denisenko-Nehrbass N, Guennoc AM, Girault JA, Brophy PJ, Lubetzki C (2002) Neurofascin is a glial receptor for the paranodin/Caspr-contactin axonal complex at the axoglial junction. Curr Biol 12:217-220.

Chen C, Bharucha V, Chen Y, Westenbroek RE, Brown A, Malhotra JD, Jones D, Avery C, Gillespie PJ, 3rd, Kazen-Gillespie KA, Kazarinova-Noyes K, Shrager P, Saunders TL, Macdonald RL, Ransom BR, Scheuer T, Catterall WA, Isom LL (2002) Reduced sodium channel density, altered voltage dependence of inactivation, and increased susceptibility to seizures in mice lacking sodium channel beta 2-subunits. Proc Natl Acad Sci U S A 99:17072-17077.

Chen C, Westenbroek RE, Xu X, Edwards CA, Sorenson DR, Chen Y, McEwen DP, O'Malley HA, Bharucha V, Meadows LS, Knudsen GA, Vilaythong A, Noebels JL, Saunders TL, Scheuer T, Shrager P, Catterall WA, Isom LL (2004) Mice lacking sodium channel beta1 subunits display defects in neuronal excitability, sodium channel expression, and nodal architecture. J Neurosci 24:4030-4042.

Chen MS, Huber AB, van der Haar ME, Frank M, Schnell L, Spillmann AA, Christ F, Schwab ME (2000) Nogo-A is a myelin-associated neurite outgrowth inhibitor and an antigen for monoclonal antibody IN-1. Nature 403:434-439.

Chiquet-Ehrismann R, Chiquet M (2003) Tenascins: regulation and putative functions during pathological stress. J Pathol 200:488-499.

Coetzee T, Fujita N, Dupree J, Shi R, Blight A, Suzuki K, Suzuki K, Popko B (1996) Myelination in the absence of galactocerebroside and sulfatide: normal structure with abnormal function and regional instability. Cell 86:209-219.

Costa C, Tortosa R, Domenech A, Vidal E, Pumarola M, Bassols A (2007) Mapping of aggrecan, hyaluronic acid, heparan sulphate proteoglycans and aquaporin 4 in the central nervous system of the mouse. J Chem Neuroanat 33:111-123.

Crossin KL, Hoffman S, Grumet M, Thiery JP, Edelman GM (1986) Site-restricted expression of cytotactin during development of the chicken embryo. J Cell Biol 102:1917-1930.

Csoka AB, Scherer SW, Stern R (1999) Expression analysis of six paralogous human hyaluronidase genes clustered on chromosomes 3p21 and 7q31. Genomics 60:356-361.

Csoka AB, Frost GI, Stern R (2001) The six hyaluronidase-like genes in the human and mouse genomes. Matrix Biol 20:499-508.

Custer AW, Kazarinova-Noyes K, Sakurai T, Xu X, Simon W, Grumet M, Shrager P (2003) The role of the ankyrin-binding protein NrCAM in node of Ranvier formation. J Neurosci 23:10032-10039.

David S, Aguayo AJ (1981) Axonal elongation into peripheral nervous system "bridges" after central nervous system injury in adult rats. Science 214:931-933.

Day AJ, Prestwich GD (2002) Hyaluronan-binding proteins: tying up the giant. J Biol Chem 277:4585-4588.

DeAngelis PL (1999) Hyaluronan synthases: fascinating glycosyltransferases from vertebrates, bacterial pathogens, and algal viruses. Cell Mol Life Sci 56:670-682.

Delpech B, Halavent C (1981) Characterization and purification from human brain of a hyaluronic acid-binding glycoprotein, hyaluronectin. J Neurochem 36:855-859.

Doege K, Sasaki M, Horigan E, Hassell JR, Yamada Y (1987) Complete primary structure of the rat cartilage proteoglycan core protein deduced from cDNA clones. J Biol Chem 262:17757-17767.

Dours-Zimmermann MT, Zimmermann DR (1994) A novel glycosaminoglycan attachment domain identified in two alternative splice variants of human versican. J Biol Chem 269:32992-32998.

Dudhia J (2005) Aggrecan, aging and assembly in articular cartilage. Cell Mol Life Sci 62:2241-2256.

Dupree JL, Girault JA, Popko B (1999) Axo-glial interactions regulate the localization of axonal paranodal proteins. J Cell Biol 147:1145-1152.

Dupree JL, Coetzee T, Blight A, Suzuki K, Popko B (1998) Myelin galactolipids are essential for proper node of Ranvier formation in the CNS. J Neurosci 18:1642-1649.

Dutt S, Kleber M, Matasci M, Sommer L, Zimmermann DR (2006) Versican V0 and V1 guide migratory neural crest cells. J Biol Chem 281:12123-12131.

Dzhashiashvili Y, Zhang Y, Galinska J, Lam I, Grumet M, Salzer JL (2007) Nodes of Ranvier and axon initial segments are ankyrin G-dependent domains that assemble by distinct mechanisms. J Cell Biol 177:857-870.

Eshed Y, Feinberg K, Carey DJ, Peles E (2007) Secreted gliomedin is a perinodal matrix component of peripheral nerves. J Cell Biol 177:551-562.

Eshed Y, Feinberg K, Poliak S, Sabanay H, Sarig-Nadir O, Spiegel I, Bermingham JR, Jr., Peles E (2005) Gliomedin mediates Schwann cell-axon interaction and the molecular assembly of the nodes of Ranvier. Neuron 47:215-229.

Faulkner JR, Herrmann JE, Woo MJ, Tansey KE, Doan NB, Sofroniew MV (2004) Reactive astrocytes protect tissue and preserve function after spinal cord injury. J Neurosci 24:2143-2155.

Fields RD, Stevens-Graham B (2002) New insights into neuron-glia communication. Science 298:556-562.

Filbin MT (2003) Myelin-associated inhibitors of axonal regeneration in the adult mammalian CNS. Nat Rev Neurosci 4:703-713.

Flannery CR (2006) MMPs and ADAMTSs: functional studies. Front Biosci 11:544-569.

Forsberg E, Hirsch E, Fröhlich L, Meyer M, Ekblom P, Aszodi A, Werner S, Fässler R (1996) Skin wounds and severed nerves heal normally in mice lacking tenascin-C. Proc Natl Acad Sci U S A 93:6594-6599.

Franzen A, Bjornsson S, Heinegard D (1981) Cartilage proteoglycan aggregate formation. Role of link protein. Biochem J 197:669-674.

Fraser JR, Laurent TC, Laurent UB (1997) Hyaluronan: its nature, distribution, functions and turnover. J Intern Med 242:27-33.

Freitag S, Schachner M, Morellini F (2003) Behavioral alterations in mice deficient for the extracellular matrix glycoprotein tenascin-R. Behav Brain Res 145:189-207.

Friedlander DR, Milev P, Karthikeyan L, Margolis RK, Margolis RU, Grumet M (1994) The neuronal chondroitin sulfate proteoglycan neurocan binds to the neural cell adhesion molecules Ng-CAM/L1/NILE and N-CAM, and inhibits neuronal adhesion and neurite outgrowth. J Cell Biol 125:669-680.

Fukamauchi F, Wang YJ, Mataga N, Kusakabe M (1997) Paradoxical behavioral response to apomorphine in tenascin-gene knockout mouse. Eur J Pharmacol 338:7-10.

Fukamauchi F, Mataga N, Wang YJ, Sato S, Youshiki A, Kusakabe M (1996) Abnormal behavior and neurotransmissions of tenascin gene knockout mouse. Biochem Biophys Res Commun 221:151-156.

Fülöp C, Walcz E, Valyon M, Glant TT (1993) Expression of alternatively spliced epidermal growth factor-like domains in aggrecans of different species. J Biol Chem 268:17377-17383.

Girard N, Courel MN, Delpech A, Bruckner G, Delpech B (1992) Staining of hyaluronan in rat cerebellum with a hyaluronectin-antihyaluronectin immune complex. Histochem J 24:21-24.

Gleghorn L, Ramesar R, Beighton P, Wallis G (2005) A mutation in the variable repeat region of the aggrecan gene (AGC1) causes a form of spondyloepiphyseal dysplasia associated with severe, premature osteoarthritis. Am J Hum Genet 77:484-490.

Gollan L, Salomon D, Salzer JL, Peles E (2003) Caspr regulates the processing of contactin and inhibits its binding to neurofascin. J Cell Biol 163:1213-1218.

Gollan L, Sabanay H, Poliak S, Berglund EO, Ranscht B, Peles E (2002) Retention of a cell adhesion complex at the paranodal junction requires the cytoplasmic region of Caspr. J Cell Biol 157:1247-1256.

Gonzenbach RR, Schwab ME (2008) Disinhibition of neurite growth to repair the injured adult CNS: Focusing on Nogo. Cell Mol Life Sci 65:161-176.

GrandPre T, Nakamura F, Vartanian T, Strittmatter SM (2000) Identification of the Nogo inhibitor of axon regeneration as a Reticulon protein. Nature 403:439-444.

Hagihara K, Miura R, Kosaki R, Berglund E, Ranscht B, Yamaguchi Y (1999) Immunohistochemical evidence for the brevican-tenascin-R interaction: colocalization in perineuronal nets suggests a physiological role for the interaction in the adult rat brain. J Comp Neurol 410:256-264.

Hardingham TE, Fosang AJ (1992) Proteoglycans: many forms and many functions. Faseb J 6:861-870.

Harroch S, Furtado GC, Brueck W, Rosenbluth J, Lafaille J, Chao M, Buxbaum JD, Schlessinger J (2002) A critical role for the protein tyrosine phosphatase receptor type Z in functional recovery from demyelinating lesions. Nat Genet 32:411-414.

Harroch S, Palmeri M, Rosenbluth J, Custer A, Okigaki M, Shrager P, Blum M, Buxbaum JD, Schlessinger J (2000) No obvious abnormality in mice deficient in receptor protein tyrosine phosphatase beta. Mol Cell Biol 20:7706-7715.

Hartline DK, Colman DR (2007) Rapid conduction and the evolution of giant axons and myelinated fibers. Curr Biol 17:R29-35.

Hascall VC, Heinegard D (1974) Aggregation of cartilage proteoglycans. I. The role of hyaluronic acid. J Biol Chem 249:4232-4241.

Haunso A, Celio MR, Margolis RK, Menoud PA (1999) Phosphacan immunoreactivity is associated with perineuronal nets around parvalbumin-expressing neurones. Brain Res 834:219-222.

Hedstrom KL, Xu X, Ogawa Y, Frischknecht R, Seidenbecher CI, Shrager P, Rasband MN (2007) Neurofascin assembles a specialized extracellular matrix at the axon initial segment. J Cell Biol 178:875-886.

Hirakawa S, Oohashi T, Su WD, Yoshioka H, Murakami T, Arata J, Ninomiya Y (2000) The brain link protein-1 (BRAL1): cDNA cloning, genomic structure, and characterization as a novel link protein expressed in adult brain. Biochem Biophys Res Commun 276:982-989.

Honke K, Hirahara Y, Dupree J, Suzuki K, Popko B, Fukushima K, Fukushima J, Nagasawa T, Yoshida N, Wada Y, Taniguchi N (2002) Paranodal junction formation and spermatogenesis require sulfoglycolipids. Proc Natl Acad Sci U S A 99:4227-4232.

Hsia HC, Schwarzbauer JE (2005) Meet the tenascins: multifunctional and mysterious. J Biol Chem 280:26641-26644.

Huang JK, Phillips GR, Roth AD, Pedraza L, Shan W, Belkaid W, Mi S, Fex-Svenningsen A, Florens L, Yates JR, 3rd, Colman DR (2005) Glial membranes at the node of Ranvier prevent neurite outgrowth. Science 310:1813-1817.

Hudson LD (2001) Oligodendrocytes. In: Encyclopedia of Life Siences: John Wiley & Sons, Ltd: Chichester.

Ikuta T, Sogawa N, Ariga H, Ikemura T, Matsumoto K (1998) Structural analysis of mouse tenascin-X: evolutionary aspects of reduplication of FNIII repeats in the tenascin gene family. Gene 217:1-13.

Iozzo RV, Murdoch AD (1996) Proteoglycans of the extracellular environment - clues from the gene and protein side offer novel perspectives in molecular diversity and function [Review]. FASEB J 10:598-614.

Ishibashi T, Dupree JL, Ikenaka K, Hirahara Y, Honke K, Peles E, Popko B, Suzuki K, Nishino H, Baba H (2002) A myelin galactolipid, sulfatide, is essential for maintenance of ion channels on myelinated axon but not essential for initial cluster formation. J Neurosci 22:6507-6514.

Isogai Z, Aspberg A, Keene DR, Ono RN, Reinhardt DP, Sakai LY (2002) Versican interacts with fibrillin-1 and links extracellular microfibrils to other connective tissue networks. J Biol Chem 277:4565-4572.

Joester A, Faissner A (1999) Evidence for combinatorial variability of tenascin-C isoforms and developmental regulation in the mouse central nervous system. J Biol Chem 274:17144-17151.

Joester A, Faissner A (2001) The structure and function of tenascins in the nervous system. Matrix Biol 20:13-22.

Johansson S, Hedman K, Kjellén L, Christner J, Vaheri A, Höök M (1985) Structure and interactions of proteoglycans in the extracellular matrix produced by cultured human fibroblasts. Biochem J 232:161-168.

Jones FS, Jones PL (2000) The tenascin family of ECM glycoproteins: structure, function, and regulation during embryonic development and tissue remodeling. Dev Dyn 218:235-259.

Jones GC, Riley GP (2005) ADAMTS proteinases: a multi-domain, multi-functional family with roles in extracellular matrix turnover and arthritis. Arthritis Res Ther 7:160-169.

Kaplan MR, Meyer-Franke A, Lambert S, Bennett V, Duncan ID, Levinson SR, Barres BA (1997) Induction of sodium channel clustering by oligodendrocytes. Nature 386:724-728.

Kazarinova-Noyes K, Shrager P (2002) Molecular constituents of the node of Ranvier. Mol Neurobiol 26:167-182.

Kiernan BW, Garcion E, Ferguson J, Frost EE, Torres EM, Dunnett SB, Saga Y, Aizawa S, Faissner A, Kaur R, Franklin RJ, ffrench-Constant C (1999) Myelination and behaviour of tenascin-C null transgenic mice. Eur J Neurosci 11:3082-3092.

Kimata K, Oike Y, Tani K, Shinomura T, Yamagata M, Uritani M, Suzuki S (1986) A large chondroitin sulfate proteoglycan (PG-M) synthesized before chondrogenesis in the limb bud of chick embryo. J Biol Chem 261:13517-13525.

Kjellén L, Lindahl U (1991) Proteoglycans: structures and interactions [published erratum appears in Annu. Rev. Biochem. (1992) **61**, following viii]. Annu Rev Biochem 60:443-475.

Kloeckener-Gruissem B, Bartholdi D, Abdou MT, Zimmermann DR, Berger W (2006) Identification of the genetic defect in the original Wagner syndrome family. Mol Vis 12:350-355.

Komada M, Soriano P (2002) [Beta]IV-spectrin regulates sodium channel clustering through ankyrin-G at axon initial segments and nodes of Ranvier. J Cell Biol 156:337-348.

Krueger RC, Jr., Kurima K, Schwartz NB (1999) Completion of the mouse aggrecan gene structure and identification of the defect in the cmd-Bc mouse as a near complete deletion of the murine aggrecan gene. Mamm Genome 10:1119-1125.

Lai HC, Jan LY (2006) The distribution and targeting of neuronal voltage-gated ion channels. Nat Rev Neurosci 7:548-562.

Landolt RM, Vaughan L, Winterhalter KH, Zimmermann DR (1995) Versican is selectively expressed in embryonic tissues that act as barriers to neural crest cell migration and axon outgrowth. Development 121:2303-2312.

Lappe-Siefke C, Goebbels S, Gravel M, Nicksch E, Lee J, Braun PE, Griffiths IR, Nave KA (2003) Disruption of Cnp1 uncouples oligodendroglial functions in axonal support and myelination. Nat Genet 33:366-374.

LeBaron RG, Zimmermann DR, Ruoslahti E (1992) Hyaluronate binding properties of versican. J Biol Chem 267:10003-10010.

Levy JB, Canoll PD, Silvennoinen O, Barnea G, Morse B, Honegger AM, Huang JT, Cannizzaro LA, Park SH, Druck T, Huebner K, Sap J, Ehrlich M, Musacchio JM, Schlessinger J (1993) The cloning of a receptor-type protein tyrosine phosphatase expressed in the central nervous system. Journal of Biological Chemistry 268:10573-10581.

Li H, Schwartz NB, Vertel BM (1993) cDNA cloning of chick cartilage chondroitin sulfate (aggrecan) core protein and identification of a stop codon in the aggrecan gene associated with the chondrodystrophy, nanomelia. J Biol Chem 268:23504-23511.

Lundell A, Olin AI, Morgelin M, al-Karadaghi S, Aspberg A, Logan DT (2004) Structural basis for interactions between tenascins and lectican C-type lectin domains: evidence for a crosslinking role for tenascins. Structure 12:1495-1506.

Mackie EJ, Tucker RP (1999) The tenascin-C knockout revisited. J Cell Sci 112 (Pt 22):3847-3853.

Maeda N, Hamanaka H, Oohira A, Noda M (1995) Purification, characterization and developmental expression of a brain-specific chondroitin sulfate proteoglycan, 6B4 proteoglycan/phosphacan. Neuroscience 67:23-35.

Maier IC, Schwab ME (2006) Sprouting, regeneration and circuit formation in the injured spinal cord: factors and activity. Philos Trans R Soc Lond B Biol Sci 361:1611-1634.

Malhotra JD, Kazen-Gillespie K, Hortsch M, Isom LL (2000) Sodium channel beta subunits mediate homophilic cell adhesion and recruit ankyrin to points of cell-cell contact. J Biol Chem 275:11383-11388.

Marcus J, Honigbaum S, Shroff S, Honke K, Rosenbluth J, Dupree JL (2006) Sulfatide is essential for the maintenance of CNS myelin and axon structure. Glia 53:372-381.

Margolis RK, Margolis RU, Preti C, Lai D (1975) Distribution and metabolism of glycoproteins and glycosaminoglycans in subcellular fractions of brain. Biochemistry 14:4797-4804.

Maroudas A, Muir H, Wingham J (1969) The correlation of fixed negative charge with glycosaminoglycan content of human articular cartilage. Biochim Biophys Acta 177:492-500.

Matsui F, Watanabe E, Oohira A (1994) Immunological identification of two proteoglycan fragments derived from neurocan, a brain-specific chondroitin sulfate proteoglycan. Neurochem Int 25:425-431.

Matsumoto K, Saga Y, Ikemura T, Sakakura T, Chiquet-Ehrismann R (1994) The distribution of tenascin-X is distinct and often reciprocal to that of tenascin-C. J Cell Biol 125:483-493.

Matthews RT, Gary SC, Zerillo C, Pratta M, Solomon K, Arner EC, Hockfield S (2000) Brain-enriched hyaluronan binding (BEHAB)/brevican cleavage in a glioma cell line is mediated by a disintegrin and metalloproteinase with thrombospondin motifs (ADAMTS) family member. J Biol Chem 275:22695-22703.

Maurel P, Rauch U, Flad M, Margolis RK, Margolis RU (1994) Phosphacan, a chondroitin sulfate proteoglycan of brain that interacts with neurons and neural cell-adhesion molecules, is an extracellular variant of a receptor-type protein tyrosine phosphatase. Proc Natl Acad Sci USA 91:2512-2516.

Maurel P, Einheber S, Galinska J, Thaker P, Lam I, Rubin MB, Scherer SS, Murakami Y, Gutmann DH, Salzer JL (2007) Nectin-like proteins mediate axon Schwann cell interactions along the internode and are essential for myelination. J Cell Biol 178:861-874.

McDonald JA, Camenisch TD (2002) Hyaluronan: genetic insights into the complex biology of a simple polysaccharide. Glycoconj J 19:331-339.

Melendez-Vasquez C, Carey DJ, Zanazzi G, Reizes O, Maurel P, Salzer JL (2005) Differential expression of proteoglycans at central and peripheral nodes of Ranvier. Glia 52:301-308.

Milev P, Friedlander DR, Sakurai T, Karthikeyan L, Flad M, Margolis RK, Grumet M, Margolis RU (1994) Interactions of the chondroitin sulfate proteoglycan phosphacan, the extracellular domain of a receptor-type protein tyrosine phosphatase, with neurons, glia, and neural cell adhesion molecules. J Cell Biol 127:1703-1715.

Milev P, Maurel P, Chiba A, Mevissen M, Popp S, Yamaguchi Y, Margolis RK, Margolis RU (1998) Differential regulation of expression of hyaluronan-binding proteoglycans in developing brain: aggrecan, versican, neurocan, and brevican. Biochem Biophys Res Commun 247:207-212.

Miura R, Aspberg A, Ethell IM, Hagihara K, Schnaar RL, Ruoslahti E, Yamaguchi Y (1999) The proteoglycan lectin domain binds sulfated cell surface glycolipids and promotes cell adhesion. J Biol Chem 274:11431-11438.

Miyamoto T, Inoue H, Sakamoto Y, Kudo E, Naito T, Mikawa T, Mikawa Y, Isashiki Y, Osabe D, Shinohara S, Shiota H, Itakura M (2005) Identification of a novel splice site mutation of the CSPG2 gene in a Japanese family with Wagner syndrome. Invest Ophthalmol Vis Sci 46:2726-2735.

Mjaatvedt C, Yamamura H, Capehart A, Turner D, Markwald R (1998) The *cspg2* gene, disrupted in the *hdf* mutant, is required for right cardiac chamber and endocardial cushion formation. Dev Biol 202:56-66.

Montag-Sallaz M, Montag D (2003) Severe cognitive and motor coordination deficits in tenascin-R-deficient mice. Genes Brain Behav 2:20-31.

Mukhopadhyay A, Nikopoulos K, Maugeri A, de Brouwer AP, van Nouhuys CE, Boon CJ, Perveen R, Zegers HA, Wittebol-Post D, van den Biesen PR, van der Velde-Visser SD, Brunner HG, Black GC, Hoyng CB, Cremers FP (2006) Erosive vitreoretinopathy and wagner disease are caused by intronic mutations in CSPG2/Versican that result in an imbalance of splice variants. Invest Ophthalmol Vis Sci 47:3565-3572.

Murai KK, Misner D, Ranscht B (2002) Contactin supports synaptic plasticity associated with hippocampal long-term depression but not potentiation. Curr Biol 12:181-190.

Mörgelin M, Heinegard D, Engel J, Paulsson M (1994) The cartilage proteoglycan aggregate: assembly through combined protein-carbohydrate and protein-protein interactions. Biophys Chem 50:113-128.

Nakao N, Hiraiwa N, Yoshiki A, Ike F, Kusakabe M (1998) Tenascin-C promotes healing of Habu-snake venom-induced glomerulonephritis: studies in knockout congenic mice and in culture. Am J Pathol 152:1237-1245.

Naso MF, Zimmermann DR, Iozzo RV (1994) Characterization of the complete genomic structure of the human versican gene and functional analysis of its promoter. J Biol Chem 269:32999-33008.

Naso MF, Morgan JL, Buchberg AM, Siracusa LD, Iozzo RV (1995) Expression pattern and mapping of the murine versican gene (Cspg2) to chromosome 13. Genomics 29:297-300.

Nave KA (1994) Neurological mouse mutants and the genes of myelin. J Neurosci Res 38:607-612.

Neidhardt J, Fehr S, Kutsche M, Lohler J, Schachner M (2003) Tenascin-N: characterization of a novel member of the tenascin family that mediates neurite repulsion from hippocampal explants. Mol Cell Neurosci 23:193-209.

Nicholson C, Sykova E (1998) Extracellular space structure revealed by diffusion analysis. Trends Neurosci 21:207-215.

Niederöst BP, Zimmermann DR, Schwab ME, Bandtlow CE (1999) Bovine CNS myelin contains neurite growth inhibitory activity associated with chondroitin sulfate proteoglycans. J Neurosci 19:8979-8989.

Niisato K, Fujikawa A, Komai S, Shintani T, Watanabe E, Sakaguchi G, Katsuura G, Manabe T, Noda M (2005) Age-dependent enhancement of hippocampal long-term potentiation and impairment of spatial learning through the Rho-associated kinase pathway in protein tyrosine phosphatase receptor type Z-deficient mice. J Neurosci 25:1081-1088.

Norenberg U, Wille H, Wolff JM, Frank R, Rathjen FG (1992) The chicken neural extracellular matrix molecule restrictin: similarity with EGF-, fibronectin type III-, and fibrinogen-like motifs. Neuron 8:849-863.

Novak U, Kaye AH (2000) Extracellular matrix and the brain: components and function. J Clin Neurosci 7:280-290.

Ogawa H, Oohashi T, Sata M, Bekku Y, Hirohata S, Nakamura K, Yonezawa T, Kusachi S, Shiratori Y, Ninomiya Y (2004) Lp3/Hapln3, a novel link protein that co-localizes with versican and is coordinately up-regulated by platelet-derived growth factor in arterial smooth muscle cells. Matrix Biol 23:287-298.

Olin AI, Morgelin M, Sasaki T, Timpl R, Heinegard D, Aspberg A (2001) The proteoglycans aggrecan and Versican form networks with fibulin-2 through their lectin domain binding. J Biol Chem 276:1253-1261.

Oohashi T, Hirakawa S, Bekku Y, Rauch U, Zimmermann DR, Su WD, Ohtsuka A, Murakami T, Ninomiya Y (2002) Bral1, a brain-specific link protein, colocalizing with the versican V2 isoform at the nodes of Ranvier in developing and adult mouse central nervous systems. Mol Cell Neurosci 19:43-57.

Oohira A, Matsui F, Watanabe E, Kushima Y, Maeda N (1994) Developmentally regulated expression of a brain specific species of chondroitin sulfate proteoglycan, neurocan, identified with a monoclonal antibody IG2 in the rat cerebrum. Neuroscience 60:145-157.

Parkinson NJ, Olsson CL, Hallows JL, McKee-Johnson J, Keogh BP, Noben-Trauth K, Kujawa SG, Tempel BL (2001) Mutant beta-spectrin 4 causes auditory and motor neuropathies in quivering mice. Nat Genet 29:61-65.

Peles E, Schlessinger J, Grumet M (1998) Multi-ligand interactions with receptor-like protein tyrosine phosphatase beta: implications for intercellular signaling. Trends in Biochemical Sciences 23:121-124.

Peles E, Nativ M, Campbell PL, Sakurai T, Martinez R, Lev S, Clary DO, Schilling J, Barnea G, Plowman GD, Grumet M, Schlessinger J (1995) The carbonic anhydrase domain of receptor tyrosine phosphatase beta is a functional ligand for the axonal cell recognition molecule contactin. Cell 82:251-260.

Perides G, Lane WS, Andrews D, Dahl D, Bignami A (1989) Isolation and partial characterization of a glial hyaluronate-binding protein. J Biol Chem 264:5981-5987.

Pesheva P, Probstmeier R (2000) The yin and yang of tenascin-R in CNS development and pathology. Prog Neurobiol 61:465-493.

Pesheva P, Gennarini G, Goridis C, Schachner M (1993) The f3/11 cell adhesion molecule mediates the repulsion of neurons by the extracellular matrix glycoprotein j1-160/180. Neuron 10:69-82.

Pesheva P, Gloor S, Schachner M, Probstmeier R (1997) Tenascin-R is an intrinsic autocrine factor for oligodendrocyte differentiation and promotes cell adhesion by a sulfatide-mediated mechanism. J Neurosci 17:4642-4651.

Poliak S, Peles E (2003) The local differentiation of myelinated axons at nodes of Ranvier. Nat Rev Neurosci 4:968-980.

Poliak S, Gollan L, Salomon D, Berglund EO, Ohara R, Ranscht B, Peles E (2001) Localization of Caspr2 in myelinated nerves depends on axon-glia interactions and the generation of barriers along the axon. J Neurosci 21:7568-7575.

Poliak S, Salomon D, Elhanany H, Sabanay H, Kiernan B, Pevny L, Stewart CL, Xu X, Chiu SY, Shrager P, Furley AJ, Peles E (2003) Juxtaparanodal clustering of Shaker-like K+ channels in myelinated axons depends on Caspr2 and TAG-1. J Cell Biol 162:1149-1160.

Porter S, Clark IM, Kevorkian L, Edwards DR (2005) The ADAMTS metalloproteinases. Biochem J 386:15-27.

Prydz K, Dalen KT (2000) Synthesis and sorting of proteoglycans. J Cell Sci 113 Pt 2:193-205.

Purves D, Augustine GJ, Fitzpatrick D, Katz LC, LaMantia AS, McNamara JO, Williams SM (2001) Neuroscience, Second Edition. Sunderland, MA: Sinauer Associates, Inc.

Ramer MS, McMahon SB, Priestley JV (2001) Axon regeneration across the dorsal root entry zone. Prog Brain Res 132:621-639.

Rasband MN, Trimmer JS (2001) Developmental clustering of ion channels at and near the node of Ranvier. Dev Biol 236:5-16.

Rasband MN, Taylor CM, Bansal R (2003) Paranodal transverse bands are required for maintenance but not initiation of Nav1.6 sodium channel clustering in CNS optic nerve axons. Glia 44:173-182.

Rasband MN, Tayler J, Kaga Y, Yang Y, Lappe-Siefke C, Nave KA, Bansal R (2005) CNP is required for maintenance of axon-glia interactions at nodes of Ranvier in the CNS. Glia 50:86-90.

Ratcliffe CF, Qu Y, McCormick KA, Tibbs VC, Dixon JE, Scheuer T, Catterall WA (2000) A sodium channel signaling complex: modulation by associated receptor protein tyrosine phosphatase beta. Nat Neurosci 3:437-444.

Rathjen FG, Wolff JM, Chiquet-Ehrismann R (1991) Restrictin: a chick neural extracellular matrix protein involved in cell attachment co-purifies with the cell recognition molecule F11. Development 113:151-164.

Rauch U (1997) Modeling an extracellular environment for axonal pathfinding and fasciculation in the central nervous system. Cell Tissue Res 290:349-356.

Rauch U (2004) Extracellular matrix components associated with remodeling processes in brain. Cell Mol Life Sci 61:2031-2045.

Rauch U, Zhou XH, Roos G (2005) Extracellular matrix alterations in brains lacking four of its components. Biochem Biophys Res Commun 328:608-617.

Rauch U, Karthikeyan L, Maurel P, Margolis RU, Margolis RK (1992) Cloning and primary structure of neurocan, a developmentally regulated, aggregating chondroitin sulfate proteoglycan of brain. J Biol Chem 267:19536-19547.

Rauch U, Clement A, Retzler C, Fröhlich L, Fässler R, Göhring W, Faissner A (1997a) Mapping of a defined neurocan binding site to distinct domains of tenascin-C. J Biol Chem 272:26905-26912.

Rauch U, Meyer H, Brakebusch C, Seidenbecher C, Gundelfinger ED, Beier DR, Fässler R (1997b) Sequence and chromosomal localization of the mouse brevican gene. Genomics 44:15-21.

Rauch U, Gao P, Janetzko A, Flaccus A, Hilgenberg L, Tekotte H, Margolis RK, Margolis RU (1991) Isolation and characterization of developmentally regulated chondroitin sulfate and chondroitin/keratan sulfate proteoglycans of brain identified with monoclonal antibodies. J Biol Chem 266:14785-14801.

Retzler C, Wiedemann H, Kulbe G, Rauch U (1996) Structural and electron microscopic analysis of neurocan and recombinant neurocan fragments. J Biol Chem 271:17107-17113.

Richardson PM, McGuinness UM, Aguayo AJ (1980) Axons from CNS neurons regenerate into PNS grafts. Nature 284:264-265.

Rios JC, Melendez-Vasquez CV, Einheber S, Lustig M, Grumet M, Hemperly J, Peles E, Salzer JL (2000) Contactin-associated protein (Caspr) and contactin form a complex that is targeted to the paranodal junctions during myelination. J Neurosci 20:8354-8364.

Rios JC, Rubin M, St Martin M, Downey RT, Einheber S, Rosenbluth J, Levinson SR, Bhat M, Salzer JL (2003) Paranodal interactions regulate expression of sodium channel subtypes and provide a diffusion barrier for the node of Ranvier. J Neurosci 23:7001-7011.

Rosenbluth J, Dupree JL, Popko B (2003) Nodal sodium channel domain integrity depends on the conformation of the paranodal junction, not on the presence of transverse bands. Glia 41:318-325.

Ruoslahti E (1996) Brain extracellular matrix [Review]. Glycobiology 6:489-492.

Russell DL, Doyle KM, Ochsner SA, Sandy JD, Richards JS (2003) Processing and localization of ADAMTS-1 and proteolytic cleavage of versican during cumulus matrix expansion and ovulation. J Biol Chem 278:42330-42339.

Rutka JT, Apodaca G, Stern R, Rosenblum M (1988) The extracellular matrix of the central and peripheral nervous systems: structure and function. J Neurosurg 69:155-170.

Saga Y, Yagi T, Ikawa Y, Sakakura T, Aizawa S (1992) Mice develop normally without tenascin. Genes Dev 6:1821-1831.

Saghatelyan A, de Chevigny A, Schachner M, Lledo PM (2004) Tenascin-R mediates activity-dependent recruitment of neuroblasts in the adult mouse forebrain. Nat Neurosci 7:347-356.

Saito F, Moore SA, Barresi R, Henry MD, Messing A, Ross-Barta SE, Cohn RD, Williamson RA, Sluka KA, Sherman DL, Brophy PJ, Schmelzer JD, Low PA, Wrabetz L, Feltri ML, Campbell KP (2003) Unique role of dystroglycan in peripheral nerve myelination, nodal structure, and sodium channel stabilization. Neuron 38:747-758.

Sakurai T, Lustig M, Nativ M, Hemperly JJ, Schlessinger J, Peles E, Grumet M (1997) Induction of neurite outgrowth through contactin and Nr-CAM by extracellular regions of glial receptor tyrosine phosphatase beta. Journal of Cell Biology 136:907-918.

Salzer JL (2003) Polarized domains of myelinated axons. Neuron 40:297-318.

Sandy JD, Westling J, Kenagy RD, Iruela-Arispe ML, Verscharen C, Rodriguez-Mazaneque JC, Zimmermann DR, Lemire JM, Fischer JW, Wight TN, Clowes AW (2001) Versican V1 proteolysis in human aorta in vivo occurs at the Glu441-Ala442 bond, a site that is cleaved by recombinant ADAMTS-1 and ADAMTS-4. J Biol Chem 276:13372-13378.

Sanes JR (1989) Extracellular matrix molecules that influence neural development. Annu Rev Neurosci 12:491-516.

Schaeren-Wiemers N, Bonnet A, Erb M, Erne B, Bartsch U, Kern F, Mantei N, Sherman D, Suter U (2004) The raft-associated protein MAL is required for maintenance of proper axon--glia interactions in the central nervous system. J Cell Biol 166:731-742.

Schafer DP, Rasband MN (2006) Glial regulation of the axonal membrane at nodes of Ranvier. Curr Opin Neurobiol 16:508-514.

Scherberich A, Tucker RP, Samandari E, Brown-Luedi M, Martin D, Chiquet-Ehrismann R (2004) Murine tenascin-W: a novel mammalian tenascin expressed in kidney and at sites of bone and smooth muscle development. J Cell Sci 117:571-581.

Scherer SS, Arroyo EJ (2002) Recent progress on the molecular organization of myelinated axons. J Peripher Nerv Syst 7:1-12.

Schmalfeldt M, Dours-Zimmermann MT, Winterhalter KH, Zimmermann DR (1998) Versican V2 is a major extracellular matrix component of the mature bovine brain. J Biol Chem 273:15758-15764.

Schmalfeldt M, Bandtlow CE, Dours-Zimmermann MT, Winterhalter KH, Zimmermann DR (2000) Brain derived versican V2 is a potent inhibitor of axonal growth. J Cell Sci 113:807-816.

Schwartz NB, Domowicz M, Krueger RC, Jr., Li H, Mangoura D (1996) Brain aggrecan. Perspect Dev Neurobiol 3:291-306.

Schweigreiter R, Roots BI, Bandtlow CE, Gould RM (2006) Understanding myelination through studying its evolution. Int Rev Neurobiol 73:219-273.

Scott AL, Ramer LM, Soril LJ, Kwiecien JM, Ramer MS (2006) Targeting myelin to optimize plasticity of spared spinal axons. Mol Neurobiol 33:91-111.

Seidenbecher CI, Gundelfinger ED, Bockers TM, Trotter J, Kreutz MR (1998) Transcripts for secreted and GPI-anchored brevican are differentially distributed in rat brain. European Journal of Neuroscience 10:1621-1630.

Seidenbecher CI, Richter K, Rauch U, Fässler R, Garner CC, Gundelfinger ED (1995) Brevican, a chondroitin sulfate proteoglycan of rat brain, occurs as secreted and cell surface glycosylphosphatidylinositol-anchored isoforms. J Biol Chem 270:27206-27212.

Sherman DL, Brophy PJ (2005) Mechanisms of axon ensheathment and myelin growth. Nat Rev Neurosci 6:683-690.

Sherman DL, Tait S, Melrose S, Johnson R, Zonta B, Court FA, Macklin WB, Meek S, Smith AJ, Cottrell DF, Brophy PJ (2005) Neurofascins are required to establish axonal domains for saltatory conduction. Neuron 48:737-742.

Sherman LS, Struve JN, Rangwala R, Wallingford NM, Tuohy TM, Kuntz Ct (2002) Hyaluronate-based extracellular matrix: keeping glia in their place. Glia 38:93-102.

Shinomura T, Nishida Y, Ito K, Kimata K (1993) cDNA cloning of PG-M, a large chondroitin sulfate proteoglycan expressed during chondrogenesis in chick limb buds. Alternative spliced multiforms of PG-M and their relationships to versican. J Biol Chem 268:14461-14469.

Shinomura T, Jensen KL, Yamagata M, Kimata K, Solursh M (1990) The distribution of mesenchyme proteoglycan (PG-M) during wing bud outgrowth. Anat Embryol (Berl) 181:227-233.

Shinomura T, Zako M, Ito K, Ujita M, Kimata K (1995) The gene structure and organization of mouse PG-M, a large chondroitin sulfate proteoglycan. Genomic background for the generation of multiple PG-M transcripts. J Biol Chem 270:10328-10333.

Shintani T, Watanabe E, Maeda N, Noda M (1998) Neurons as well as astrocytes express proteoglycan-type protein tyrosine phosphatase zeta/RPTPbeta: analysis of mice in which the PTPzeta/RPTPbeta gene was replaced with the LacZ gene. Neuroscience Letters 247:135-138.

Siegel GJ, Agranoff BW, Fisher SK, Albers RW, Uhler MD (1999) Basic Neurochemistry. Molecular, Cellular and Medical Aspects, Sixth Edition. Philadelphia, PA: Lippincott Williams and Wilkins.

Silver J, Miller JH (2004) Regeneration beyond the glial scar. Nat Rev Neurosci 5:146-156.

Simons M, Trajkovic K (2006) Neuron-glia communication in the control of oligodendrocyte function and myelin biogenesis. J Cell Sci 119:4381-4389.

Snow DM, Watanabe M, Letourneau PC, Silver J (1991) A chondroitin sulfate proteoglycan may influence the direction of retinal ganglion cell outgrowth. Development 113:1473-1485.

Somerville RP, Longpre JM, Jungers KA, Engle JM, Ross M, Evanko S, Wight TN, Leduc R, Apte SS (2003) Characterization of ADAMTS-9 and ADAMTS-20 as a distinct ADAMTS subfamily related to Caenorhabditis elegans GON-1. J Biol Chem 278:9503-9513.

Spicer AP, McDonald JA (1998) Characterization and molecular evolution of a vertebrate hyaluronan synthase gene family. Journal of Biological Chemistry 273:1923-1932.

Spicer AP, Tien JY (2004) Hyaluronan and morphogenesis. Birth Defects Res C Embryo Today 72:89-108.

Spicer AP, Joo A, Bowling RA, Jr. (2003) A hyaluronan binding link protein gene family whose members are physically linked adjacent to chondroitin sulfate proteoglycan core protein genes: the missing links. J Biol Chem 278:21083-21091.

Spicer AP, Tien JL, Joo A, Bowling Jr RA (2002) Investigation of hyaluronan function in the mouse through targeted mutagenesis. Glycoconj J 19:341-345.

Spiegel I, Adamsky K, Eshed Y, Milo R, Sabanay H, Sarig-Nadir O, Horresh I, Scherer SS, Rasband MN, Peles E (2007) A central role for Necl4 (SynCAM4) in Schwann cell-axon interaction and myelination. Nat Neurosci 10:861-869.

Srinivasan J, Schachner M, Catterall WA (1998) Interaction of voltage-gated sodium channels with the extracellular matrix molecules tenascin-C and tenascin-R. Proc Natl Acad Sci U S A 95:15753-15757.

Tammi MI, Day AJ, Turley EA (2002) Hyaluronan and homeostasis: a balancing act. J Biol Chem 277:4581-4584.

Tamura H, Fukada M, Fujikawa A, Noda M (2006) Protein tyrosine phosphatase receptor type Z is involved in hippocampus-dependent memory formation through dephosphorylation at Y1105 on p190 RhoGAP. Neurosci Lett 399:33-38.

Tani E, Ametani T (1971) Extracellular distribution of ruthenium red-positive substance in the cerebral cortex. J Ultrastruct Res 34:1-14.

Toole BP (2000) Hyaluronan is not just a goo! J Clin Invest 106:335-336.

Toole BP (2001) Hyaluronan in morphogenesis. Semin Cell Dev Biol 12:79-87.

Toole BP (2004) Hyaluronan: from extracellular glue to pericellular cue. Nat Rev Cancer 4:528-539.

Tortorella MD, Burn TC, Pratta MA, Abbaszade I, Hollis JM, Liu R, Rosenfeld SA, Copeland RA, Decicco CP, Wynn R, Rockwell A, Yang F, Duke JL, Solomon K, George H, Bruckner R, Nagase H, Itoh Y, Ellis DM, Ross H, Wiswall BH, Murphy K, Hillman MC, Jr., Hollis GF, Newton RC, Magolda RL, Trzaskos JM, Arner EC (1999) Purification and cloning of aggrecanase-1: a member of the ADAMTS family of proteins. Science 284:1664-1666.

Traka M, Goutebroze L, Denisenko N, Bessa M, Nifli A, Havaki S, Iwakura Y, Fukamauchi F, Watanabe K, Soliven B, Girault JA, Karagogeos D (2003) Association of TAG-1 with Caspr2 is essential for the molecular organization of juxtaparanodal regions of myelinated fibers. J Cell Biol 162:1161-1172.

Ujita M, Shinomura T, Ito K, Kitagawa Y, Kimata K (1994) Expression and binding activity of the carboxyl-terminal portion of the core protein of PG-M, a large chondroitin sulfate proteoglycan. J Biol Chem 269:27603-27609.

Viapiano MS, Matthews RT (2006) From barriers to bridges: chondroitin sulfate proteoglycans in neuropathology. Trends Mol Med 12:488-496.

Watanabe H, Kimata K, Line S, Strong D, Gao LY, Kozak CA, Yamada Y (1994) Mouse cartilage matrix deficiency (cmd) caused by a 7 bp deletion in the aggrecan gene. Nat Genet 7:154-157.

Weber P, Bartsch U, Rasband MN, Czaniera R, Lang Y, Bluethmann H, Margolis RU, Levinson SR, Shrager P, Montag D, Schachner M (1999) Mice deficient for tenascin-R display alterations of the extracellular matrix and decreased axonal conduction velocities in the CNS. J Neurosci 19:4245-4262.

Weigel PH, Hascall VC, Tammi M (1997) Hyaluronan synthases. J Biol Chem 272:13997-14000.

Westling J, Gottschall PE, Thompson VP, Cockburn A, Perides G, Zimmermann DR, Sandy JD (2004) ADAMTS4 (aggrecanase-1) cleaves human brain versican V2 at Glu405-Gln406 to generate glial hyaluronate binding protein. Biochem J 377:787-795.

Xiao ZC, Taylor J, Montag D, Rougon G, Schachner M (1996) Distinct effects of recombinant tenascin-R domains in neuronal cell functions and identification of the domain interacting with the neuronal recognition molecule F3/11. Eur J Neurosci 8:766-782.

Xiao ZC, Bartsch U, Margolis RK, Rougon G, Montag D, Schachner M (1997) Isolation of a tenascin-R binding protein from mouse brain membranes - a phosphacan-related chondroitin sulfate proteoglycan. J Biol Chem 272:32092-32101.

Xiao ZC, Ragsdale DS, Malhotra JD, Mattei LN, Braun PE, Schachner M, Isom LL (1999) Tenascin-R is a functional modulator of sodium channel beta subunits. J Biol Chem 274:26511-26517.

Xie F, Zheng B (2008) White matter inhibitors in CNS axon regeneration failure. Exp Neurol 209:302-312.

Yamada H, Watanabe K, Shimonaka M, Yamaguchi Y (1994) Molecular cloning of brevican, a novel brain proteoglycan of the aggrecan/versican family. J Biol Chem 269:10119-10126.

Yamada H, Fredette B, Shitara K, Hagihara K, Miura R, Ranscht B, Stallcup WB, Yamaguchi Y (1997) The brain chondroitin sulfate proteoglycan brevican associates with astrocytes ensheathing cerebellar glomeruli and inhibits neurite outgrowth from granule neurons. J Neurosci 17:7784-7795.

Yamaguchi Y (1996) Brevican - a major proteoglycan in adult brain. Perspectives on Developmental Neurobiology 3:307-317.

Yamaguchi Y (2000) Lecticans: organizers of the brain extracellular matrix. Cell Mol Life Sci 57:276-289.

Yamamura H, Zhang M, Markwald RR, Mjaatvedt CH (1997) A heart segmental defect in the anterior-posterior axis of a transgenic mutant mouse. Developmental Biology 186:58-72.

Yasuhara O, Akiyama H, McGeer EG, McGeer PL (1994) Immunohistochemical localization of hyaluronic acid in rat and human brain. Brain Res 635:269-282.

Yiu G, He Z (2006) Glial inhibition of CNS axon regeneration. Nat Rev Neurosci 7:617-627.

Zako M, Shinomura T, Ujita M, Ito K, Kimata K (1995) Expression of PG-M (V3), an alternative splice form of PG-M without a chondroitin sulfate attachment region in mouse and human tissues. J Biol Chem 270:3914-3918.

Zheng B, Lee JK, Xie F (2006) Genetic mouse models for studying inhibitors of spinal axon regeneration. Trends Neurosci 29:640-646.

Zhou XH, Brakebusch C, Matthies H, Oohashi T, Hirsch E, Moser M, Krug M, Seidenbecher CI, Boeckers TM, Rauch U, Buettner R, Gundelfinger ED, Fassler R (2001) Neurocan is dispensable for brain development. Mol Cell Biol 21:5970-5978.

Zimmermann DR, Ruoslahti E (1989) Multiple domains of the large fibroblast proteoglycan, versican. EMBO J 8:2975-2981.

Zimmermann DR, Dours-Zimmermann MT, Schubert M, Bruckner-Tuderman L (1994) Versican is expressed in the proliferating zone in the epidermis and in association with the elastic network of the dermis. J Cell Biol 124:817-825.

Zonta B, Tait S, Melrose S, Anderson H, Harroch S, Higginson J, Sherman DL, Brophy PJ (2008) Glial and neuronal isoforms of Neurofascin have distinct roles in the assembly of nodes of Ranvier in the central nervous system. J Cell Biol 181:1169-1177.

Zurn AD, Bandtlow CE (2006) Regeneration failure in the CNs: cellular and molecular mechanisms. Adv Exp Med Biol 557:54-76.

2.4. Published review article:

Zimmermann DR, Dours-Zimmermann MT (2008) Extracellular matrix of the central nervous system: from neglect to challenge. Histochem Cell Biol 130:635-653.

Histochem Cell Biol (2008) 130:635–653
DOI 10.1007/s00418-008-0485-9

REVIEW

Extracellular matrix of the central nervous system: from neglect to challenge

Dieter R. Zimmermann · María T. Dours-Zimmermann

Accepted: 26 July 2008 / Published online: 12 August 2008

Abstract The basic concept, that specialized extracellular matrices rich in hyaluronan, chondroitin sulfate proteoglycans (aggrecan, versican, neurocan, brevican, phosphacan), link proteins and tenascins (Tn-R, Tn-C) can regulate cellular migration and axonal growth and thus, actively participate in the development and maturation of the nervous system, has in recent years gained rapidly expanding experimental support. The swift assembly and remodeling of these matrices have been associated with axonal guidance functions in the periphery and with the structural stabilization of myelinated fiber tracts and synaptic contacts in the maturating central nervous system. Particular interest has been focused on the putative role of chondroitin sulfate proteoglycans in suppressing central nervous system regeneration after lesions. The axon growth inhibitory properties of several of these chondroitin sulfate proteoglycans in vitro, and the partial recovery of structural plasticity in lesioned animals treated with chondroitin sulfate degrading enzymes in vivo have significantly contributed to the increased awareness of this long time neglected structure.

Keywords CSPG · Lectican · Hyalectan · ADAMTS · Hyaluronan synthase · Perineuronal net · Node of Ranvier · Knockout · Tenascin · Link protein · Central nervous system

D. R. Zimmermann (✉) · M. T. Dours-Zimmermann
Division of Diagnostic Molecular Pathology,
Institute of Surgical Pathology, University Hospital Zurich,
Schmelzbergstrasse 12, 8091 Zurich, Switzerland
e-mail: dieterzi@pathol.uzh.ch; dieter.zimmermann@usz.ch

Introduction

It was not until 1971 that the existence of an extracellular matrix (ECM) in the central nervous system (CNS) was generally acknowledged (Tani and Ametani 1971). Then a predominance of hyaluronan and chondroitin sulfate proteoglycans (CSPG) (Margolis et al. 1975) and the paucity of otherwise frequent ECM molecules, like fibronectin or collagens, have been described (Carbonetto 1984; Rutka et al. 1988; Sanes 1989). Today we know that this distinctive ECM is mainly composed of proteoglycans of the lectican/hyalectan-family and their binding partners, hyaluronan, link proteins and tenascins (Bandtlow and Zimmermann 2000; Novak and Kaye 2000; Rauch 1997, 2004; Ruoslahti 1996; Yamaguchi 2000). In the following, we will focus on the structure, expression and putative functions of this major matrix components that form this extraordinary extracellular meshwork. Not discussed in this review are less abundant, but nonetheless functionally important macromolecules of the nervous system, such as reelin, agrin and thrombospondins. For detailed information about these large glycoproteins, which are involved in the control of neuronal migration and establishment of synapses we would like to refer the reader to recent reviews and publications (Bezakova and Ruegg 2003; Christopherson et al. 2005; Herz and Chen 2006; Tissir and Goffinet 2003).

Structures and ligands of the major constituents of the neural ECM

Proteoglycans and hyaluronan

Proteoglycans (PGs) are glycoproteins carrying, in addition to variable numbers of N- and O-linked oligosaccharides, at

least one glycosaminoglycan (GAG) side chain, which is covalently bound to a core protein. The GAGs themselves are long unbranched polymers of repetitive disaccharide units consisting of an uronic acid (glucuronic or iduronic) or galactose and an amino-sugar (*N*-acetylglucosamine or *N*-acetylgalactosamine). According to the combination of these sugars, the GAGs are subclassified into heparin/heparan-, keratan- or chondroitin/dermatan-sulfates (Bandtlow and Zimmermann 2000; Kjellén and Lindahl 1991; Prydz and Dalen 2000). The GAG chains are in general 20–200 disaccharide-repeats long. Whereas keratan sulfates are usually attached to the core proteins via short standard N- or O-glycan links to asparagine or serine/threonine, respectively, the binding of chondroitin/dermatan sulfate and of heparin/heparan sulfate chains is mediated by a serine residue and a specific linker tetrasaccharide composed of a xylose, two consecutive galactoses and a glucuronic acid molecule. Numerous modifications that include O- and N-sulfation and epimerization of glucuronic acid at the C5-position lead to a high structural variability and open up countless possibilities for the modulation of GAG-dependent interactions (Bulow and Hobert 2006; Kusche-Gullberg and Kjellen 2003). Moreover, the highly negatively charged GAGs attract and bind considerable amount of water and cations.

In contrast to the protein-bound GAGs, hyaluronan (also known as hyaluronic acid or hyaluronate) is incorporated into the extracellular matrix as a core protein-free glycosaminoglycan (Toole 2000, 2004). Hyaluronan is a very large linear polymer built of repetitive disaccharides units consisting of glucuronic acid and *N*-acetylglucosamine. This carbohydrate filament reaches a molecular mass of up to 10^7 Da and extends over lengths of 2–25 μm. Unlike the other GAGs, hyaluronan is not sulfated and the glucuronic acid units are not epimerized.

While the more complex core protein-bound GAGs are assembled and modified by a large set of glycosyl- and sulfotransferases, the structurally simpler hyaluronan is synthesized by a single enzyme, the hyaluronan synthase (HAS). Three vertebrate genes (*HAS1*, *HAS2*, and *HAS3*) giving rise to three HAS isoenzymes have been identified (DeAngelis 1999; Itano and Kimata 2002; Spicer and McDonald 1998; Weigel et al. 1997). The HAS are rather unique, as they catalyze the incorporation of two different monosaccharides and are, in contrast to most other glycosyltransferases, localized at the inner surface of the cell membrane. From there the growing hyaluronan string directly extrudes into the pericellular space, while being still attached to the producing enzyme (Spicer and Tien 2004; Weigel et al. 1997).

The most prominent binding partners of hyaluronan in the nervous system are the extracellular matrix proteoglycans of the lectican family (also called hyalectans) (reviewed by Bandtlow and Zimmermann 2000; Iozzo and Murdoch 1996; Rauch 2004; Ruoslahti 1996; Yamaguchi 2000). In mammals, four distinct lectican genes encode brevican, neurocan, aggrecan and versican (Table 1; Fig. 1). Shared features among these large chondroitin sulfate proteoglycans are the highly homologous G1 and G3 domains, which appear in rotary shadowing electron microscopy as compact globular structures at either end of an extended, but flexible central region (Mörgelin et al. 1989; Retzler et al. 1996). This poorly sequence-conserved middle part carries most of the O- and N-linked oligosaccharides and all glycosaminoglycan side chains. It varies among the different family members in size and also in the number of carbohydrate substitutions. Occasionally, the GAGs might even be absent, like in a fraction of the part-time preoteoglycan brevican, or they may be greatly diminished, as in CNS-derived aggrecan in relation to its cartilage counterpart. Apart from the variations within the carbohydrate moiety, alternative splicing also greatly adds to the structural diversity of lecticans. Four versican isoforms (V0, V1, V2 and V3) exist as a result of alternative usage of two giant exons encoding the central GAG-α and GAG-β domains (Dours-Zimmermann and Zimmermann 1994; Zako et al. 1995; Zimmermann and Ruoslahti 1989). Versican V0 contains both of these GAG-attachment modules, whereas versican V1 and V2 include only the GAG-β or GAG-α, respectively. Versican V3, the smallest lectican,

Table 1 Extracellular matrix CSPGs in the central nervous system

Name	Core size[a]		GAGs		Cellular origin	CNS-specific
	Calculated[b]	SDS-PAGE[c]	Type	Number		
Aggrecan	244	370	CS	?	Neurons/astrocytes	No
Versican V0	371	≈550	CS	17–23	Neurons/astrocytes?	No
Versican V1	263	≈500	CS	12–15	Astrocytes?	No
Versican V2	180	400	CS	5–8	Oligodendroglial lineage	Yes
Neurocan	141	245	CS	3	Astrocytes/neurons	Yes[d]
Brevican	97	145	CS	0–5	Glial cells/neurons	Yes
Phosphacan (-KS)	172	400	CS/(KS)	3–4	Glial cells/neurons	Yes

[a] kDa

[b] Mature polypeptide

[c] Core glycoprotein after glycosaminoglycan removal

[d] Minor expression in peripheral nervous system

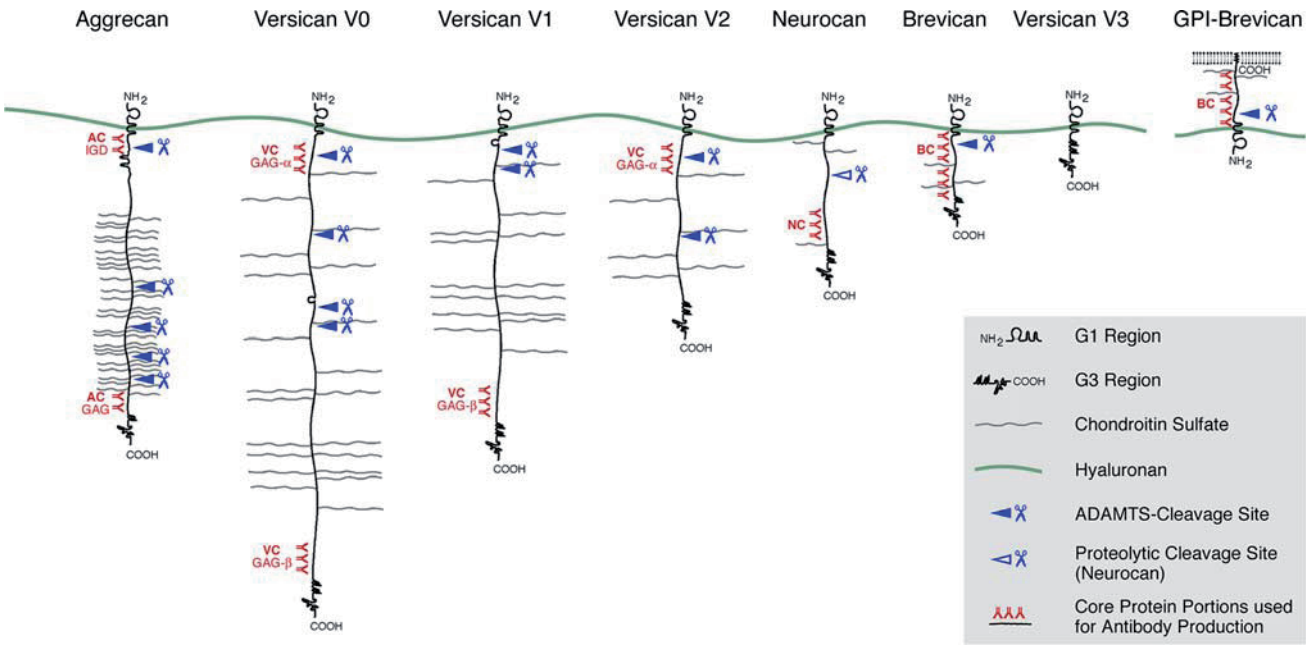

Fig. 1 Structural models of the chondroitin sulfate proteoglycans of the lectican family. ADAMTS cleavage sites and binding regions of the polyclonal antibodies used in immunohistochemical stainings displayed in the following figures are indicated

lacks both of these alternatively spliced elements and consequently carries no glycosaminoglycans.

In contrast to these largely diversified GAG-binding regions, the modules that form the globular G1 and G3 structures display little variability. For instance, all N-terminal G1 regions of the different lecticans include an immunoglobulin (Ig)-like loop and two link-protein-like tandem repeats that are involved in the binding of hyaluronan and link proteins (LeBaron et al. 1992; Mörgelin et al. 1989; Neame et al. 1987; Rauch et al. 2004). The G3 globule at the other end of the core protein contains a C-type lectin-like element, which is flanked by one or two EGF-repeats and a Sushi (SCR/CCP) domain, respectively. The entire G3 region is only absent in a GPI-anchored brevican-variant arising from alternative transcription termination (Seidenbecher et al. 1995). Recombinantly expressed G3 domains and/or the C-type lectin elements alone bind in vitro simple carbohydrates and heparin or heparan sulfate (Ujita et al. 1994), fibulin-1 and -2 (Aspberg et al. 1999; Olin et al. 2001), fibrillin-1 (Isogai et al. 2002), sulfoglycolipids (Miura et al. 1999) and the tenascins, Tn-C and Tn-R (Aspberg et al. 1995, 1997; Day and Prestwich 2002; Rauch et al. 1997). Of note, the majority of the G1- and G3-ligands are recognized by all lecticans, albeit differences in the affinities exist. Completing the structural models of the lecticans and their splice-variants by including the singular GAG-attachment regions between the largely homologous globular ends makes evident that this proteoglycan family forms an almost perfect array of functionally closely related but differently sized modular proteins (Fig. 1).

Besides the large aggregating proteoglycans of the lectican family, phosphacan, a secreted CSPG-isoform of the receptor-type protein-tyrosine phosphatase β (RPTPβ), plays a prominent role in the brain ECM (Barnea et al. 1994; Maurel et al. 1994; Shitara et al. 1994). Like the other alternative splice products of the RPTPβ gene, it is composed of a carbonic anhydrase domain, a fibronectin type III repeat and a spacer element, but lacks the transmembrane domain and the cytoplasmic tyrosine phosphatase modules. An additional element, present in phosphacan and the larger phosphatase variant, carries three to four chondroitin sulfate chains and sporadically also a few keratan sulfates (Rauch et al. 1991).

Phosphacan/RPTPβ binds in a calcium-dependent manner to the ECM glycoproteins tenascin-R and tenascin-C (Milev et al. 1997; Xiao et al. 1997). It furthermore interacts in vitro with various cell adhesion molecules of the Ig-superfamily (IgCAMs) including N-CAM, Ng-CAM, axonin-1 (TAG-1) and contactin (F3/F11) (Milev et al. 1994, 1996; Peles et al. 1995), and it binds to the extracellular portion of voltage-gated sodium channels (Ratcliffe et al. 2000). The interaction with contactin and the sodium channels seems to be mediated by the carbonic anhydrase (CAH) domain of RPTPβ/phosphacan (Peles et al. 1995; Ratcliffe et al. 2000).

Link proteins

The interaction between hyaluronan and lecticans is reinforced by small link proteins, collectively denominated

HAPLNs (hyaluronan and proteoglycan binding link proteins) (Spicer et al. 2003). This family of ancillary glycoproteins consists of four members, including the classical cartilage link protein (HAPLN1 = Crtl1) (Neame and Barry 1993). Since its discovery several decades ago, HAPLN1 Crtl1 has also been detected in brain, where it joins two other link proteins, the CNS-restricted HAPLN2/Bral1 and HPLN4/Bral2 (Bekku et al. 2003; Hirakawa et al. 2000). Only HAPLN3/Lp3 seems to be absent from the brain parenchyma, however, being expressed by the smooth muscle cells of larger blood vessels (Ogawa et al. 2004; Spicer et al. 2003).

The structure of the link proteins strongly resembles the globular G1 regions of lecticans, as they are all built-up of an Ig-fold and a hyaluronan-binding tandem repeat. There is some evidence that the interaction with lecticans may either be mediated by the Ig-fold (aggrecan) or by the tandem repeat of the link protein (versican). This functional relationship between HAPLNs and lecticans is also reflected in their chromosomal location and genomic organization. Intriguingly, each of the link protein genes is paired up with one of the lectican genes: *HAPLN1* with *VCAN, HAPLN2* with *BCAN, HAPLN3* with *AGC* and *HAPLN4* with *NCAN* (Spicer et al. 2003). Despite this particularity, the expression and binding preferences of link proteins and lecticans seem to be uncoupled from their genomic setup. For instance, HAPLN1/Crtl1 is co-expressed and interacts with aggrecan in cartilage and possibly in brain, while versican, V0 and V1, and HAPLN3/Lp3 are both synthesized in smooth muscle tissues and may bind to each other at these locations (Ogawa et al. 2004). Alternatively, the same versican isoforms or neurocan may team up with HAPLN1/Crtl1 to form ternary complexes with hyaluronan during brain development (Hirakawa et al. 2000; Matsumoto et al. 2003; Rauch et al. 2004; Seyfried et al. 2005; Shi et al. 2004). Finally, there are strong indications that pairs of HAPLN2/Bral1 and versican V2 (Oohashi et al. 2002) and of HAPLN4/Bral2 and brevican associate in mature brain tissues with hyaluronan (Bekku et al. 2003).

Tenascins

Apart from hyaluronan, lecticans and link proteins, tenascins represent the fourth class of molecules that form the basic constituents of the brain ECM. Tenascins (Tn) are very large multimeric glycoproteins that are well conserved among vertebrates (reviewed by Chiquet-Ehrismann and Chiquet 2003; Hsia and Schwarzbauer 2005; Joester and Faissner 2001; Jones and Jones 2000). In mammals, the family consists of four members namely tenascin-C, -R, -X and -W (-N). The macromolecular structures of the different tenascin monomers are highly alike as they follow the same modular arrangement. They are built of an amino-terminal cysteine-rich oligomerization region composed of three to four α-helical heptad repeats, EGF-like elements, fibronectin type III-repeats (FN III) and a carboxyl-terminal fibrinogen-like globular domain.

The heptad domains allow an N-terminal association of the individual subunits that primarily form homotrimers. In tenascin-C and tenascin-W, an additional cysteine residue in this region permits these trimers to further assemble into large hexameric structures, the so-called hexabrachions. Although this cysteine is also present in tenascin-R, only trimers of this ECM molecule have been observed so far.

While the number of EGF-like repeats varies only between the different tenascins, some of the FN III domains are also subjected to alternative splicing. Since different combinations of these variable FNIII repeats are possible, several isoforms of the individual tenascins exist (Jones and Jones 2000). For instance, the tenascin-C monomers bear 14.5 EGF-repeats plus 17 FN III repeats, 9 of which can be alternative spliced. As a result, up to 27 different tenascin-C transcripts may be expressed during mouse brain development (Joester and Faissner 1999), each subunit comprising molecular weights in the range of 180–300 kDa. In contrast, tenascin-R, which includes 4.5 EGF and 9 FN III repeats, gives rise only to two splice variants of 180 and 160 kDa per subunit. This difference depends on the presence or absence of a supplementary FN III module between the FN III-repeats 5 and 6 (Fuss et al. 1993). Alternative splicing seems also to generate different isoforms of Tn-X (Ikuta et al. 1998) and Tn-W/Tn-N, the latter representing variants originating from the same gene (Neidhardt et al. 2003; Scherberich et al. 2004). Because the neural expression of Tn-W/Tn-N is currently still rather controversial (Neidhardt et al. 2003; Scherberich et al. 2004) and because Tn-X does not reach significant levels in the central nervous system (Matsumoto et al. 1994), we will focus in the following only onto the two other tenascin-family members.

Both, tenascin-C and tenascin-R bind to a wealth of extracellular matrix and cell surface ligands (Jones and Jones 2000). These interactions are mainly mediated by the FN III modules. The majority of the cellular receptors for tenascin-C and tenascin-R belong to the integrins, to the cell surface heparan sulfate proteoglycans (syndecans, glypicans) or to the cell adhesion molecules of the immunoglobulin superfamily (Ig-CAMs contactin/F11/F3, axonin/TAG-1 and neurofascin). Other cell surface binding partners are annexin II and the receptor protein tyrosine phosphatase (RPTP-ζ/β). Albeit of uncertain physiological relevance, a low affinity of the EGF-like repeats of Tn-C for EGF-receptors has also been reported (Swindle et al. 2001). Among the major ECM binding partners of these tenascins are fibronectin, phosphacan and particularly lecticans.

Supramolecular assembly

The ability of the brain ECM-components to selectively aggregate, leads to the establishment of large, relatively loose and flexible meshworks where hyaluronan acts as backbone. The current concept of supramolecular organization and assembly is mainly based on affinity measurements in vitro (mentioned before) and on recent rotary shadowing electron micrographs displaying the corresponding large multi-molecular complexes (Lundell et al. 2004). In this model, filamentous hyaluronan-molecules extruding from the neuronal cell membrane associate first with the G1 domains of distinct lecticans and link proteins that stabilize the complex. At the other end of the lectican core protein, the G3 domains engage in an interaction with one of the arms of the tenascin oligomers. This way tenascins may cross-link up to three (Tn-R) or up to six lecticans (Tn-C) and consequently bridge neighboring hyaluronan/lectican/link protein-complexes to complete the extracellular network. Supposing that the different components are proportionally expressed, the mesh size of this structure will be determined by the length of the tenascin arm, the distance between the lectican G1/link protein-aggregates along the hyaluronan molecules and most importantly by the dimension of the lectican core protein. Hence, the network would become roughly twice as dense by replacing for instance the V0 isoform of versican by the V2 variant and switching from Tn-C to Tn-R. Along with the change of lectican expression, the proportion of negatively charged carbohydrates and consequently the amounts of attracted water and cations may alter the gel-like properties of the extracellular matrix that occupies the intercellular spaces within the central nervous system. Indeed, the estimated change of the extracellular volume from roughly 40% in the developing brain to about 20% in adults (Nicholson and Sykova 1998) may at least partly be linked to the general tendency to express smaller lectican variants in the course of tissue maturation.

Expression and distribution

Gaining a clear insight into the expression and distribution of ECM components in development and adulthood has not been an easy task as especially antibodies widely employed in the earlier immunohistochemical studies were often not monospecific. Since ex vivo isolates of the highly glycosylated molecules were frequently used for immunization, several monoclonal antibodies have recognized carbohydrate epitopes, which could be found in glycans of several glycoproteins and/or were sometimes only present in subfractions of a particular ECM component (Lander et al. 1997; Matthews et al. 2002; Yamagata et al. 1993; Zako et al. 2002). Another cause for antibody cross-reactivity has also been the high protein sequence conservation, as in the G1 and G3 domains of the lecticans, and the consequent epitope sharing (Bignami et al. 1993; Perides et al. 1993; Yamada et al. 1997b). With the increasing availability of cDNAs and the advent of recombinant expression systems in bacteria, however, antibody production could be directed against more selective sites in little or non-glycosylated regions of the proteins (Milev et al. 1998b; Schmalfeldt et al. 1998; Zimmermann et al. 1994) (Fig. 1). Consequently, a set of highly specific and sensitive polyclonal antibodies with well-defined immunoreactivity has revealed a more consistent picture of ECM expression.

Tenascins C and R, phosphacan, most of the link proteins and all lecticans, including alternative splice-variants, are at some stage present in the central nervous system (Bandtlow and Zimmermann 2000; Jones and Jones 2000; Rauch 2004; Yamaguchi 2000). While Tn-R, phosphacan, HAPLN2/Bral1, HAPLN4/Bral2, brevican, neurocan and versican V2 are uniquely expressed in brain and spinal cord, Tn-C and the versican isoforms V0, V1 and V3 are also found in many mesenchymal tissues during embryogenesis and later in association with remodeling processes induced by, e.g., injury, neovascularization, inflammation or neoplasia. Likewise, aggrecan and HAPLN1/Crtl1, which participate in the establishment of some specialized brain ECMs, are primarily components of developing and mature cartilage. Finally, hyaluronan, which interacts with all the lecticans, displays the widest tissue distribution, being (also outside the nervous system) most abundantly produced by morphogenetically active zones during development and adult remodeling processes (Toole 2001, 2004).

Juvenile matrix type

During late embryonic and early postnatal phases of mammalian development, a juvenile type of extracellular matrix is initially formed in the CNS (Fig. 2). It mostly consists of hyaluronan, neurocan, versican V0, versican V1, tenascin-C and HAPLN1/Crtl1 (Milev et al. 1998b; Rauch 2004). In addition, prominent CNS-expression of aggrecan has been reported in chick embryos (Schwartz and Domowicz 2004), while only very small amounts have been detected in prenatal rodent brains (Matthews et al. 2002; Milev et al. 1998c). Cellular origin of neurocan and the large versican variants are neurons (Engel et al. 1996; Yamagata and Sanes 2005), whereas aggrecan appears to be mainly expressed by cells of astroglial lineage at this early time point (Domowicz et al. 2008). The transient deposition of neurocan and versican V0/V1, peaks in rats shortly after birth (Fig. 3) (Meyer-Puttlitz et al. 1995; Milev et al. 1998a). Preferential accumulations are the marginal zone and the subplate of the

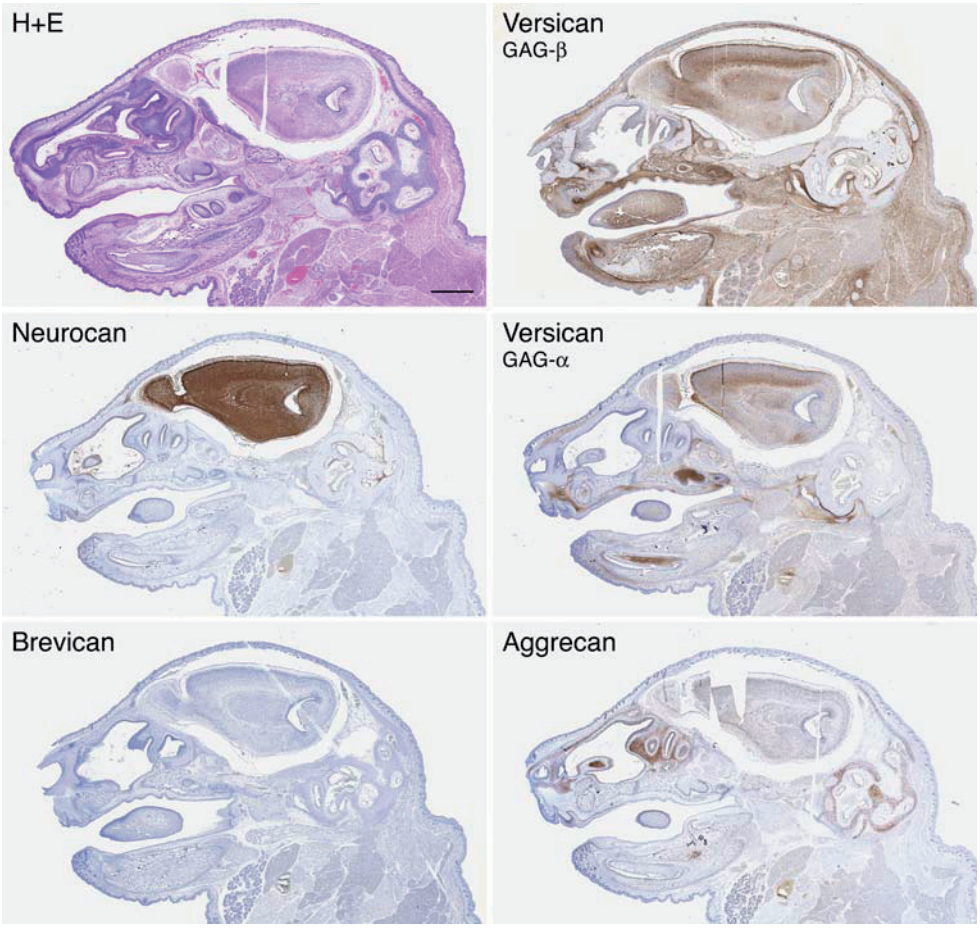

Fig. 2 Immunohistochemical analyzes of the lectican distribution in the head region of E18.5 mouse embryos. Note the strong brain-specific staining of antibodies against neurocan. The antibodies against versican detect at this time point mainly the versican splice-variants V0 (GAG-α and GAG-β reactive) and V1 (only GAG-β reactive). These versicans are deposited in the CNS and in most of the mesenchymal tissues of the embryo. Aggrecan is practically absent from the brain, but is strongly expressed in cartilaginous tissues. No brevican staining can be detected at this embryonic stage. Sagittal sections. *Bar* 100 μm

neocortex, parts of the hypothalamus, the amygdala and the developing hippocampus and dentate gyrus (Meyer-Puttlitz et al. 1996; Miller et al. 1995; Popp et al. 2003). Early postnatally, neurocan and the versican isoforms V0 and V1 are also found in the presumptive white matter and in the internal granule cell layer of the cerebellum (Meyer-Puttlitz et al. 1996; Popp et al. 2003). Starting from the second week after birth they are down-regulated and finally only persist in a few specialized locations in the adult CNS.

The time course of this early lectican expression is paralleled by their ligands, hyaluronan and the HAPLN1/Crtl1 link protein. In fact, the content of hyaluronan peaks in rodent brain shortly after birth, being subsequently reduced to one-fourth of its maximal level in the adult tissue (Margolis et al. 1975). In the developing cerebellum, hyaluronan is mostly present in the granular cell layer and prospective white matter (Ripellino et al. 1988), where it seems to be organized into extracellular arrays of fiber-like structures (Baier et al. 2007). There is evidence that glial cells synthesize hyaluronan in the early phase of the CNS formation (Deyst and Toole 1995), the hyaluronan synthase responsible for its production at this early stage has yet to be identified. Similar to hyaluronan, HAPLN1/Crtl1, which may stabilize the interaction of hyaluronan with neurocan, versican and aggrecan, is up to about postnatal day 10 increasingly expressed and then gradually diminishes in the maturating nervous tissue (Hirakawa et al. 2000).

A relatively early CNS expression is also observed for the glia-derived ECM glycoprotein Tn-C. It first accumulates around the fibrous processes of radial and Bergmann glial cells that direct the migration of neuronal precursors during cortical and cerebellar development, respectively (Crossin et al. 1986; Prieto et al. 1990). In rodents, it is rather widely distributed shortly after birth and displays at least in the cerebral cortex, hippocampus and cerebellum partial overlaps with neurocan and versican V0/V1 depositions (Bartsch et al. 1992; Laywell and Steindler 1991; Meyer-Puttlitz et al. 1996; Popp et al. 2003). Particularly intriguing is the transient association of Tn-C with the glial boundary tissues surrounding the functional sets of neurons, like for instance the vibrissae-related barrel fields of the developing somatosensory cortex (Steindler et al. 1989). About 2–3 weeks after birth, Tn-C levels decrease continuously, maintaining only a significant expression level in the neurogenetically active areas of the adult brain that encompass the subependymal zone and the hippocampus

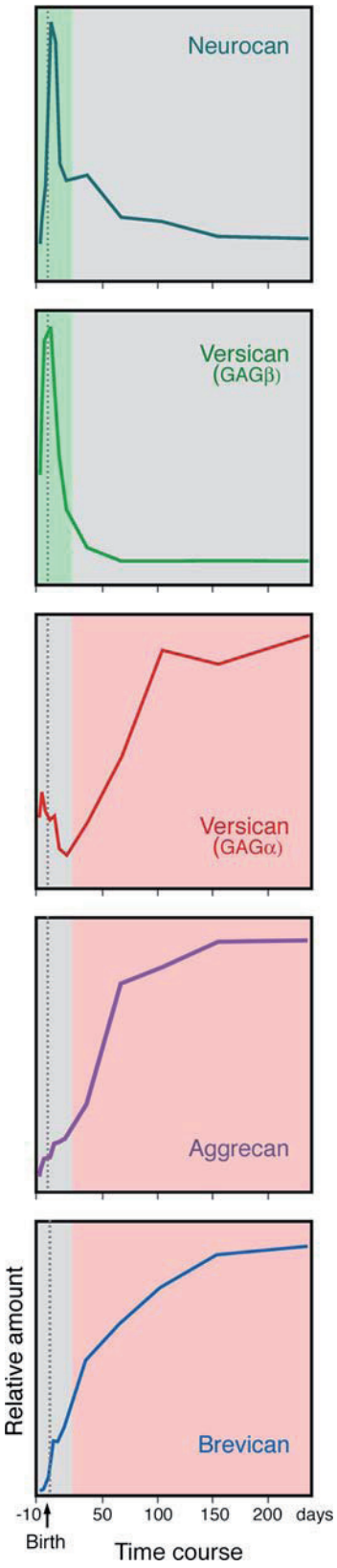

Fig. 3 Time course of lectican levels in extracts of embryonic and postnatal rat brains. Note the transition from the expression of the juvenile-type of matrix to its mature form around postnatal day 20. Diagrams adapted from (Milev et al. 1998b)

(Bartsch et al. 1992; Dorries and Schachner 1994; Gates et al. 1995; Thomas et al. 1996).

Mature matrix type

Initiating about 2 weeks after birth, a major remodeling process takes place (Fig. 3), which replaces most of the juvenile type of matrix by its mature form (Rauch 2004). This exchange transforms the relatively loose embryonic and early postnatal ECM to a significantly firmer meshwork, which is subsequently maintained throughout adulthood. The large majority of the early matrix components are along the conversion substituted by a different, but homologous set of ECM proteins that include versican V2, aggrecan, brevican, phosphacan, tenascin-R and the brain link proteins HAPLN2/Bral1 and HAPLN4/Bral2 (Bekku et al. 2003; Hirakawa et al. 2000; Meyer-Puttlitz et al. 1995; Milev et al. 1998b; Pesheva et al. 1989).

In the adult CNS, various combinations of lecticans and link protein, which are generally associated with hyaluronan, Tn-R and phosphacan condense at some strategic locations (Fig. 4.). Versican V2 and the secreted brevican isoform emerge around the second and third week postpartum and subsequently evolve to the predominant constituents in the adult brain and spinal cord (Schmalfeldt et al. 1998; Yamaguchi 1996). Matrices that contain mainly versican V2 and some brevican are most prevalent in the white matter surrounding the myelinated fibers of all calibers (Ogawa et al. 2001; Schmalfeldt et al. 2000). Particularly dense accumulation of versican V2, HAPLN2/Bral1, Tn-R and phosphacan appear as ring-like structures around the CNS nodes of Ranvier (Dours-Zimmermann et al. unpublished; Melendez-Vasquez et al. 2005; Oohashi et al. 2002; Pesheva et al. 1989; Xiao et al. 1997). Origins of the Tn-R and versican V2 deposits in the white matter are primarily oligodendrocytes and their precursors (Asher et al. 2002; Pesheva et al. 1989; Schmalfeldt et al. 2000), while HAPLN2/Bral1 expression has been attributed to neurons (Oohashi et al. 2002) or oligodendrocytes (Carulli et al. 2006). Interestingly, the brevican expression shifts at the end of myelination from oligodendroglial to astrocytic lineage in the white matter (Ogawa et al. 2001). Starting from postnatal day 28, astrocytes seem to give rise to another particularly brevican-rich zone that forms after completion of the neuronal migration in the granular cell layer of the rat cerebellum. This more compact extracellular matrix ensheathes cerebellar glomeruli, in which the incoming mossy fibers contact the local neuronal processes (Yamada et al. 1997a).

The by far best studied extracellular matrix condensation in the adult central nervous system is the perineuronal net (PNN). This lattice-like structure engulfs the cell bodies, proximal dendrites and axon initial segments of specific

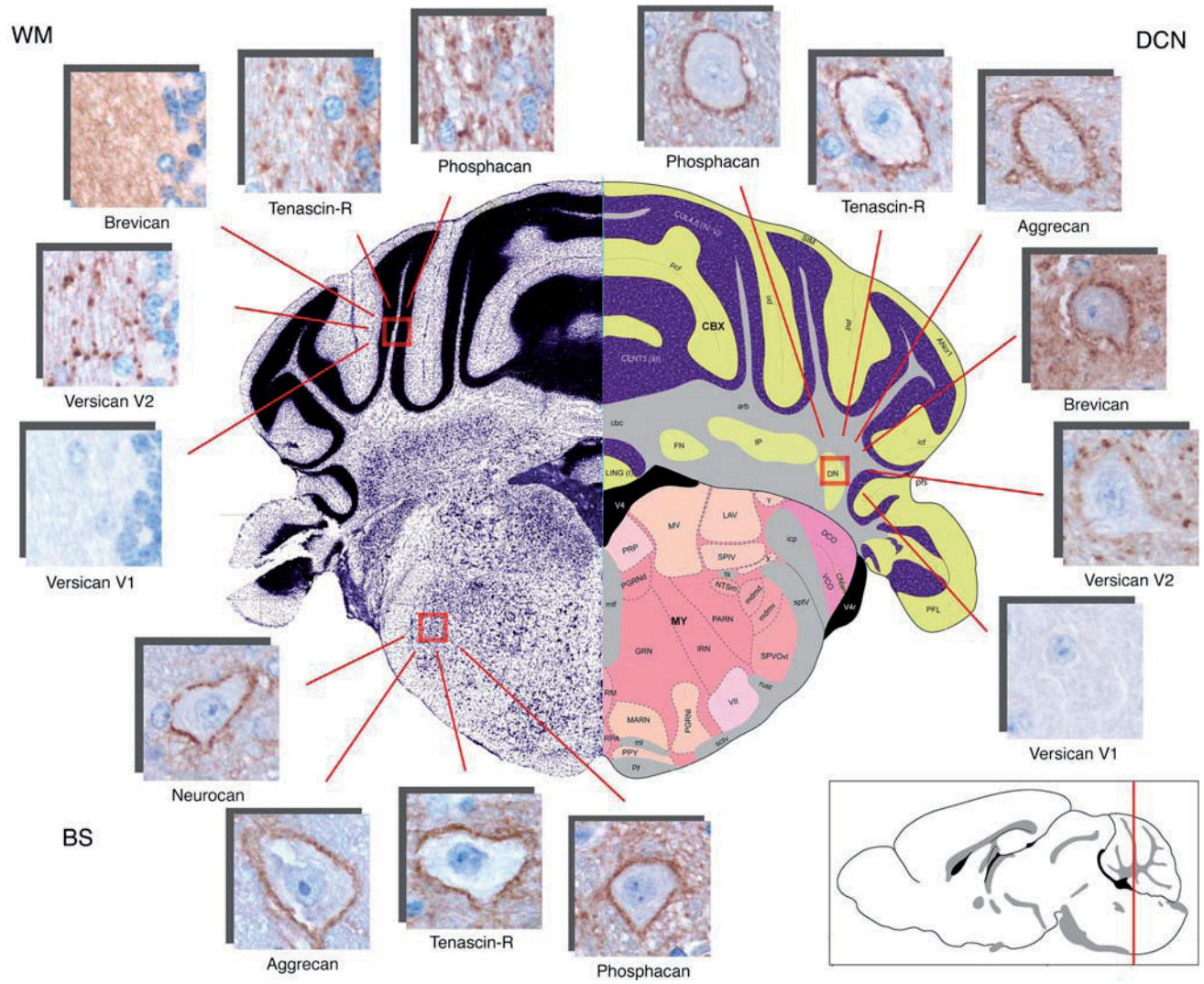

Fig. 4 Localization of lecticans and tenascins in coronal sections through adult cerebellum and medulla at Bregma −6.18 mm. Note the perineuronal net staining of aggrecan, tenascin-R and phosphacan in the deep cerebellar nuclei (*DCN*) and the brain stem (*BS*). Brevican and neurocan are only present in some of the PNNs. Versican V2, which stains exclusively with GAG-α-, but not with GAG-β-specific antibodies is accumulating at the nodes of Ranvier in the white matter (*WM*), while brevican staining is rather diffused in the myelinated fiber tracts. Versican V0 and V1, which are recognized by the GAG-β-specific antibodies are absent from these brain regions in adult mice. Graphics modified from the Allen Brain Atlas (http://www.brain-map.org) (Lein et al. 2007)

subsets of neurons and embeds, with exception of the synaptic clefts, the presynaptic boutons that contact them (Bruckner et al. 1993, 2006; Celio and Blumcke 1994; Celio et al. 1998; Galtrey and Fawcett 2007; Murakami and Ohtsuka 2003; Rhodes and Fawcett 2004; Yamaguchi 2000). PNNs can be observed in many areas of the CNS including the cerebral cortex, the hippocampus, the thalamus, the cerebellum, the brain stem and the spinal cord. They most frequently surround parvalbumin-expressing GABAergic interneurons and certain cortical pyramidal neurons, as well as projection and large motor neurons of the brain stem and spinal cord. The formation of perineuronal nets occurs relatively late in postnatal development (in rodents 2–5 weeks after birth) and coincides with the ending of the experience-dependent refinement of the synaptic network and the closure of the critical period, e.g., in the visual system and spinal cord (Guimaraes et al. 1990; Kalb and Hockfield 1988, 1990; Pizzorusso et al. 2002).

This specialized matrix consists of hyaluronan, different lecticans, the link proteins HAPLN1/Crtl1 and HAPLN4/Bral2, Tn-R, and phosphacan (Asher et al. 1995; Bekku et al. 2003; Bruckner et al. 2000; Carulli et al. 2006; Haunso et al. 1999; Maeda et al. 1995). The perineuronally accumulating hyaluronan is synthesized by HAS2 and HAS3 expressed in the net-carrying neurons, while HAS1 is generally absent from the CNS (Carulli et al. 2006, 2007). During the PNN-formation, HAS3 may slightly precede HAS2. The expression of both of these hyaluronan

synthases is subsequently attenuated, but pertains throughout adulthood.

Among the lectican family members, aggrecan is the most common perineuronal net component. Although present in all PNNs, it may contribute to a certain sub-specialization by varying its glycan structures between distinctive sets of neuronal coats (Matthews et al. 2002). Brevican and neurocan display in many CNS regions an expression pattern similar to aggrecan (Fig. 4) and there is indeed some evidence that they co-localize within the same perineuronal structure (Carulli et al. 2006; Galtrey et al. 2008). At least hyaluronan, aggrecan and Tn-R seem to be rather uniformly distributed within a single net covering the cell body, proximal dendrites and the axon initial segment (AIS) irrespective of the presence of synapses (Bruckner et al. 2006). In contrast, a certain preference of brevican deposition around the AIS has been observed in neuronal cell cultures (Hedstrom et al. 2007; John et al. 2006). Using a monoclonal antibody (12C5) against the hyaluronan-binding G1 domain of versican, immunohistological examinations of brain and spinal cord sections have also suggested that the fourth lectican member is present in PNNs (Carulli et al. 2006; Deepa et al. 2006). Surprisingly, none of our antibodies against the two GAG-attachment regions (Fig. 1) has displayed a similar perineuronal net staining (Fig. 4). It is therefore conceivable that the 12C5 antibody, in fact does not detect intact versican V2 in the PNNs, but rather a proteolytic remnant of the early postnatal versican V0 and V1 expressions that correspond to the versican fragment, formerly named as glial hyaluronate-binding protein (GHAP) or hyaluronectin (Delpech and Halavent 1981; Perides et al. 1989). Also neurocan in the PNNs may at least partly be present in form of a hyaluronan-binding truncation product (Neurocan-*N*) (Deepa et al. 2006), which eventually has become trapped after the conversion of the juvenile matrix.

No matter whether the lecticans are intact or truncated, their interactions with hyaluronan seem to be either stabilized by HAPLN1/Crtl1 or by HAPLN4/Bral2 (Bekku et al. 2003; Carulli et al. 2006, 2007). Both of these link proteins form an integral part of perineuronal nets. Whereas HAPLN1/Crtl1 seems to bind to its classical partner aggrecan and probably also to neurocan or neurocan-*N*, there is some indication from knockout mice that brevican may be required for the PNN localization of HAPLN4/Bral2 (Bekku et al. 2003).

Most of the perineuronal net constituents seem to be expressed by the engulfed neurons themselves (Carulli et al. 2006). Nonetheless, contributions from surrounding astrocytes that extend cellular processes into the reticular structure cannot be excluded (Carulli et al. 2007). This concerns particularly brevican and to some extent also neurocan, which may be produced bilaterally by the ensheathed neurons and the contacting astrocytes. Co-culture experiments of primary hippocampal neurons and glial cells indeed revealed that the perineuronal deposits of brevican are in vitro primarily astrocyte-derived (John et al. 2006), although perineuronal net-like structures develop apparently also in the virtual absence of glial cells (Miyata et al. 2005).

Lesion-associated reactive matrix

Once established, the composition of the mature type of extracellular matrix is rather stable with little or no turnover of their components. This changes, however, radically, when lesions to the adult central nervous system occur. Under these circumstances, the expression of various extracellular matrix molecules is highly up-regulated and major depositions are observed in and around the lesion site, in particular, in association with the glial scar tissue that forms (Bradbury and McMahon 2006; Galtrey and Fawcett 2007; Gonzenbach and Schwab 2008; Morgenstern et al. 2002; Zurn and Bandtlow 2006). The freshly produced ECM components may be secreted by reactive astrocytes, oligodendrocyte precursors, microglia/macrophages and eventually by meningeal cells. The lesion and consequent reactive processes induce a matrix accumulation that strongly resembles the juvenile-type of meshwork previously observed during early nervous system development. For instance, surgical incisions in the cerebral cortex or spinal cord provoke a relatively fast and transient up-regulation of Tn-C and neurocan (Asher et al. 2000; Haas et al. 1999; Jones et al. 2003; Laywell et al. 1992; Matsui et al. 2002; McKeon et al. 1999; Tang et al. 2003). Also the expression of versican V2, brevican and phosphacan appear to be affected. Yet, recent reports about alterations in the production of versican V2 (direction of regulation) and brevican (timing) are somewhat controversial (Asher et al. 2002; Jones et al. 2003; Tang 2003). There are nevertheless indications that the lecticans brevican, aggrecan and versican V2 follow the time course of phosphacan, whose content first diminishes during the acute phase and then increases in a late attempt to restore the mature type of matrix at the injury site (Lemons et al. 2001; Tang et al. 2003).

A similar post-traumatic upregulation of Tn-C and lecticans has also been observed after disruption of sensory axons at the dorsal root (Beggah et al. 2005; Pindzola et al. 1993). Importantly, this type of lesion near the PNS/CNS interface lacks a scar formation within the CNS, but still leads to a reactive gliosis in the dorsal root entry zone (DREZ) and Wallerian degeneration of the central axon branches, now separated from their cell bodies. Despite the absence of a glial scar tissue, elevated depositions of neurocan and versicans (also V1 isoform) are prominent in the DREZ suggesting that the remodeling process temporally

reactivates a juvenile matrix-like expression profile analogous to direct damages to the CNS.

Matrix turnover

The rapid switch from embryonic and early postnatal extracellular matrices to their mature form in the normal adult CNS (Rauch 2004), the fast disappearance of CSPGs from the predestined axonal pathways observed in the developing periphery (Landolt et al. 1995; Oakley and Tosney 1991), as well as the reactive changes following nervous system lesions (Galtrey and Fawcett 2007; Zurn and Bandtlow 2006) cannot solely be attributed to adjustments in the ECM expression patterns, but must also depend on highly active proteolytic processes (Agrawal et al. 2008; Ethell and Ethell 2007; Flannery 2006; Gottschall et al. 2005; Milward et al. 2007; Porter et al. 2005). The selective turnover of lecticans may in this context be essential for altering the cell migration and axon growth properties of many nervous tissues. Metalloendopeptidases of the ADAMTS family seem to be primarily responsible for the lectican catabolism (ADAMTS: a disintegrin and metalloproteinase with thrombospondin motifs). Conversely, matrix metalloproteases (MMPs) may only play a subordinate role in the proteoglycan degradation, but they could preferentially target the link proteins and tenascins of the central nervous system. In any case, the proteolysis is tightly controlled by the tissue inhibitors of metalloproteinases (TIMPs), which are physiological antagonists of both enzyme types, MMPs (TIMP-1 to -4) and ADAMTSs (TIMP-3).

Various ADAMTS-enzymes cleave lecticans at a few specific sites in vitro and corresponding digestion products have been identified in vivo (Flannery 2006; Gottschall et al. 2005; Porter et al. 2005). The secreted ADAMTSs are close relatives of the cell membrane-bound ADAM metalloproteases. ADAMs and ADAMTSs are expressed as zymogens containing a prodomain and a zinc-binding catalytic element linked to a disintegrin-like motif. In ADAMTSs, several additional modules may control tissue localization and contribute to the substrate specificity. This C-terminal set of ancillary domains includes a central thrombospondin type I repeat, a cysteine-rich region, a spacer element and several supplementary thrombospondin motifs in most of the family members. The ADAMTS-zymogens are in the trans-Golgi or at the cell surface activated by N-terminal propeptide cleavage mediated by furin or furin-like convertases. Additional proteolytic or autocatalytic removal of a C-terminal portion has been demonstrated to modulate the enzymatic activity of some of these metalloproteases (Gao et al. 2002; Rodriguez-Manzaneque et al. 2000; Zeng et al. 2006).

Five ADAMTS sites have been characterized in the aggrecan core protein (Caterson et al. 2000; Lemons et al. 2001), two to four in the proteoglycan isoforms of versican (V2–V0) (Jonsson-Rylander et al. 2005; Sandy et al. 2001; Westling et al. 2004) and one in brevican (Matthews et al. 2000; Yamada et al. 1995). Interestingly, in all of these lecticans one ADAMTS-site is located next to the globular G1-domain allowing the selective release of the large GAG-carrying portions from the complex with hyaluronan and link proteins. Finally, also neurocan, which is in adult tissues often present in form of two well-defined N- and C-terminal fragments, may be cleaved by an ADAMTS- or MMP-protease. Based on comparisons of known substrates, specific sites for by MMP-2- and ADAMTS-processing have been postulated. Whereas MMP-2 indeed cleaves neurocan in vitro, the susceptibility to ADAMTS-digestion still has to be confirmed in an experimental setting (Sandy et al. 2001; Turk et al. 2001).

Among the 19 ADAMTSs, seven exhibit cleavage capacity towards lecticans (ADAMTS-1, -4, -5, -8, -9, -15 and -20; ADAMTS-5 and -11 are identical). The classical aggrecanases are ADAMTS-4 and -5 (Abbaszade et al. 1999; Tortorella et al. 1999). Albeit less efficient, aggrecan-processing activities have also been observed of ADAMTS-1, -8, -9 and -15 (Collins-Racie et al. 2004; Flannery 2006; Kuno et al. 2000; Somerville et al. 2003). At least four ADAMTS-proteases including ADAMTS-1, -4, -9 and -20 recognize versican substrates in vitro (Sandy et al. 2001; Silver et al. 2008; Somerville et al. 2003; Westling et al. 2004), whereas only cleavage by ADAMTS-4 and -5 has been demonstrated for brevican (Matthews et al. 2000; Nakada et al. 2005; Nakamura et al. 2000).

Until now, only a few studies have explored the expression of distinct ADAMTSs during nervous system development and virtually no data are available for peri- and early postnatal phases that are particularly interesting regarding the remodeling of the neural ECM. From the limited insights one can currently conclude, that ADAMTS-1 and -9 are expressed relatively early in the embryonic CNS (Gunther et al. 2005; Jungers et al. 2005; Thai and Iruela-Arispe 2002), while ADAMTS-4 appears only in adult nervous tissues (Abbaszade et al. 1999; Jungers et al. 2005). Moderate to low expression of ADAMTS-4, for instance has been detected in pyramidal neurons of various cortical areas and in granule cells of the dentate gyrus in normal adult brain (Yuan et al. 2002).

This base-expression of ADAMTSs rises considerably in the presence of different types of lesions. After a kainate-induced excitotoxic insult, a transient up-regulation of ADAMTS-4 and ADAMTS-1 coincides with a marked increase of brevican proteolysis (Mayer et al. 2005; Yuan et al. 2002). A similar reaction is also observed in an experimental model of cerebral ischemia (Cross et al. 2006). Moreover, motor axon disruption induces the ADAMTS-1 production in the affected neurons (Sasaki et al. 2001) and

there is growing evidence that the same enzyme is also over-expressed in association with various neurodegenerative disorders (Miguel et al. 2005; Satoh et al. 2000). In addition, glioblastomas display elevated levels of brevican and its proteolytic fragments (Nutt et al. 2001) are associated with an increased expression of ADAMTS-5 and, although somewhat controversial, possibly also with ADAMTS-4 (Held-Feindt et al. 2006; Nakada et al. 2005). This close relationship between ECM remodeling and ADAMTS expression under traumatic and pathogenic conditions, provides an indirect indication for an analogous functional involvement of ADAMTSs in the matrix conversion of normal neural development.

Putative functions

The progress in unraveling the precise functions of the extracellular matrix in the central nervous system has for long been rather slow due to the high structural variability of its main constituents and the great complexity of the dynamic remodeling process involved in normal development and disease conditions. Albeit correlations of the distribution of specific ECM components with cellular processes like proliferation, migration, axonal growth or synapse formation have been very valuable for gaining insights into the putative functions in vivo, they may have been somewhat distorted by the fact that most antibodies used in these studies are unable to discriminate between intact and ADAMTS- or MMP-processed forms of a particular molecule. This distinction could be of considerable importance as the specific cleavage may attenuate or even neutralize certain ECM functions without becoming apparent in the immunohistological stainings.

Moreover, partial overlapping rather than completely different functions of structurally related matrix proteins may be responsible for the unexpectedly mild phenotypes of several knockout mice, while the absence of potential key components has in contrast resulted in embryonic or perinatal lethality that prevents the study of their role in the mainly postnatal neural development (Table 2). Nevertheless, evidence for an extracellular matrix involvement in neural migration, axon guidance, plasticity restriction and fiber tract stabilization has in recent years come from various in vitro and in vivo observations.

Axon growth inhibition

Phosphacan and all lecticans of the central nervous system inhibit in their intact form axonal growth in vitro (Bandtlow and Zimmermann 2000; Yamaguchi 2000). This functional property appears to be mostly core protein-dependent in versican V0, V1 and V2 (Dutt, Stöckli and Zimmermann unpublished; Niederöst et al. 1999; Schmalfeldt et al. 2000;), neurocan (Margolis et al. 1996) and phosphacan (Maeda and Noda 1996), whereas no inhibition of brevican (Yamada et al. 1997a) and cartilage-derived aggrecan (Snow et al. 1990) has been detected after chondroitinase ABC digestion. Notably, we also observed two- to three-fold reductions, but never an abolition of the inhibitory capacity of versican V2 in stripe choice experiments after complete glycosaminoglycan-removal (Schmalfeldt et al.

Table 2 Available ECM-knockout mouse strains

Gene	Viability	CNS phenotype
Brevican (*Bcan*)	Normal	Reduced LTP
Neurocan (*Ncan*)	Normal	Reduced LTP
Versican (*Vcan*/*hdf*-strain)	Die at E10.5	–
Aggrecan (*Acan*/*cmd*-strain)	Die at birth	ND
RPTP-*β*/phosphacan (*Ptprz1*)	Normal	Enhanced LTP; impaired recovery from EAE (transmembrane variants?)
Tenascin-R (*Tnr*)	Normal	Aberrant PNNs; reduced conduction velocity; disturbed neuroblast migration in olfactory bulb; some behavioral abnormalities
Tenascin-C (*Tnc*)	Normal	Reduced LTP; mild behavioral abnormalities
HAPLN1/Crtl1 (*Hapln1*)	Die at birth	ND
HAS2 (*Has2*)	Die at E10.5	–
HAS3 (*Has3*)	Normal	ND

LTP Hippocampal long-term potentiation, *EAE* experimental autoimmune encephalomyelitis, *PNN* perineuronal net, *ND* not described

Brevican (Brakebusch et al. 2002); neurocan (Zhou et al. 2001); versican (Mjaatvedt et al. 1998); aggrecan (Watanabe et al. 1994); RPTP-*β*/phosphacan (Harroch et al. 2000, 2002; Niisato et al. 2005); TnR (Bruckner et al. 2000; Freitag et al. 2003; Haunso et al. 2000; Montag-Sallaz and Montag 2003; Saghatelyan et al. 2004; Weber et al. 1999); TnC (Evers et al. 2002; Forsberg et al. 1996; Fukamauchi et al. 1996; Kiernan et al. 1999; Saga et al. 1992); HAPLN1/Crtl1 (Watanabe and Yamada 1999); HAS2 (Camenisch et al. 2000); HAS3 (Bai et al. 2005)

2000). This moderate decrease might be related to the partial collapse of the extended core protein structure after elimination of the highly negatively charged chondroitin sulfate side chains.

The axonal growth inhibition is likely dependent on the presence of a pericellular hyaluronan coat that covers many cell types and often includes variable amounts of lecticans, link proteins and tenascins (Evanko et al. 2007). Synthesis of hyaluronan alone promotes in various cell types the formation of plasma membrane protrusions (Kultti et al. 2006; Rilla et al. 2008). It is therefore conceivable that a coat containing exclusively hyaluronan has a similar effect in generating growth cone filopodia exploring the environment at the tip of growing axons. In situations, in which these filopodia encounter areas expressing lecticans, they may incorporate the CSPGs into the pericellular hyaluronan structure and consequently increase the hydration capacity and thus the thickness of their coat. Depending on the extent of this coat swelling, the contacts to the surface of neighboring cells or the extracellular matrix may be increasingly compromised by sterical hindrance. Accordingly, the advancing growth cone should slow down, turn away or retract from the lectican-containing zones. Furthermore, the expression level, core protein size and carbohydrate substitution of the encountered lecticans would control the coat dimensions and thus, modulate the inhibitory effect. In line with this hypothesis are the concentration-dependency of the versican inhibition (Schmalfeldt et al. 2000) and a certain tendency to accentuate the effect by using larger splice-variants in vitro (Dutt, Stöckli and Zimmermann, unpublished). In addition, neurons may regulate the coat size by the extent of the hyaluronan synthesis and/or by secreting ADAMTS-proteases, which would reduce the inhibitory activity through release of the GAG-carrying core protein portions from the pericellular structure.

While high-versican concentrations provoke retraction, low concentrations still allow a reduced growth, but promote enlargement of presynaptic varicosities in chick retinal axons in vitro (Yamagata and Sanes 2005). This finding is corroborated by RNA interference experiments in vivo, where depletion of versican causes a significant size reduction of the varicosities in the retinal arbors of the optic tectum suggesting that low-versican expression attenuates axonal growth and induces lamina-specific presynaptic maturation. Conversely, high expression of versican V0/V1 may also contribute to the formation of molecular barriers that block axon extension and may in addition, direct migratory neural crest cells in the developing peripheral nervous system (Dutt et al. 2006; Landolt et al. 1995; Oakley and Tosney 1991). Unfortunately, these suspected modulator functions of the V0/V1 isoforms cannot be verified in versican null mice (*hdf* strain), as they suffer from problems in heart segmentation and consequently die early, at around embryonic day 10.5 (Mjaatvedt et al. 1998).

Although the highest matrix protein expression in the CNS during early neural development has been attributed to Tn-C and neurocan, their in vivo functions in the juvenile-type of matrix are still largely unknown. Single knockouts of neurocan and Tn-C showed no apparent anatomical abnormalities in the CNS (Steindler et al. 1995; Zhou et al. 2001). A potential compensation by up-regulation of the closely related brevican or Tn-R, respectively, has not been observed. Nonetheless, recent generation of a Tn-C, Tn-R, neurocan and brevican quadruple knockout suggested a partial replacement of the tenascins by fibulin-1 and -2, which are generally not expressed in the brain parenchyma, but may similarly cross-link the C-terminal domains of the remaining lecticans (Rauch et al. 2005). This complex may however, be less stable as suggested by the partly disturbed structure of the perineuronal nets in these quadruple and in the Tn-R single knockout mice (Bruckner et al. 2000; Haunso et al. 2000; Rauch et al. 2005; Weber et al. 1999).

Regulation of plasticity

There are increasing indications that the transition from the juvenile type of matrix to its mature form terminates the highly dynamic periods of cell and axonal migrations and restricts plasticity and regeneration in the adult central nervous system (Galtrey and Fawcett 2007; Rauch 2004). In white matter, specialized matrices rich in brevican and versican V2 contribute to axon growth inhibitory environment associated with CNS myelin (Niederöst et al. 1999) and possibly prevent abnormal axon branching by accumulating at the nodes of Ranvier. In addition, the establishment of perineuronal nets seems to stabilize the neuronal circuitry by suppressing the formation of new synaptic contacts (Galtrey and Fawcett 2007; Hockfield et al. 1990; Rauch 2004; Yamaguchi 2000). These speculations that are mostly based on the inhibitory properties of lecticans in vitro, have been further nourished by observations that injections of bacterial chondroitinase into the visual cortex of rats affect the integrity of perineuronal nets and restore ocular dominance plasticity even after closure of the critical period (Berardi et al. 2004; Hooks and Chen 2007; Pizzorusso et al. 2002, 2006). Similarly enhanced plasticity after chondroitinase treatment has been reported from experimental brain and spinal cord injuries (Barritt et al. 2006; Bradbury et al. 2002; Moon et al. 2001). In these studies, the digestion of chondroitin sulfates at the lesion sites resulted in increased axonal sprouting and some axonal re-growth across the normally non-permissive glial scar tissue, which expresses CSPGs abundantly. In addition, in adult brevican and neurocan double-knockout mice, the obstruction of the lectican-rich dorsal root entry

zone appears to be partly lifted, as a significant number of sensory axons cross back into the DREZ after proximal nerve disruption and subsequent growth stimulation through a late conditioning lesion of the peripheral branch (Quaglia et al. 2008). Because the suppression of a single myelin- or ECM-associated CNS-inhibitor typically leads to less than 10% robust re-growth of cut axons in all different experimental lesion systems tested (Bradbury and McMahon 2006; Gonzenbach and Schwab 2008; Zheng et al. 2006), such multimodal strategies may be required to achieve an improved neutralization of the inhibition and a more effective promotion of the regenerative response in the CNS.

Other putative functions

Apart from these putative roles connected to axon growth inhibition, the condensed matrices in the mature central nervous system may take part in axo-glial interactions and regulate the ion homeostasis required for the rapid and timely induction and propagation of action potentials at the axon initial segments (AIS) and at the nodes of Ranvier, respectively (Bruckner et al. 1993, 2006; Hedstrom and Rasband 2006; Poliak and Peles 2003; Salzer 2003). In this context it is interesting to note, that neurocan, brevican, RPTP-β/phosphacan and also Tn-C null-mice display certain alterations of hippocampal long-term potentiation (in RPTP-β knockout mice probably only linked to transmembrane variants), while a decreased axonal conductance has been measured in the optic nerve of Tn-R mutants (Brakebusch et al. 2002; Evers et al. 2002; Weber et al. 1999; Zhou et al. 2001).

It has also been suggested that proteoglycans in the extracellular meshwork surrounding myelin-free and thus, exposed nodal regions and axon initial segments may be implemented in neuroprotective functions (Miyata et al. 2007; Morawski et al. 2004).

Finally, abrogation of Tn-R expression impairs in adult knockout mice the detachment and radial migration of neuroblasts into the outer layers of the olfactory bulb. In contrast, ectopic expression reroutes the neuroblasts that originate from the subventricular zone of the lateral ventricles and first move tangentially in the rostral migratory stream. This suggests that Tn-R alone may also act as positive cue for adult neuroblast migration (Saghatelyan et al. 2004).

Despite the panoply of putative functions of the extracellular matrix in the nervous system presented in the last years, the picture of its main roles in development and maturation has remained largely fragmented. It is to hope, that after a long period of neglect, the recently renewed research interests will boost the assembly of this fascinating puzzle.

Acknowledgments We thank Holger Moch for support and our lab-team for taking care of our diagnostic duties during the writing of this review. Our work has been partly financed by the University of Zurich, the Swiss National Science Foundation and the Velux-Foundation.

References

Abbaszade I, Liu RQ, Yang F, Rosenfeld SA, Ross OH, Link JR, Ellis DM, Tortorella MD, Pratta MA, Hollis JM, Wynn R, Duke JL, George HJ, Hillman MC Jr, Murphy K, Wiswall BH, Copeland RA, Decicco CP, Bruckner R, Nagase H, Itoh Y, Newton RC, Magolda RL, Trzaskos JM, Burn TC et al (1999) Cloning and characterization of ADAMTS11, an aggrecanase from the ADAMTS family. J Biol Chem 274:23443–23450

Agrawal SM, Lau L, Yong VW (2008) MMPs in the central nervous system: where the good guys go bad. Semin Cell Dev Biol 19:42–51

Asher RA, Scheibe RJ, Keiser HD, Bignami A (1995) On the existence of a cartilage-like proteoglycan and link proteins in the central nervous system. Glia 13:294–308

Asher RA, Morgenstern DA, Fidler PS, Adcock KH, Oohira A, Braistead JE, Levine JM, Margolis RU, Rogers JH, Fawcett JW (2000) Neurocan is upregulated in injured brain and in cytokine-treated astrocytes. J Neurosci 20:2427–2438

Asher RA, Morgenstern DA, Shearer MC, Adcock KH, Pesheva P, Fawcett JW (2002) Versican is upregulated in CNS injury and is a product of oligodendrocyte lineage cells. J Neurosci 22:2225–2236

Aspberg A, Binkert C, Ruoslahti E (1995) The versican C-type lectin domain recognizes the adhesion protein tenascin-R. Proc Natl Acad Sci USA 92:10590–10594

Aspberg A, Miura R, Bourdoulous S, Shimonaka M, Heinegård D, Schachner M, Ruoslahti E, Yamaguchi Y (1997) The C-type lectin domains of lecticans, a family of aggregating chondroitin sulfate proteoglycans, bind tenascin-R by protein–protein interactions independent of carbohydrate moiety. Proc Natl Acad Sci USA 94:10116–10121

Aspberg A, Adam S, Kostka G, Timpl R, Heinegard D (1999) Fibulin-1 is a ligand for the C-type lectin domains of aggrecan and versican. J Biol Chem 274:20444–20449

Bai KJ, Spicer AP, Mascarenhas MM, Yu L, Ochoa CD, Garg HG, Quinn DA (2005) The role of hyaluronan synthase 3 in ventilator-induced lung injury. Am J Respir Crit Care Med 172:92–98

Baier C, Baader SL, Jankowski J, Gieselmann V, Schilling K, Rauch U, Kappler J (2007) Hyaluronan is organized into fiber-like structures along migratory pathways in the developing mouse cerebellum. Matrix Biol 26:348–358

Bandtlow CE, Zimmermann DR (2000) Proteoglycans in the developing brain—new conceptual insights for old proteins. Physiol Rev 80:1267–1290

Barnea G, Grumet M, Milev P, Silvennoinen O, Levy JB, Sap J, Schlessinger J (1994) Receptor tyrosine phosphatase beta is expressed in the form of proteoglycan and binds to the extracellular matrix protein tenascin. J Biol Chem 269:14349–14352

Barritt AW, Davies M, Marchand F, Hartley R, Grist J, Yip P, McMahon SB, Bradbury EJ (2006) Chondroitinase ABC promotes sprouting of intact and injured spinal systems after spinal cord injury. J Neurosci 26:10856–10867

Bartsch U, Bartsch S, Dorries U, Schachner M (1992) Immunohistological localization of tenascin in the developing and lesioned adult mouse optic nerve. Eur J Neurosci 4:338–352

Beggah AT, Dours-Zimmermann MT, Barras FM, Brosius A, Zimmermann DR, Zurn AD (2005) Lesion-induced differential expression and cell association of neurocan, brevican, versican V1 and V2 in the mouse dorsal root entry zone. Neuroscience 133:749–762

Bekku Y, Su WD, Hirakawa S, Fassler R, Ohtsuka A, Kang JS, Sanders J, Murakami T, Ninomiya Y, Oohashi T (2003) Molecular cloning of Bral2, a novel brain-specific link protein, and immunohistochemical colocalization with brevican in perineuronal nets. Mol Cell Neurosci 24:148–159

Berardi N, Pizzorusso T, Maffei L (2004) Extracellular matrix and visual cortical plasticity: freeing the synapse. Neuron 44:905–908

Bezakova G, Ruegg MA (2003) New insights into the roles of agrin. Nat Rev Mol Cell Biol 4:295–308

Bignami A, Perides G, Rahemtulla F (1993) Versican, a hyaluronate-binding proteoglycan of embryonal precartilaginous mesenchyma, is mainly expressed postnatally in rat brain. J Neurosci Res 34:97–106

Bradbury EJ, McMahon SB (2006) Spinal cord repair strategies: why do they work? Nat Rev Neurosci 7:644–653

Bradbury EJ, Moon LD, Popat RJ, King VR, Bennett GS, Patel PN, Fawcett JW, McMahon SB (2002) Chondroitinase ABC promotes functional recovery after spinal cord injury. Nature 416:636–640

Brakebusch C, Seidenbecher CI, Asztely F, Rauch U, Matthies H, Meyer H, Krug M, Bockers TM, Zhou X, Kreutz MR, Montag D, Gundelfinger ED, Fassler R (2002) Brevican-deficient mice display impaired hippocampal CA1 long-term potentiation but show no obvious deficits in learning and memory. Mol Cell Biol 22:7417–7427

Bruckner G, Brauer K, Hartig W, Wolff JR, Rickmann MJ, Derouiche A, Delpech B, Girard N, Oertel WH, Reichenbach A (1993) Perineuronal nets provide a polyanionic, glia-associated form of microenvironment around certain neurons in many parts of the rat brain. Glia 8:183–200

Bruckner G, Grosche J, Schmidt S, Hartig W, Margolis RU, Delpech B, Seidenbecher CI, Czaniera R, Schachner M (2000) Postnatal development of perineuronal nets in wild-type mice and in a mutant deficient in tenascin-R. J Comp Neurol 428:616–629

Bruckner G, Szeoke S, Pavlica S, Grosche J, Kacza J (2006) Axon initial segment ensheathed by extracellular matrix in perineuronal nets. Neuroscience 138:365–375

Bulow HE, Hobert O (2006) The molecular diversity of glycosaminoglycans shapes animal development. Annu Rev Cell Dev Biol 22:375–407

Camenisch TD, Spicer AP, Brehm-Gibson T, Biesterfeldt J, Augustine ML, Calabro A Jr, Kubalak S, Klewer SE, McDonald JA (2000) Disruption of hyaluronan synthase-2 abrogates normal cardiac morphogenesis and hyaluronan-mediated transformation of epithelium to mesenchyme. J Clin Invest 106:349–360

Carbonetto S (1984) The extracellular matrix of the nervous system. Trends Neurosci 7:382–387

Carulli D, Rhodes KE, Brown DJ, Bonnert TP, Pollack SJ, Oliver K, Strata P, Fawcett JW (2006) Composition of perineuronal nets in the adult rat cerebellum and the cellular origin of their components. J Comp Neurol 494:559–577

Carulli D, Rhodes KE, Fawcett JW (2007) Upregulation of aggrecan, link protein 1, and hyaluronan synthases during formation of perineuronal nets in the rat cerebellum. J Comp Neurol 501:83–94

Caterson B, Flannery CR, Hughes CE, Little CB (2000) Mechanisms involved in cartilage proteoglycan catabolism. Matrix Biol 19:333–344

Celio MR, Blumcke I (1994) Perineuronal nets–a specialized form of extracellular matrix in the adult nervous system. Brain Res Brain Res Rev 19:128–145

Celio MR, Spreafico R, De Biasi S, Vitellaro-Zuccarello L (1998) Perineuronal nets: past and present. Trends Neurosci 21:510–515

Chiquet-Ehrismann R, Chiquet M (2003) Tenascins: regulation and putative functions during pathological stress. J Pathol 200:488–499

Christopherson KS, Ullian EM, Stokes CC, Mullowney CE, Hell JW, Agah A, Lawler J, Mosher DF, Bornstein P, Barres BA (2005) Thrombospondins are astrocyte-secreted proteins that promote CNS synaptogenesis. Cell 120:421–433

Collins-Racie LA, Flannery CR, Zeng W, Corcoran C, Annis-Freeman B, Agostino MJ, Arai M, DiBlasio-Smith E, Dorner AJ, Georgiadis KE, Jin M, Tan XY, Morris EA, LaVallie ER (2004) ADAMTS-8 exhibits aggrecanase activity and is expressed in human articular cartilage. Matrix Biol 23:219–230

Cross AK, Haddock G, Stock CJ, Allan S, Surr J, Bunning RA, Buttle DJ, Woodroofe MN (2006) ADAMTS-1 and -4 are up-regulated following transient middle cerebral artery occlusion in the rat and their expression is modulated by TNF in cultured astrocytes. Brain Res 1088:19–30

Crossin KL, Hoffman S, Grumet M, Thiery JP, Edelman GM (1986) Site-restricted expression of cytotactin during development of the chicken embryo. J Cell Biol 102:1917–1930

Day AJ, Prestwich GD (2002) Hyaluronan-binding proteins: tying up the giant. J Biol Chem 277:4585–4588

DeAngelis PL (1999) Hyaluronan synthases: fascinating glycosyltransferases from vertebrates, bacterial pathogens, and algal viruses. Cell Mol Life Sci 56:670–682

Deepa SS, Carulli D, Galtrey C, Rhodes K, Fukuda J, Mikami T, Sugahara K, Fawcett JW (2006) Composition of perineuronal net extracellular matrix in rat brain: a different disaccharide composition for the net-associated proteoglycans. J Biol Chem 281:17789–17800

Delpech B, Halavent C (1981) Characterization and purification from human brain of a hyaluronic acid-binding glycoprotein, hyaluronectin. J Neurochem 36:855–859

Deyst KA, Toole BP (1995) Production of hyaluronan-dependent pericellular matrix by embryonic rat glial cells. Brain Res Dev Brain Res 88:122–125

Domowicz MS, Sanders TA, Ragsdale CW, Schwartz NB (2008) Aggrecan is expressed by embryonic brain glia and regulates astrocyte development. Dev Biol 315:114–124

Dorries U, Schachner M (1994) Tenascin mRNA isoforms in the developing mouse brain. J Neurosci Res 37:336–347

Dours-Zimmermann MT, Zimmermann DR (1994) A novel glycosaminoglycan attachment domain identified in two alternative splice variants of human versican. J Biol Chem 269:32992–32998

Dutt S, Kleber M, Matasci M, Sommer L, Zimmermann DR (2006) Versican V0 and V1 guide migratory neural crest cells. J Biol Chem 281:12123–12131

Engel M, Maurel P, Margolis RU, Margolis RK (1996) Chondroitin sulfate proteoglycans in the developing central nervous system. I. cellular sites of synthesis of neurocan and phosphacan. J Comp Neurol 366:34–43

Ethell IM, Ethell DW (2007) Matrix metalloproteinases in brain development and remodeling: synaptic functions and targets. J Neurosci Res 85:2813–2823

Evanko SP, Tammi MI, Tammi RH, Wight TN (2007) Hyaluronan-dependent pericellular matrix. Adv Drug Deliv Rev 59:1351–1365

Evers MR, Salmen B, Bukalo O, Rollenhagen A, Bosl MR, Morellini F, Bartsch U, Dityatev A, Schachner M (2002) Impairment of L-type Ca2+ channel-dependent forms of hippocampal synaptic plasticity in mice deficient in the extracellular matrix glycoprotein tenascin-C. J Neurosci 22:7177–7194

Flannery CR (2006) MMPs and ADAMTSs: functional studies. Front Biosci 11:544–569

Forsberg E, Hirsch E, Fröhlich L, Meyer M, Ekblom P, Aszodi A, Werner S, Fässler R (1996) Skin wounds and severed nerves heal normally in mice lacking tenascin-C. Proc Natl Acad Sci USA 93:6594–6599

Freitag S, Schachner M, Morellini F (2003) Behavioral alterations in mice deficient for the extracellular matrix glycoprotein tenascin-R. Behav Brain Res 145:189–207

Fukamauchi F, Mataga N, Wang YJ, Sato S, Youshiki A, Kusakabe M (1996) Abnormal behavior and neurotransmissions of tenascin gene knockout mouse. Biochem Biophys Res Commun 221:151–156

Fuss B, Wintergerst ES, Bartsch U, Schachner M (1993) Molecular characterization and in situ mRNA localization of the neural recognition molecule J1-160/180: a modular structure similar to tenascin. J Cell Biol 120:1237–1249

Galtrey CM, Fawcett JW (2007) The role of chondroitin sulfate proteoglycans in regeneration and plasticity in the central nervous system. Brain Res Rev 54:1–18

Galtrey CM, Kwok JC, Carulli D, Rhodes KE, Fawcett JW (2008) Distribution and synthesis of extracellular matrix proteoglycans, hyaluronan, link proteins and tenascin-R in the rat spinal cord. Eur J Neurosci 27:1373–1390

Gao G, Westling J, Thompson VP, Howell TD, Gottschall PE, Sandy JD (2002) Activation of the proteolytic activity of ADAMTS4 (aggrecanase-1) by C-terminal truncation. J Biol Chem 277:11034–11041

Gates MA, Thomas LB, Howard EM, Laywell ED, Sajin B, Faissner A, Gotz B, Silver J, Steindler DA (1995) Cell and molecular analysis of the developing and adult mouse subventricular zone of the cerebral hemispheres. J Comp Neurol 361:249–266

Gonzenbach RR, Schwab ME (2008) Disinhibition of neurite growth to repair the injured adult CNS: Focusing on Nogo. Cell Mol Life Sci 65:161–176

Gottschall PE, Sandy JD, Zimmermann DR (2005) Substrates for metalloendopeptidases in the central nervous system. In: Conant K, Gottschall PE (eds) Matrix metalloproteinases in the central nervous system. Imperial College Press, London, pp 87–118

Guimaraes A, Zaremba S, Hockfield S (1990) Molecular and morphological changes in the cat lateral geniculate nucleus and visual cortex induced by visual deprivation are revealed by monoclonal antibodies Cat-304 and Cat-301. J Neurosci 10:3014–3024

Gunther W, Skaftnesmo KO, Arnold H, Bjerkvig R, Terzis AJ (2005) Distribution patterns of the anti-angiogenic protein ADAMTS-1 during rat development. Acta Histochem 107:121–131

Haas CA, Rauch U, Thon N, Merten T, Deller T (1999) Entorhinal cortex lesion in adult rats induces the expression of the neuronal chondroitin sulfate proteoglycan neurocan in reactive astrocytes. J Neurosci 19:9953–9963

Harroch S, Palmeri M, Rosenbluth J, Custer A, Okigaki M, Shrager P, Blum M, Buxbaum JD, Schlessinger J (2000) No obvious abnormality in mice deficient in receptor protein tyrosine phosphatase beta. Mol Cell Biol 20:7706–7715

Harroch S, Furtado GC, Brueck W, Rosenbluth J, Lafaille J, Chao M, Buxbaum JD, Schlessinger J (2002) A critical role for the protein tyrosine phosphatase receptor type Z in functional recovery from demyelinating lesions. Nat Genet 32:411–414

Haunso A, Celio MR, Margolis RK, Menoud PA (1999) Phosphacan immunoreactivity is associated with perineuronal nets around parvalbumin-expressing neurones. Brain Res 834:219–222

Haunso A, Ibrahim M, Bartsch U, Letiembre M, Celio MR, Menoud P (2000) Morphology of perineuronal nets in tenascin-R and parvalbumin single and double knockout mice. Brain Res 864:142–145

Hedstrom KL, Rasband MN (2006) Intrinsic and extrinsic determinants of ion channel localization in neurons. J Neurochem 98:1345–1352

Hedstrom KL, Xu X, Ogawa Y, Frischknecht R, Seidenbecher CI, Shrager P, Rasband MN (2007) Neurofascin assembles a specialized extracellular matrix at the axon initial segment. J Cell Biol 178:875–886

Held-Feindt J, Paredes EB, Blomer U, Seidenbecher C, Stark AM, Mehdorn HM, Mentlein R (2006) Matrix-degrading proteases ADAMTS4 and ADAMTS5 (disintegrins and metalloproteinases with thrombospondin motifs 4 and 5) are expressed in human glioblastomas. Int J Cancer 118:55–61

Herz J, Chen Y (2006) Reelin, lipoprotein receptors and synaptic plasticity. Nat Rev Neurosci 7:850–859

Hirakawa S, Oohashi T, Su WD, Yoshioka H, Murakami T, Arata J, Ninomiya Y (2000) The brain link protein-1 (BRAL1): cDNA cloning, genomic structure, and characterization as a novel link protein expressed in adult brain. Biochem Biophys Res Commun 276:982–989

Hockfield S, Kalb RG, Zaremba S, Fryer H (1990) Expression of neural proteoglycans correlates with the acquisition of mature neuronal properties in the mammalian brain. Cold Spring Harb Symp Quant Biol 55:505–514

Hooks BM, Chen C (2007) Critical periods in the visual system: changing views for a model of experience-dependent plasticity. Neuron 56:312–326

Hsia HC, Schwarzbauer JE (2005) Meet the tenascins: multifunctional and mysterious. J Biol Chem 280:26641–26644

Ikuta T, Sogawa N, Ariga H, Ikemura T, Matsumoto K (1998) Structural analysis of mouse tenascin-X: evolutionary aspects of reduplication of FNIII repeats in the tenascin gene family. Gene 217:1–13

Iozzo RV, Murdoch AD (1996) Proteoglycans of the extracellular environment—clues from the gene and protein side offer novel perspectives in molecular diversity and function (review). FASEB J 10:598–614

Isogai Z, Aspberg A, Keene DR, Ono RN, Reinhardt DP, Sakai LY (2002) Versican interacts with fibrillin-1 and links extracellular microfibrils to other connective tissue networks. J Biol Chem 277:4565–4572

Itano N, Kimata K (2002) Mammalian hyaluronan synthases. IUBMB Life 54:195–199

Joester A, Faissner A (1999) Evidence for combinatorial variability of tenascin-C isoforms and developmental regulation in the mouse central nervous system. J Biol Chem 274:17144–17151

Joester A, Faissner A (2001) The structure and function of tenascins in the nervous system. Matrix Biol 20:13–22

John N, Krugel H, Frischknecht R, Smalla KH, Schultz C, Kreutz MR, Gundelfinger ED, Seidenbecher CI (2006) Brevican-containing perineuronal nets of extracellular matrix in dissociated hippocampal primary cultures. Mol Cell Neurosci 31:774–784

Jones FS, Jones PL (2000) The tenascin family of ECM glycoproteins: structure, function, and regulation during embryonic development and tissue remodeling. Dev Dyn 218:235–259

Jones LL, Margolis RU, Tuszynski MH (2003) The chondroitin sulfate proteoglycans neurocan, brevican, phosphacan, and versican are differentially regulated following spinal cord injury. Exp Neurol 182:399–411

Jonsson-Rylander AC, Nilsson T, Fritsche-Danielson R, Hammarstrom A, Behrendt M, Andersson JO, Lindgren K, Andersson AK, Wallbrandt P, Rosengren B, Brodin P, Thelin A, Westin A, Hurt-Camejo E, Lee-Sogaard CH (2005) Role of ADAMTS-1 in atherosclerosis: remodeling of carotid artery, immunohistochemistry, and proteolysis of versican. Arterioscler Thromb Vasc Biol 25:180–185

Jungers KA, Le Goff C, Somerville RP, Apte SS (2005) Adamts9 is widely expressed during mouse embryo development. Gene Expr Patterns 5:609–617

Kalb RG, Hockfield S (1988) Molecular evidence for early activity-dependent development of hamster motor neurons. J Neurosci 8:2350–2360

Kalb RG, Hockfield S (1990) Large diameter primary afferent input is required for expression of the Cat-301 proteoglycan on the surface of motor neurons. Neuroscience 34:391–401

Kiernan BW, Garcion E, Ferguson J, Frost EE, Torres EM, Dunnett SB, Saga Y, Aizawa S, Faissner A, Kaur R, Franklin RJ, ffrench-Constant C (1999) Myelination and behaviour of tenascin-C null transgenic mice. Eur J Neurosci 11:3082–3092

Kjellén L, Lindahl U (1991) Proteoglycans: structures, interactions (published erratum appears in Annu Rev Biochem (1992) 61, following viii). Annu Rev Biochem 60:443–475

Kultti A, Rilla K, Tiihonen R, Spicer AP, Tammi RH, Tammi MI (2006) Hyaluronan synthesis induces microvillus-like cell surface protrusions. J Biol Chem 281:15821–15828

Kuno K, Okada Y, Kawashima H, Nakamura H, Miyasaka M, Ohno H, Matsushima K (2000) ADAMTS-1 cleaves a cartilage proteoglycan, aggrecan. FEBS Lett 478:241–245

Kusche-Gullberg M, Kjellen L (2003) Sulfotransferases in glycosaminoglycan biosynthesis. Curr Opin Struct Biol 13:605–611

Lander C, Kind P, Maleski M, Hockfield S (1997) A family of activity-dependent neuronal cell-surface chondroitin sulfate proteoglycans in cat visual cortex. J Neurosci 17:1928–1939

Landolt RM, Vaughan L, Winterhalter KH, Zimmermann DR (1995) Versican is selectively expressed in embryonic tissues that act as barriers to neural crest cell migration and axon outgrowth. Development 121:2303–2312

Laywell ED, Steindler DA (1991) Boundaries and wounds, glia and glycoconjugates. Cellular and molecular analyses of developmental partitions and adult brain lesions. Ann NY Acad Sci 633:122–141

Laywell ED, Dorries U, Bartsch U, Faissner A, Schachner M, Steindler DA (1992) Enhanced expression of the developmentally regulated extracellular matrix molecule tenascin following adult brain injury. Proc Natl Acad Sci USA 89:2634–2638

LeBaron RG, Zimmermann DR, Ruoslahti E (1992) Hyaluronate binding properties of versican. J Biol Chem 267:10003–10010

Lein ES, Hawrylycz MJ, Ao N, Ayres M, Bensinger A, Bernard A, Boe AF, Boguski MS, Brockway KS, Byrnes EJ, Chen L, Chen L, Chen TM, Chin MC, Chong J, Crook BE, Czaplinska A, Dang CN, Datta S, Dee NR, Desaki AL, Desta T, Diep E, Dolbeare TA, Donelan MJ, Dong HW, Dougherty JG, Duncan BJ, Ebbert AJ, Eichele G, Estin LK, Faber C, Facer BA, Fields R, Fischer SR, Fliss TP, Frensley C, Gates SN, Glattfelder KJ, Halverson KR, Hart MR, Hohmann JG, Howell MP, Jeung DP, Johnson RA, Karr PT, Kawal R, Kidney JM, Knapik RH, Kuan CL, Lake JH, Laramee AR, Larsen KD, Lau C, Lemon TA, Liang AJ, Liu Y, Luong LT, Michaels J, Morgan JJ, Morgan RJ, Mortrud MT, Mosqueda NF, Ng LL, Ng R, Orta GJ, Overly CC, Pak TH, Parry SE, Pathak SD, Pearson OC, Puchalski RB, Riley ZL, Rockett HR, Rowland SA, Royall JJ, Ruiz MJ, Sarno NR, Schaffnit K, Shapovalova NV, Sivisay T, Slaughterbeck CR, Smith SC, Smith KA, Smith BI, Sodt AJ, Stewart NN, Stumpf KR, Sunkin SM, Sutram M, Tam A, Teemer CD, Thaller C, Thompson CL, Varnam LR, Visel A, Whitlock RM, Wohnoutka PE, Wolkey CK, Wong VY, Wood M, Yaylaoglu MB, Young RC, Youngstrom BL, Yuan XF, Zhang B, Zwingman TA, Jones AR (2007) Genome-wide atlas of gene expression in the adult mouse brain. Nature 445:168–176

Lemons ML, Sandy JD, Anderson DK, Howland DR (2001) Intact aggrecan and fragments generated by both aggrecanse and metalloproteinase-like activities are present in the developing and adult rat spinal cord and their relative abundance is altered by injury. J Neurosci 21:4772–4781

Lundell A, Olin AI, Morgelin M, al-Karadaghi S, Aspberg A, Logan DT (2004) Structural basis for interactions between tenascins and lectican C-type lectin domains: evidence for a crosslinking role for tenascins. Structure 12:1495–1506

Maeda N, Noda M (1996) 6B4 proteoglycan/phosphacan is a repulsive substratum but promotes morphological differentiation of cortical neurons. Development 122:647–658

Maeda N, Hamanaka H, Oohira A, Noda M (1995) Purification, characterization and developmental expression of a brain-specific chondroitin sulfate proteoglycan, 6B4 proteoglycan/phosphacan. Neuroscience 67:23–35

Margolis RK, Margolis RU, Preti C, Lai D (1975) Distribution and metabolism of glycoproteins and glycosaminoglycans in subcellular fractions of brain. Biochemistry 14:4797–4804

Margolis RK, Rauch U, Maurel P, Margolis RU (1996) Neurocan and phosphacan–two major nervous tissue-specific chondroitin sulfate proteoglycans. Perspect Dev Neurobiol 3:273–290

Matsui F, Kawashima S, Shuo T, Yamauchi S, Tokita Y, Aono S, Keino H, Oohira A (2002) Transient expression of juvenile-type neurocan by reactive astrocytes in adult rat brains injured by kainate-induced seizures as well as surgical incision. Neuroscience 112:773–781

Matsumoto K, Saga Y, Ikemura T, Sakakura T, Chiquet-Ehrismann R (1994) The distribution of tenascin-X is distinct and often reciprocal to that of tenascin-C. J Cell Biol 125:483–493

Matsumoto K, Shionyu M, Go M, Shimizu K, Shinomura T, Kimata K, Watanabe H (2003) Distinct interaction of versican/PG-M with hyaluronan and link protein. J Biol Chem 278:41205–41212

Matthews RT, Gary SC, Zerillo C, Pratta M, Solomon K, Arner EC, Hockfield S (2000) Brain-enriched hyaluronan binding (BEHAB)/brevican cleavage in a glioma cell line is mediated by a disintegrin and metalloproteinase with thrombospondin motifs (ADAMTS) family member. J Biol Chem 275:22695–22703

Matthews RT, Kelly GM, Zerillo CA, Gray G, Tiemeyer M, Hockfield S (2002) Aggrecan glycoforms contribute to the molecular heterogeneity of perineuronal nets. J Neurosci 22:7536–7547

Maurel P, Rauch U, Flad M, Margolis RK, Margolis RU (1994) Phosphacan, a chondroitin sulfate proteoglycan of brain that interacts with neurons and neural cell-adhesion molecules, is an extracellular variant of a receptor-type protein tyrosine phosphatase. Proc Natl Acad Sci USA 91:2512–2516

Mayer J, Hamel MG, Gottschall PE (2005) Evidence for proteolytic cleavage of brevican by the ADAMTSs in the dentate gyrus after excitotoxic lesion of the mouse entorhinal cortex. BMC Neurosci 6:52

McKeon RJ, Jurynec MJ, Buck CR (1999) The chondroitin sulfate proteoglycans neurocan and phosphacan are expressed by reactive astrocytes in the chronic CNS glial scar. J Neurosci 19:10778–10788

Melendez-Vasquez C, Carey DJ, Zanazzi G, Reizes O, Maurel P, Salzer JL (2005) Differential expression of proteoglycans at central and peripheral nodes of Ranvier. Glia 52:301–308

Meyer-Puttlitz B, Milev P, Junker E, Zimmer I, Margolis RU, Margolis RK (1995) Chondroitin sulfate and chondroitin/keratan sulfate proteoglycans of nervous tissue: developmental changes of neurocan and phosphacan. J Neurochem 65:2327–2337

Meyer-Puttlitz B, Junker E, Margolis RU, Margolis RK (1996) Chondroitin sulfate proteoglycans in the developing central nervous system. II. Immunocytochemical localization of neurocan and phosphacan. J Comp Neurol 366:44–54

Miguel RF, Pollak A, Lubec G (2005) Metalloproteinase ADAMTS-1 but not ADAMTS-5 is manifold overexpressed in neurodegenerative disorders as Down syndrome, Alzheimer's and Pick's disease. Brain Res Mol Brain Res 133:1–5

Milev P, Friedlander DR, Sakurai T, Karthikeyan L, Flad M, Margolis RK, Grumet M, Margolis RU (1994) Interactions of the chondroitin sulfate proteoglycan phosphacan, the extracellular domain of a receptor-type protein tyrosine phosphatase, with neurons, glia, and neural cell adhesion molecules. J Cell Biol 127:1703–1715

Milev P, Maurel P, Haring M, Margolis RK, Margolis RU (1996) TAG-1/axonin-1 is a high-affinity ligand of neurocan, phosphacan/protein-tyrosine phosphatase-zeta/beta, and N-CAM. J Biol Chem 271:15716–15723

Milev P, Fischer D, Haring M, Schulthess T, Margolis RK, Chiquet-Ehrismann R, Margolis RU (1997) The fibrinogen-like globe of tenascin-C mediates its interactions with neurocan and phosph-

acan/protein-tyrosine phosphatase-zeta/beta. J Biol Chem 272:15501–15509

Milev P, Chiba A, Haring M, Rauvala H, Schachner M, Ranscht B, Margolis RK, Margolis RU (1998a) High affinity binding and overlapping localization of neurocan and phosphacan protein-tyrosine phosphatase-zeta/beta with tenascin-R, amphoterin, and the heparin-binding growth-associated molecule. J Biol Chem 273:6998–7005

Milev P, Maurel P, Chiba A, Mevissen M, Popp S, Yamaguchi Y, Margolis RK, Margolis RU (1998b) Differential regulation of expression of hyaluronan-binding proteoglycans in developing brain: aggrecan, versican, neurocan, and brevican. Biochem Biophys Res Commun 247:207–212

Milev P, Monnerie H, Popp S, Margolis RK, Margolis RU (1998c) The core protein of the chondroitin sulfate proteoglycan phosphacan is a high-affinity ligand of fibroblast growth factor-2 and potentiates its mitogenic activity. J Biol Chem 273:21439–21442

Miller B, Sheppard AM, Bicknese AR, Pearlman AL (1995) Chondroitin sulfate proteoglycans in the developing cerebral cortex: the distribution of neurocan distinguishes forming afferent and efferent axonal pathways. J Comp Neurol 355:615–628

Milward EA, Fitzsimmons C, Szklarczyk A, Conant K (2007) The matrix metalloproteinases and CNS plasticity: an overview. J Neuroimmunol 187:9–19

Miura R, Aspberg A, Ethell IM, Hagihara K, Schnaar RL, Ruoslahti E, Yamaguchi Y (1999) The proteoglycan lectin domain binds sulfated cell surface glycolipids and promotes cell adhesion. J Biol Chem 274:11431–11438

Miyata S, Nishimura Y, Hayashi N, Oohira A (2005) Construction of perineuronal net-like structure by cortical neurons in culture. Neuroscience 136:95–104

Miyata S, Nishimura Y, Nakashima T (2007) Perineuronal nets protect against amyloid beta-protein neurotoxicity in cultured cortical neurons. Brain Res 1150:200–206

Mjaatvedt C, Yamamura H, Capehart A, Turner D, Markwald R (1998) The *cspg2* gene, disrupted in the *hdf* mutant, is required for right cardiac chamber and endocardial cushion formation. Dev Biol 202:56–66

Montag-Sallaz M, Montag D (2003) Severe cognitive and motor coordination deficits in tenascin-R-deficient mice. Genes Brain Behav 2:20–31

Moon LD, Asher RA, Rhodes KE, Fawcett JW (2001) Regeneration of CNS axons back to their target following treatment of adult rat brain with chondroitinase ABC. Nat Neurosci 4:465–466

Morawski M, Bruckner MK, Riederer P, Bruckner G, Arendt T (2004) Perineuronal nets potentially protect against oxidative stress. Exp Neurol 188:309–315

Morgenstern DA, Asher RA, Fawcett JW (2002) Chondroitin sulphate proteoglycans in the CNS injury response. Prog Brain Res 137:313–332

Murakami T, Ohtsuka A (2003) Perisynaptic barrier of proteoglycans in the mature brain and spinal cord. Arch Histol Cytol 66:195–207

Mörgelin M, Paulsson M, Malmström A, Heinegård D (1989) Shared and distinct structural features of interstitial proteoglycans from different bovine tissues revealed by electron microscopy. J Biol Chem 264:12080–12090

Nakada M, Miyamori H, Kita D, Takahashi T, Yamashita J, Sato H, Miura R, Yamaguchi Y, Okada Y (2005) Human glioblastomas overexpress ADAMTS-5 that degrades brevican. Acta Neuropathol 110:239–246

Nakamura H, Fujii Y, Inoki I, Sugimoto K, Tanzawa K, Matsuki H, Miura R, Yamaguchi Y, Okada Y (2000) Brevican is degraded by matrix metalloproteinases and aggrecanase-1 (ADAMTS4) at different sites. J Biol Chem 275:38885–38890

Neame PJ, Barry FP (1993) The link proteins. Experientia 49:393–402

Neame PJ, Christner JE, Baker JR (1987) Cartilage proteoglycan aggregates. The link protein and proteoglycan amino-terminal globular domains have similar structures. J Biol Chem 262:17768–17778

Neidhardt J, Fehr S, Kutsche M, Lohler J, Schachner M (2003) Tenascin-N: characterization of a novel member of the tenascin family that mediates neurite repulsion from hippocampal explants. Mol Cell Neurosci 23:193–209

Nicholson C, Sykova E (1998) Extracellular space structure revealed by diffusion analysis. Trends Neurosci 21:207–215

Niederöst BP, Zimmermann DR, Schwab ME, Bandtlow CE (1999) Bovine CNS myelin contains neurite growth inhibitory activity associated with chondroitin sulfate proteoglycans. J Neurosci 19:8979–8989

Niisato K, Fujikawa A, Komai S, Shintani T, Watanabe E, Sakaguchi G, Katsuura G, Manabe T, Noda M (2005) Age-dependent enhancement of hippocampal long-term potentiation and impairment of spatial learning through the Rho-associated kinase pathway in protein tyrosine phosphatase receptor type Z-deficient mice. J Neurosci 25:1081–1088

Novak U, Kaye AH (2000) Extracellular matrix and the brain: components and function. J Clin Neurosci 7:280–290

Nutt CL, Matthews RT, Hockfield S (2001) Glial tumor invasion: a role for the upregulation and cleavage of BEHAB/brevican. Neuroscientist 7:113–122

Oakley RA, Tosney KW (1991) Peanut agglutinin and chondroitin-6-sulfate are molecular markers for tissues that act as barriers to axon advance in the avian embryo. Dev Biol 147:187–206

Ogawa T, Hagihara K, Suzuki M, Yamaguchi Y (2001) Brevican in the developing hippocampal fimbria: differential expression in myelinating oligodendrocytes and adult astrocytes suggests a dual role for brevican in central nervous system fiber tract development. J Comp Neurol 432:285–295

Ogawa H, Oohashi T, Sata M, Bekku Y, Hirohata S, Nakamura K, Yonezawa T, Kusachi S, Shiratori Y, Ninomiya Y (2004) Lp3/Hapln3, a novel link protein that co-localizes with versican and is coordinately up-regulated by platelet-derived growth factor in arterial smooth muscle cells. Matrix Biol 23:287–298

Olin AI, Morgelin M, Sasaki T, Timpl R, Heinegard D, Aspberg A (2001) The proteoglycans aggrecan and Versican form networks with fibulin-2 through their lectin domain binding. J Biol Chem 276:1253–1261

Oohashi T, Hirakawa S, Bekku Y, Rauch U, Zimmermann DR, Su WD, Ohtsuka A, Murakami T, Ninomiya Y (2002) Bral1, a brain-specific link protein, colocalizing with the versican V2 isoform at the nodes of Ranvier in developing and adult mouse central nervous systems. Mol Cell Neurosci 19:43–57

Peles E, Nativ M, Campbell PL, Sakurai T, Martinez R, Lev S, Clary DO, Schilling J, Barnea G, Plowman GD, Grumet M, Schlessinger J (1995) The carbonic anhydrase domain of receptor tyrosine phosphatase beta is a functional ligand for the axonal cell recognition molecule contactin. Cell 82:251–260

Perides G, Lane WS, Andrews D, Dahl D, Bignami A (1989) Isolation and partial characterization of a glial hyaluronate-binding protein. J Biol Chem 264:5981–5987

Perides G, Erickson HP, Rahemtulla F, Bignami A (1993) Colocalization of tenascin with versican, a hyaluronate-binding chondroitin sulfate proteoglycan. Anat Embryol Berl 188:467–479

Pesheva P, Spiess E, Schachner M (1989) J1-160 and J1-180 are oligodendrocyte-secreted nonpermissive substrates for cell adhesion. J Cell Biol 109:1765–1778

Pindzola RR, Doller C, Silver J (1993) Putative inhibitory extracellular matrix molecules at the dorsal root entry zone of the spinal cord during development and after root and sciatic nerve lesions. Dev Biol 156:34–48

Pizzorusso T, Medini P, Berardi N, Chierzi S, Fawcett JW, Maffei L (2002) Reactivation of ocular dominance plasticity in the adult visual cortex. Science 298:1248–1251

Pizzorusso T, Medini P, Landi S, Baldini S, Berardi N, Maffei L (2006) Structural and functional recovery from early monocular deprivation in adult rats. Proc Natl Acad Sci USA 103:8517–8522

Poliak S, Peles E (2003) The local differentiation of myelinated axons at nodes of Ranvier. Nat Rev Neurosci 4:968–980

Popp S, Andersen JS, Maurel P, Margolis RU (2003) Localization of aggrecan and versican in the developing rat central nervous system. Dev Dyn 227:143–149

Porter S, Clark IM, Kevorkian L, Edwards DR (2005) The ADAMTS metalloproteinases. Biochem J 386:15–27

Prieto AL, Jones FS, Cunningham BA, Crossin KL, Edelman GM (1990) Localization during development of alternatively spliced forms of cytotactin mRNA by in situ hybridization. J Cell Biol 111:685–698

Prydz K, Dalen KT (2000) Synthesis and sorting of proteoglycans. J Cell Sci 113(Pt 2):193–205

Quaglia X, Beggah AT, Seidenbecher C, Zurn AD (2008) Delayed priming promotes CNS regeneration post-rhizotomy in neurocan and brevican-deficient mice. Brain 131:240–249

Ratcliffe CF, Qu Y, McCormick KA, Tibbs VC, Dixon JE, Scheuer T, Catterall WA (2000) A sodium channel signaling complex: modulation by associated receptor protein tyrosine phosphatase beta. Nat Neurosci 3:437–444

Rauch U (1997) Modeling an extracellular environment for axonal pathfinding and fasciculation in the central nervous system. Cell Tissue Res 290:349–356

Rauch U (2004) Extracellular matrix components associated with remodeling processes in brain. Cell Mol Life Sci 61:2031–2045

Rauch U, Gao P, Janetzko A, Flaccus A, Hilgenberg L, Tekotte H, Margolis RK, Margolis RU (1991) Isolation and characterization of developmentally regulated chondroitin sulfate and chondroitin/keratan sulfate proteoglycans of brain identified with monoclonal antibodies. J Biol Chem 266:14785–14801

Rauch U, Clement A, Retzler C, Fröhlich L, Fässler R, Göhring W, Faissner A (1997) Mapping of a defined neurocan binding site to distinct domains of tenascin-C. J Biol Chem 272:26905–26912

Rauch U, Hirakawa S, Oohashi T, Kappler J, Roos G (2004) Cartilage link protein interacts with neurocan, which shows hyaluronan binding characteristics different from CD44 and TSG-6. Matrix Biol 22:629–639

Rauch U, Zhou XH, Roos G (2005) Extracellular matrix alterations in brains lacking four of its components. Biochem Biophys Res Commun 328:608–617

Retzler C, Wiedemann H, Kulbe G, Rauch U (1996) Structural and electron microscopic analysis of neurocan and recombinant neurocan fragments. J Biol Chem 271:17107–17113

Rhodes KE, Fawcett JW (2004) Chondroitin sulphate proteoglycans: preventing plasticity or protecting the CNS? J Anat 204:33–48

Rilla K, Tiihonen R, Kultti A, Tammi M, Tammi R (2008) Pericellular hyaluronan coat visualized in live cells with a fluorescent probe is scaffolded by plasma membrane protrusions. J Histochem Cytochem (in press)

Ripellino JA, Bailo M, Margolis RU, Margolis RK (1988) Light and electron microscopic studies on the localization of hyaluronic acid in developing rat cerebellum. J Cell Biol 106:845–855

Rodriguez-Manzaneque JC, Milchanowski AB, Dufour EK, Leduc R, Iruela-Arispe ML (2000) Characterization of METH-1/ADAMTS1 processing reveals two distinct active forms. J Biol Chem 275:33471–33479

Ruoslahti E (1996) Brain extracellular matrix (review). Glycobiology 6:489–492

Rutka JT, Apodaca G, Stern R, Rosenblum M (1988) The extracellular matrix of the central and peripheral nervous systems: structure and function. J Neurosurg 69:155–170

Saga Y, Yagi T, Ikawa Y, Sakakura T, Aizawa S (1992) Mice develop normally without tenascin. Genes Dev 6:1821–1831

Saghatelyan A, de Chevigny A, Schachner M, Lledo PM (2004) Tenascin-R mediates activity-dependent recruitment of neuroblasts in the adult mouse forebrain. Nat Neurosci 7:347–356

Salzer JL (2003) Polarized domains of myelinated axons. Neuron 40:297–318

Sandy JD, Westling J, Kenagy RD, Iruela-Arispe ML, Verscharen C, Rodriguez-Mazaneque JC, Zimmermann DR, Lemire JM, Fischer JW, Wight TN, Clowes AW (2001) Versican V1 proteolysis in human aorta in vivo occurs at the Glu441-Ala442 bond, a site that is cleaved by recombinant ADAMTS-1 and ADAMTS-4. J Biol Chem 276:13372–13378

Sanes JR (1989) Extracellular matrix molecules that influence neural development. Annu Rev Neurosci 12:491–516

Sasaki M, Seo-Kiryu S, Kato R, Kita S, Kiyama H (2001) A disintegrin and metalloprotease with thrombospondin type1 motifs (ADAMTS-1) and IL-1 receptor type 1 mRNAs are simultaneously induced in nerve injured motor neurons. Brain Res Mol Brain Res 89:158–163

Satoh K, Suzuki N, Yokota H (2000) ADAMTS-4 (a disintegrin and metalloproteinase with thrombospondin motifs) is transcriptionally induced in beta-amyloid treated rat astrocytes. Neurosci Lett 289:177–180

Scherberich A, Tucker RP, Samandari E, Brown-Luedi M, Martin D, Chiquet-Ehrismann R (2004) Murine tenascin-W: a novel mammalian tenascin expressed in kidney and at sites of bone and smooth muscle development. J Cell Sci 117:571–581

Schmalfeldt M, Dours-Zimmermann MT, Winterhalter KH, Zimmermann DR (1998) Versican V2 is a major extracellular matrix component of the mature bovine brain. J Biol Chem 273:15758–15764

Schmalfeldt M, Bandtlow CE, Dours-Zimmermann MT, Winterhalter KH, Zimmermann DR (2000) Brain derived versican V2 is a potent inhibitor of axonal growth. J Cell Sci 113:807–816

Schwartz NB, Domowicz M (2004) Proteoglycans in brain development. Glycoconj J 21:329–341

Seidenbecher CI, Richter K, Rauch U, Fässler R, Garner CC, Gundelfinger ED (1995) Brevican, a chondroitin sulfate proteoglycan of rat brain, occurs as secreted and cell surface glycosylphosphatidylinositol-anchored isoforms. J Biol Chem 270:27206–27212

Seyfried NT, McVey GF, Almond A, Mahoney DJ, Dudhia J, Day AJ (2005) Expression and purification of functionally active hyaluronan-binding domains from human cartilage link protein, aggrecan and versican: formation of ternary complexes with defined hyaluronan oligosaccharides. J Biol Chem 280:5435–5448

Shi S, Grothe S, Zhang Y, O'Connor-McCourt MD, Poole AR, Roughley PJ, Mort JS (2004) Link protein has greater affinity for versican than aggrecan. J Biol Chem 279:12060–12066

Shitara K, Yamada H, Watanabe K, Shimonaka M, Yamaguchi Y (1994) Brain-specific receptor-type protein-tyrosine phosphatase RPTP beta is a chondroitin sulfate proteoglycan in vivo. J Biol Chem 269:20189–20193

Silver DL, Hou L, Somerville R, Young ME, Apte SS, Pavan WJ (2008) The secreted metalloprotease ADAMTS20 is required for melanoblast survival. PLoS Genet 4:e1000003

Snow DM, Lemmon V, Carrino DA, Caplan AI, Silver J (1990) Sulfated proteoglycans on astroglial barriers inhibit neurite outgrowth in vitro. Exp Neurol 109:111–130

Somerville RP, Longpre JM, Jungers KA, Engle JM, Ross M, Evanko S, Wight TN, Leduc R, Apte SS (2003) Characterization of ADAMTS-9 and ADAMTS-20 as a distinct ADAMTS subfamily related to Caenorhabditis elegans GON-1. J Biol Chem 278:9503–9513

Spicer AP, McDonald JA (1998) Characterization and molecular evolution of a vertebrate hyaluronan synthase gene family. J Biol Chem 273:1923–1932

Spicer AP, Tien JY (2004) Hyaluronan and morphogenesis. Birth Defects Res C Embryo Today 72:89–108

Spicer AP, Joo A, Bowling RA Jr (2003) A hyaluronan binding link protein gene family whose members are physically linked adjacent to chondroitin sulfate proteoglycan core protein genes: the missing links. J Biol Chem 278:21083–21091

Steindler DA, Cooper NG, Faissner A, Schachner M (1989) Boundaries defined by adhesion molecules during development of the cerebral cortex: the J1/tenascin glycoprotein in the mouse somatosensory cortical barrel field. Dev Biol 131:243–260

Steindler DA, Settles D, Erickson HP, Laywell ED, Yoshiki A, Faissner A, Kusakabe M (1995) Tenascin knockout mice: barrels, boundary molecules, and glial scars. J Neurosci 15:1971–1983

Swindle CS, Tran KT, Johnson TD, Banerjee P, Mayes AM, Griffith L, Wells A (2001) Epidermal growth factor (EGF)-like repeats of human tenascin-C as ligands for EGF receptor. J Cell Biol 154:459–468

Tang BL (2003) Inhibitors of neuronal regeneration: mediators and signaling mechanisms. Neurochem Int 42:189–203

Tang X, Davies JE, Davies SJ (2003) Changes in distribution, cell associations, and protein expression levels of NG2, neurocan, phosphacan, brevican, versican V2, and tenascin-C during acute to chronic maturation of spinal cord scar tissue. J Neurosci Res 71:427–444

Tani E, Ametani T (1971) Extracellular distribution of ruthenium red-positive substance in the cerebral cortex. J Ultrastruct Res 34:1–14

Thai SN, Iruela-Arispe ML (2002) Expression of ADAMTS1 during murine development. Mech Dev 115:181–185

Thomas LB, Gates MA, Steindler DA (1996) Young neurons from the adult subependymal zone proliferate and migrate along an astrocyte, extracellular matrix-rich pathway. Glia 17:1–14

Tissir F, Goffinet AM (2003) Reelin and brain development. Nat Rev Neurosci 4:496–505

Toole BP (2000) Hyaluronan is not just a goo!. J Clin Invest 106:335–336

Toole BP (2001) Hyaluronan in morphogenesis. Semin Cell Dev Biol 12:79–87

Toole BP (2004) Hyaluronan: from extracellular glue to pericellular cue. Nat Rev Cancer 4:528–539

Tortorella MD, Burn TC, Pratta MA, Abbaszade I, Hollis JM, Liu R, Rosenfeld SA, Copeland RA, Decicco CP, Wynn R, Rockwell A, Yang F, Duke JL, Solomon K, George H, Bruckner R, Nagase H, Itoh Y, Ellis DM, Ross H, Wiswall BH, Murphy K, Hillman MC Jr, Hollis GF, Newton RC, Magolda RL, Trzaskos JM, Arner EC (1999) Purification and cloning of aggrecanase-1: a member of the ADAMTS family of proteins. Science 284:1664–1666

Turk BE, Huang LL, Piro ET, Cantley LC (2001) Determination of protease cleavage site motifs using mixture-based oriented peptide libraries. Nat Biotechnol 19:661–667

Ujita M, Shinomura T, Ito K, Kitagawa Y, Kimata K (1994) Expression and binding activity of the carboxyl-terminal portion of the core protein of PG-M, a large chondroitin sulfate proteoglycan. J Biol Chem 269:27603–27609

Watanabe H, Yamada Y (1999) Mice lacking link protein develop dwarfism and craniofacial abnormalities. Nat Genet 21:225–229

Watanabe H, Kimata K, Line S, Strong D, Gao LY, Kozak CA, Yamada Y (1994) Mouse cartilage matrix deficiency (cmd) caused by a 7 bp deletion in the aggrecan gene. Nat Genet 7:154–157

Weber P, Bartsch U, Rasband MN, Czaniera R, Lang Y, Bluethmann H, Margolis RU, Levinson SR, Shrager P, Montag D, Schachner M (1999) Mice deficient for tenascin-R display alterations of the extracellular matrix and decreased axonal conduction velocities in the CNS. J Neurosci 19:4245–4262

Weigel PH, Hascall VC, Tammi M (1997) Hyaluronan synthases. J Biol Chem 272:13997–14000

Westling J, Gottschall PE, Thompson VP, Cockburn A, Perides G, Zimmermann DR, Sandy JD (2004) ADAMTS4 (aggrecanase-1) cleaves human brain versican V2 at Glu405-Gln406 to generate glial hyaluronate binding protein. Biochem J 377:787–795

Xiao ZC, Bartsch U, Margolis RK, Rougon G, Montag D, Schachner M (1997) Isolation of a tenascin-R binding protein from mouse brain membranes—a phosphacan-related chondroitin sulfate proteoglycan. J Biol Chem 272:32092–32101

Yamada H, Watanabe K, Shimonaka M, Yamasaki M, Yamaguchi Y (1995) cDNA cloning and the identification of an aggrecanase-like cleavage site in rat brevican. Biochem Biophys Res Commun 216:957–963

Yamada H, Fredette B, Shitara K, Hagihara K, Miura R, Ranscht B, Stallcup WB, Yamaguchi Y (1997a) The brain chondroitin sulfate proteoglycan brevican associates with astrocytes ensheathing cerebellar glomeruli and inhibits neurite outgrowth from granule neurons. J Neurosci 17:7784–7795

Yamada K, Yamada T, Sasaki T, Rahemtulla F, Takagi M (1997b) Light and electron microscopical immunohistochemical localization of large proteoglycans in human tooth germs at the bell stage. Histochem J 29:167–175

Yamagata M, Sanes JR (2005) Versican in the developing brain: lamina-specific expression in interneuronal subsets and role in presynaptic maturation. J Neurosci 25:8457–8467

Yamagata M, Shinomura T, Kimata K (1993) Tissue variation of two large chondroitin sulfate proteoglycans (PG-M/versican and PG-H/aggrecan) in chick embryos. Anat Embryol Berl 187:433–444

Yamaguchi Y (1996) Brevican—a major proteoglycan in adult brain. Perspect Dev Neurobiol 3:307–317

Yamaguchi Y (2000) Lecticans: organizers of the brain extracellular matrix. Cell Mol Life Sci 57:276–289

Yuan W, Matthews RT, Sandy JD, Gottschall PE (2002) Association between protease-specific proteolytic cleavage of brevican and synaptic loss in the dentate gyrus of kainate-treated rats. Neuroscience 114:1091–1101

Zako M, Iwaki M, Yoneda M, Miyaishi O, Zhao J, Suzuki Y, Takeuchi M, Miyake G, Ikagawa H, Kimata K (2002) Molecular cloning and characterization of chick sialoprotein associated with cones and rods, a developmentally regulated glycoprotein of interphotoreceptor matrix. J Biol Chem 277:25592–25600

Zako M, Shinomura T, Ujita M, Ito K, Kimata K (1995) Expression of PG-M (V3), an alternative splice form of PG-M without a chondroitin sulfate attachment region in mouse and human tissues. J Biol Chem 270:3914–3918

Zeng W, Corcoran C, Collins-Racie LA, Lavallie ER, Morris EA, Flannery CR (2006) Glycosaminoglycan-binding properties and aggrecanase activities of truncated ADAMTSs: comparative analyses with ADAMTS-5, -9, -16 and -18. Biochim Biophys Acta 1760:517–524

Zheng B, Lee JK, Xie F (2006) Genetic mouse models for studying inhibitors of spinal axon regeneration. Trends Neurosci 29:640–646

Zhou XH, Brakebusch C, Matthies H, Oohashi T, Hirsch E, Moser M, Krug M, Seidenbecher CI, Boeckers TM, Rauch U, Buettner R, Gundelfinger ED, Fassler R (2001) Neurocan is dispensable for brain development. Mol Cell Biol 21:5970–5978

Zimmermann DR, Ruoslahti E (1989) Multiple domains of the large fibroblast proteoglycan, versican. EMBO J 8:2975–2981

Zimmermann DR, Dours-Zimmermann MT, Schubert M, Bruckner-Tuderman L (1994) Versican is expressed in the proliferating zone in the epidermis and in association with the elastic network of the dermis. J Cell Biol 124:817–825

Zurn AD, Bandtlow CE (2006) Regeneration failure in the CNs: cellular and molecular mechanisms. Adv Exp Med Biol 557:54–76

3. Aims of the project

Prior to the initiation of this PhD project we had shown that the versican isoform V2 is a major constituent of the adult brain ECM (Dours-Zimmermann and Zimmermann, 1994; Schmalfeldt et al., 1998) and we described its characteristic expression pattern in myelinated fiber tracts of the CNS (Schmalfeldt et al., 2000). Moreover, we had demonstrated its potent inhibitory properties on axonal growth in vitro.

These data from our previous experiments together with additional work from other laboratories indicated that versicans could function in axonal guidance during development, participate in the stabilization of the myelinated fiber tracts during CNS maturation and contribute to the suppression of structural regeneration in the mature brain and spinal cord after injury.

In order to obtain a mouse model and to study the potential role of versican V2 in vivo, following specific goals were formulated:

1) To generate a mutant mouse constitutively lacking the versican splice-variant V2.
2) To screen the mutants for gross anatomical, histological and molecular aberrations focusing in particular on the myelinated fiber tracts in the CNS.
3) To produce domain-specific antibodies against mouse versicans and other mouse lecticans in order to detect alterations of their deposition in knockout mice.
4) To analyze the differential expression pattern of CSPGs in CNS injury models by discriminating between the different lecticans (in collaboration with other laboratories).

References:

Dours-Zimmermann MT, Zimmermann DR (1994) A novel glycosaminoglycan attachment domain identified in two alternative splice variants of human versican. J Biol Chem 269:32992-32998.

Schmalfeldt M, Dours-Zimmermann MT, Winterhalter KH, Zimmermann DR (1998) Versican V2 is a major extracellular matrix component of the mature bovine brain. J Biol Chem 273:15758-15764.

Schmalfeldt M, Bandtlow CE, Dours-Zimmermann MT, Winterhalter KH, Zimmermann DR (2000) Brain derived versican V2 is a potent inhibitor of axonal growth. J Cell Sci 113:807-816.

4. Results

4.1. Original publication I (submitted manuscript):

Dours-Zimmermann MT, Rauch U, Stoffel W, Fässler R, Zimmermann DR. (2008) Versican V2 assembles the extracellular matrix surrounding the nodes of Ranvier in the central nervous system (submitted to J. Neuroscience).

Submitted to Journal of Neuroscience

Section: Cellular & Molecular Neuroscience

Versican V2 assembles the extracellular matrix surrounding the nodes of Ranvier in the central nervous system

(Abbreviated title: ECM assembly at CNS-nodes of Ranvier)

María T. Dours-Zimmermann[1], Uwe Rauch[2], Wilhelm Stoffel[3], Reinhard Fässler[4], and Dieter R. Zimmermann[1]

[1] Institute of Surgical Pathology, University Hospital Zurich, CH-8091 Zurich, Switzerland

[2] Vascular Wall Biology, Department of Experimental Medical Science, University of Lund, S-221 00 Lund, Sweden

[3] Center for Biochemistry, Medical Faculty, University of Cologne, D-50931 Cologne, Germany

[4] Department of Molecular Medicine, Max Planck Institute of Biochemistry, D-82152 Martinsried, Germany

Corresponding author: Dieter R. Zimmermann, Institute of Surgical Pathology, University Hospital Zurich, Schmelzbergstrasse 12, CH-8091 Zürich, Switzerland. Email: dieterzi@pathol.uzh.ch

Numbers of figures / tables: **10 / none**

Numbers of supplementary tables: **1**

Numbers of pages: **19**

Numbers of words for Abstract / Introduction / Discussion: **161 / 499 / 1497**

Keywords: Versican; Chondroitin Sulfate Proteoglycan; Extracellular Matrix; Node of Ranvier; Matrix Assembly; Knockout

Acknowledgements

We thank Anders Aspberg and Takako Sasaki for the generous gift of antibodies, Marie-Therese Abdou, Belinda Senn and Karin Hansen for preparing tissue sections Mathias Hoechli and Nicole Schaeren-Wiemers for technical advice and Holger Moch for support.

This work was financed in part by grants from the Swiss National Science Foundation and the Velux-Foundation to D.R.Z.

Abstract

The central nervous system-restricted versican splice-variant V2 is a large chondroitin sulfate proteoglycan incorporated in the extracellular matrix surrounding myelinated fibers and particularly accumulating at nodes of Ranvier. In vitro, it is a potent inhibitor of axonal growth and therefore considered to participate in the reduction of structural plasticity connected to myelination. To study the role of versican V2 during postnatal development, we designed a novel isoform-specific gene inactivation approach circumventing early embryonic lethality of the complete knockout and preventing compensation by the remaining versican splice-variants. These mice are viable and fertile, display however, major molecular alterations at the nodes of Ranvier. While the clustering of nodal sodium channels and paranodal structures appear in versican V2-deficient mice unaffected, the formation of the extracellular matrix surrounding the nodes is largely impaired. The conjoint loss of tenascin-R and phosphacan from the perinodal matrix provide strong evidence that versican V2, possibly controlled by a nodal receptor, organizes the extracellular matrix assembly in vivo.

Introduction

Neuronal and glial cells of the adult central nervous system (CNS) are surrounded by specialized extracellular matrices (ECM) that assemble during maturation and replace the loose meshwork of the late embryonic and early postnatal phase (for reviews see (Bandtlow and Zimmermann, 2000; Yamaguchi, 2000; Rauch, 2004; Zimmermann and Dours-Zimmermann, 2008)). Both, juvenile and mature forms of the CNS-matrix are composed of chondroitin sulfate proteoglycans (CSPG), tenascins, link proteins and hyaluronan. The majority of the CSPGs belong to the lectican family that includes brevican, neurocan, aggrecan and versican. Lecticans share N- and C-terminal globular structures (G1 and G3, respectively) separated by unique glycosaminoglycan (GAG) carrying middle portions of variable size. Moreover, alternative incorporation of the two glycosaminoglycan attachment regions, GAG-α and GAG-β, results in four versican splice-variants (V0 contains the GAG-α and GAG-β-domain, V1 only GAG-β, V2 only GAG-α and V3 neither of these domains) (Dours-Zimmermann and Zimmermann, 1994; Zako et al., 1995).

All lecticans bind via their G1-domain to hyaluronan. This interaction is stabilized by one of four link proteins (HAPLN1-4) (Spicer et al., 2003). In addition, the lectin-like element in the C-terminal G3-domain displays in vitro moderate to high binding-affinities towards tenascin-R (TnR) (Aspberg et al., 1997), tenascin-C (TnC) (Day et al., 2004) and sulfated glycolipids (Miura et al., 1999). The trimeric TnR and the hexameric TnC glycoproteins may crosslink the G3 domains of lecticans and thus, tie up the extracellular network (Lundell et al., 2004). Finally, phosphacan, a secreted CSPG-form of the receptor-like protein tyrosine phosphatase β (RPTPβ) (Maurel et al., 1994), joins the complex.

In the adult CNS, versican V2 and HAPLN2/Bral1 are the prominent components of the white matter ECM and particularly accumulate at the nodes of Ranvier (Schmalfeldt et al., 1998; Schmalfeldt et al., 2000; Oohashi et al., 2002; Melendez-Vasquez et al., 2005). Conversely, aggrecan, HAPLN4/Bral2 and neurocan associate with perineuronal nets (Bruckner et al., 2000; Bekku et al., 2003). Brevican, hyaluronan, TnR and phosphacan are observed in both of these meshworks.

Since lecticans strongly inhibit axonal growth in vitro, these specialized ECMs might participate in consolidating myelinated fiber tracts, limiting structural plasticity and restricting regeneration in the maturating CNS (Yamaguchi, 2000; Zurn and Bandtlow, 2006; Galtrey and Fawcett, 2007; Zimmermann and Dours-Zimmermann, 2008). Furthermore, they may regulate the assembly of axo-glial complexes and facilitate the induction and propagation of action potentials at the axon initial segments (AIS) and the nodes of Ranvier (Bruckner et al., 1993; Poliak and Peles, 2003; Salzer, 2003; Sherman and Brophy, 2005; Bruckner et al., 2006; Hedstrom and Rasband, 2006) or they could fulfill neuroprotective functions (Morawski et al., 2004).

To further explore these potential roles in vivo, we have now suppressed the expression of versican V2, one of the main constituents of the mature neural ECM. We avoided the early embryonic lethality of the complete gene knockout (Mjaatvedt et al., 1998) by employing an

unconventional isoform-specific gene targeting strategy. The newly generated mouse strain is viable and fertile, but displays major aberrations in the matrix assembly.

Materials and Methods

Generation of versican V0/V2 KO mice

Using a targeting vector containing a floxed neomycin–thymidine kinase (neo–tk) selection cassette under the control of the HSV-tk promoter, we introduced an ER-retention signal followed by an early translational stop codon into the GAG-α encoding exon VII of the mouse versican gene (codon-insertion KDELstop after E749, Swiss-Prot Q62059; **figure 1**). The two 3.9 kb-long genomic arms of the construct included corresponding parts of exon VII plus adjacent intron sequences, previously cloned from syngeneic DNA by PCR *(primer sequences and PCR-conditions available on request).* Electroporation of the linearized construct into R1 129Sv embryonic stem (ES) cells (Nagy et al., 1993), selection and screening of ES cell clones were done as previously described (Talts et al., 1999). Homologous recombinants were identified by Southern blot analysis using a digoxigenin (DIG)-labeled probe (Roche Applied Science) downstream of the target site. The ES cells were injected into C57Bl/6J blastocysts and transferred into a foster mother. The chimaeric offsprings were cross-bred with C57Bl/6J WT mice. Germline transmission of the mutated versican allele was verified by Southern blotting and long-distance PCR.

The floxed neo-tk selection cassette was removed in vivo by cross-breeding heterozygous V0/V2 neo-tk animals with a mouse strain expressing the CRE transgene under the control of the cytomegalovirus promoter (Schwenk et al., 1995). Correct target integration and recombination was verified by PCR and sequencing of the modified allele. The mutant mice, named $VCAN^{(tm1Zim)}$, were back-crossed to establish 129Sv inbred and C57BL/6J outbred strains.

Northern blotting and Quantitative RT-PCR

Primary fibroblasts were isolated from E14.5 embryos and maintained in culture (Talts et al., 1999). Total RNA extraction, Northern blotting and DIG-labeling of a riboprobe hybridizing with the hyaluronan-binding region of the mouse versican mRNA (HABR, positions 458 to 1203, GenBank D28599) were done as described (Zimmermann et al., 1994).

To determine relative amounts of versican mRNA expression in the mutant versus WT mouse brains, quantitative RT-PCR was performed with an ABI PRISM 7700 Sequence Detection System using the QuantiTect SYBR Green RT-PCR Kit (Qiagen). Total RNAs from brains of littermates were extracted with RNeasy Protect kit (Qiagen). Primers detecting the different splice-variants of versican were designed to cover the isoform specific exon-exon boundaries *(supplementary table)*. Threshold cycle-values (C_T) from at least three animals per genotype and per developmental time point were normalized against glyceraldehyde-3-phosphate dehydrogenase mRNA (mGAPDH, GenBank M32599) as endogenous control. Relative mRNA amounts ($2^{-\Delta\Delta C_T}$) were calculated on the basis of the comparative C_T method, applying the formula $\Delta\Delta C_T = (\Delta C_T \text{ KO} - \Delta C_T \text{ WT})$. The ΔC_T of each measurement was determined by subtracting the GAPDH-C_T from the versican-C_T value (ΔC_T= VC C_T - GAPDH C_T).

Antibodies

All polyclonal antibodies have been raised against recombinant core protein fragments as described previously (Zimmermann et al., 1994). The GAG-α specific antibodies (Schmalfeldt et al., 2000) recognize the N-terminal portion of this domain of mouse versican (amino acids 362 to 585, Swiss-Prot Q62059), also present in the potentially translated truncated V0/V2-polypetide of the mutant mice. The GAG-β antigen comprised amino acids 2750 to 3040. Both versican fragments were used to generate rabbit and guinea pig antisera in parallel. Recombinant portions of aggrecan (mAC-IGD: residues 368-481 and mAC-GAG: 1678-1896; Swiss-Prot Q61282) and neurocan (mNC-C: residues 645-944; Swiss-Prot P55066) served as antigens for the immunization of guinea pigs. Rabbit antisera against rat brevican (Thon et al., 2000) and TnR (Day et al., 2004) were kind gifts of Takako Sasaki and Anders Aspberg, respectively.

The anti-phosphacan monoclonal antibody 3F8 (Rauch et al., 1991) was purchased from the Developmental Studies Hybridoma Bank (University of Iowa). Other commercial antibodies used were: goat anti-human-contactin-1 polyclonal antibodies (R&D Systems), mouse monoclonal antibody K14/16 against the $K_v1.2$ α-subunit (Upstate),
rabbit anti-rat-voltage gated sodium channel 1.6 ($Na_v1.6$) polyclonal antibodies (Alomone Labs, Israel), mouse monoclonal antibody anti-Caspr clone K65/35 (obtained from the UC Davis/NIH NeuroMab Facility, University of California), rabbit anti-human MBP polyclonal antibodies (Dako), mouse anti-human MBP monoclonal antibody 67-74 (Chemicon), rabbit polyclonal antibodies against bovine GFAP (Dako), mouse (pan-)sodium channel monoclonal antibody K58/35 (Sigma) and mouse anti-neurofilament-200 monoclonal antibody NE14 (Sigma).

Protein extraction and immunoblots

Brain extracts were prepared as described (Schmalfeldt et al., 1998); each step of sample preparations included Pefabloc and 'complete protease inhibitors' (Roche Applied Science). In brief, tissues were disrupted in a Polytron homogenizer with 4 volumes of extraction buffer (0.5 M NaCl, 50 mM Tris, pH 7.5, 25 mM EDTA, 0.5% Nonidet P-40) and stirred overnight at 4°C. The homogenates were centrifuged at 100,000 *g* for 1 h and the supernatants dialyzed against chondroitinase buffer (40 mM Tris, 40 mM sodium acetate, 10 mM EDTA, pH 8). The protein concentration was determined with the BCA System (Pierce).

Samples were run on 4-15% PHAST polyacrylamide gels (GE Healthcare) under reducing conditions and blotted onto Immobilon-P membranes (Millipore) by diffusion transfer at 70°C for 20 minutes. Alkaline phosphatase-conjugated secondary antibodies (Biosource or Jackson Immuno Research Laboratories) and color reaction with Western Blue substrate (Promega) were employed. To detect lecticans, samples were digested with chondroitinase ABC (Seikagaku) (1-2 mU/μg protein) at 37°C overnight prior to electrophoresis. Spent medium from primary embryonic fibroblast culture was extensively dialyzed against chondroitinase buffer before chondroitinase ABC digestion.

Immunohistochemistry and immunofluorescence

All animal studies were approved by our institutional review boards. Animals were euthanized by CO_2-inhalation and decapitated. The tissues were dissected, immediately fixed in 4% paraformaldehyde (PFA) in PBS, paraffin embedded and sectioned according to routine protocols. If needed, unmasking of the antigen prior to staining was done in a controlled antigen-retrieval device (FSG 120-T/T from Milestone), filled with appropriate buffer (10 mM tri-sodium citrate pH 6.0 or 2 mM Tris, 1.7 mM EDTA, 1 mM tri-sodium citrate, pH 7.8).

In some cases, mice were anesthetized with a lethal dose of pentobarbital and transcardially perfused with PBS, followed by perfusion-fixation with 4% PFA in PBS as described (Beggah et al., 2005). Brains and spinal cords were removed, post-fixed overnight at 4°C and either paraffin-embedded or cryo-protected and rapidly frozen in O.C.T. compound (Tissue-Tek).

Immunohistochemistry followed the avidin-biotinylated peroxidase method (VECTASTAIN Elite ABC Reagent, Vector Laboratories) using biotinylated secondary antibodies from Jackson Immuno Research Laboratories (biotin-SP-conjugated donkey anti-goat, guinea pig or rabbit IgG (H+L)). Counterstaining was done with Mayer's hematoxylin. With mouse monoclonal primary antibodies, the M.O.M. kit (Vector Laboratories) was used to avoid non-specific reactions.

To stain hyaluronan in tissue sections, biotinylated hyaluronic acid binding protein (B-HABP) (Seikagaku) was applied as 0.5 μg/ml-solution in PBS overnight at 4°C, then detected with the ABC method.

Hyaluronan was eliminated from the tissue sections by pre-treatment with either 0.1% testicular hyaluronidase (Roche Applied Science) or 10 U/ml hyaluronate-lyase from Streptomyces hyalurolyticus (Sigma) in 30 mM sodium acetate, 125 mM NaCl, pH 5.2 containing 'complete protease inhibitors'. Digestions went on for 2 hs at 37°C in a humid chamber. Control sections were processed in parallel with buffer alone. Sections were washed with PBS before blocking and immunostaining.

Immunofluorescence staining by standard procedures employed Alexa secondary antibodies: Fluor-488 or Fluor-594 highly cross-adsorbed goat anti-rabbit, guinea pig or mouse IgG (H+L), or Fluor-594 donkey anti-goat. For triple immunofluorescence: Alexa Fluor-488 donkey anti-rabbit, Alexa Fluor-555 donkey anti-goat and Alexa Fluor-647 donkey anti-mouse IgGs. Counterstaining was with Hoechst H33258 bis-benzimide (all from Invitrogen). Blocking reagent of the M.O.M. kit was used for mouse primary antibodies.

Photomicrographs were taken with an Olympus BX61 microscope equipped with a F-view camera. The image capture was controlled with the AnalySISPro software (Soft Imaging System, Münster, Germany). Confocal Laser Scanning Microscopy was done with a Leica TCS4D, and 3D image-processing using IMARIS software (Bitplane, Switzerland).

Results

Generation of versican V0 and V2 specific knockout mice

The constitutive knockout of all versican isoforms is lethal at an early embryonic stage (Mjaatvedt et al., 1998). We therefore chose a splice-variant-specific gene inactivation approach to explore the function of versican V2 in the adult mouse CNS in vivo. For this purpose, we introduced a translational stop codon into exon VII of the versican gene (*VCAN*) preceded by an ER-retention signal (**figure 1**). This minimal modification, supplemented only by a loxP site, was sought to circumvent potential splicing errors or compensatory expression of other isoforms and to suppress the secretion of a truncated protein in the recombinant mice. Due to the splicing modality of the versican gene the elimination of the expression of the largest V0 isoform conjointly with versican V2 has been unavoidable, however.

Heterozygous and homozygous mice of the newly generated knockout mouse strain $VCAN^{(tm1Zim)}$ are viable and fertile, have a normal life span, exhibit in comparison to their wildtype littermates no immediately obvious phenotype in the nervous system and display within the cage environment an inconspicuous behavior. Litters of heterozygous breeding pairs follow a normal Mendelian inheritance indicating no increased lethality in association with the versican mutant genotype.

Expression of the versican transcripts in V0/V2 knockout mice

In line with our targeting strategy to abrogate the versican V0 and V2 production only on the protein level and to preserve correct splicing and normal expression of versican transcripts, we could find mRNAs of all splice variants in knockout animals. Nevertheless, the ratios of the different versican transcripts were to some extend affected in the mutant mice. For instance, Northern blot analysis of RNA isolated from E14.5 embryonic fibroblasts showed that versican V0 transcripts were reduced in cells from heterozygous mice or even evaded detection when they were isolated from homozygous animals (**figure 2A**). In both cases the level of the V1 message remained unchanged in embryonic fibroblasts. A more sensitive approach using RT-PCR with isoform-specific primers confirmed however, the presence of versican V0 transcripts in all mutant fibroblast cultures (not shown). Relative quantification of versican transcripts in brains of homozygous versus wildtype littermates by real-time RT-PCR finally demonstrated that the total amount of versican mRNA was diminished in knockout animals of all ages examined (P0, P30 and P100). In homozygous mice this change in expression resulted from a 90%-reduction of versican V2 mRNA (all ages tested) and a decline of V0 mRNA to about 20% (P0) or 50% (P30, P100) of the level measured in the wildtype animals (**figure 2B**). In contrast, the relative expression level of versican V1 mRNA in brain was not influenced by the mutation and also the V3-transcript stayed rather stably low.

Proof of absence of versican V0 and V2 core proteins in homozygous mutants

The efficient elimination of the V0 and V2 core protein expression in homozygous animals was demonstrated in comparisons with adult wildtype and heterozygous littermates. Immunoblots of brain extracts with GAG-α domain specific antibodies showed that versican V2 protein was significantly reduced in heterozygous and abolished in homozygous mice (**figure 2C**). Moreover, the absence of the truncated form of V0 and V2 provided indirect evidence for a successful intracellular degradation in neural cells. Similarly, immunoblot of spent medium from primary cultures of E14.5 mutant embryonic fibroblasts with anti-GAG-β domain antibodies revealed that homozygous fibroblasts secreted normal levels of the V1 isoform, but completely lacked the versican V0 core protein confirming the effectiveness of our targeting approach also in mesenchymal cells (**figure 2D**).

The complete absence of the V0 and V2 core proteins in the homozygote mice could ultimately be proven by comparative immunohistological analyses of wildtype animals and mutants using our GAG-domain specific antibodies. In wildtype mice, versican V0 is normally present during early CNS development mostly disappearing after birth (not shown). In exchange versican V2 expression initiates postnatally increasing continuously until it reaches a plateau (mRNA level around P30 / protein level around P90). At this time point versican V2 has become a major component of the brain ECM being associated with the white matter of the central nervous system (**figures 3 and 4**). In the knockout strain, neither the core proteins of versican V0 (includes GAG-α and GAG-β) nor of versican V2 (contains only GAG-α) could be detected by immunohistochemical stainings of embryonic (not shown) or postnatal tissues confirming their effective abrogation (**figures 3A, 4, 6 and 7** display examples of cerebellum, cerebrum, optic nerve and spinal cord).

Effects of the versican V0/V2 knockout on the expression of other lecticans

In accordance with our strategy to minimize the impact on the transcriptional level and to evade potential feedback mechanisms, the lack of versican V2 in the adult CNS of homozygous mutants was not compensated by increased expression and deposition of the remaining V1 and V3 splice-variants (**fig. 2B, 3**). In fact, immunostaining with GAG-β specific antibodies revealed that versican V1 stayed in wildtype and knockout littermates confined to a few tissues such as the choroid plexus, meninges and blood vessels (not shown). Also other lecticans retained their normal protein levels and distribution in the absence of versican V2. This is exemplified by immunohistochemical stainings of cerebellar white matter and granular cell layer and by immunoblotting of whole brain extracts employing antibodies against brevican, neurocan and aggrecan (**fig 3A and B,** respectively). Similarly, brain ECM-structures typically devoid of versican V2 (e.g. the specialized perineuronal nets in the deep cerebellar nuclei and/or the brain stem) displayed in the knockout mice their characteristic staining patterns for aggrecan, brevican and neurocan **(fig. 3, insets)**. Finally, no compensatory upregulation of other brain ECM molecules, like tenascin-R (TnR) and its binding partner phosphacan, could be observed in the initial immunoblotting experiments (**figure 3B**).

Histological and molecular analysis of myelinated fiber tracts

Despite the complete absence of versican V2 and the lack of a compensatory expression of a related lectican, postnatal brain development seemed to be mostly unaffected in knockout mice **(figure 4)**. Hematoxylin-eosin stainings revealed no significant differences in comparisons of brain sections from wildtype and mutant littermates aged P10 or older (not shown). Also the formation of the major fiber tracts and myelination appeared normal, since no alterations could be observed by light microscopical examination of Nissl stained sections or after immunohistochemistry with antibodies against neurofilament-200 (not shown) and myelin basic protein (MBP, **figure 4**). Likewise, the distribution of glial fibrillary acidic protein (GFAP)-positive astrocytes was comparable in wildtype and in knockout mice (not shown).

Although the CNS-specific versican V2 is in wildtype mice present all along the myelinated fibers, it is preferentially deposited at the nodes of Ranvier. Therefore, we focused next onto the nodal region. For this purpose, we prepared double and triple immunofluorescence stainings of cerebellum, spinal cord and optic nerve sections using antibodies against nodal, paranodal and juxtaparanodal markers. Our confocal images displayed in the CNS of wildtype mice a versican V2- and TnR-enriched extracellular matrix that engulfs the nodes between the compact MBP-positive myelin sheaths (**figure 5**). Surprisingly, the absence of versican from this structure had in the mouse mutants no effect on the distribution of MBP (not shown), the juxtaparanodal voltage-gated potassium channel 1.2 (K_v1.2) or the paranodal Caspr and contactin (**figures 6 and 7**). Also the compact clustering of the voltage-gated sodium channel 1.6 (Na_v1.6) embedded in the axolemma at the node of Ranvier appeared unaltered in versican V0/V2 null mice.

Disturbed assembly of the extracellular matrix around the node of Ranvier

In contrast to the normal localization of these membranous components, the molecular organization of extracellular matrix surrounding the myelin-free portion of the CNS nodes is in the V0/V2 knockout animals severely affected. This rather compact ECM forms a 1 to 2 μm-wide ring with an outer diameter of 3-4 μm (**figures 5 to 7**). It includes, apart from the tightly intermingled versican V2 and tenascin-R (TnR), also phosphacan (the secreted proteoglycan isoform of RPTPβ) and hyaluronan. Intriguingly, this specialized meshwork structure is practically absent in our mutant mice, as the selective ablation of the V2 isoform is accompanied by the complete loss of tenascin-R and phosphacan, suggesting a key regulatory function of versican in the assembly of the perinodal extracellular matrix. Nevertheless, TnR and phosphacan maintain their normal distribution in locations where versican V2 is usually not present. This includes the perineuronal nets of the deep cerebellar nuclei (TnR and phosphacan, **figure 7**) as well as the molecular layer of the cerebellum (phosphacan/RPTPβ, not shown). This specific loss of tenascin-R and phosphacan from the nodal ECM of versican V0/V2 knockout mice could also be corroborated in other CNS tissues such as spinal cord **(figure 7)** and optic nerve (not shown).

In order to confirm that versican V2 recruits tenascin-R to the nodal matrix and not vice versa, we made a comparative analysis of cerebellar sections from a TnR knockout strain (Rauch et al., 2005) with tissue sections from our versican V0/V2 mutant. These immunohistological experiments indeed demonstrated that versican V2 incorporated normally into the extracellular matrix at the nodes of Ranvier, even in the absence of tenascin-R, while TnR implicitly required versican V2 for its deposition at this location (**figure 8**). Interestingly, phosphacan was missing from the nodal matrix of both knockout strains indicating that its loss in the CNS of versican V0/V2 knockout mice is caused indirectly by the absence of TnR (data not shown).

Previous in vitro experiments have demonstrated that the C-type lectin domain within the C-terminal G3-region of versican mediates the binding to tenascin-R (Aspberg et al., 1997), whereas the N-terminal G1-domain interacts with hyaluronan (LeBaron et al., 1992). Because versican V2 is recruited to the nodal matrix independently of tenascin-R, we subsequently tested, whether hyaluronan, its second ligand at the node of Ranvier, could be responsible for anchoring the large molecular complex of versican V2, TnR and phosphacan. We therefore removed hyaluronan from wildtype cerebellar sections by cleavage with the highly specific *Streptomyces hyalurolyticus* hyaluronate-lyase or with ovine testicular hyaluronidase, an enzyme known to degrade also chondroitin and chondroitin sulfate. Despite the effective elimination of hyaluronan by either enzyme the distribution of versican V2 and tenascin-R remained unchanged (**figure 9**). Only phosphacan disappeared from the nodes of Ranvier after treatment with testicular hyaluronidase, while the more specific hyaluronate-lyase had no effect. Consequently, we have attributed the loss of phosphacan from the complex to the chondroitinase side-activity of this enzyme. The versican V2 immunostaining was also not affected in hyaluronan-depleted cerebellum sections of tenascin-R null mutants demonstrating that neither ligand is absolutely necessary for its anchorage in the ECM (not shown).

Finally, cell surface sulfatides interact *in vitro* with the C-terminal globular domain of lecticans, including versican (Miura et al., 1999). We therefore concluded our studies of the versican ligands by analyzing the distribution of the V2 isoform in the myelinated fiber tracts of brains from mice deficient in UDP-galactose ceramide galactosyltransferase (CGT) (Bosio et al., 1996). CGT is a key enzyme in the biosynthesis of galactocerebroside (GalC) and its sulfated-derivative, sulfatide, both major lipid constituents of myelin. Although CGT-knockout mice completely lack axoglial junctions in the CNS-paranodes and die shortly after onset of myelination, they displayed about 19 days after birth no abnormal distribution of versican V2 and tenascin-R in cerebrum and cerebellum **(figure 10)**. Even additional enzymatic removal of hyaluronan from the brain sections of CGT null mice did not result in the release of versican V2 from the newly formed nodes of Ranvier. In sum, these experiments indicate, that the cell surface sulfatide lipids are, unlike versican V2, not directly involved in the assembly of the nodal extracellular matrix.

Discussion

Our previous studies, first identifying the versican isoform V2 as a major constituent of the adult brain extracellular matrix (Dours-Zimmermann and Zimmermann, 1994; Schmalfeldt et al., 1998), then revealing its characteristic expression pattern in myelinated fiber tracts of the central nervous system and subsequently demonstrating its potent inhibitory properties on axonal growth (Schmalfeldt et al., 2000) in vitro, prompted us to generate a knockout mouse model to further explore the function of this CNS-specific lectican in vivo. Due to the early intra-uterine lethality caused by the constitutive elimination of all versican splice-variants in *hdf* mice (Mjaatvedt et al., 1998), we had to choose between 1) a conditional knockout approach, potentially facing difficulties with efficiency, timing and tissue-specificity of the versican gene ablation, or 2) an isoform-selective knockout, which would only affect the alternatively spliced exon VII, but would also abolish the expression of the more widely distributed V0 splice-variant along with the CNS-restricted versican V2. Since versican V0 appears to be always co-expressed together with versican V1 (Dours-Zimmermann and Zimmermann, 1994; Zimmermann et al., 1994; Landolt et al., 1995; Dutt et al., 2006), we considered the collateral elimination of versican V0 the minor problem, and finally opted for the latter approach. For this purpose, we designed a novel strategy that ultimately left the expression of versican V1 and V3 intact, effectively prevented compensation by other versican splice-variants and successfully circumvented the secretion of an artificially truncated core protein that potentially could cause a dominant side effect. Although we originally attempted to maintain normal mRNA levels of all versican splice-variants in the genetically manipulated VCAN$^{(tm1Zim)}$ strain and to disrupt V0- and V2-production and secretion only via a premature stop codon and an ER-retention signal instead, the complete annihilation of versican V0 and V2 in the mutants has most probably to be attributed to a combined action of a nonsense-mediated-decay (NMD) mechanism reducing the proportion of V0 and V2 transcripts (for review see (Kuzmiak and Maquat, 2006)) and an efficient intracellular clearance of the few truncated core proteins translated from the mutated mRNAs.

The normal reproduction behavior, litter size and the Mendelian distribution of wildtype, heterozygous and homozygous progeny indeed confirmed our prediction, that the early embryonic lethality of *hdf* mice is mostly caused by the absence of versican V1 and consequently could be overcome by keeping the expression of this isoform unchanged in our mutant strain. Similar to the single gene inactivation of other prominent myelin-derived inhibitors of axonal growth like Nogo, myelin-associated glycoprotein (MAG) and oligodendrocyte myelin glycoprotein (OMgp) (Zurn and Bandtlow, 2006), the abolition of the CNS-restricted versican V2 alone had no apparent effect on the formation of the fiber tracts. Versican V2-deficency neither led to excessive axonal sprouting nor caused myelination defects in the developing central nervous system. Albeit very difficult to discern from immunofluorescence experiments, increased collateral axon branching at the CNS-nodes of Ranvier or enlargement of the nodal region were not evident. Since the proper formation and stabilization of fiber tracts and synaptic contacts in the CNS certainly involves inhibitory activities of many cell surface and ECM molecules, functional redundancy may explain, why

dramatic histological changes are only rarely observed in single mutants. These include also the brevican and neurocan knockout strains, which both displayed no alterations upon histological examination (Zhou et al., 2001; Brakebusch et al., 2002). While neurocan forms mostly part of the embryonic and perinatal extracellular matrix of the CNS, brevican expression is initiated postnatally and overlaps to a certain extend with versican V2 in the interstitial space between the myelinated fibers. It is therefore conceivable that a lack of versican V2 at this location would at least partly be compensated by brevican. Eliminating both of these CNS-lecticans that are expressed more or less simultaneously during late developmental phases by cross-breeding the strains may provide more conclusive answers about their functional relation in regard to fiber tract stabilization. Based on our experiments, a rescue of a potential versican V2-null phenotype by compensatory up-regulation of other lecticans can be excluded, however.

Whereas brevican, aggrecan and neurocan are along with TnR highly concentrated in the perineuronal nets engulfing the perikaryon, the proximal dendrites and particularly the axon initial segment (AIS) of large neurons in various CNS regions, versican V2 is predominantly deposited in an analogous extracellular matrix structure surrounding the CNS nodes of Ranvier. Despite this intriguing accumulation that occurs already during the establishment of the nodes (Oohashi et al., 2002), versican V2 seems not to be directly involved in controlling the initial steps of nodal formation. Unaffected clustering of the Na_v channels at the CNS nodes and accurate localization of paranodal and juxtaparanodal components in our knockout mice argue against a role of versican V2 as a functional analogue of gliomedin, the glial organizer of the nodal structure in the peripheral nervous system (Eshed et al., 2005). Furthermore, the concomitant absence of node associated TnR and phosphacan and the lack of compensatory expression of other lecticans in our mouse mutant provide evidence that none of these extracellular matrix proteins are related to the oligodendrocyte-derived soluble factors reported to induce node-like Na_v clustering in vitro (Kaplan et al., 1997). Even a functional redundancy, leading to a substitution of the hypothetical clustering-activity of versican V2 by its close relative brevican, appears highly unlikely, as brevican retains its firm association with perineuronal nets and its uniform distribution along the myelinated fiber tracts without particularly concentrating around the nodes of Ranvier in knockout animals.

Instead, the data from our versican V0/V2 knockout mouse model clearly point towards a key role of versican V2 in the assembly of the extracellular structure surrounding and possibly stabilizing the CNS nodes. The conjoint loss of versican V2, tenascin-R and phosphacan from the nodal matrix in our mutant strain now confirms in vivo, macromolecular interactions formerly postulated on the basis of in vitro-findings. This includes the binding of versican V2 to tenascin-R (Aspberg et al., 1997) and the interactions between tenascin-R and phosphacan (Xiao et al., 1997; Milev et al., 1998). Since phosphacan is also absent from the nodes of Ranvier in TnR null mice (Weber et al., 1999), we conclude that versican V2 first recruits tenascin-R, which in turn integrates phosphacan into the matrix. Additional components joining the extracellular complex are hyaluronan and its binding partner Bral1, which shortly follows versican V2 expression during postnatal development (Oohashi et al., 2002). Bral1 possibly stabilizes the interaction between

hyaluronan and the N-terminal G1 domain of versican, whereas TnR may cross-link the versican G3 domains at the other end of the core protein. Hyaluronan certainly forms a general backbone for the aggregation of versican in the CNS. Yet, hyaluronan is unlikely to increase the versican deposition around the nodes of Ranvier because of its uniform distribution along the myelinated fiber tracts. Moreover, our hyaluronan-degradation experiments demonstrate that the binding of versican V2 is not crucially depending on interactions with hyaluronan and TnR alone or in combination. Considering all these observations, we propose a model, in which the accumulation of versican V2 around the CNS nodes of Ranvier forms the extracellular nucleation point for the subsequent assembly of the perinodal matrix.

Accordingly, the deposition of the versican-enriched matrix at the nodes is likely to be initiated by a firm interaction of versican V2 with the nodal axolemma or, less probable, with the paranodal structure, while previously reported binding activities of its partner TnR and/or phosphacan to paranodal contactin (Brummendorf et al., 1993; Peles et al., 1995) and Neurofascin-155 (NF-155) (Volkmer et al., 1998) or to the nodal sodium channels (Srinivasan et al., 1998; Ratcliffe et al., 2000) may either play no or only subordinate roles in matrix-anchoring. The prominent paranodal components contactin, NF-155, Caspr and sulfatides (known to interact with versican in vitro (Miura et al., 1999)) seem also not to be required for the selective deposition and binding of versican V2 at the nodes. In CGT-null mice, they are all virtually absent from the severely disturbed terminal glial loop structures of the CNS paranodes (Poliak et al., 2001; Marcus et al., 2002). Nevertheless, versican V2 and TnR accumulate normally in CGT-mutants, as demonstrated by our immunohistochemical analyses. Hence, cell surface proteins selectively localized within the nodal axolemma are more promising candidates for the versican-dependent anchoring of the perinodal extracellular matrix. In the adult CNS potential membrane receptors of versican are voltage gated sodium channels (mainly Na_v 1.6) and neurofascin-186 (NF-186). Hedstrom et al (Hedstrom et al., 2007) could recently show that the knockdown of NF-186 by RNA interference abolished the recruitment of the close versican-relative brevican to the perineuronal net covering the axon initial segment (AIS) of several subsets of CNS neurons. Since NF-186 is also crucially involved in the nodal assembly (Zonta et al., 2008), it seems conceivable that it similarly accumulates and immobilizes the ECM at the CNS nodes of Ranvier via a versican V2-mediated interaction. Yet, a direct binding of NF-186 to brevican and versican V2 has still to be demonstrated.

References

Aspberg A, Miura R, Bourdoulous S, Shimonaka M, Heinegård D, Schachner M, Ruoslahti E, Yamaguchi Y (1997) The C-type lectin domains of lecticans, a family of aggregating chondroitin sulfate proteoglycans, bind tenascin-R by protein-protein interactions independent of carbohydrate moiety. Proc Natl Acad Sci USA 94:10116-10121.

Bandtlow CE, Zimmermann DR (2000) Proteoglycans in the developing brain - new conceptual insights for old proteins. Physiol Rev 80:1267-1290.

Beggah AT, Dours-Zimmermann MT, Barras FM, Brosius A, Zimmermann DR, Zurn AD (2005) Lesion-induced differential expression and cell association of Neurocan, Brevican, Versican V1 and V2 in the mouse dorsal root entry zone. Neuroscience 133:749-762.

Bekku Y, Su WD, Hirakawa S, Fassler R, Ohtsuka A, Kang JS, Sanders J, Murakami T, Ninomiya Y, Oohashi T (2003) Molecular cloning of Bral2, a novel brain-specific link protein, and immunohistochemical colocalization with brevican in perineuronal nets. Mol Cell Neurosci 24:148-159.

Bosio A, Binczek E, Stoffel W (1996) Functional breakdown of the lipid bilayer of the myelin membrane in central and peripheral nervous system by disrupted galactocerebroside synthesis. Proc Natl Acad Sci U S A 93:13280-13285.

Brakebusch C, Seidenbecher CI, Asztely F, Rauch U, Matthies H, Meyer H, Krug M, Bockers TM, Zhou X, Kreutz MR, Montag D, Gundelfinger ED, Fassler R (2002) Brevican-deficient mice display impaired hippocampal CA1 long-term potentiation but show no obvious deficits in learning and memory. Mol Cell Biol 22:7417-7427.

Bruckner G, Szeoke S, Pavlica S, Grosche J, Kacza J (2006) Axon initial segment ensheathed by extracellular matrix in perineuronal nets. Neuroscience 138:365-375.

Bruckner G, Grosche J, Schmidt S, Hartig W, Margolis RU, Delpech B, Seidenbecher CI, Czaniera R, Schachner M (2000) Postnatal development of perineuronal nets in wild-type mice and in a mutant deficient in tenascin-R. J Comp Neurol 428:616-629.

Bruckner G, Brauer K, Hartig W, Wolff JR, Rickmann MJ, Derouiche A, Delpech B, Girard N, Oertel WH, Reichenbach A (1993) Perineuronal nets provide a polyanionic, glia-associated form of microenvironment around certain neurons in many parts of the rat brain. Glia 8:183-200.

Brummendorf T, Hubert M, Treubert U, Leuschner R, Tarnok A, Rathjen FG (1993) The axonal recognition molecule F11 is a multifunctional protein: specific domains mediate interactions with Ng-CAM and restrictin. Neuron 10:711-727.

Day JM, Olin AI, Murdoch AD, Canfield A, Sasaki T, Timpl R, Hardingham TE, Aspberg A (2004) Alternative splicing in the aggrecan G3 domain influences binding interactions with tenascin-C and other extracellular matrix proteins. J Biol Chem 279:12511-12518.

Dours-Zimmermann MT, Zimmermann DR (1994) A novel glycosaminoglycan attachment domain identified in two alternative splice variants of human versican. J Biol Chem 269:32992-32998.

Dutt S, Kleber M, Matasci M, Sommer L, Zimmermann DR (2006) Versican V0 and V1 guide migratory neural crest cells. J Biol Chem 281:12123-12131.

Eshed Y, Feinberg K, Poliak S, Sabanay H, Sarig-Nadir O, Spiegel I, Bermingham JR, Jr., Peles E (2005) Gliomedin mediates Schwann cell-axon interaction and the molecular assembly of the nodes of Ranvier. Neuron 47:215-229.

Galtrey CM, Fawcett JW (2007) The role of chondroitin sulfate proteoglycans in regeneration and plasticity in the central nervous system. Brain Res Rev 54:1-18.

Hedstrom KL, Rasband MN (2006) Intrinsic and extrinsic determinants of ion channel localization in neurons. J Neurochem 98:1345-1352.

Hedstrom KL, Xu X, Ogawa Y, Frischknecht R, Seidenbecher CI, Shrager P, Rasband MN (2007) Neurofascin assembles a specialized extracellular matrix at the axon initial segment. J Cell Biol 178:875-886.

Kaplan MR, Meyer-Franke A, Lambert S, Bennett V, Duncan ID, Levinson SR, Barres BA (1997) Induction of sodium channel clustering by oligodendrocytes. Nature 386:724-728.

Kuzmiak HA, Maquat LE (2006) Applying nonsense-mediated mRNA decay research to the clinic: progress and challenges. Trends Mol Med 12:306-316.

Landolt RM, Vaughan L, Winterhalter KH, Zimmermann DR (1995) Versican is selectively expressed in embryonic tissues that act as barriers to neural crest cell migration and axon outgrowth. Development 121:2303-2312.

LeBaron RG, Zimmermann DR, Ruoslahti E (1992) Hyaluronate binding properties of versican. J Biol Chem 267:10003-10010.

Lundell A, Olin AI, Morgelin M, al-Karadaghi S, Aspberg A, Logan DT (2004) Structural basis for interactions between tenascins and lectican C-type lectin domains: evidence for a crosslinking role for tenascins. Structure 12:1495-1506.

Marcus J, Dupree JL, Popko B (2002) Myelin-associated glycoprotein and myelin galactolipids stabilize developing axo-glial interactions. J Cell Biol 156:567-577.

Maurel P, Rauch U, Flad M, Margolis RK, Margolis RU (1994) Phosphacan, a chondroitin sulfate proteoglycan of brain that interacts with neurons and neural cell-adhesion molecules, is an extracellular variant of a receptor-type protein tyrosine phosphatase. Proc Natl Acad Sci USA 91:2512-2516.

Melendez-Vasquez C, Carey DJ, Zanazzi G, Reizes O, Maurel P, Salzer JL (2005) Differential expression of proteoglycans at central and peripheral nodes of Ranvier. Glia 52:301-308.

Milev P, Chiba A, Haring M, Rauvala H, Schachner M, Ranscht B, Margolis RK, Margolis RU (1998) High affinity binding and overlapping localization of neurocan and phosphacan protein-tyrosine phosphatase-zeta/beta with tenascin-R, amphoterin, and the heparin-binding growth-associated molecule. J Biol Chem 273:6998-7005.

Miura R, Aspberg A, Ethell IM, Hagihara K, Schnaar RL, Ruoslahti E, Yamaguchi Y (1999) The proteoglycan lectin domain binds sulfated cell surface glycolipids and promotes cell adhesion. J Biol Chem 274:11431-11438.

Mjaatvedt C, Yamamura H, Capehart A, Turner D, Markwald R (1998) The *cspg2* gene, disrupted in the *hdf* mutant, is required for right cardiac chamber and endocardial cushion formation. Dev Biol 202:56-66.

Morawski M, Bruckner MK, Riederer P, Bruckner G, Arendt T (2004) Perineuronal nets potentially protect against oxidative stress. Exp Neurol 188:309-315.

Nagy A, Rossant J, Nagy R, Abramow-Newerly W, Roder JC (1993) Derivation of completely cell culture-derived mice from early-passage embryonic stem cells. Proc Natl Acad Sci U S A 90:8424-8428.

Oohashi T, Hirakawa S, Bekku Y, Rauch U, Zimmermann DR, Su WD, Ohtsuka A, Murakami T, Ninomiya Y (2002) Bral1, a brain-specific link protein, colocalizing with the versican V2 isoform at the nodes of Ranvier in developing and adult mouse central nervous systems. Mol Cell Neurosci 19:43-57.

Peles E, Nativ M, Campbell PL, Sakurai T, Martinez R, Lev S, Clary DO, Schilling J, Barnea G, Plowman GD, Grumet M, Schlessinger J (1995) The carbonic anhydrase domain of receptor tyrosine phosphatase beta is a functional ligand for the axonal cell recognition molecule contactin. Cell 82:251-260.

Poliak S, Peles E (2003) The local differentiation of myelinated axons at nodes of Ranvier. Nat Rev Neurosci 4:968-980.

Poliak S, Gollan L, Salomon D, Berglund EO, Ohara R, Ranscht B, Peles E (2001) Localization of Caspr2 in myelinated nerves depends on axon-glia interactions and the generation of barriers along the axon. J Neurosci 21:7568-7575.

Rasband MN, Trimmer JS (2001) Developmental clustering of ion channels at and near the node of Ranvier. Dev Biol 236:5-16.

Ratcliffe CF, Qu Y, McCormick KA, Tibbs VC, Dixon JE, Scheuer T, Catterall WA (2000) A sodium channel signaling complex: modulation by associated receptor protein tyrosine phosphatase beta. Nat Neurosci 3:437-444.

Rauch U (2004) Extracellular matrix components associated with remodeling processes in brain. Cell Mol Life Sci 61:2031-2045.

Rauch U, Zhou XH, Roos G (2005) Extracellular matrix alterations in brains lacking four of its components. Biochem Biophys Res Commun 328:608-617.

Rauch U, Gao P, Janetzko A, Flaccus A, Hilgenberg L, Tekotte H, Margolis RK, Margolis RU (1991) Isolation and characterization of developmentally regulated chondroitin sulfate and chondroitin/keratan sulfate proteoglycans of brain identified with monoclonal antibodies. J Biol Chem 266:14785-14801.

Salzer JL (2003) Polarized domains of myelinated axons. Neuron 40:297-318.

Schmalfeldt M, Dours-Zimmermann MT, Winterhalter KH, Zimmermann DR (1998) Versican V2 is a major extracellular matrix component of the mature bovine brain. J Biol Chem 273:15758-15764.

Schmalfeldt M, Bandtlow CE, Dours-Zimmermann MT, Winterhalter KH, Zimmermann DR (2000) Brain derived versican V2 is a potent inhibitor of axonal growth. J Cell Sci 113:807-816.

Schwenk F, Baron U, Rajewsky K (1995) A cre-transgenic mouse strain for the ubiquitous deletion of loxP-flanked gene segments including deletion in germ cells. Nucleic Acids Res 23:5080-5081.

Sherman DL, Brophy PJ (2005) Mechanisms of axon ensheathment and myelin growth. Nat Rev Neurosci 6:683-690.

Spicer AP, Joo A, Bowling RA, Jr. (2003) A hyaluronan binding link protein gene family whose members are physically linked adjacent to chondroitin sulfate proteoglycan core protein genes: the missing links. J Biol Chem 278:21083-21091.

Srinivasan J, Schachner M, Catterall WA (1998) Interaction of voltage-gated sodium channels with the extracellular matrix molecules tenascin-C and tenascin-R. Proc Natl Acad Sci U S A 95:15753-15757.

Talts JF, Brakebusch C, Fassler R (1999) Integrin gene targeting. Methods Mol Biol 129:153-187.

Thon N, Haas CA, Rauch U, Merten T, Fassler R, Frotscher M, Deller T (2000) The chondroitin sulphate proteoglycan brevican is upregulated by astrocytes after entorhinal cortex lesions in adult rats. Eur J Neurosci 12:2547-2558.

Volkmer H, Zacharias U, Norenberg U, Rathjen FG (1998) Dissection of complex molecular interactions of neurofascin with axonin-1, F11, and tenascin-R, which promote attachment and neurite formation of tectal cells. J Cell Biol 142:1083-1093.

Weber P, Bartsch U, Rasband MN, Czaniera R, Lang Y, Bluethmann H, Margolis RU, Levinson SR, Shrager P, Montag D, Schachner M (1999) Mice deficient for tenascin-R display alterations of the extracellular matrix and decreased axonal conduction velocities in the CNS. J Neurosci 19:4245-4262.

Xiao ZC, Bartsch U, Margolis RK, Rougon G, Montag D, Schachner M (1997) Isolation of a tenascin-R binding protein from mouse brain membranes - a phosphacan-related chondroitin sulfate proteoglycan. J Biol Chem 272:32092-32101.

Yamaguchi Y (2000) Lecticans: organizers of the brain extracellular matrix. Cell Mol Life Sci 57:276-289.

Zako M, Shinomura T, Ujita M, Ito K, Kimata K (1995) Expression of PG-M (V3), an alternative splice form of PG-M without a chondroitin sulfate attachment region in mouse and human tissues. J Biol Chem 270:3914-3918.

Zhou XH, Brakebusch C, Matthies H, Oohashi T, Hirsch E, Moser M, Krug M, Seidenbecher CI, Boeckers TM, Rauch U, Buettner R, Gundelfinger ED, Fassler R (2001) Neurocan is dispensable for brain development. Mol Cell Biol 21:5970-5978.

Zimmermann DR, Dours-Zimmermann MT (2008) Extracellular matrix of the central nervous system: from neglect to challenge. Histochem Cell Biol. Published online Aug 12, 2008.

Zimmermann DR, Dours-Zimmermann MT, Schubert M, Bruckner-Tuderman L (1994) Versican is expressed in the proliferating zone in the epidermis and in association with the elastic network of the dermis. J Cell Biol 124:817-825.

Zonta B, Tait S, Melrose S, Anderson H, Harroch S, Higginson J, Sherman DL, Brophy PJ (2008) Glial and neuronal isoforms of Neurofascin have distinct roles in the assembly of nodes of Ranvier in the central nervous system. J Cell Biol 181:1169-1177.

Zurn AD, Bandtlow CE (2006) Regeneration failure in the CNs: cellular and molecular mechanisms. Adv Exp Med Biol 557:54-76.

Figure 1

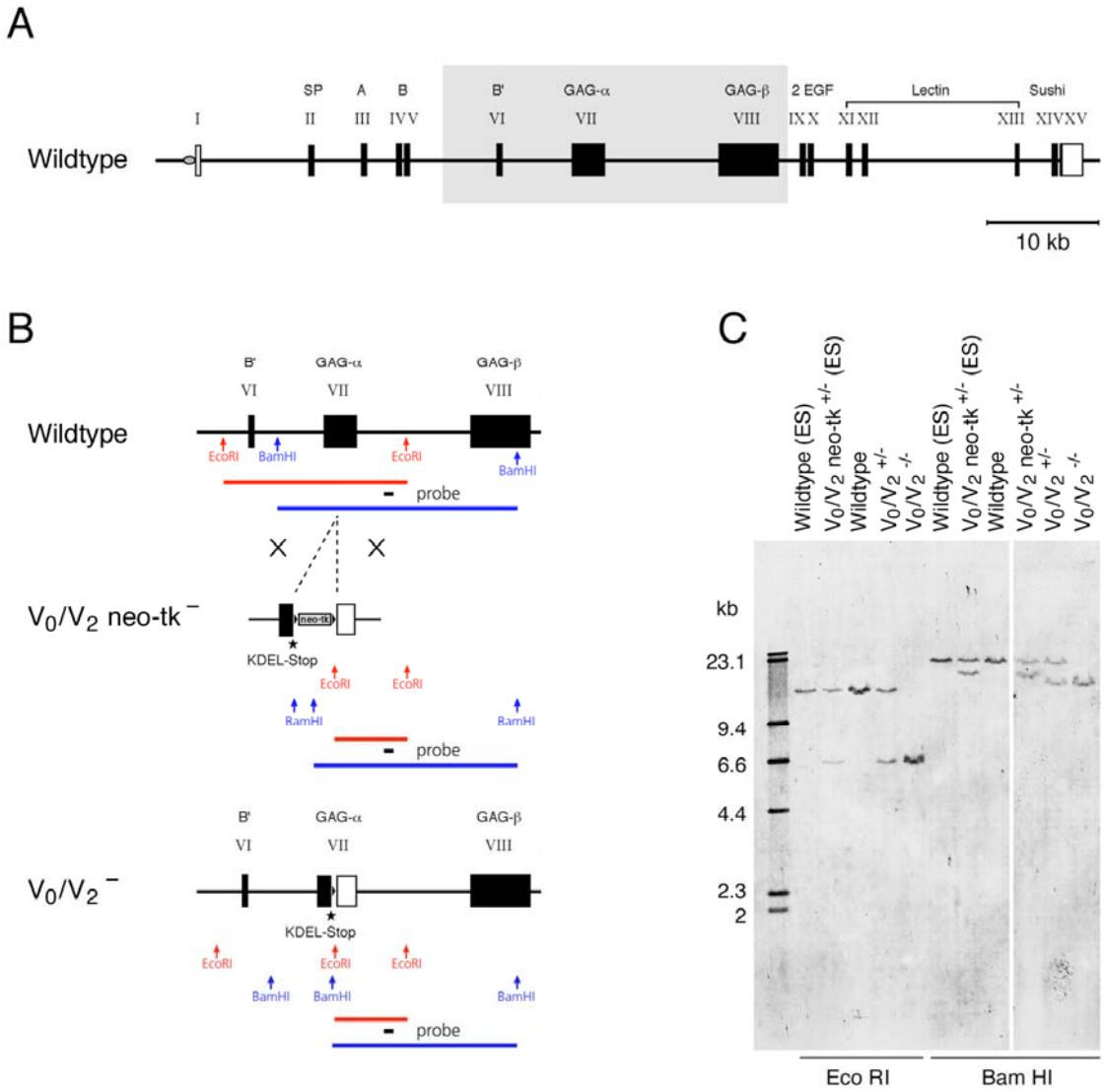

***Figure 1**. Generation of versican V0/V2 KO mice.*

A) Intron/exon organization of the mouse versican gene giving rise to four different versican isoforms (V0-V3) due to alternative splicing of exons VII and VIII encoding the GAG-attachment domains (GAG-α and GAG-β). Grey box shows region of interest displayed in B.
B) Locus diagram and targeting strategy: introduction of an ER retention signal, a translational stop codon and a floxed neo-tk cassette into exon VII of the versican gene (V0/V2 neo-tk). Removal of selection cassette by cross-breeding with a CRE-deleter strain leaves only the KDEL coding sequence and a stop codon plus one loxP site in exon VII of the mutated versican allele (V0/V2^{-}). Corresponding restriction fragments detected in Southern blot are depicted below.
C) Southern blot analysis of genomic DNA from mice and embryonic stem cells (ES): the DIG-probe downstream of the targeting locus hybridizes to the 17 Kb EcoRI-fragment of the WT allele, which converts to a 6.6 Kb-fragment in versican V0/V2 null mutants. BamHI restriction allows a distinction between WT, V0/V2 neo-tk $^{-}$, and V0/V2 $^{-}$ allele confirming the successful targeting.

Figure 2

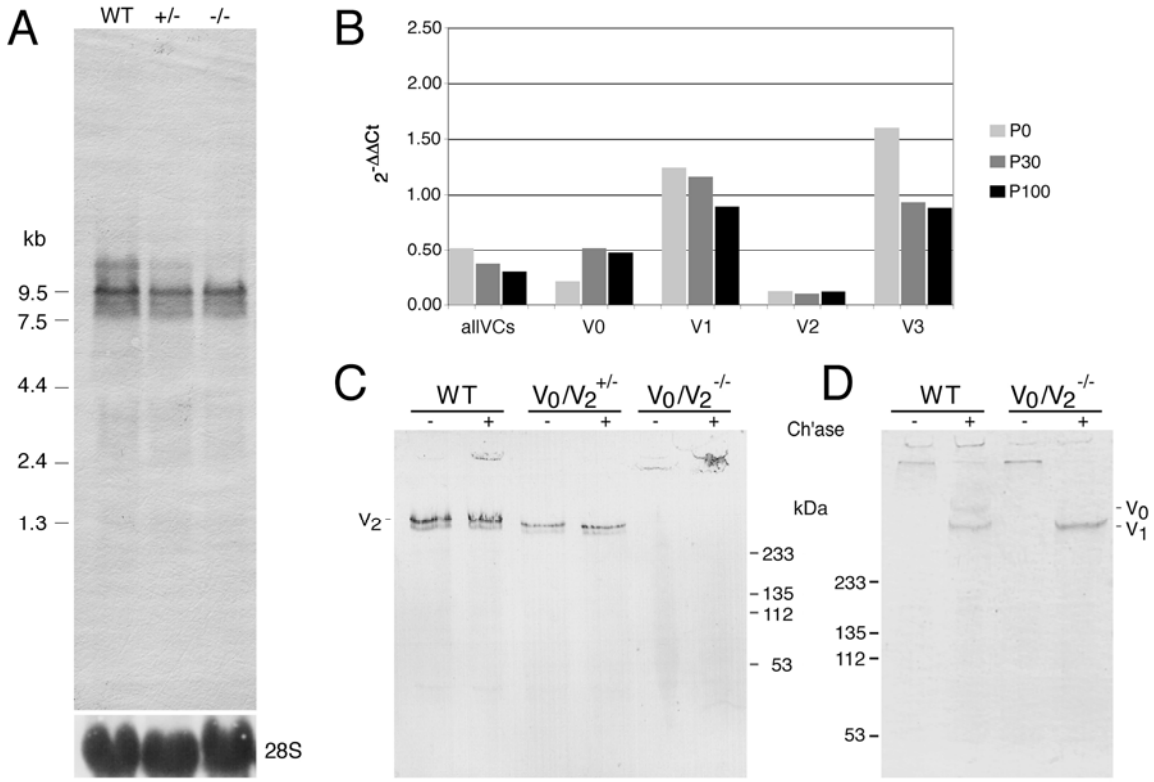

***Figure 2**. RNA expression analysis.*

A) Northern blot of total RNA from E14.5 embryonic fibroblasts hybridized with a riboprobe detecting all versican splice variants. The approximately 10 kb and 13 kb-bands correspond to mRNAs of versican V1 and V0, respectively. Minor fragments are products of alternative polyadenylation sites. Loading control: 28S ribosomal RNA.
B) Relative expression of alternative versican transcripts in brains of KO and WT mice at postnatal stages P0, P30 and P100 using quantitative RT-PCR. mRNA ratios of mutants versus WT ($2^{-\Delta\Delta Ct}$) were calculated as described in 'materials and methods'.
C) Immunoblot of brain extracts using GAG-α domain-specific antibodies demonstrates the reduction and the complete loss of versican V2 in heterozygous V0/V2$^{+/-}$ and homozygous V0/V2$^{-/-}$ animals, respectively. Note that the main portion of mouse versican V2 from WT mouse brains seems to be devoid of chondroitin sulfate (band also visible before chondroitinase ABC digestion). The lower V2 core protein band may represent intracellular precursor protein prior to full O-glycosylation.
D) Immunoblot with antibodies against the GAG-β domain. Supernatants from embryonic fibroblast cultures lack the V0 isoform in cells from homozygous mice. Samples in C) and D) were loaded with (+) or without (-) preceding treatment with chondroitinase ABC (Ch'ase).

Figure 3

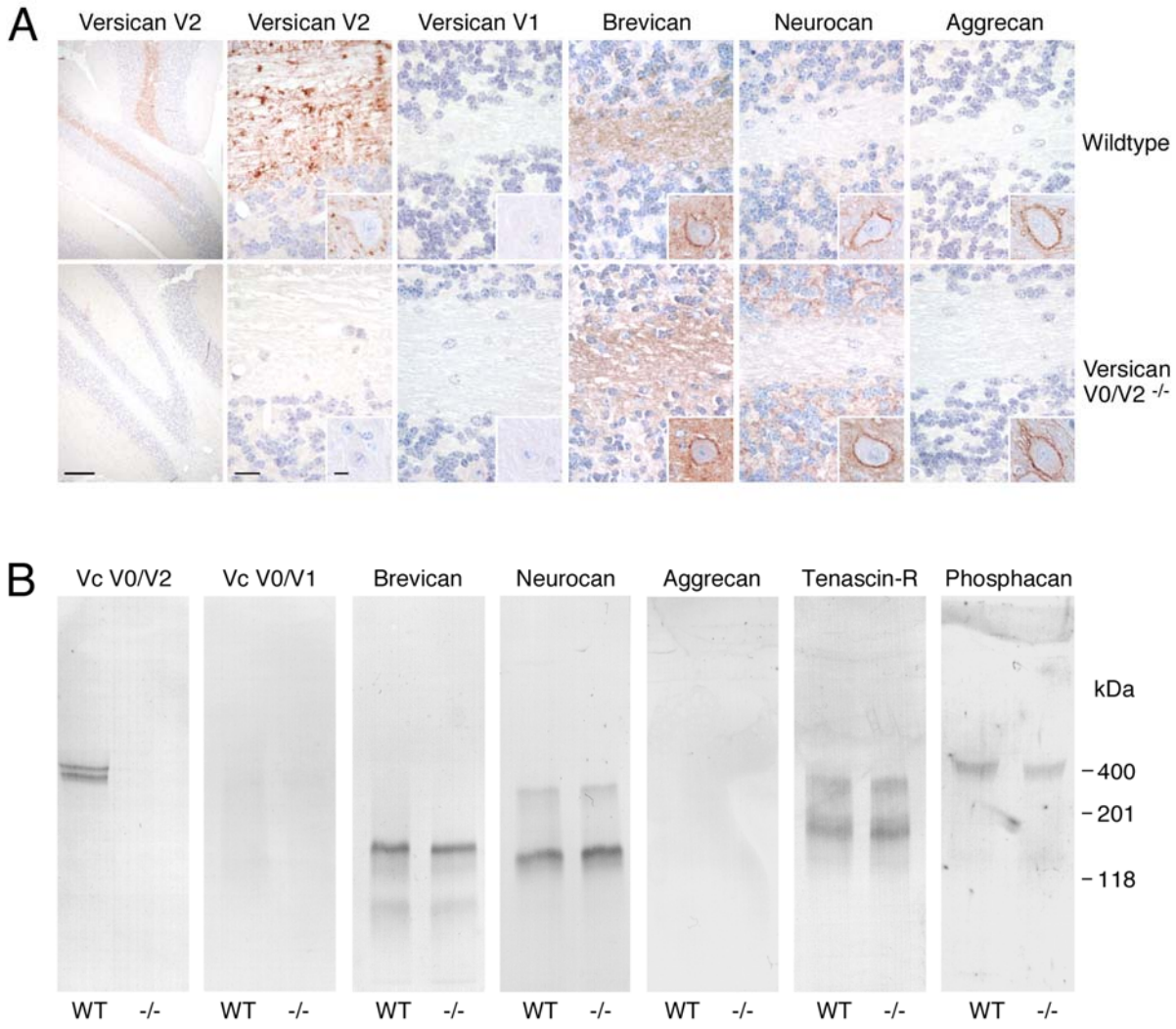

***Figure 3**. Absence of compensatory expression of other ECM components in versican V0/V2-deficient mice.*

A) Immunohistochemistry of cerebellar sections of two months old littermates with antibodies against versican GAG-α (versican V2) and GAG-β domains (versican V1), brevican, neurocan-C and aggrecan reveal no compensatory over-expression of versican V1 and other lecticans in V0/V2-deficient mice. In WT mice versican V2 and brevican are both present along myelinated fibers, but only versican V2 accumulates at nodes of Ranvier (punctate staining). Brevican and aggrecan, but not versican V2, form part of perineuronal nets in the deep cerebellar nuclei, while neurocan-C is associated with perineuronal nets of brain stem nuclei (small insets). Scale bars: 500 μm (overview on the left); 10 μm (insets); 20 μm (remaining images).
B) Immunoblots corroborate the unaltered content of lecticans, TnR and phosphacan in brain extracts of P30 WT and versican V0/V2 deficient mice. Aggrecan and versican V1 evade detection due to their limited expression in mature brain tissues.

Figure 4

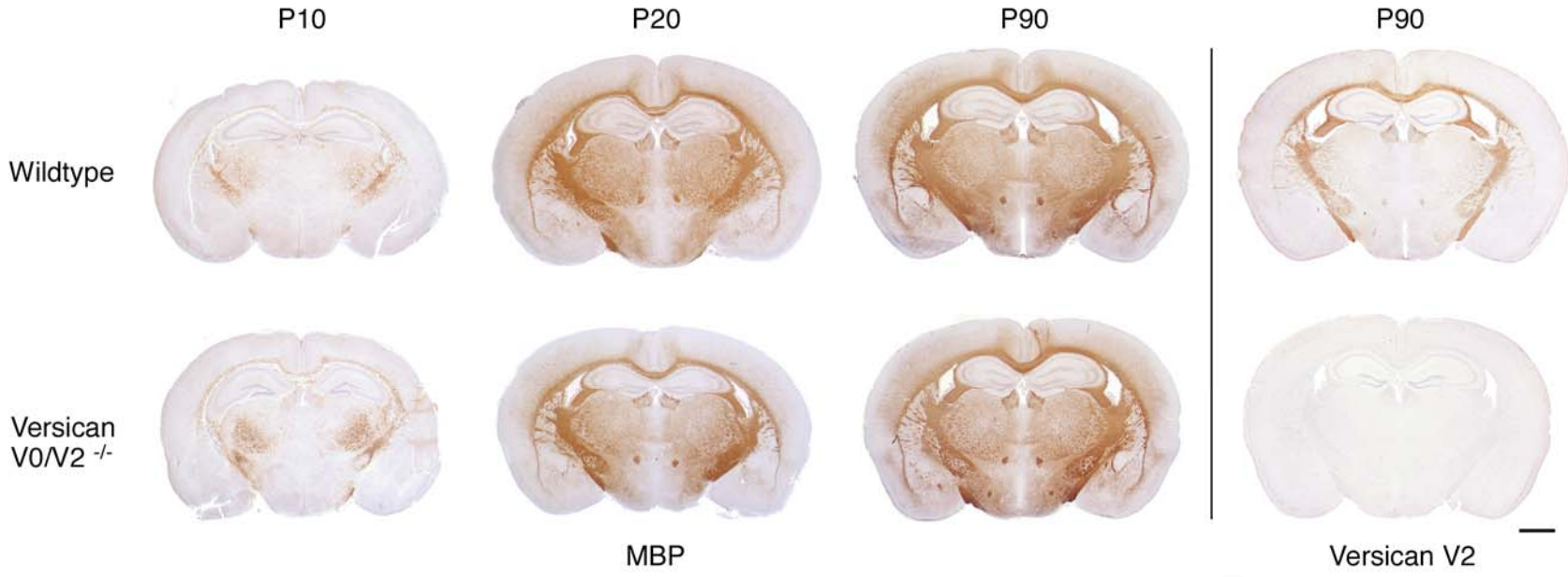

***Figure 4**. Comparative analysis of myelinated fiber tracts in WT and versican V0/V2$^{-/-}$ mutants.*

Coronal brain sections of postnatal stages P10, P20 and P90 stained with antibodies against myelin basic protein (MBP) display no morphological aberrations in spite of the complete absence of versican V2 in the KO mice. Scale bar: 1 mm.

Figure 5

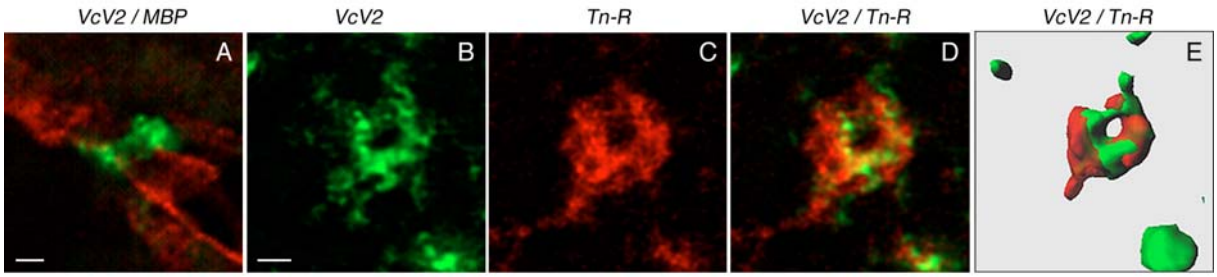

***Figure 5**. Visualization of the ECM around the CNS nodes of Ranvier.*

Double immunofluorescence of cerebellar sections reveals in wildtype mice the nodal accumulation of versican V2 in relation to the myelin component MBP (A: VcV2; green / MBP; red; sagittal view) and demonstrates its co-localization with TnR (B to D: VcV2; green / TnR; red, transverse view) intermingling with versican in the perinodal ECM (E: 3D-reconstruction based on confocal image stack). Scale bars (A and B-E): 1 μm.

Figure 6

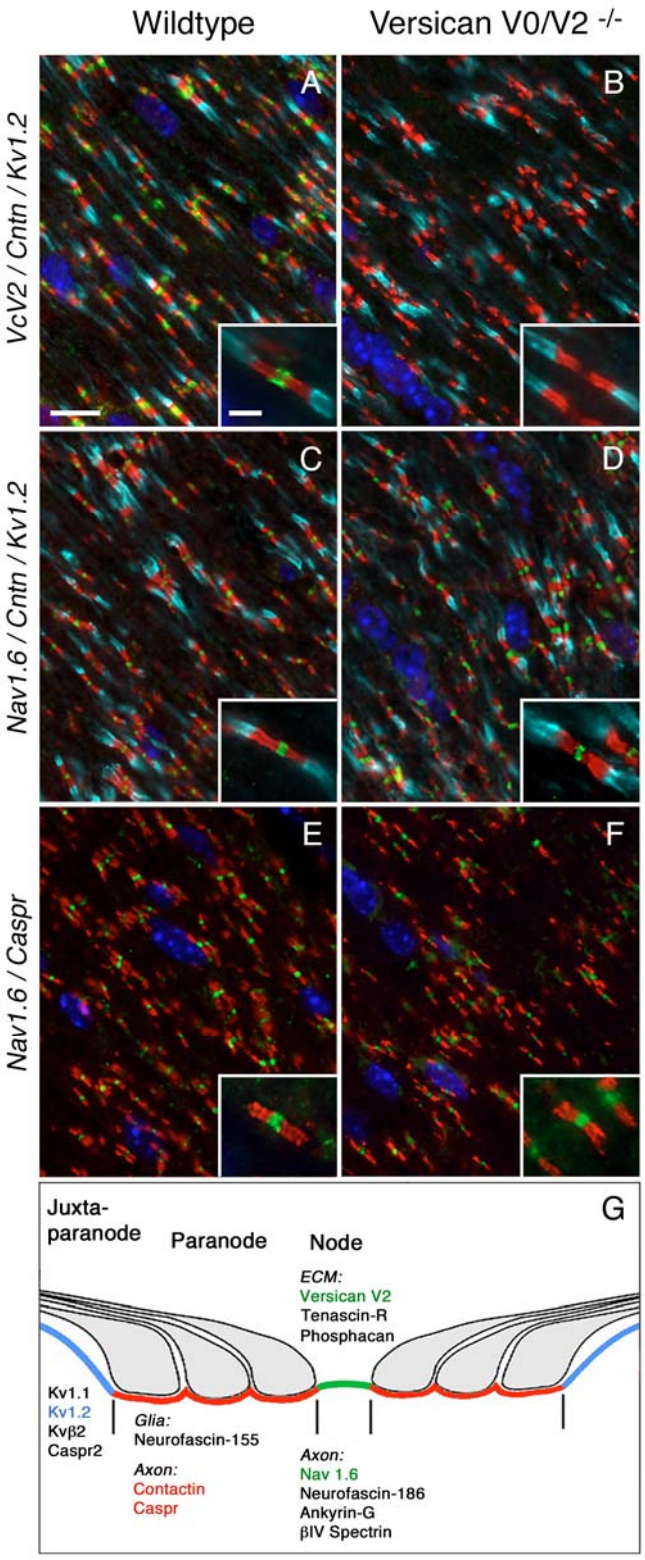

***Figure 6**. Effect of the versican V2-deficiency on the distribution of nodal, paranodal and juxtaparanodal components.*

In triple/double immunofluorescence of optic nerve tissue from wildtype (A, C, E) and versican V2-deficient mice (B, D, F) no difference in the distribution of paranodal contactin (Cntn: red in A-D) and Caspr (red in E and F) or juxtaparanodal potassium channels $K_v1.2$ (turquoise in A-D) can be observed (VcV2: green in A and B; Hoechst nuclear staining: blue in A-F). Also the clustering of the sodium channel $Na_v1.6$ (green in C-F) is not impaired. The localization of key components of the CNS-nodes of Ranvier is depicted in the sketch (G) modified from (Rasband and Trimmer, 2001). Scale bars: 10 μm; 2.5 μm (insets).

Figure 7

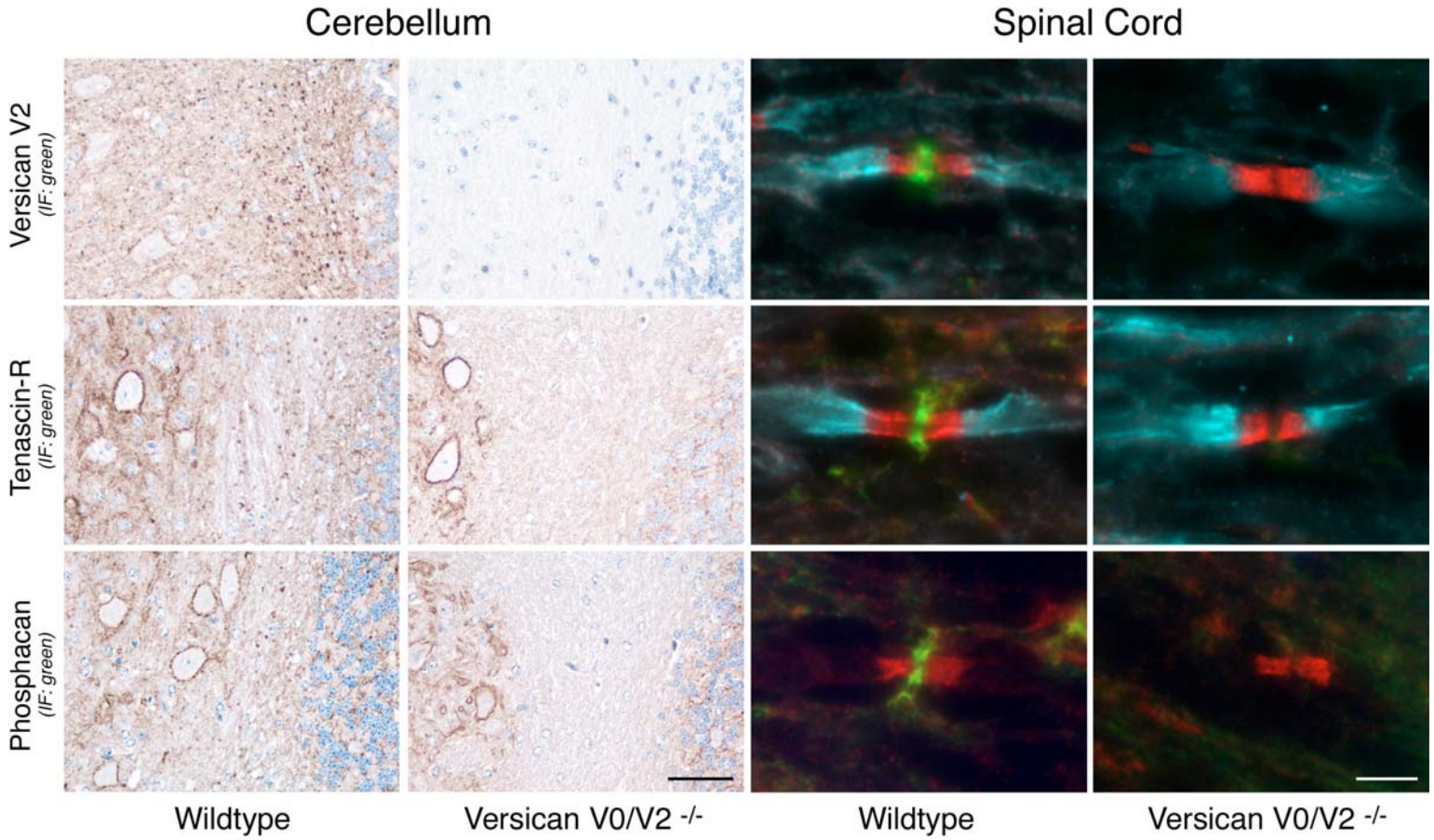

***Figure 7**. Simultaneous loss of TnR and phosphacan from nodes of Ranvier in versican V2 mutants.*

Immunochemical and immunfluorescence analysis of cerebellum and spinal cord white matter, respectively with antibodies against versican V2 (GAG-α domain), TnR and phosphacan demonstrates their co-localization in the perinodal ECM in wildtype mice. In versican V2-deficient mice, TnR and phosphacan are both absent from the CNS-nodes of Ranvier, while keeping their normal distribution in perineuronal nets of deep cerebellar nuclei. Paranodal contactin (red) and juxtaparanodal potassium channel Kv1.2 (turquoise) were immunostained in spinal cord for node localization. Scale bars: 50 μm (cerebellum) and 5 μm (spinal cord).

Figure 8

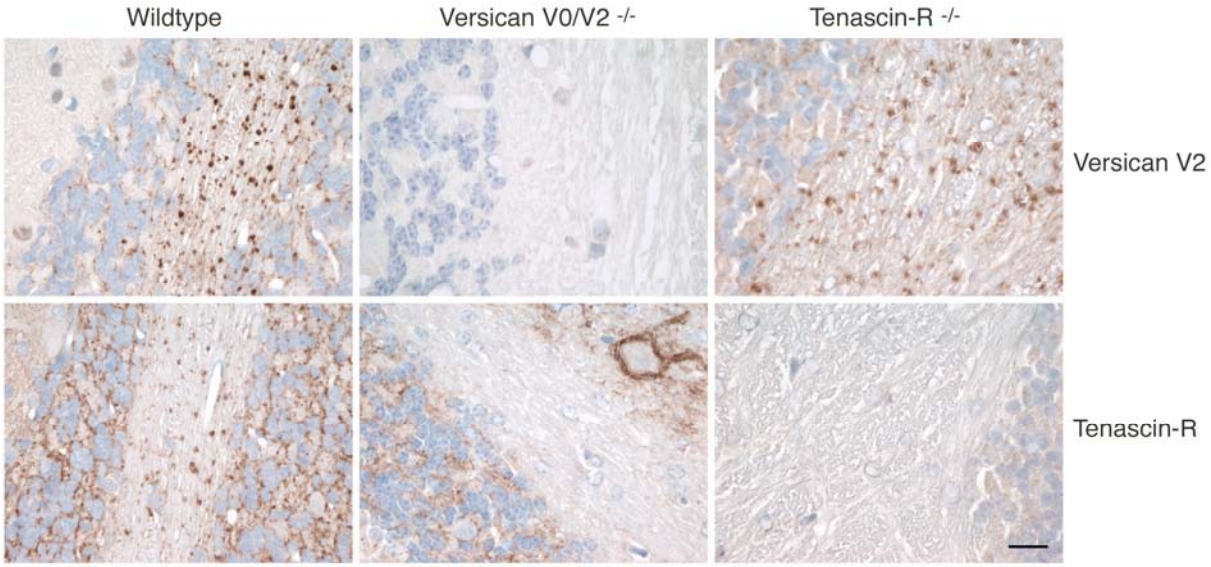

***Figure 8**. Perinodal localization of versican V2 is not affected by absence of TnR.*

Immunhistochemistry of cerebellar sections demonstrates that TnR is selectively lost from the nodes of Ranvier in versican V2-deficient animals, while versican V2 maintains its normal distribution in $TnR^{-/-}$ mice. Scale bar: 10 μm.

Figure 9

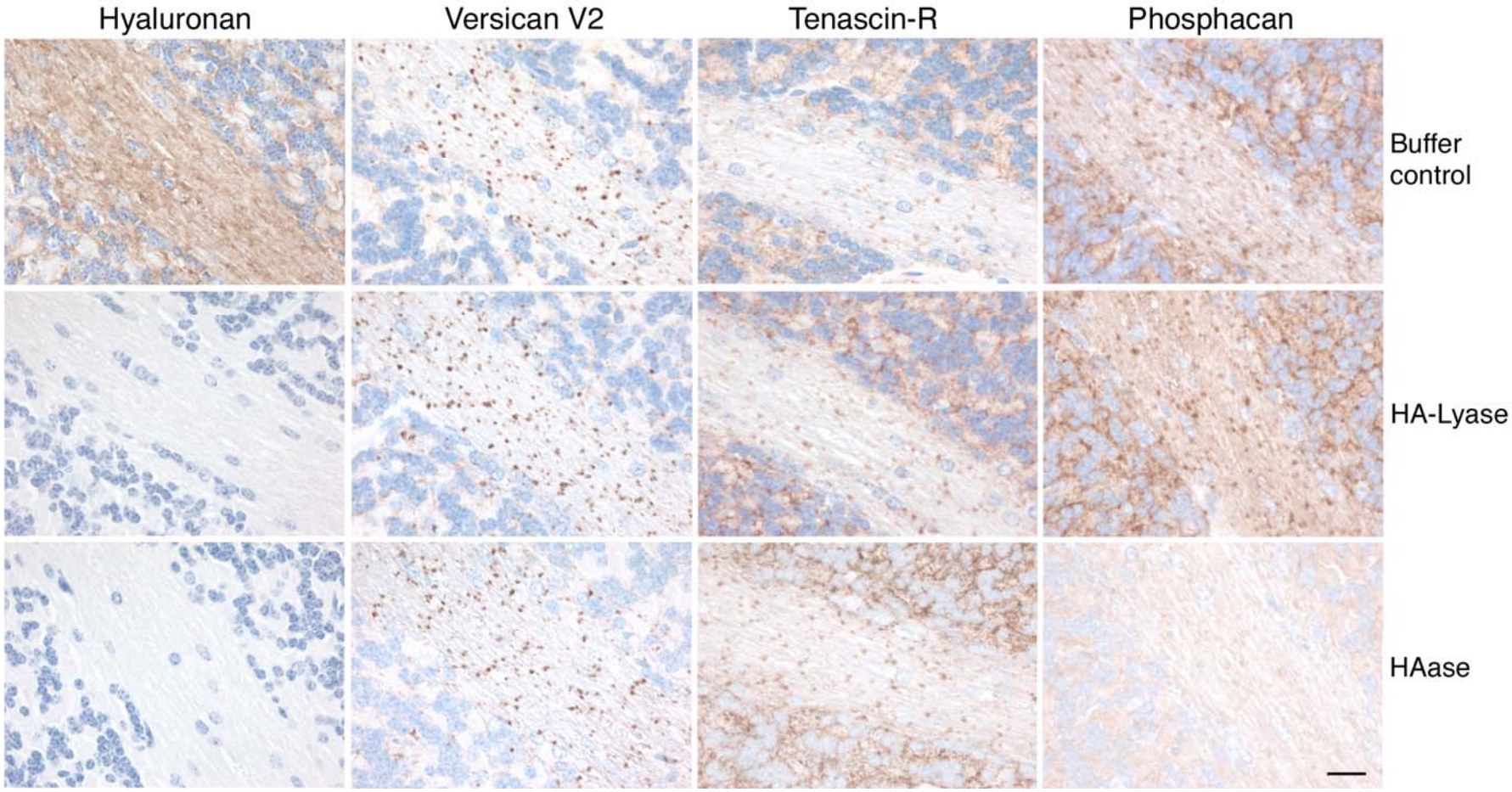

***Figure 9**. Hyaluronan is not responsible for anchoring the perinodal matrix.*

Complete removal of hyaluronan by treating cerebellar sections with *Streptomyces hyalurolyticus* hyaluronate-lyase (HA-lyase) or with ovine testicular hyaluronidase (HAase) has no effect on the distribution of versican V2 and TnR in WT mice. The disappearance of phosphacan upon HAase digestion is most likely attributable to a contaminating enzyme activity in this preparation. Sections were stained with corresponding antibodies to reveal the localization of the ECM proteins and with biotinylated hyaluronic acid binding protein (B-HABP) to visualize hyaluronan. Scale bar: 20 μm.

Figure 10

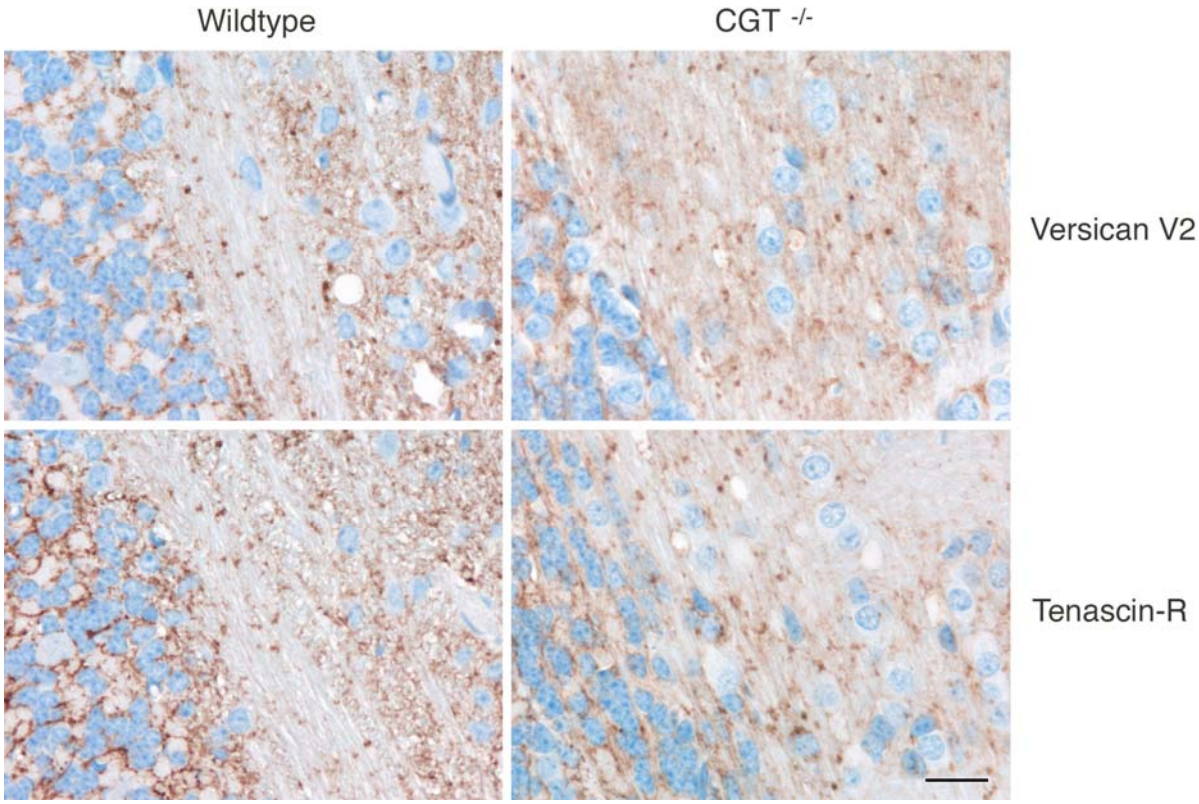

***Figure 10**. The perinodal accumulation of versican V2 does not depend on sulfatide-mediated cell surface-binding.*

Immunohistochemical analysis of cerebellar sections reveals the normal deposition of versican V2 and TnR around the newly formed nodes of Ranvier in 19 days old ($CGT^{-/-}$) mice in spite of their deficiency in the biosynthesis of sulfatides, a glycolipid-ligand of versican in vitro. Scale bar: 20 μm.

Supplementary table (Materials and Methods)

Quantitative RT-PCR

Isoform-specific versican primers

Splice variant	Primer pairs
all VCs	CCACCTCACAAGCATCCTTTCT / TGAGGCCGATCCACTGGTA
V0*	TGAGGTCAGAGAAAACAAGACA / CTGCAAGGTTCCTCTTCTTTAGATTC
V1*	CAGATTTGATGCCTACTGCTTTAAAC / CTGCAAGGTTCCTCTTCTTTAGATTC
V2*	TGAGGTCAGAGAAAACAAGACA / GATAACAGGTGCCTCCGTTGA
V3*	CAGATTTGATGCCTACTGCTTTAAAC / GATAACAGGTGCCTCCGTTGA

*Primers spanning over splice variant specific exon-exon boundaries.

Primers for reference gene expression (GAPDH)

mGAPDH	AACGACCCCTTCATTGAC / TCCACGACATACTCAGCAC

RT-PCR conditions

30 min at 50°C (Reverse transcription)	
15 min at 95°C	
40 cycles:	30 sec at 94°C 30 sec at 60°C 1 min at 72°C
8 min at 72°C	
soak at 4°C	

ABI PRISM 7700 Sequence Detection System set-up:

Dye layer: SYBR, single reporter, internal reference ROX.

Fluorescence emission was measured at the end of each cycle. For all samples two different negative control reactions omitting either the template or the reverse transcription-step were performed.

4.1.1. Supplementary Methods Part I

4.1.1.1. Isolation of genomic clones and preparation of the targeting construct

Since the complete sequence of the mouse genome was at the beginning of this project not yet known, several PCR approaches were used to isolate and sequence the fragments covering the target region. Exon VII was cloned by PCR from genomic 129/Sv mouse DNA using Ampli-Taq Gold (Applied Biosystems) and primers at the 5' and 3' end of the GAG-α encoding sequence (suppl. table 1). Likewise, the flanking introns were cloned with Expand-long template PCR kit (Roche Applied Science) using a hot start procedure (wax beads, Applied Biosystems) and primers hybridizing at the 3' or 5' end of adjacent exons, correspondingly (3' end of exon VI and 5' end of exon VII or 3' end of exon VII and 5' end of exon VIII).

Supplementary table 1: Primers and reaction conditions used to subclone the targeting region

Primer name	Sequence	PCR-type	Product	Annealing / extension	Cycles / elongation
Intron67up	CCCAGTGTGGAGGAGGTC	Expand-long	~6 kb	65°C/6min@68°C	15
Intron67low	TGATGAAGTTTCTGCGAGGAT				35 (+20sec)
Exon7up	AAATGAATATCCTCGCAGAAACT	ampliTaq-Gold	~3 kb	58°C/2min@72°C	10
Exon7low	GATGGTCTTGTTGGCTGTGT				30 (+20sec)
I78-up2	ACACAGCCAACAAGACCATCAGTT	Expand-long	~10 kb	68°C/6min@68°C	15
I78-low2	AACACTATGCCCCGTTTACTTCTCTG				35 (+20sec)

All PCR products were subcloned in pGEM-T Easy (Promega) and grown in the E. coli host strains SURE or JM110 (Stratagene). Sequencing of the clones was done on an ABI 377 DNA Sequencer using dye terminator chemistry (Applied Biosystems).

Based on the sequence data obtained from these primary PCR products, specific primers were designed and the gene fragment later used as 5'-arm of the targeting construct was amplified from genomic DNA by long template-PCR (suppl. table 2 and suppl. fig. 1). For cloning purposes, the upper primer (KO5'-up, hybridizing in intron 6-7) had been modified to include a 5'-Not I restriction site, while at the 3'-end, a BstZ I site, a translational stop codon and the coding sequence for the ER retention signal KDEL had been incorporated into the lower primer sequence (KO5'-low, containing 5' end sequence of exon VII, 22 bp up to position 2428, GenBank D28599). The resulting Not I-BstZ I fragment was inserted into the Not I site of a pBluescript vector bearing a floxed neo-tk cassette under the HSV promoter. The resulting vectors has been named pKO5'Arm-neotk.

To assemble the 3' arm we designed an upper primer hybridizing proximally to the 3'-end of the 5'-arm in exon VII (KO3'-up) and a lower primer placed in intron 7-8 (KO3'-low). Both primers were modified with Cla I sites. The entire fragment had beforehand been joined from two smaller amplificates by PCR-ligation (with Expand polymerase). For the generation of these pieces (with

AmpliTaq-Gold) the cloned GAG-α sequence (GAG-α-pGEM) and an Nco I-fragment of the intron 7-8 plasmid had been used as templates, respectively (suppl. fig. 1).

At last, the completed 3' arm was subcloned into the unique Cla I site of KO5'Arm-neotk and the final targeting construct was verified by sequencing. Prior to electroporation into R 1 ES cells, it was linearized by cleavage with Not I.

Supplementary table 2: Primers and reaction conditions used to generate the targeting construct

Primer	Sequence	PCR type	Product	Anneal./ extension	Cycles/ elongation
KO5'-up	AAATCGGCCGCAGAATGGCTCAAACAAATGGCACA	Expand-long	~4 kb	68°C/68°C	15 and 35 (+20sec)
KO5'-low	AAATCGGCCGTTAGAGCTCATCCTTCTCAATTGTCA ATGCAGGGGAA				
KO3'-up	ATTTATCGATCCAACAGAAGCAAGAGATGT	Ligation-PCR / Expand-long	~1.5 kb	65°C/72°C	15 and 25 (+20sec)
Exon7low	GATGGTCTTGTTGGCTGTGT			30 cycles	
I78-up2	ACACAGCCAACAAGACCATCAGTT		~2.5 kb	65°C/72°C	
KO3'-low	ATTTATCGATGTTAATGTTTTCATGGGTAAAGT			30 cycles	

CGGCCG: Not I / BstZ I compatiple sites TTA: stop codon GAGCTCATCCTT: KDEL coding sequence ATCGAT: Cla I site

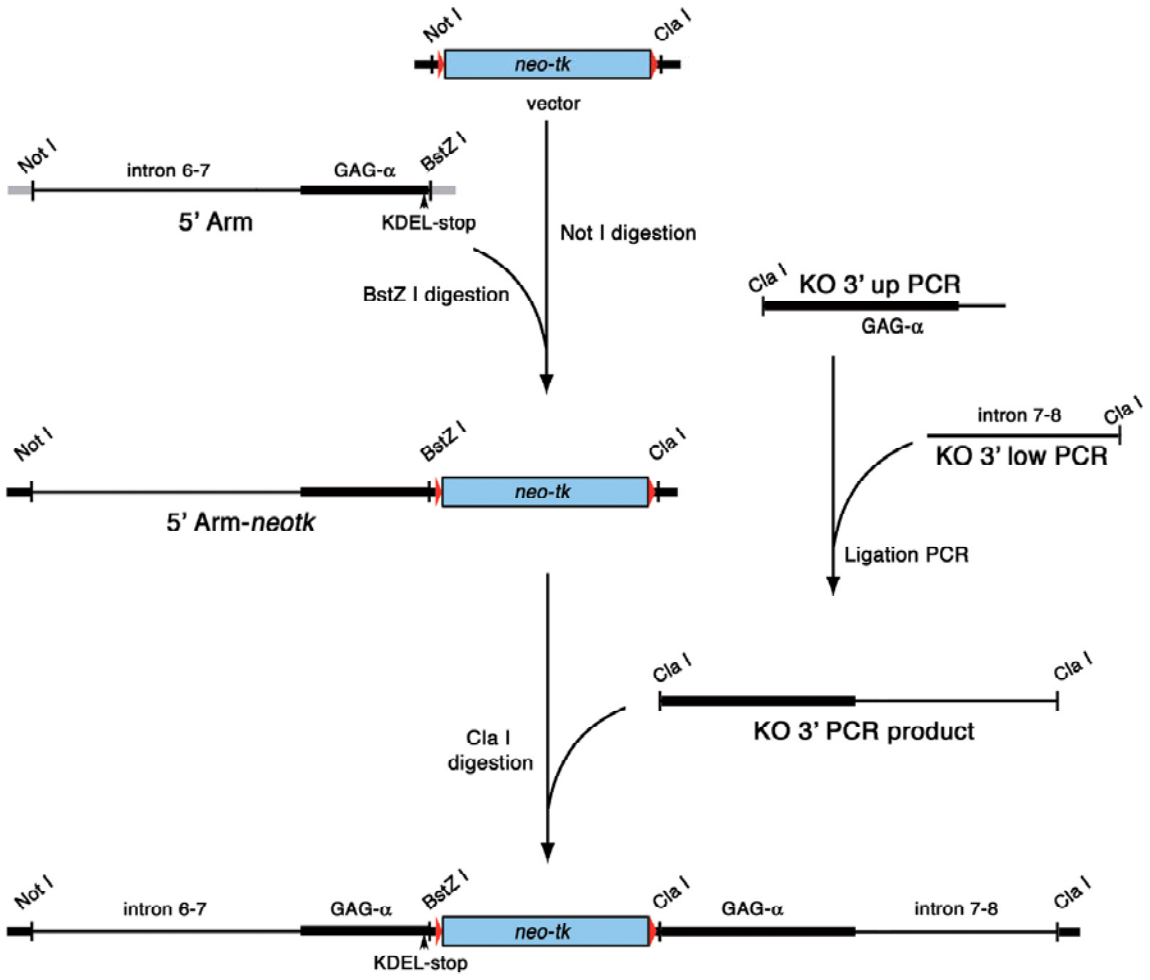

Supplementary figure 1: Strategy followed to prepare the targeting construct.

(Blue box: vector sequence encoding the neo-tk selection cassette; red triangles: loxP sites)

4.1.1.2. Preparation of the Southern blot probe

Using a cloned Nco I fragment of intron 7-8 as template, the 953 bp-long Southern blot probe was PCR amplified (primers GTGCATGCATACTGTTGT and CAGCCATGGTCTCAATA) and simultaneously DIG-labeled (Roche Applied Science).

4.1.1.3. Verification of target integration and screening of mutant mice

Long distance PCR products from genomic DNA of ES clones and mutant mice were sequenced to check the correct transgene integration into the versican locus. Amplifications were performed with TaKaRa LA Taq (TaKaRa Biomedicals). The primer pairs employed were complementary to the neo-tk and the contiguous intron sequences, respectively (5'PCR-up and 5'PCR-low or 3'PCR-up and 3'PCR-low) (suppl. table 3).

To screen the mutants by PCR, primers were designed flanking the mutation in exon VII (loxed-up and loxed-low). CRE-transgenic mice used to remove the neo-tk selection cassette in cross-breedings were genotyped with cre-up and cre-low primers.

Supplementary table 3: Primers and reaction conditions used to verify integration of the targeting construct

Primer	Sequence	PCR type	Product	Anneal./ extension	Cycles/ elongation
5'PCR-up	GACATTTCTTTGTAGACGGTGTTTTA	LD-PCR (TaKaRa)	~4.3 kb	65°C/68°C	15 and 35 (+20sec)
5'PCR-low	CCTTAATATGCGAAGTGGACCT				
3'PCR-up	CCACCGAGACCCCATTG	LD-PCR (TaKaRa)	~4.7 kb	65°C/68°C	15 and 35 (+20sec)
3'PCR-low	CACCCCACAGCATTTTTCAG				
loxed-up	GAGAGGACAGAAACACCAAG	AmpliTaq Gold	WT: 312 bp	55°C/72°C	35
loxed-low	ACTGTGGGTCAAATGAACTC		KO: 454 bp		
cre-up	CCAAAATTTGCCTGCATTAC	AmpliTaq Gold	166 bp	55°C/72°C	35
cre-low	CCATTTCCGGTTATTCAACT				

4.1.1.4. Preparation of the Northern blot riboprobe

A cDNA fragment covering G1 domain-encoding sequences of mouse versican (positions 458 to 1203, GenBank D28599) was obtained by RT-PCR from total RNA of brain (OneStep RT-PCR, Qiagen; primers mLINK-up/low GGTCAGGACTACAAGGG/ TCAAATCTGCTATCAGG). After T/A cloning in pGEM-T, a second amplification was performed using the low-primer modified with the T7-promoter sequence at the 5' end. (mLINK-low-T7: CGAAATTAATACGACTCACTATAGGGAGA TCAAATCTGCTATCAGG) (T7-sequence in red). The resulting product was then *in vitro* transcribed and DIG labeled (DIG RNA Labeling Kit, Roche Applied Science).

4.1.1.5. Generation of domain-specific antibodies against mouse versican and other lecticans

Immunization of rabbits or guinea pigs was done using recombinant core protein fragments as antigens (suppl. fig. 2). In all cases, PCR amplificates from genomic DNA were cloned into the pDS56/RBSII, 6xHis expression vector (= pDS9) (Stüber et al., 1990), previously modified by introducing a synthetic cassette with Sfi I and Not I sites (pDS9-cassette) (Zimmermann et al., 1994). The N-terminally His-tagged fusion proteins were expressed in M15[pREP] bacteria and subsequently purified under denaturing conditions on a Ni^{2+}-NTA-agarose (Qiagen) column. Briefly, after transformation and consecutive IPTG induction of the protein expression in bacteria cultures, the peptides were extracted with 6 M guanidine hydrochloride/100 mM sodium phosphate, pH 8.0. Once the lysate was cleared by centrifugation, the supernatant was bound to the Ni^{2+}-column, washed with 8 M urea/100 mM sodium phosphate/10 mM Tris pH 8.0, and eluted stepwise by lowering the pH to 6.3 and 5.9. For the preparation of bacterial control extracts, M15[pREP] were transformed with the empty pDS9-cassette vector and processed similarly.

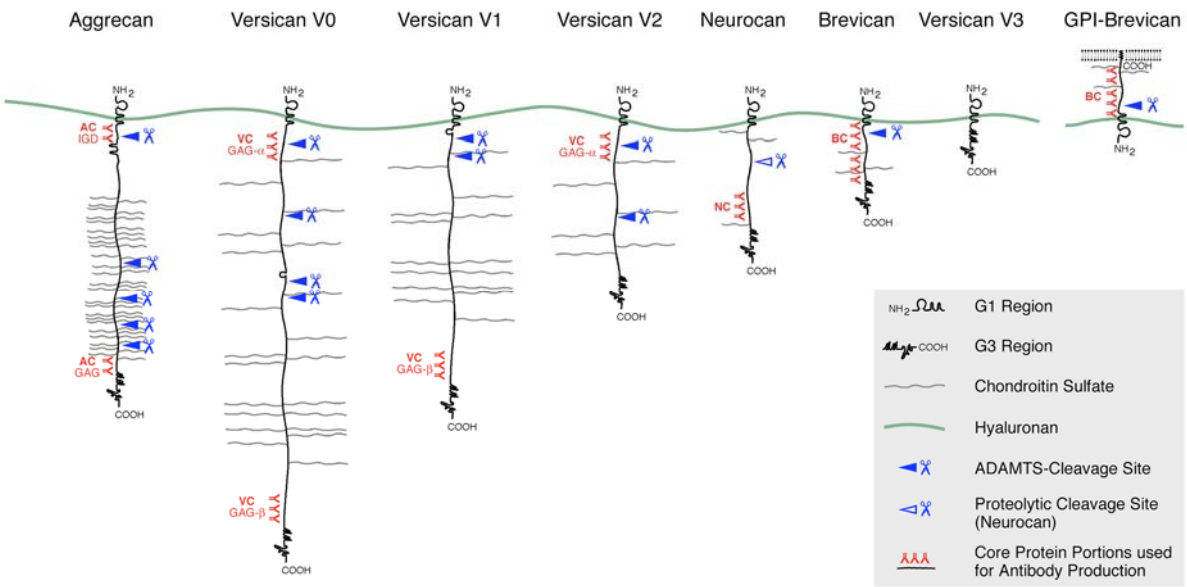

Supplementary figure 2: Cartoon showing the location of recombinant antigens used to immunize rabbits (versicans) and guinea pigs (versicans, neurocan and aggrecan); brevican antiserum (Thon et al., 2000) was a gift from Takako Sasaki (MPI Martinsried).

Rabbits were immunized with 300-400 μg of purified fusion proteins emulsified in incomplete Freund's adjuvant and boosted two to four times with one tenth of the original amount of antigen. Rabbit antisera were affinity purified on the corresponding fusion protein column (antigen coupled to NHS-activated HiTrap, Amersham) after pre-absorption on a bacterial control extract column. Eluted antibodies were then precipitated with $(NH_4)_2SO_4$ to 50% saturation and resuspended in TBS/ 1% BSA/ 0.02% sodium azide. The specificity of antibodies was controlled on immunoblots of

fusion proteins and whole brain extracts (not shown) as well as by immunohistochemical analysis (suppl. fig. 3).

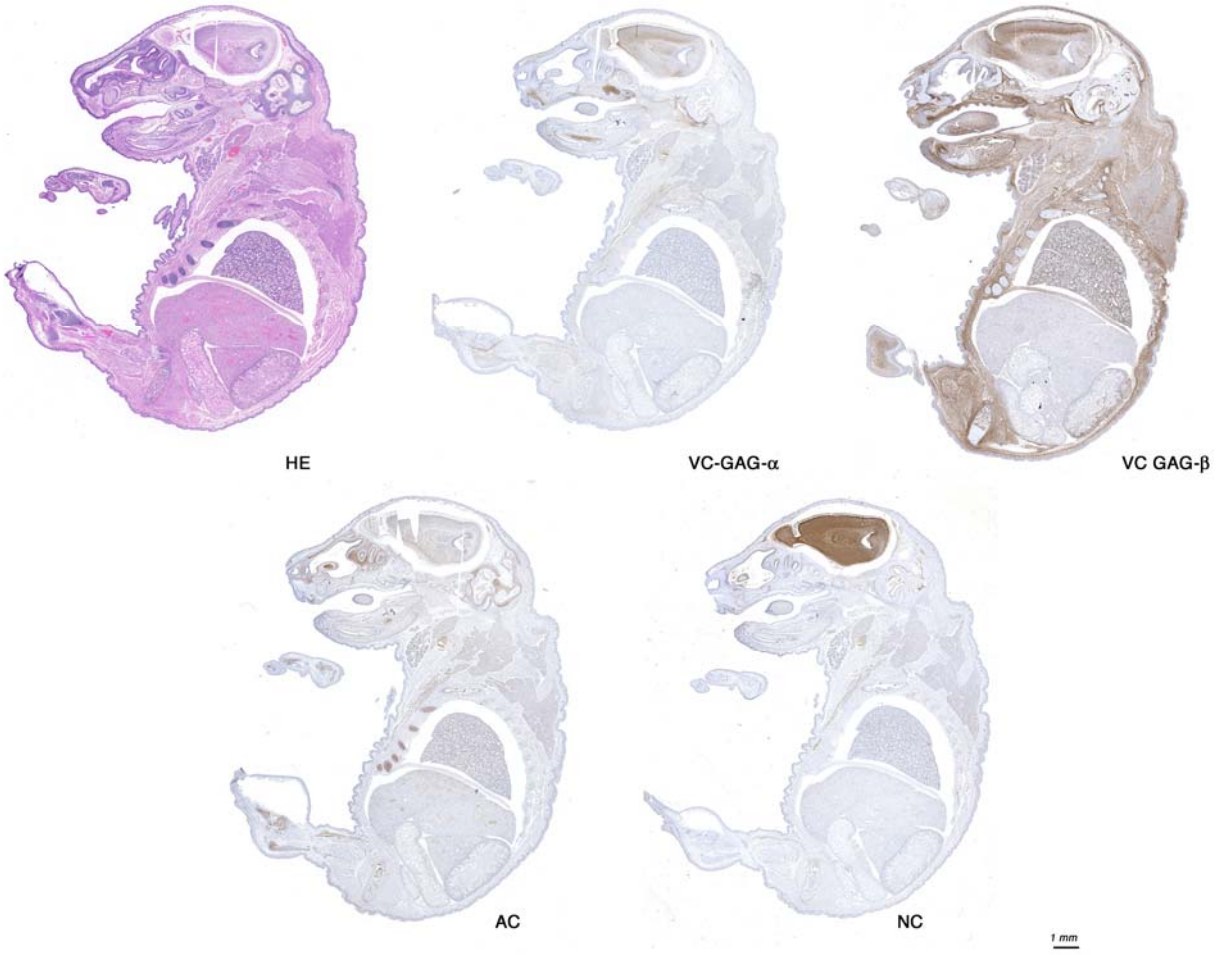

Supplementary figure 3: Immunohistochemistry of para-sagittal sections of a wildtype E18.5 mouse embryo using the newly produced rabbit and guinea pig antibodies. For antigen description see supplementary figure 2.

4.1.2. Supplementary Results Part I:

Distribution of ECM components in perineuronal nets of versican V0/V2 null mice

Since previous reports described an association of versican with perineuronal nets (PNNs) (Carulli et al., 2006; Deepa et al., 2006), we have analyzed the distribution of all lecticans as well as phosphacan and tenascin-R in the deep cerebellar nuclei and in the brain stem of wildtype and of versican V2 null mice (suppl. fig. 4). In these experiments, we did not observe any versican immunoreactivity, neither in wildtype nor in knockout PNNs. Moreover, no alterations in the localization of the known PNN components could be detected in mutant mice.

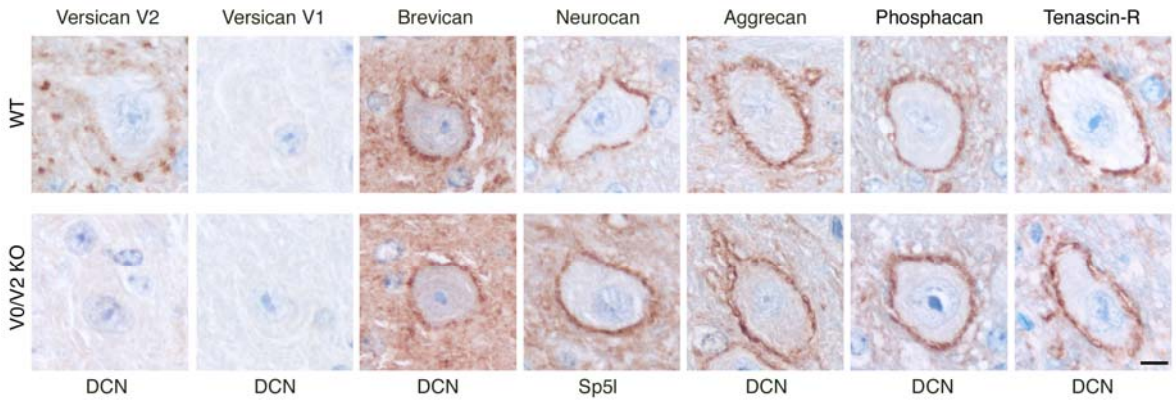

Supplementary figure 4: Immunohistochemistry on adult WT and VCV0/V2 KO brains depicting lecticans, phosphacan and Tn-R (bar: 8 μm). *DCN: deep cerebellar nuclei; Sp5I: spinal trigeminal nucleus*.

4.1.3. References

Carulli D, Rhodes KE, Brown DJ, Bonnert TP, Pollack SJ, Oliver K, Strata P, Fawcett JW (2006) Composition of perineuronal nets in the adult rat cerebellum and the cellular origin of their components. J Comp Neurol 494:559-577.

Deepa SS, Carulli D, Galtrey C, Rhodes K, Fukuda J, Mikami T, Sugahara K, Fawcett JW (2006) Composition of perineuronal net extracellular matrix in rat brain: a different disaccharide composition for the net-associated proteoglycans. J Biol Chem 281:17789-17800.

Stüber D, Matile H, Garotta G (1990) System for high-level production in Escherichia coli and rapid purification of recombinant proteins: Application to epitope mapping, preparation of antibodies, and structure-function analysis. In: Immunological Methods (Lefkovits I, Pernis B, eds), pp 121-152. San Diego: Academic Press.

Thon N, Haas CA, Rauch U, Merten T, Fassler R, Frotscher M, Deller T (2000) The chondroitin sulphate proteoglycan brevican is upregulated by astrocytes after entorhinal cortex lesions in adult rats. Eur J Neurosci 12:2547-2558.

Zimmermann DR, Dours-Zimmermann MT, Schubert M, Bruckner-Tuderman L (1994) Versican is expressed in the proliferating zone in the epidermis and in association with the elastic network of the dermis. J Cell Biol 124:817-825.

4.2 Original publication II:

Beggah AT, Dours-Zimmermann MT, Barras FM, Brosius A, Zimmermann DR, Zurn AD (2005) Lesion-induced differential expression and cell association of Neurocan, Brevican, Versican V1 and V2 in the mouse dorsal root entry zone. Neuroscience 133:749-762.

Neuroscience 133 (2005) 749–762

LESION-INDUCED DIFFERENTIAL EXPRESSION AND CELL ASSOCIATION OF NEUROCAN, BREVICAN, VERSICAN V1 AND V2 IN THE MOUSE DORSAL ROOT ENTRY ZONE

A. T. BEGGAH,[a,b] M. T. DOURS-ZIMMERMANN,[c] F.M. BARRAS,[a,b1] A. BROSIUS,[a,b] D. R. ZIMMERMANN[c] AND A. D. ZURN[a,b*]

[a]*Department of Experimental Surgery, University Medical School, Pavillon 4, CHUV, CH-1011 Lausanne, Switzerland*

[b]*Laboratory of Stem Cell Dynamics, School of Life Sciences, Swiss Federal Institute of Technology, CH-1015 Lausanne, Switzerland*

[c]*Institute of Clinical Pathology, University of Zürich, CH-8091 Zürich, Switzerland*

Abstract—Lack of regeneration in the CNS has been attributed to many causes, including the presence of inhibitory molecules such as chondroitin sulfate proteoglycans (CSPGs). However, little is known about the contribution of CSPGs to regeneration failure *in vivo*, in particular at the dorsal root entry zone (DREZ), a unique CNS region that blocks regeneration of sensory fibers following dorsal root injury without glial scar formation. The goal of the present study was to evaluate the presence, regulation, and cellular identity of the proteoglycans Brevican, Neurocan, Versican V1 and Versican V2 in the DREZ using CSPG-specific antibodies and nucleic acid probes. Brevican and Versican V2 synthesized before the lesion were still present at high levels in the extracellular matrix of the DREZ several weeks after injury. In addition, Brevican was transiently expressed by reactive oligodendrocytes, and by a subset of astrocytes thereafter. Versican V2 mRNA appeared in NG2-positive cells with the morphology of oligodendrocyte precursor cells. Neurocan and Versican V1 levels were low before injury, and appeared in nestin-positive astrocytes and in NG2-positive cells, respectively, following lesion. Versican V1, but not V2, was also transiently increased in the peripheral dorsal root post-lesion. This is the first thorough description of the expression and cell association of individual proteoglycans following dorsal root lesion. It demonstrates that the proteoglycans Brevican, Neurocan, Versican V1, and Versican V2 are abundant in the DREZ at the time regenerating sensory fibers reach the PNS/CNS border and may therefore participate in growth-inhibition in this region.

Key words: CNS injury, glial cells, nerve regeneration, axonal growth, proteoglycans.

[1] Present address: Department of Otorhinolaryngology and Head and Neck Surgery, University Medical School, Lausanne, Switzerland.
*Correspondence to: A. D. Zurn, Department of Experimental Surgery, University Medical School, Pavillon 4, CHUV, CH-1011 Lausanne, Switzerland. Tel: +41-21-314-2462; fax: +41-21-314-2468.
E-mail address: Anne.Zurn@chuv.hospvd.ch (A. D. Zurn).

Abbreviations: APC, *Adenomatous polyposis coli*; CGRP, calcitonin gene-related peptide; CSPG, chondroitin sulfate proteoglycan; dpl, days post-lesion; DREZ, dorsal root entry zone; DRG, dorsal root ganglion; ECM, extracellular matrix; GAG, glycosaminoglycan; GFAP, glial fibrillary acidic protein; IHC, immunohistochemistry; ISH, *in situ* hybridization; NGS, normal goat serum; OPC, oligodendrocyte precursor cells; PBS, phosphate buffered saline; PNS, peripheral nervous system; ROD, relative optical density; SSC, standard saline citrate.

Traumatic injuries to the brain and spinal cord cause severe and irreversible disabilities due to the inability of the CNS, in contrast to the peripheral nervous system (PNS), to regenerate injured fibers. For instance, although sensory axons can regenerate through the peripheral dorsal root after dorsal root injury (rhizotomy), they stop growing once they reach the spinal cord at the dorsal root entry zone (DREZ), and do not cross the PNS/CNS border. Connections within the dorsal horn of the spinal cord can thus not be restored (Carlstedt, 1983). In humans, brachial plexus injury results in severe impairment of hand function associated with chronic pain (Carlstedt, 1995). CNS injury leads to a reaction which is characterized by a number of changes, including astrocyte hypertrophy, up-regulation of intermediate filament proteins and various extracellular matrix (ECM) molecules, and to the formation of a glial scar (reviewed in Fawcett and Asher, 1999). Similarly, rhizotomy results in reactive gliosis at the DREZ associated with disintegration of axons and myelin sheaths during Wallerian degeneration, but no scar formation (Murray et al., 1990; Liu et al., 2000; reviewed in Ramer et al., 2001a). Chondroitin sulfate proteoglycans (CSPGs) are the first ECM molecules with growth-inhibitory properties that have been described to be enhanced around the lesion site following various types of CNS injuries (Rudge and Silver, 1990; McKeon et al., 1991). Further evidence for a role of CSPGs in restricting regeneration is provided by the demonstration that enzymatic treatment to remove the carbohydrate side chains of CSPGs allows partial regeneration after spinal cord lesion in rats (Bradbury et al., 2002). In addition, grafts of adult sensory neurons can regenerate axons in degenerating white matter tracts of the spinal cord, but not through the central area of the glial scar containing high concentrations of CSPGs (Davies et al., 1999). Current evidence thus suggests that CSPGs contribute, together with other inhibitory molecules, to growth inhibition in the CNS.

CSPGs are ECM glycoproteins carrying varying degrees of covalently bound sulfated glycosaminoglycan (GAG) chains (for review, see Bandtlow and Zimmermann, 2000). The CSPGs Brevican, Neurocan, and the V1 and V2 isoforms of Versican belong to a subgroup of proteoglycans called hyalectans which share similar globular N-terminal hyaluronan-binding domains and C-terminal selectin-like domains, but have a central region which is not conserved (for review see Yamaguchi, 2000). Hyalectans thus cross-link hyaluronan to other ECM components, including tenascins and surface molecules such as L1, neural cell adhesion molecule (N-CAM), and integrins

0306-4522/05$30.00+0.00
doi:10.1016/j.neuroscience.2005.03.005

(Hagihara et al., 1999; Grumet et al., 1994; Wu et al., 2002). Brevican and Versican V2 are the most abundant hyalectans in the adult CNS and are, together with Neurocan, exclusively expressed in the CNS (Yamaguchi, 1996; Bode-Lesniewska et al., 1996; Schmalfeldt et al., 1998; Niederöst et al., 1999; Rauch et al., 2001). In contrast, the V1 isoform of Versican has a wider tissue distribution, being expressed in embryonic tissues that act as barriers for neural crest migration and in the adult aorta (Yao et al., 1994; Landolt et al., 1995). Brevican, Neurocan, and Versican V2 have been shown to inhibit neurite outgrowth from cerebellar granule cells and/or dorsal root ganglion (DRG) neurons *in vitro* (Friedlander et al., 1994; Yamada et al., 1997; Niederöst et al., 1999; Schmalfeldt et al., 2000). In addition, various reports have shown that Neurocan and Brevican expression is increased around the lesion following brain injury, supporting a physiological contribution of CSPGs as growth-inhibitors *in vivo* (Haas et al., 1999; Jaworski et al., 1999; McKeon et al., 1999; Thon et al., 2000). The role of CSPGs in the DREZ is however less clear. Although there have been reports of the increase in CSPG expression in the DREZ following rhizotomy (Pindzola et al., 1993; Zhang et al., 2001), none has addressed the presence, potential regulation, and cell association of the individual proteoglycans Neurocan, Brevican, Versican V1, and Versican V2 in this area. The DREZ is a particularly attractive region to study the potential involvement of CSPGs in regeneration failure since it is inhibitory in the absence of direct CNS damage and glial scar formation.

EXPERIMENTAL PROCEDURES

Animals and surgery

Dorsal cervical spinal roots of 2–3 month-old C57BL/6 mice were unilaterally transected based on the model described previously in the rat (Ramer et al., 2000). Briefly, animals were anesthetized with an i.p. injection of a mix of xylazine (7 mg/kg) and ketamine (140 mg/kg). Hemilaminectomy of the right side of the dorsolateral cervical spine was performed from C5 to T1 to expose the dorsal roots. A longitudinal slit in the dura matter allowed the insertion of a pair of microscissors to completely transect dorsal roots C6 to C8, midway between the DRG and the entry zone (0.5–0.8 mm from each). This was done very carefully to avoid even minimal damage to the spinal cord. Six animals were subjected to sham operations: hemilaminectomy was performed and the meninges were opened, but the roots were left intact. The wound was then closed with sutures. Particular care was taken to minimize the number of animals used. Furthermore, the mice were injected intraperitoneally with bupremorphine (2.5 mg/Kg) at the time of the operation to attenuate post-operation suffering. All animal protocols were approved by the local veterinary commission in Lausanne, Switzerland, and carried out in accordance with their guidelines.

Immunohistochemistry (IHC)

At 3, 7, 14 or 28 days post-rhizotomy, the animals were anesthetized with a lethal dose of pentobarbital and transcardially perfused with phosphate buffered saline (PBS), followed by perfusion fixation with 50 ml 4% paraformaldehyde in PBS. The cervical part of the spinal cord together with DRGs was carefully removed and postfixed overnight at 4 °C. For Versican V2 immunolabeling, the animals were perfused with 50 ml saline only. The spinal cords were subsequently cryoprotected in 30% sucrose in PBS and rapidly frozen in O.C.T. compound (Tissue-Teck, Netherlands) over liquid nitrogen. Ten to 12 μm thick transverse sections were cut on a cryostat (CM3000, Leica, Germany), collected on Superfrost Plus slides (Menzel-Glaser, Braunschweig, Germany), and processed for immunohistochemistry as follows: Brevican [1:5000; raised in rabbits against the entire core protein of the recombinant secreted form of rat Brevican (kind gift of Dr. R, Timpl, Max-Planck-Institute for Biochemistry, Martinsried, Germany)]; Neurocan [1:200; raised in rabbits against purified rat Neurocan (Haas et al., 1999), or 1:1000; raised in guinea-pigs against a C-portion of the GAG-binding region of mouse Neurocan (amino acids 645–944; D. Zimmermann, unpublished observations)]; Versican V1 and V2 [1:1000 and 1:200, respectively; raised in rabbits against the recombinant core protein fragments of the GAGα (amino acids 362–585) and GAGβ domains (amino acids 2751–3041) of Versican V0 (Schmalfeldt et al., 2000; and Dours-Zimmermann et al., manuscript in preparation, respectively); glial fibrillary acidic protein (GFAP, 1:500, mouse clone G-A-5, Chemicon International, Germany) for astrocytes; nestin (mouse Rat 401 clone, Chemicon International, Germany) for reactive astrocytes; NG2 (1:400; rabbit anti-rat NG2, Chemicon International, Germany) for oligodendrocyte precursor cells (OPCs) or more generally for NG2-positive cells; *Adenomatous polyposis coli* antigen (APC, 1:100, mouse clone Ab-7, Oncogene Research Products, USA) for mature oligodendrocyte cell bodies; calcitonin gene-related peptide (CGRP, 1:10,000, Peninsula Laboratories, San Carlos, CA, USA) for the identification of a subpopulation of regenerating sensory fibers; laminin (1:100, mouse monoclonal antibodies to the α2-chain of laminin) (Alexis Biochemicals, Lausen, Switzerland) as a marker of the dorsal root; Mac-1 (CD11b) (1:50, Serotec, France) as a marker of activated microglia and macrophages. The slides were air-dried for 1 h at room temperature, then incubated with 0.1% phenylhydrazine (Merck, Switzerland) in PBS for 30 min at 37 °C. After extensive washing in PBS, the slides were blocked with normal goat serum (NGS, Vector Laboratoires, USA) in PBS. The sections were then exposed overnight at 4 °C to the primary antibody diluted in NGS/PBS solution. After washing, the slides were incubated with a biotin-conjugated IgG secondary antibody (Vector Laboratories, USA) in NGS/PBS for 1 h at room temperature. The sections were then incubated for 30 min in avidin-biotinylated peroxidase complex using the Vectastain ABC amplification kit (Vector Laboratories, USA) according to the manufacturer's recommendations. When mouse monoclonal antibodies were used, the immunohistochemistry was performed using the M.O.M.™ kit (Vector Laboratories, USA) according to the manufacturer's recommendations. The signal was visualized using a DAB/Ni solution (0.05% 3,3′-diaminobenzidine, 2% ammonium nickel sulfate, 0.1 M sodium acetate, 0.1 M acetic acid, 0.001% H_2O_2). The sections were lightly counterstained with Fast Red (Sigma, Switzerland), dehydrated, and coverslipped using Permount mounting medium (Fisher Scientific, Switzerland). Controls for non-specific labeling were performed in the absence of primary antibodies. An average of three to four animals per lesion time-point was analyzed.

For immunofluorescence double labeling, sections were blocked with 5% NGS in PBS and exposed to primary antibodies (Neurocan, 1:2000; GFAP, 1:4000; NG2, 1:150; CGRP, 1:10,000) overnight at 4 °C as described above. Primary antibodies were visualized with the Alexa Fluor 594 goat anti-guinea-pig secondary antibody, Alexa Fluor 488 goat anti-mouse or Alexa Fluor 488 goat anti-rabbit antibody (at 1:250; Molecular Probes, Netherlands). The slides were then coverslipped using Gel Mount™ (Sigma-Aldrich, Switzerland). Digital images were captured with an Axioskop epifluorescence microscope (Zeiss, Germany) equipped with an Axiocam MRc digital camera (Zeiss, Germany), and processed using Adobe Photoshop software (Adobe Systems, USA).

Densitometric analysis

Semi-quantitative analysis of the relative amounts of Brevican, Neurocan, Versican V1 and Versican V2 immunoreactivity present in the DREZ before and after rhizotomy were determined by densitometric analysis of digital images (Axiocam MRc digital camera, Zeiss, Germany) of immunoperoxidase-labeled spinal cord sections using the MetaMorph 3 image analysis system (Visitron, Puchheim, Germany). Multiple densitometric measurements were made for each proteoglycan as well as for the astrocyte marker GFAP by delineating a field of approximately 5 μm^2 within the main DREZ area. Microscope settings were kept constant, stored, and recalled throughout all measurements. The relative optical densities (ROD) were calculated as follows. Briefly, the background ROD present in the DREZ on the lesioned and non-lesioned side of sections exposed to the second antibody alone (no primary antibody) was always subtracted from all data in the same series of experiments. The labeling intensities were then quantified and expressed as the percentage difference in ROD of the lesioned DREZ compared with the contralateral control DREZ of the same spinal cord section. A minimum of 11 and a maximum of 21 different sections were evaluated per proteoglycan and per time point after lesion.

Nucleic acid probes for *in situ* hybridization (ISH)

The digoxigenin-labeled cRNA probes were generated on the basis of the mouse cDNAs of Versican V1 (Ito et al., 1995), Versican V2 (Ito et al., 1995), Brevican (Rauch et al., 1997), and Neurocan (Rauch et al., 1995). The sense and antisense DNA templates, fused to the T7 DNA polymerase promoter, were obtained by PCR using the oligonucleotide primers. The Versican V1 probe extends over the bases 5371–6240 of the mouse Verscian V1 cDNA located within the 3′-end portion of the GAGβ domain (GenBank accession number D16263). The Versican V2 probe covers the first 655 bp of the GAGα domain including bases 1262–1916 of the mouse Versican cDNA (GenBank accession number D28599). The Brevican probe covers the 570 bp of the non-homologous central domain, common to the secreted and GPI-anchored splice variants, including bases 1444–2013 of the mouse Brevican cDNA (GenBank accession number X87096). The Neurocan probe covers the 720 bp starting from −86 in the untranslated region, to +659 in the first N-terminal region (GenBank accession number X84727). All *in vitro* transcripts were partially hydrolyzed at alkaline pH prior to hybridization. Sense strands served as probes in negative control experiments. The relative amount of digoxigenin-labeled sense and antisense probe was estimated by comparison with the DIG-labeled control RNA (Roche, Switzerland).

ISH

ISH with DIG-labeled riboprobes was performed as described by Schaeren-Wiemers and Gerfin-Moser (1993). Briefly, spinal cord cryostat sections cut at 12 μm were thaw-mounted onto Superfrost Plus slides (Menzel-Glaser). The sections were air-dried 30 min at room temperature and fixed with 4% paraformaldehyde in PBS 10 min at 4 °C. After washing in PBS, sections were treated with 1% Triton X-100 in PBS, then washed in PBS, incubated in 0.1 M triethanolamine containing 0.25% acetic anhydride, and again washed in PBS. Prehybridization was carried out at room temperature for 3 h with prehybridization buffer (50% formamid, 5× SSC, 5× Denhardt's solution, 100 mM maleic acid pH 7.5, 150 mM NaCl, 400 μg/ml herring sperm DNA, 250 μg/ml baker's yeast RNA). Fifty nanograms of cRNA probe were mixed with the prehybridization buffer. Sections were coverslipped using Hybriship^R membranes (Schleicher and Schuell, Germany) to ensure the presence of a homogeneous volume of probe over the tissue. Hybridization was performed overnight at 63 °C in a moist, sealed container. After hybridization, sections were washed in 5× standard saline citrate (SSC, containing 750 mM NaCl and 75 mM sodium citrate, pH 7.0) for 5 min at 63 °C, then washed in 0.1× SSC for 1 h at 63 °C and finally washed again in the same buffer for 5 min at room temperature. Sections were equilibrated with 1× maleic acid buffer (100 mM maleic acid, 150 mM NaCl; pH 7.5) and incubated in buffer 1 [1% blocking reagent (Roche Diagnostics, Switzerland) in 1× maleic acid buffer] for 1 h at room temperature, then incubated with alkaline phosphatase-coupled antibodies to digoxigenin (Roche Diagnostics, Switzerland) at a dilution of 1:2000 in buffer 1 for 5 h at room temperature. Sections were washed twice with 1× maleic acid buffer, equilibrated in buffer 2 (100 mM Tris–HCl, 100 mM NaCl, 50 mM $MgCl_2$; pH 9.5) and developed in the dark with buffer 2 containing 0.34 mg/ml 4-nitroblue-tetrazolium-chloride (Roche Diagnostics, Switzerland), 0.175 mg/ml 5-bromo-4-chloro-3-indolylphosphate (Roche Diagnostics, Switzerland), and 0.25 mg/ml levamisol (Sigma-Aldrich, Switzerland). Development was stopped by washing in buffer 3 (10 mM Tris–HCl, 1 mM EDTA, pH 8.0). Finally the slides were coverslipped with long term storage buffer (50% glycerol, 5% gelatin). Digital images were captured as described for immunocytochemistry. The number of ISH signals present in the DREZ region, i.e. the number of cells expressing CSPG mRNA, was evaluated non-stereologically in an average of 56 sections from four distinct experiments for each proteoglycan and each time-point after lesion. The data were expressed as number of cells in the DREZ/section.

Double labeling ISH/IHC

ISH for Brevican, Neurocan, Versican V1, and Versican V2 mRNA was combined with immunohistochemistry for GFAP, nestin, APC, or NG2. Tissue sections processed for ISH were rinsed extensively in PBS, followed by a blocking step in PBS containing 1% NGS or the M.O.M.™ kit (Vector Laboratoires, USA) for 1 h. Primary antibodies were incubated overnight at 4 °C and detected using biotinylated secondary antibodies and diaminobenzidine/nickel intensification as described above for immunohistochemical (IHC) staining alone. The slides were then coverslipped with long term storage buffer (50% glycerol, 5% gelatin). Digital images were captured with an Axioskop microscope (Zeiss), a digital camera (Axiocam MRc, Zeiss, Germany), and processed using Adobe Photoshop software (Adobe Systems, USA).

Statistical analysis

The Prism 4 Graph statistic program (GraphPad Software, USA) was used. For the densitometric analysis, the paired Student's *t*-test was applied to compare the ROD of the DREZ region on the lesioned versus the contralateral control side. The difference in the number of cells expressing CSPG mRNA in the DREZ before and after lesion was evaluated using one-way ANOVA followed by the Kruskal-Wallis test.

RESULTS

Brevican, Neurocan, Versican V1, and Versican V2 expression in the unlesioned DREZ and spinal cord

Proteoglycan type-specific antibodies were used to evaluate the expression patterns of individual CSPGs in transverse sections of the DREZ and spinal cord of unlesioned mice. Labeling with antibodies raised against the entire core protein of Brevican revealed strong expression of the proteoglycan throughout the spinal cord gray and white matter, including the cone of the DREZ protruding into the dorsal root, but not in the peripheral dorsal root itself (Fig. 1b). Brevican immunoreactivity, like immunoreactivity for GFAP, a marker of

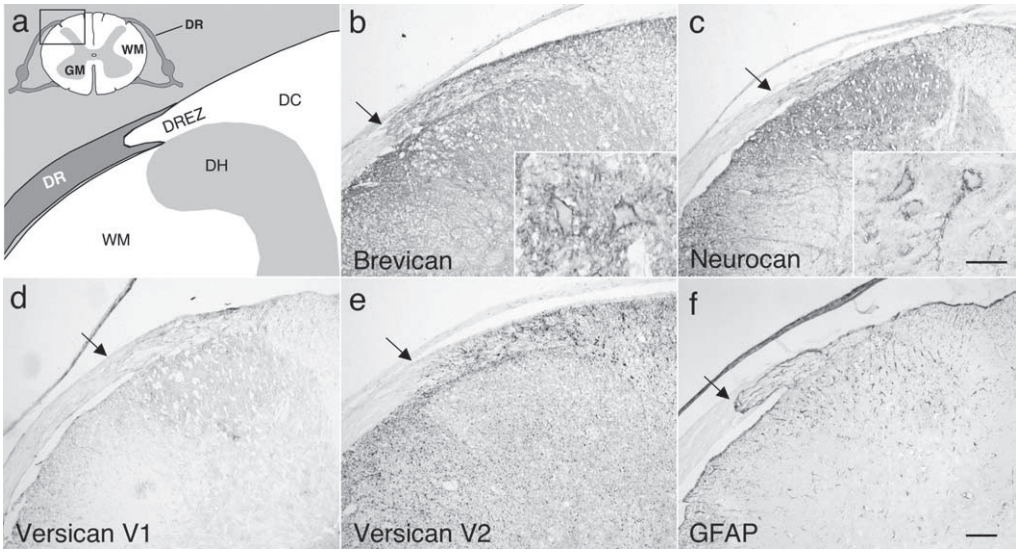

Fig. 1. Immunoreactivity for Brevican, Neurocan, Versican V1, Versican V2 and GFAP in the non-lesioned control spinal cord and DREZ. Schematic representation of a transverse section of spinal cord and dorsal root (DR) (a): DC, dorsal column; DH, dorsal horn; GM, gray matter; WM, white matter. Transverse spinal cord sections labeled with antibodies against Brevican (b), Neurocan (c), Versican V1 (d), Versican V2 (e) and the astrocyte marker GFAP (f). Strong immunoreactivity for Brevican and Versican V2 is present throughout the spinal cord GM and WM, including the DREZ (b, e). Neurocan staining is lower, particularly in the DREZ (c), whereas Versican V1 labeling is very weak over the entire spinal cord and DREZ (d). The arrows indicate the PNS/CNS border at the tip of the DREZ. Note the absence of labeling in the DR of all sections (b–f). Perineuronal nets of ventral spinal cord motoneurons stained for Brevican and Neurocan are shown in the insets (b, c). No immunoreactivity is observed in the absence of primary antibodies (not shown); Scale bar=50 μm; 10 μm in insets.

astrocytes, thus allows to delineate the PNS/CNS border (Fig. 1b and f, arrows). Intense Brevican staining was also present in perineuronal nets surrounding neurons of the ventral and dorsal spinal cord gray matter (Fig. 1b, inset). A similar, although less intense staining pattern was found for Neurocan throughout the white matter, the DREZ, and in perineuronal nets in the gray matter (Fig. 1c, and inset). Using antibodies specific for the V1 and V2 isoforms of Versican, entirely distinct labeling patterns were observed in the spinal cord and DREZ. Only weak Versican V1 immunoreactivity, was seen in the DREZ and throughout the spinal cord gray and white matter (Fig. 1d). Conversely, strong punctate immunoreactivity was observed throughout the spinal cord gray and white matter, including the DREZ, using Versican V2-specific antibodies (Fig. 1e). No signal was present in the peripheral dorsal root.

Astrocyte activation and CSPG expression following rhizotomy

Dorsal root lesion has previously been shown to lead to strong astrocyte activation in the DREZ of the rat (Murray et al., 1990). Because the response to rhizotomy has not been described in mice so far, we first evaluated astrocyte activation at the murine DREZ using anti-GFAP antibodies. At 7 days post-lesion (dpl), the signal intensity of GFAP immunoreactivity was increased by 31±4.5% compared with control. Hypertrophic astrocytic processes were mainly confined to the original outlines of the DREZ (Fig. 2a and b). No upregulation of GFAP expression was observed on the contralateral, unlesioned side when compared with unlesioned control animals (not shown). The contralateral side was therefore used as an internal control in all experiments. By 28dpl, astrocytic processes were tightly packed in the distal cone of the DREZ protruding into the root, with hypertrophic processes extending as far as 300–500 μm into the root (Fig. 2c). Brevican immunoreactivity in the DREZ was increased by 28±4.2% compared with the control side at 7dpl (Fig. 2e, f and h) and by 37±6.4% at 28dpl (Fig. 2g and h). However, hypertrophic astrocytic processes extending into the root beyond the PNS/CNS border, as well as the peripheral dorsal root itself, were not labeled. Immunoreactivity for Neurocan was also exclusively increased in the DREZ, with increases of 58±5.4% and 51±6.4% compared with control at 7 and 28dpl, respectively, but not on astrocytic processes beyond the PNS/CNS interface nor in the dorsal root (Fig. 2i–l). Increased intensity of staining was already observed at 3dpl (not shown). Immunolabeling with the isoform-specific Versican V1 and V2 antibodies revealed a distinct expression pattern in the DREZ and dorsal root following lesion. Versican V1 expression strongly increased, both in the DREZ (95±31%) and the dorsal root at 7dpl (Fig. 2n and p). Increased intensity of staining was already observed at 3dpl (not shown). Strong immunoreactivity was still detected throughout the entire DREZ at 28dpl (249±26.5%), but it had disappeared from the dorsal root (Fig. 2o). From 7–28dpl, staining was also present in the fibrous tissue over the DREZ (Fig. 2n and o, asterisk). In contrast, there was a small increase in Versican V2 immunoreactivity in the DREZ at 7dpl (25±5.5%) (Fig. 2r and t), but not in the dorsal root. By 28dpl, immunolabeling was slightly, but

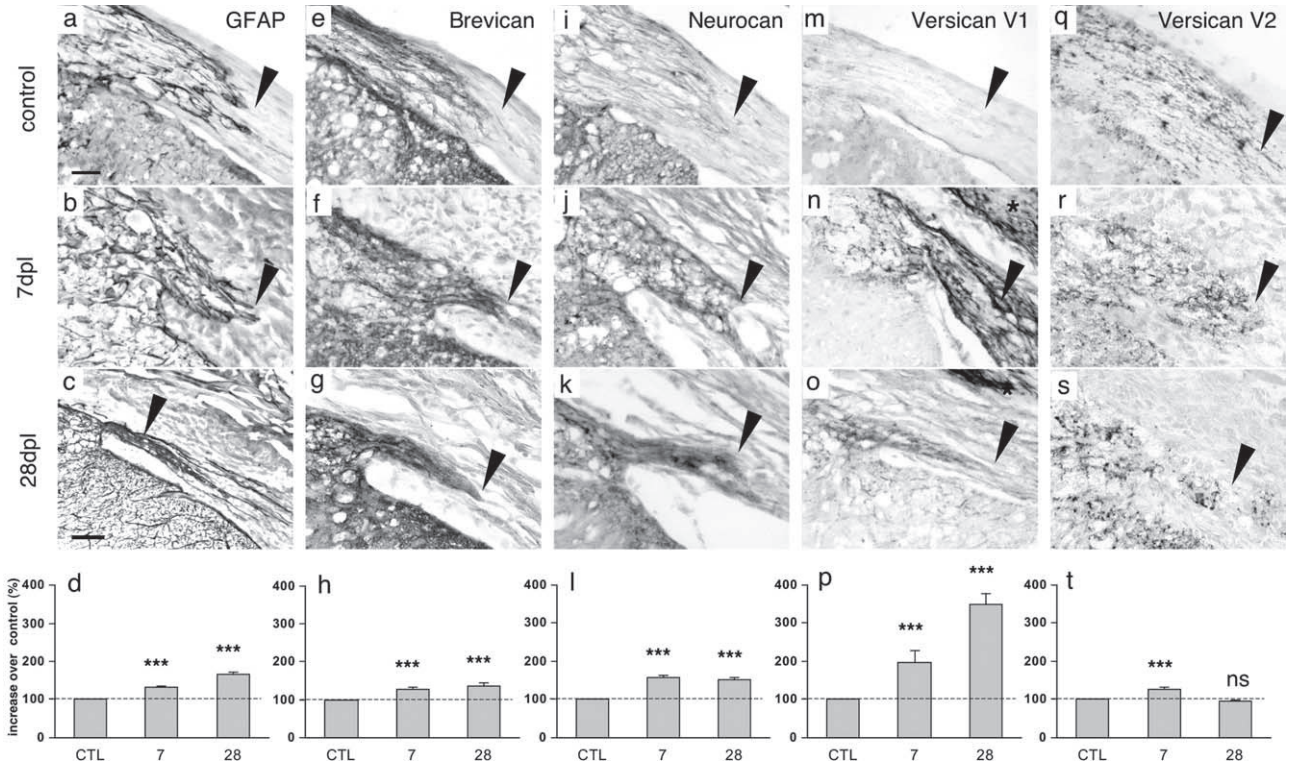

Fig. 2. Immunolocalization of GFAP, Brevican, Neurocan, Verican V1 and Versican V2 in the DREZ following dorsal root lesion. GFAP immunoreactivity at 7dpl shows hypertrophic astrocytic processes present mainly within the limits of the original DREZ area (a, b, arrowheads). At 28dpl, glial processes have extended as far as 300–500 μm into the peripheral root (c). The distribution of Brevican immunoreactivity is more compact at 7dpl (f) compared with non-lesioned controls (e). The PNS/CNS border is clearly visible (arrowhead), with strong Brevican labeling persisting in the DREZ until 28dpl, but none present in the dorsal root (g). Neurocan immunoreactivity is low in the DREZ of controls (i) and is increased at 7dpl and until 28dpl (j, k). Versican V1 expression is very weak in the control DREZ (m) and is strongly increased at 7 and 28dpl (n, o). An important and transient increase in immunoreactivity is also observed in the dorsal root (n). Note also the labeling of the fibrous tissue at 7 and 28dpl (n, o; asterisk). A periodic punctate Versican V2 staining pattern is revealed in the DREZ of controls (q). The pattern of immunoreactivity is altered at 7dpl (r) and 28dpl (s). The PNS/CNS border is indicated with arrowheads. Scale bar=20 μm in a–s except c, 50 μm. Densitometric analysis showing the ROD of the immunoreactivity for GFAP (d), Brevican (h), Neurocan (l), Versican V1 (p) and Versican V2 (t) post-lesion compared with control (CTL). The data are expressed as mean values±S.E.M. ns, not significant. ($11<n<21$, *** $P<0.001$).

not significantly decreased compared with control (Fig. 2s and t).

Brevican, Neurocan, and Versican V1 and V2 mRNA expression in the DREZ following rhizotomy

ISH in unlesioned animals revealed the presence of Brevican mRNA in most of the neurons of spinal cord gray matter, as well as lower mRNA expression in scattered cells of the white matter and the DREZ (Fig. 3a). The hybridization signal was particularly intense in motoneurons (not shown). The number of Brevican mRNA-expressing cells was transiently decreased in the DREZ at 3dpl from a mean number of 4.32±0.4–2.86±0.22 cells per section (Fig. 3b and e). At 7dpl, the number of positive cells was back to control values (4.6±0.25 cells/section), but the intensity of the signals was increased (Fig. 3c and e). At 14dpl, Brevican mRNA was mainly present in the distal portion of the DREZ protruding into the dorsal root (Fig. 3d).

Using the Neurocan-specific nucleic acid probe, no Neurocan mRNA-expressing cells could be detected over the entire spinal cord and DREZ in unlesioned controls (Fig. 3f). Neurocan mRNA-positive cells appeared in the proximal area and the tip of the DREZ at 3dpl (3.67±0.33 cells/section, Fig. 3g, j). Their number progressively decreased at 7dpl (2.32±0.14) and 14dpl (1.9±0.38 cells/section) (Fig. 3h–j). At 14dpl, the ISH signals were mainly found in the tip of the DREZ (Fig. 3i).

Low Versican V1 mRNA levels were detected in isolated cells scattered throughout the spinal cord white matter, including the DREZ, of non-lesioned animals (Fig. 3k). The number of Versican V1-expressing cells present in the DREZ transiently increased from an average of 0.7±0.12–2.5±1.5 cells per section at 3dpl (Fig. 3l and o) and returned to control levels at 7 and 14dpl (Fig. 3m–o). Cells expressing Versican V1 mRNA were also present in the dorsal root at 3 and 7, but not at 14dpl (l–n; arrowheads in m). Note the presence of V1-positive cells in the fibrous tissue at 7 and 14dpl (Fig. 3m and n, asterisks).

Versican V2 mRNA was detected in isolated cells scattered throughout the spinal cord white and gray matter, including the DREZ, of non-lesioned animals (Fig. 3p). The number of V2 mRNA-positive cells progressively increased to a maximal level of 3.4±0.25 cells/section at 7dpl (Fig. 3q–t). Hybridization with the sense probes for Brevican, Neurocan,

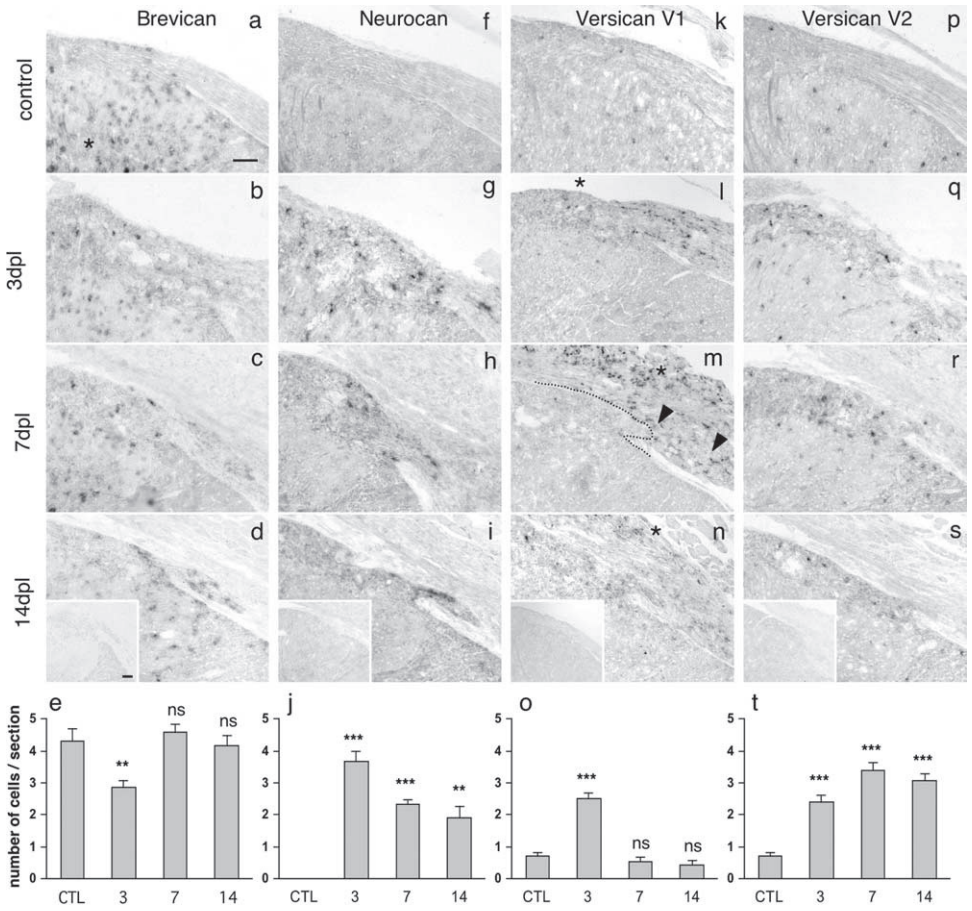

Fig. 3. ISH with Brevican-, Neurocan-, Versican V1-, and Versican V2-specific nucleic acid probes. Brevican mRNA transcripts are present in the DREZ of controls (a), and are maintained until 14dpl (b–d). Strong hybridization signals are also found in neurons of the gray matter (a; asterisk). Neurocan transcripts are not found in the DREZ and the entire control spinal cord (f). They appear in the DREZ at 3dpl (g) and are maintained, but decreased, at 7 and 14dpl (h, i). Versican V1 transcripts are found in scattered cells throughout the spinal cord of controls (k). There is a transient increase in the number of signals in the DREZ at 3dpl (l, asterisk) which returns to control levels at 7 and 14dpl (m, n). Versican V1 transcripts are also increased in the dorsal root at 3 and 7dpl (l, m, arrowheads) and are present in fibrous tissue (m, n, astersks). Versican V2 transcripts are also found in scattered cells throughout the control spinal cord (p). The number of Versican V2 hybridization signals is exclusively increased in the DREZ at 3, 7, and 14dpl (q–s). No signal was observed with any of the sense probes (insets d, i, n, s). Scale bar=50 μm. Quantification of the number of ISH signals per DREZ and per section is indicated in e, j, o, and t. The data are expressed as mean values±S.E.M. ns, not significant. ($10<n<124$, ** $P<0.01$; *** $P<0.001$).

or Versican V1 and V2 did not show any hybridization signals, confirming the specificity of the ISH protocols (Fig. 3d, i, n, s; insets). Taken together, these results demonstrate that expression of Brevican, Neurocan, Versican V1 and Versican V2 is regulated in a differential spatial and temporal manner in the DREZ following lesion.

Identity of Brevican, Neurocan, Versican V1, and Versican V2 mRNA expressing cells

Because most CSPGs are secreted ECM molecules, it is difficult to identify their cellular origin using double-immunofluorescence techniques. We therefore performed ISH with CSPG-specific probes, followed by IHC with cell type-specific antibodies. To assess the identity of the Brevican mRNA expressing cells present in the DREZ and spinal cord white matter, ISH was combined with IHC detection of astrocytes (GFAP), reactive astrocytes (nestin, an intermediate filament protein re-expressed in activated astrocytes {Clarke et al., 1994; Levine and Nishima, 1996}), oligodendrocyte precursor cells (NG2; Levine and Nishiyama, 1996), and oligodendrocytes (APC, a marker of mature oligodendrocytes labeling only the cell soma and not myelin sheaths {Watanabe et al., 2002}). At 3dpl, Brevican mRNA was detected in APC- (Fig. 4c), occasionally in NG2- (Fig. 4d), but not in GFAP- (Fig. 4a), or nestin- (Fig. 4b) positive cells in the DREZ. Conversely, at 7dpl, the transcripts were exclusively found in GFAP-positive DREZ astrocytes (Fig. 4e), but not in nestin-, APC-, or NG2-positive cells (Fig. 4f–h). This suggests that Brevican is transiently expressed by reactive oligodendrocytes post-lesion and in a subpopulation of astroglial cells that are nestin-negative thereafter. On the contralateral, non-lesioned side, most Brevican transcripts in the spinal cord white matter and the DREZ were associated with a subpopulation of astrocytes (Fig. 4i),

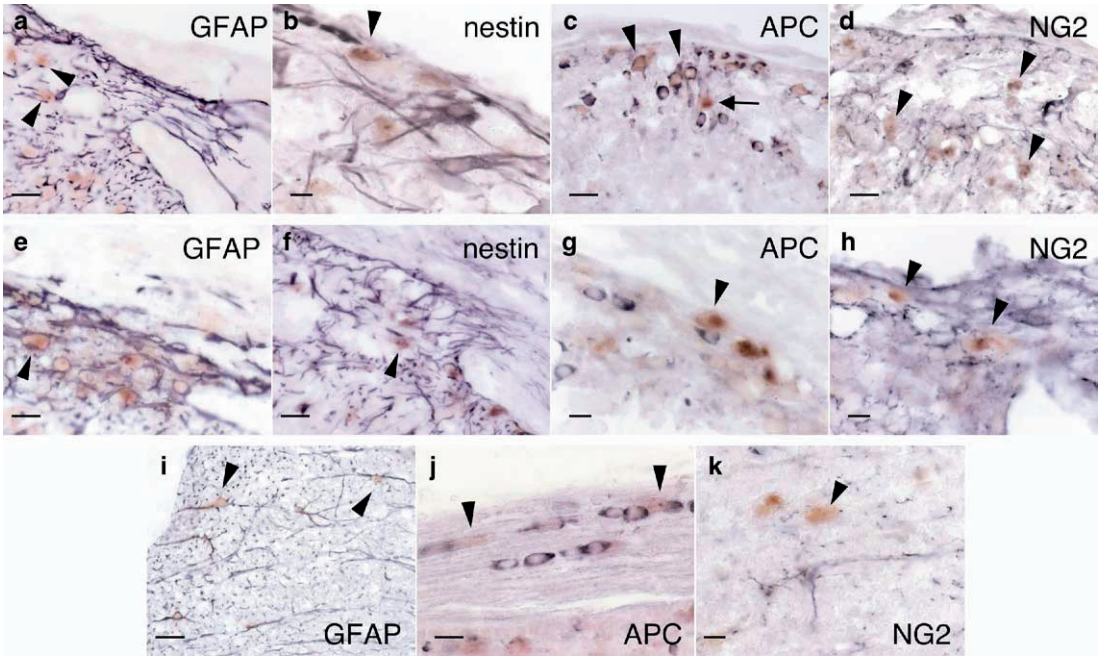

Fig. 4. Identity of Brevican mRNA expressing cells. DREZ labeled with a Brevican-specific probe (brown), followed by immunohistochemistry for GFAP (a, e, i), nestin (b, f), APC (c, g, j), and NG2 (d, h, k) (black). At 3dpl, Brevican mRNA co-localizes in the DREZ with APC (c, arrowheads), but not with GFAP (a), nestin (b), or NG2 (d) immunoreactivity. In contrast, at 7dpl, the *in situ* signal appears in GFAP-positive astrocytes (e), but is not present in nestin- (f), APC- (g), nor NG2-positive cells (h). The same cell-association is found in spinal cord white matter and DREZ of controls (i–k). Arrowheads in i indicate Brevican mRNA-expressing resting astrocytes in control white matter. Rows of APC-positive oligodendrocytes in the DREZ of an unlesioned animal are shown in j, with two interposed Brevican-positive cells (arrowheads). The *in situ* signal is not co-localized with with NG2 in control white matter (k). Scale bar=20 μm in a, c, e, f, i–k; 10 μm in b, d, g, h.

but not with APC- (Fig. 4j) or NG2-positive cells (Fig. 4k). Fig. 4j shows rows of APC-positive oligodendrocytes with interposed Brevican-positive cells in the DREZ of an unlesioned animal (arrowheads). This is reminiscent of the rows of contiguous oligodendrocytes with interspersed isolated astrocytes previously described in longitudinal sections of the rat fimbria (Suzuki and Raisman, 1992).

Neurocan mRNA transcripts that appeared in the DREZ at 3dpl were associated with both nestin (Fig. 5a and b) and GFAP immunoreactivity (Fig. 5c). The same cell-association was revealed at 7dpl (GFAP, Fig. 5d and e; nestin not shown). The hybridization signal was only occasionally found to be co-localized with NG2 (Fig. 5f), but not with APC immunoreactivity (not shown).

Versican V1 mRNA transcripts were expressed by a subpopulation of NG2-positive cells in both the DREZ at 3dpl (Fig. 6a) and in the control spinal cord white matter (Fig. 6e). No co-localization of the signal was found with GFAP, neither in the DREZ post-lesion (Fig. 6b), nor in the control white matter (Fig. 6f). The transcripts present in the dorsal root were located on the PNS side of the PNS/CNS border, marked by the extremity of the GFAP-positive astrocytic processes (Fig. 6c, arrowheads). High peripheral Versican V1 immunoreactivity was shown to delineate the DREZ in the lesioned dorsal root at 3dpl (Fig. 6d). Immunolabeling was still present at 7dpl (see Fig. 2n), but had disappeared from the dorsal root by 14dpl (not shown) (see Fig. 2o for 28dpl). The Versican V1 mRNA-expressing cells present in the dorsal root post-lesion did not co-localize with NG2 immunolabeling (Fig. 7b), and only occasionally with the macrophage marker Mac-1 (Fig. 7f–h). In addition, Versican V1 immunostaining only partially overlaps with laminin, an ECM glycoprotein produced by Schwann cells (Fig. 7c–e). Note the presence of Versican V1 transcripts in the meninges (Fig. 7a, arrowheads).

Most Versican V2 mRNA transcripts were detected in NG2-positive cells with the morphology of oligodendrocyte precursor cells present in the DREZ after lesion (Fig. 8a), but did not co-localize with GFAP or the oligodendrocyte marker APC (Fig. 8b, c). Similarly, the hybridization signal was expressed by many NG2-positive cells throughout the control spinal cord white matter (Fig. 8d), but not by APC- and GFAP-positive cells (Fig. 8e, f).

A comparative overview of the IHC stainings, message distribution (ISH), and cell association (ISH/IHC) of Brevican Neurocan, Versican V1 and Versican V2 in the DREZ area before and after rhizotomy is shown in Table 1.

Regeneration of CGRP-positive sensory fibers following lesion

To evaluate whether there was a correlation between the presence of CSPGs in the DREZ and the failure of axonal regeneration through this region after rhizotomy, spinal cord cryosections from animals killed at 28dpl were processed for double-immunofluorescence labeling using antibodies raised against CGRP (a peptide

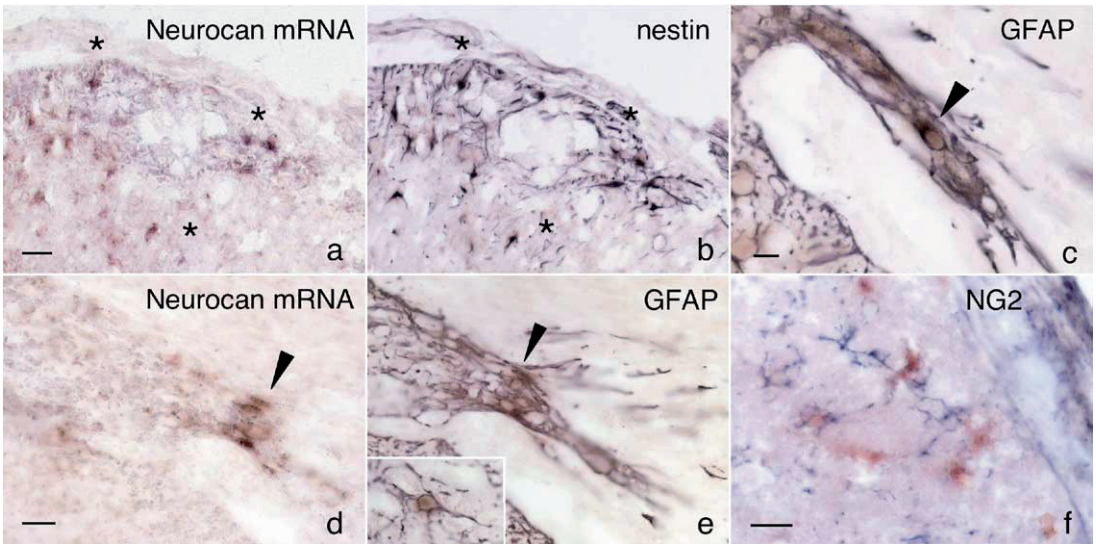

Fig. 5. Identity of Neurocan mRNA expressing cells. DREZ 3dpl labeled with a Neurocan-specific probe (a), followed by immunohistochemistry for nestin (b). The asterisks indicate the ISH signal in a (brown), and nestin-immunoreactivity in b (black), revealing the expression of Neurocan in nestin-positive cells. Co-localization of Neurocan mRNA with GFAP staining is shown in c (arrowhead). Neurocan transcripts are often found at the tip of the DREZ at 7dpl (d) and co-localize with GFAP immunostaining (e). The inset in e shows co-localization of Neurocan mRNA and GFAP staining in another DREZ section of the same animal. The Neurocan signal was only occasionally found to be co-localized with NG2 immunoreactivity (f). Scale bar=20 μm in a, b, d–f; 10 μm in c.

present in a subpopulation of large diameter myelinated and small diameter non-myelinated sensory fibers) and against Neurocan, GFAP, or laminin. Many CGRP-positive fibers regenerated through the dorsal root (PNS), but they stopped growing as soon as they reached the DREZ (CNS) containing high Neurocan concentrations (Fig. 9a–c). Failure to regrow through the PNS/CNS transitional zone was also visualized by double-labeling with GFAP, a marker of astrocytes (Fig. 9d–f), and laminin, an ECM glycoprotein produced by Schwann cells present in the dorsal root (Fig. 9g–i). CGRP-positive axons can grow along astrocytic processes that extend long distances into the dorsal root (Fig. 9f, inset, arrows) and are occasionally seen to penetrate short distances into the outskirts of the DREZ, but not through the DREZ (Fig. 9b, c; asterisk).

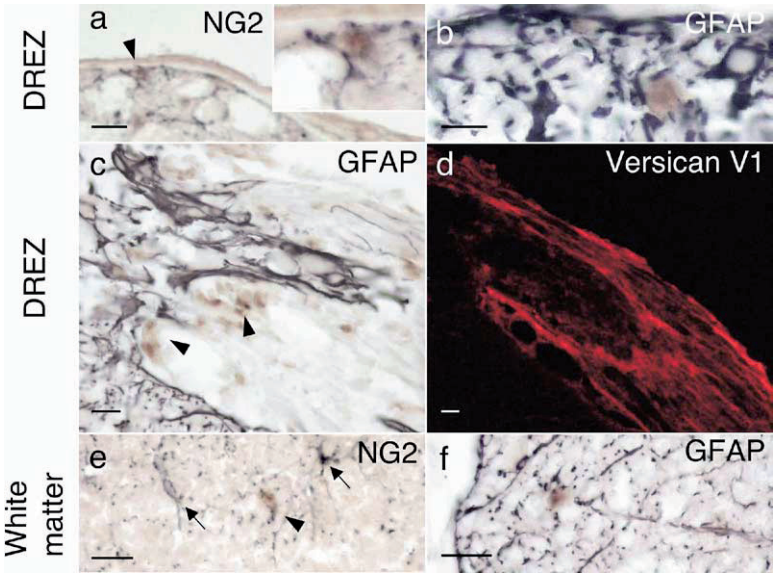

Fig. 6. Identity of Versican V1 mRNA expressing cells. Spinal cord sections labeled with a Versican V1-specific probe, followed by immunohistochemistry for NG2 or GFAP. The ISH signal is present in a subpopulation of NG2- (a, e, arrowhead), but not GFAP- (b, c, f) positive cells, both in the DREZ 3dpl (a–c) and in the spinal cord white matter of controls (e and f). Note that not all NG2-positive cells express the Versican V1 transcripts in the control white matter (e, arrows). The transcripts visible at the PNS/CNS border in Fig. 3C, are located on the PNS side of the transition zone marked by GFAP-positive astrocytic processes (c, arrowheads). Similarly, the presence of Versican V1 immunolabeling in the dorsal root allows to delineate the PNS/CNS border (d). Scale bar=10 μm in b; 20 μm in a, c–f.

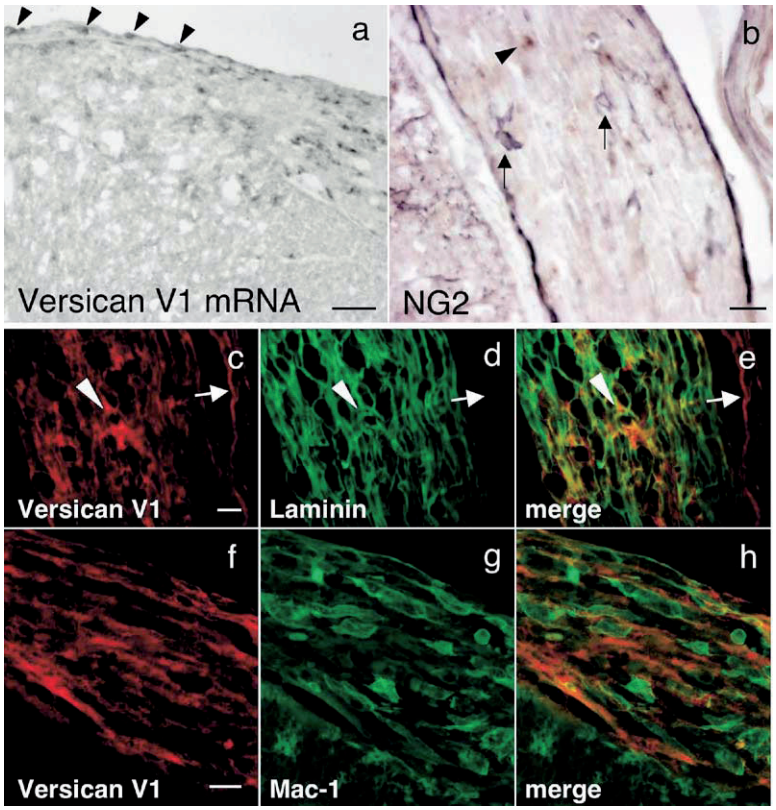

Fig. 7. Versican V1 expression in the dorsal root. Spinal cord section labeled with a Versican V1 specific probe reveals positive cells in meningeal membranes (a, arrowheads). Cells expressing Versican V1 transcripts in the dorsal root (b, arrowhead) do not co-localize with NG2 immunoreactivity (b, arrows). Double-immunofluorescence labeling using antibodies against Versican V1 and laminin (c–e) or Mac-1, a macrophage marker (f–h), shows only partial overlap with laminin and only rarely co-localization with Mac-1. Note the Versican V1 labeling of the meninges in c and e (arrows). Scale bar=50 μm in a; 20 μm in b–h.

DISCUSSION

Brevican, Neurocan, Versican V1 and Versican V2 have all been shown to have potent growth-inhibitory properties *in vitro*. However, little is known about their involvement in regeneration failure *in vivo*, especially in the DREZ, a region that is particularly inhibitory following dorsal root lesion, and

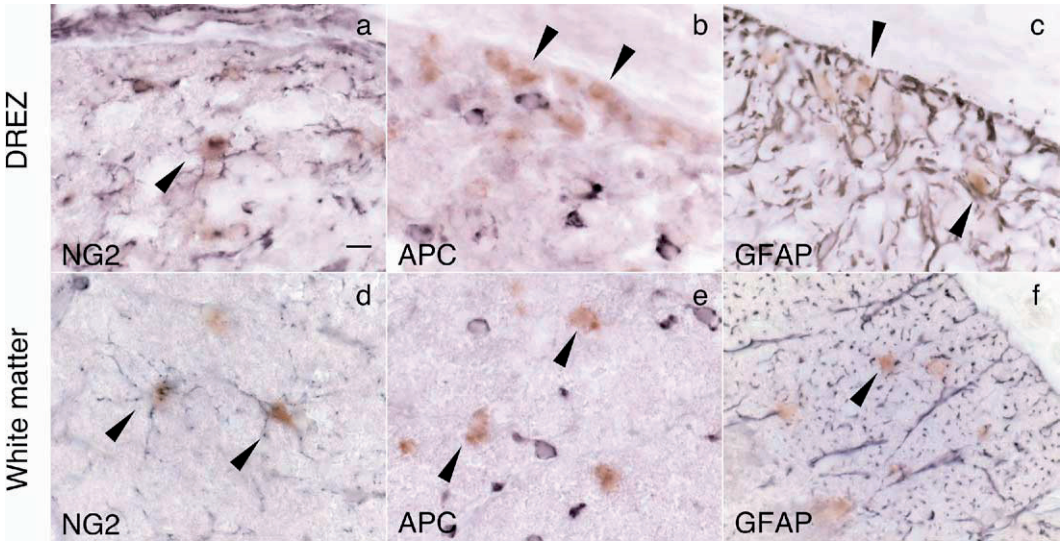

Fig. 8. Identity of Versican V2 mRNA expressing cells. Spinal cord sections labeled with a Versican V2-specific probe followed by immunohistochemistry for NG2 (a, d), APC (b, e), and GFAP (c, f). The ISH signal only co-localizes with NG2-positive cells both in the DREZ 7dpl (a–c) and in the control spinal cord white matter (d–f). Scale bar=10 μm.

Table 1. Summary of immunohistochemical staining, message distribution, and cell-association of Brevican, Neurocan, Versican V1 and Versican V2 in the DREZ before and after rhizotomy

	Increase in immunoreactivity post-lesion (fold-increase)		Number of mRNA expressing cells/DREZ/section				Cell-association of CSPGs	
	7 dpl	28 dpl	Control	3 dpl	7 dpl	14 dpl	Non-lesioned	Lesioned
GFAP	1.31±0.04	1.67±0.04	ND	ND	ND	ND	—	—
Brevican	1.28±0.04	1.37±0.06	4.3±0.4	2.9±0.2	4.6±0.2	4.2±0.3	Astrocytes	Oligodendrocytes (transient), astrocytes (nestin-neg.)
Neurocan	1.58±0.05	1.51±0.06	0	3.7±0.3	2.3±0.1	1.9±0.4	—	Astrocytes (nestin-pos.)
Versican V1	1.95±0.03	2.49±0.03	0.7±0.1	2.5±0.1	0.5±0.1	0.4±0.1	OPCs	OPCs
Versican V2	1.25±0.05	0.6±0.05	0.7±0.1	2.4±0.2	3.4±0.3	3.1±0.2	OPCs	OPCs

this in the absence of glial scar formation. The present study demonstrates, using CSPG-specific antibodies and nucleic acid probes, that the investigated proteoglycans are differentially distributed in the DREZ of unlesioned mice and that changes in their spatiotemporal expression occur upon dorsal root lesion. Furthermore, these proteoglycans are ex-

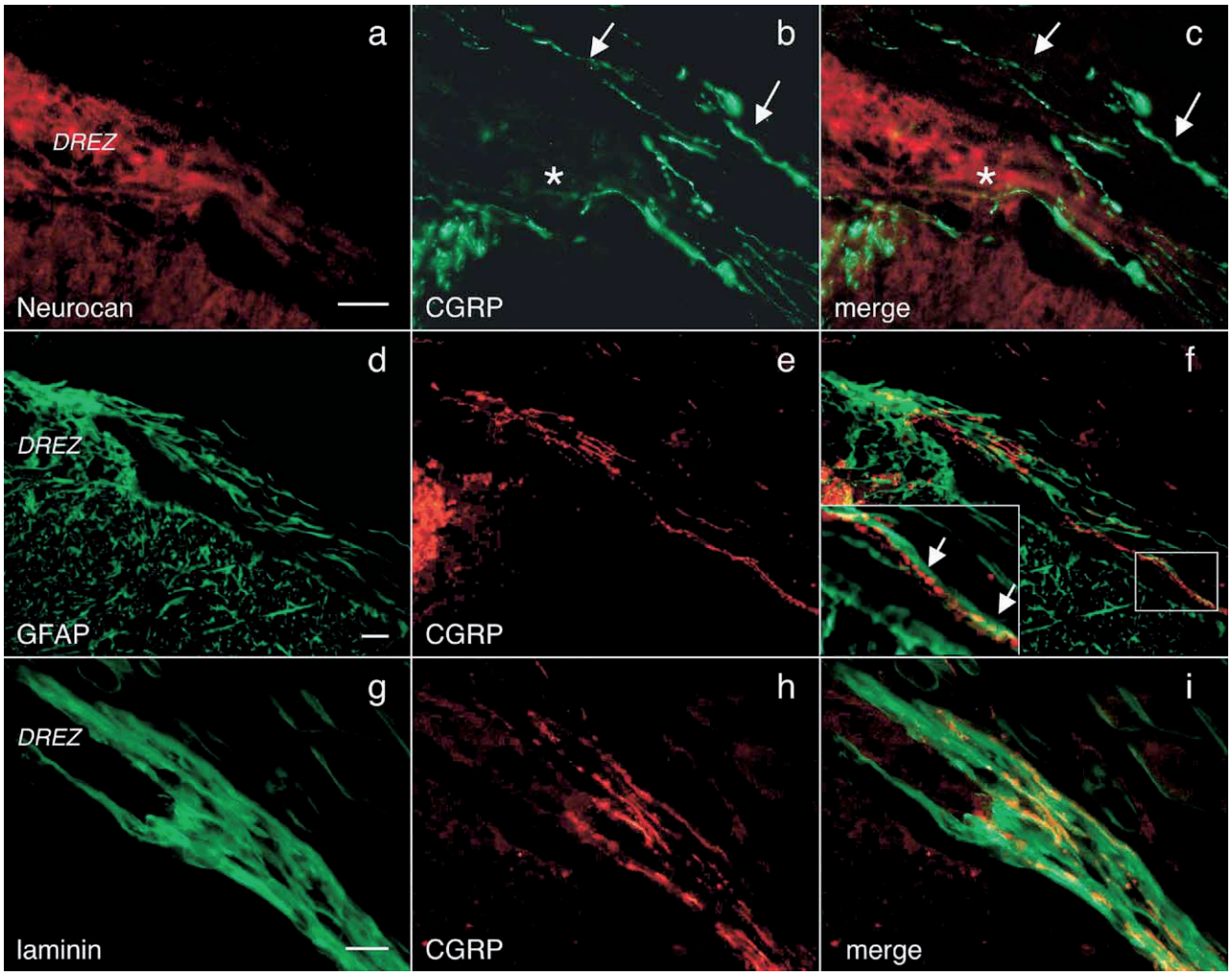

Fig. 9. Regeneration of CGRP-positive sensory fibers following rhizotomy. Double-immunofluorescence labeling using antibodies raised against CGRP (b, e, h), Neurocan (a), GFAP (d), or laminin (g). Merged images (c, f, i) illustrate the inability of the nerve fibers to regenerate through the DREZ containing high Neurocan concentrations (c). In addition, CGRP-positive axons stop at the PNS/CNS transitional zone marked on the CNS side with GFAP (f), and on the PNS side with laminin, an ECM glycoprotein produced by Schwann cells (i). CGRP-positive axons can grow along astrocytic processes extending into the dorsal root (f, inset) and into the fibrous tissue above the DREZ (b, c, arrows). They can occasionally be seen to penetrate short distances into the outskirts of the DREZ (c; asterisks). Scale bar=20 μm.

pressed by distinct reactive glial cells post-injury and are abundant in the DREZ at the time regenerating sensory fibers reach the PNS-CNS transitional zone.

CSPG expression in the unlesioned DREZ and spinal cord

Immunohistochemistry using CSPG-specific antibodies revealed the presence and differential distribution of Brevican, Neurocan, and Versican V1 and V2, in the DREZ and spinal cord of unlesioned animals. Labeling with Brevican antibodies recognizing both the secreted and the GPI-anchored isoform of the proteoglycan (Seidenbecher et al., 1995) revealed strong expression throughout the spinal cord gray and white matter, but not in the dorsal root. This confirms previous observations demonstrating that Brevican is CNS-specific and is abundantly expressed in adult brain (Yamada et al., 1997; Seidenbecher et al., 1998; reviewed in Yamaguchi, 1996). Neurocan immunoreactivity showed a pattern of distribution similar to that of Brevican, but labeling was less intense (Margolis et al., 1996). Perineuronal nets surrounding gray matter neurons, in particular ventral motoneurons, were also immunoreactive. In the rat, perineuronal Neurocan has been demonstrated to be expressed by glial cell processes surrounding neuronal cell bodies (Matsui et al., 1998). Using antibodies specific for the V1 and V2 isoforms of Versican, entirely distinct labeling patterns were observed in the spinal cord and DREZ of unlesioned mice. Only weak immunoreactivity for Versican V1 was present throughout the spinal cord, and labeling was absent from the dorsal root. In contrast, Versican V2 was strongly expressed throughout the spinal cord gray and white matter, but not in the peripheral dorsal root. Immunolabeling revealed a punctate staining pattern reminiscent of the distribution of nodes of Ranvier (see Fig. 2q), in agreement with the recent finding that Versican V2 is highly concentrated at nodes of Ranvier in adult mouse cerebellum (Oohashi et al., 2002). Despite strong labeling revealed by immunohistochemistry, relatively low mRNA levels for Brevican and Versican V2 were detected in the control spinal cord white matter and DREZ. This discrepancy may be due to the slow turnover rate of these proteoglycans in unlesioned tissue and the difficulty to detect very low abundant mRNA transcripts by ISH. This also holds true for Neurocan.

Astrocyte activation at the murine DREZ following rhizotomy

Cervical rhizotomy in mice led to astrocyte activation in the DREZ characterized by astrocyte hypertrophy and upregulation of GFAP. Starting a few days after injury, astrocytic processes started to elongate beyond the PNS/CNS border into the peripheral environment of the dorsal root and reached several hundred micrometers (up to 500 μm at 28dpl). Thus, astrogliosis at the DREZ in mice, as evaluated with antibodies against GFAP, appears to be largely similar to the response previously observed in the rat (Liu et al., 2000; Ramer et al., 2001b). This is interesting to note since the reaction to spinal cord injury in mice has been described to be different from that in rats and human, probably due to a distinct inflammatory reaction (Inman et al., 2002; Sroga et al., 2003). The similarity in the astrogliotic response to dorsal root lesion may therefore be related to the weak inflammatory reaction occurring in the DREZ upon rhizotomy (George and Griffin, 1994; Liu et al., 2000).

Brevican expression in the DREZ following rhizotomy

Brevican has previously been demonstrated to be upregulated in the glial scar following CNS injury (Jaworski et al., 1999; Thon et al., 2000). However, the glial reaction that occurs at the DREZ following rhizotomy is distinct from the cellular response to direct CNS injury that leads to breakage of the blood–brain-barrier and to glial scar formation. Semi-quantitative evaluation of the labeling intensity by densitometric analysis revealed the maintenance, but only a small increase in Brevican immunostaining at both 7 and 28dpl. This small increase may be in part due to the reduced size of the DREZ subsequent to the loss of the integrity of the axons and myelin sheaths during Wallerian degeneration. It may also be due to newly synthesized Brevican produced by glial cells since the intensity, although not the number, of the ISH signals was increased in the DREZ at 7dpl. Thus, in the absence of glial scar formation and breakage of the blood–brain-barrier, only moderate increases in Brevican immunoreactivity were observed which could be attributed to a combination of slow degradation, shrinkage of the DREZ, and increased production by activated glial cells. Note that Brevican immunolabeling could only be detected in the DREZ region that contains tightly packed astrocytic processes, but not on glial processes extending long distances into the peripheral root, i.e. beyond the PNS/CNS border. This may indicate a possible differential distribution of the CSPG on astrocytes. Combined ISH and immunohistochemistry revealed that Brevican mRNA was transiently expressed by APC-positive oligodendrocytes at 3dpl. This increase in Brevican expression may be a reactive response of oligodendrocytes to axonal loss during Wallerian degeneration, leading to re-expression of the proteoglycan in these cells (Ogawa et al., 2001). At 7dpl, Brevican was no longer detected in oligodendrocytes, but appeared in GFAP-positive astrocytes. Interestingly, no co-localization of Brevican was found with nestin, an intermediate filament protein present in glial and neuronal precursors and re-expressed in some activated astrocytes (Clarke et al., 1994; Lin et al., 1995). Brevican thus appears to be mainly expressed by a subset of reactive astrocytes in the DREZ that are nestin-negative.

Neurocan expression in the DREZ following rhizotomy

Both Neurocan immunoreactivity and Neurocan mRNA were increased in the DREZ upon rhizotomy, as has previously been shown to occur upon direct CNS injury (Haas et al., 1999; McKeon et al., 1999). The Neurocan transcripts were present as early as 3dpl and were maintained there until 14dpl. Neurocan is thus present in the DREZ at

the time sensory fibers reach the PNS/CNS interface (between 3 and 7 days following lesion {unpublished observation; Wujek and Lasek, 1983}). Neurocan mRNA co-localized both with GFAP and nestin immunoreactivity in the DREZ. Co-localization with NG2 was found only occasionally. Neurocan thus appears to be mainly produced by a sub-population of nestin-positive reactive astrocytes. This is in agreement with previous studies reporting Neurocan expression by activated astrocytes following direct CNS injury (Haas et al., 1999; McKeon et al., 1999). Alternatively, Neurocan may be synthesized by nestin-positive glial precursor cells that have been described to appear in the spinal cord following rhizotomy in the rat. These cells have been suggested to originate from the subpial region of the dorsal spinal cord and migrate ventrally (Kozlova, 2003). However, lateral migration of these precursors from the pial region into the DREZ has not been evaluated in this work. Taken together, reactive astrocytes in the DREZ may consist of a heterogeneous population of cells, some expressing Brevican but not nestin, while others express Neurocan and nestin.

Versican V1 expression in the DREZ following rhizotomy

Although there have been reports showing modulation of Versican expression upon CNS injury (Asher et al., 2002; Tang et al., 2003), these studies were performed with a monoclonal antibody that recognizes an epitope in the protein domain that is common to all Versican isoforms. Using an isoform-specific antibody, Versican V1 immunoreactivity that is low in the entire control spinal cord, was shown to be increased three-four-fold in the DREZ post-injury and to remain high until 28dpl. In contrast, Versican V1 mRNA was only transiently increased post-lesion. This discrepancy could reflect a slow turnover rate of this proteoglycan, leading to its persistence in the DREZ for several weeks. Versican V1 mRNA was localized to a subpopulation of NG2-positive cells with the morphology of oligodendrocyte precursors, both in the DREZ post-injury and in the spinal cord white matter of controls. This indicates that Versican V1, which is predominantly expressed outside the CNS (Yao et al., 1994; Bode-Lesniewska et al., 1996), may participate in growth-inhibition in the brain following injury. A growth-inhibitory role for Versican V1 in peripheral tissues has previously been suggested since it is present in regions that act as barriers for the migration of neural crest cells (Landolt et al., 1995). Furthermore, Versican V1 strongly inhibits neurite outgrowth from chicken embryonic DRG neurons in a stripe choice assay *in vitro* (S. Dutt and D. R. Zimmermann, manuscript in preparation).

In addition to an increase in the DREZ, there was a strong increase in both Versican V1 mRNA and immunostaining in the dorsal root at 3 and 7dpl. Both the transcripts and the immunoreactivity had disappeared from the dorsal root by 14dpl. This transient expression appears to coincide with axonal destruction, macrophage invasion, and Schwann cell proliferation occurring during the first few days of Wallerian degeneration. Because Versican V1 is still present at the time the first regenerating sensory axons reach the DREZ (3–7dpl, unpublished observation), its inhibitory properties may be masked by the presence of growth-promoting molecules such as laminin and tenascin C that are strongly up-regulated in the dorsal root after lesion (Kozlova et al., 1997; Zhang et al., 2001). A balance between growth-inhibitory and growth-promoting molecules has been postulated to be important for inhibition to be effective (Jones et al., 2003). Laminin, for instance, has been shown to override the inhibitory effects of myelin-associated glycoprotein, a growth-inhibitor present in both CNS and PNS myelin (David et al., 1995). Furthermore, NG2, a growth-inhibitory proteoglycan that is up-regulated after CNS injury (Levine, 1994), is also increased in the growth-permissive environment of the rat sciatic nerve after lesion (Morgenstern et al., 2003). Thus, although Versican V1 may inhibit axonal growth in other contexts, growth-permissive molecules present in the lesioned dorsal root may override its inhibitory properties.

Versican V1 was found to be present in the fibrous tissue forming above the DREZ, as well as in cells of the meninges, probably fibroblasts. Versican V1 may therefore be expressed by endoneurial fibroblasts present in the root following lesion. NG2 proteoglycan has recently been suggested to be expressed by endoneurial and perineurial fibroblasts in the peripheral nerve following sciatic nerve lesion in the rat (Morgenstern et al., 2003). However, no co-localization of Versican V1 mRNA and NG2 was found in our hands in the mouse. The lack of availability of appropriate markers for mouse fibroblasts did not allow us to evaluate further the cellular identity of Versican V1 expressing cells in the lesioned dorsal root.

Versican V2 expression in the DREZ following rhizotomy

Using Versican V2-specific antibodies, immunoreactivity was found to be slightly, but significantly increased in the DREZ at 7dpl. This increase may be due to Versican V2 mRNA production by reactive cells in the DREZ post-lesion, as visualized using ISH. Concomitantly, constitutively expressed Versican V2 visualized by IHC appears to remain in the DREZ for several weeks post-lesion. Like Brevican, Versican V2 may therefore be rather stable despite the ongoing Wallerian degeneration. This may also explain the low mRNA expression detected in spinal cord white matter using *in situ* hybridization that contrasts with the high intensity of both Brevican and Versican V2 immunostaining (Fig. 1b and e; Fig. 3a and p). Combined ISH and immunohistochemistry revealed the selective co-localization of Versican V2 mRNA with NG2-immunoreactivity, both in the DREZ after lesion, and in the intact spinal cord white matter. Versican V2 therefore appears to be mainly produced by a subpopulation of NG2-positive cells with the morphology of oligodendrocyte precursors, as previously shown to occur after direct cortical injury (Asher et al., 2002). Taken together, there are spatiotemporal changes in the expression pattern of Versican V1 and Versican V2 following dorsal root lesion. Both Versican isoforms appear to be expressed by NG2-positive cells of the oligodendrocyte lineage in the DREZ. However, it remains to be de-

termined whether they are expressed by the same population, or by distinct subpopulations of oligodendrocyte lineage cells.

Regenerating sensory fibers stop at the DREZ following rhizotomy

Regeneration of sensory fibers after dorsal root lesion, as evaluated using antibodies against the peptide CGRP, was shown to stop as soon as the axons reached the DREZ containing high Neurocan concentrations. There is therefore a good correlation between the presence of this proteoglycan in the DREZ and the failure of axonal regeneration through this region. Thus, together with other CSPGs, Neurocan produced by reactive astrocytes may participate in the non-permissiveness of this area. In addition, the high levels of laminin present in the root post-lesion may prevent the regenerating axons from leaving the growth-promoting environment of the peripheral root, as suggested recently using *in vitro* models of regeneration (Adcock et al., 2004; Grimpe et al., 2005).

Taken together, this is a detailed description showing that Brevican, Neurocan, and Versican V1 and V2 are abundant in the DREZ following rhizotomy at the time regenerating sensory axons reach the PNS/CNS border. Furthermore, we demonstrate that Brevican and Neurocan are produced by two distinct subpopulations of reactive astrocytes, and Versican V1 and V2 by subpopulations of cells of the oligodendrocyte lineage. These four proteoglycans are thus appropriately located to contribute to the non-permissive environment of the DREZ.

Acknowledgments—This work was supported by the Swiss National Science Foundation Grants No. 3100–065405 (A.D.Z.) and No. 3100–103717 (D.R.Z.), and the IRP Foundation-Geneva International Institute for Research in Paraplegia (A.D.Z.). We thank Drs. U. Rauch and R. Timpl for the generous gift of Neurocan and Brevican antibodies and S. Streuli, X. Quaglia, and E. Sarrasin for technical assistance.

REFERENCES

Adcock KH, Brown DJ, Shearer MC, Shewan D, Schachner M, Smith GM, Geller HM, Fawcett JW (2004) Axon behaviour at Schwann cell-astrocyte boundaries: manipulation of axon signalling pathways and the neural adhesion molecule L1 can enable axons to cross. Eur J Neurosci 20:1425–1435.

Asher RA, Morgenstern DA, Shearer MC, Adcock KH, Pesheva P, Fawcett JW (2002) Versican is upregulated in CNS injury and is a product of oligodendrocyte lineage cells. J Neurosci 22:2225–2236.

Bandtlow CE, Zimmermann DR (2000) Proteoglycans in the developing brain: new conceptual insights for old proteins. Physiol Rev 80:1267–1290.

Bode-Lesniewska B, Dours-Zimmermann MT, Odermatt BF, Briner J, Heitz PU, Zimmermann DR (1996) Distribution of the large aggregating proteoglycan versican in adult human tissues. J Histochem Cytochem 44:303–312.

Bradbury EJ, Moon LD, Popat RJ, King VR, Bennett GS, Patel PN, Fawcett JW, McMahon SB (2002) Chondroitinase ABC promotes functional recovery after spinal cord injury. Nature 416:636–640.

Carlstedt T (1983) Regrowth of anastomosed ventral root nerve fibers in the dorsal root of rats. Brain Res 272:162–165.

Carlstedt TP (1995) Spinal nerve root injuries in brachial plexus lesions: basic science and clinical application of new surgical strategies. A review. Microsurgery 16:13–16.

Clarke SR, Shetty AK, Bradley JL, Turner DA (1994) Reactive astrocytes express the embryonic intermediate neurofilament nestin. Neuroreport 5:1885–1888.

David S, Braun PE, Jackson DL, Kottis V, McKerracher L (1995) Laminin overrides the inhibitory effects of peripheral nervous system and central nervous system myelin-derived inhibitors of neurite growth. J Neurosci Res 42:594–602.

Davies SJ, Goucher DR, Doller C, Silver J (1999) Robust regeneration of adult sensory axons in degenerating white matter of the adult rat spinal cord. J Neurosci 19:5810–5822.

Fawcett JW, Asher RA (1999) The glial scar and central nervous system repair. Brain Res Bull 49:377–391.

Friedlander DR, Milev P, Karthikeyan L, Margolis RK, Margolis RU, Grumet M (1994) The neuronal chondroitin sulfate proteoglycan neurocan binds to the neural cell adhesion molecules Ng-CAM/L1/NILE and N-CAM, and inhibits neuronal adhesion and neurite outgrowth. J Cell Biol 125:669–680.

George R, Griffin JW (1994) Delayed macrophage responses and myelin clearance during Wallerian degeneration in the central nervous system: the dorsal radiculotomy model. Exp Neurol 129:225–236.

Grimpe B, Pressman Y, Bunge MB, Silver J (2005) The role of proteoglycans in Schwann cell/astrocyte interactions and in regeneration failure at PNS/CNS interfaces. Mol Cell Neurosci 28:18–29.

Grumet M, Milev P, Sakurai T, Karthikeyan L, Bourdon M, Margolis RK, Margolis RU (1994) Interactions with tenascin and differential effects on cell adhesion of neurocan and phosphacan, two major chondroitin sulfate proteoglycans of nervous tissue. J Biol Chem 269:12142–12146.

Haas CA, Rauch U, Thon N, Merten T, Deller T (1999) Entorhinal cortex lesion in adult rats induces the expression of the neuronal chondroitin sulfate proteoglycan neurocan in reactive astrocytes. J Neurosci 19:9953–9963.

Hagihara K, Miura R, Kosaki R, Berglund E, Ranscht B, Yamaguchi Y (1999) Immunohistochemical evidence for the brevican-tenascin-R interaction: colocalization in perineuronal nets suggests a physiological role for the interaction in the adult rat brain. J Comp Neurol 410:256–264.

Inman D, Guth L, Steward O (2002) Genetic influences on secondary degeneration and wound healing following spinal cord injury in various strains of mice. J Comp Neurol 451:225–235.

Ito K, Shinomura T, Zako M, Ujita M, Kimata K (1995) Multiple forms of mouse PG-M, a large chondroitin sulfate proteoglycan generated by alternative splicing. J Biol Chem 270:958–965.

Jaworski DM, Kelly GM, Hockfield S (1999) Intracranial injury acutely induces the expression of the secreted isoform of the CNS-specific hyaluronan-binding protein BEHAB/brevican. Exp Neurol 157:327–337.

Jones LL, Sajed D, Tuszynski MH (2003) Axonal regeneration through regions of chondroitin sulfate proteoglycan deposition after spinal cord injury: a balance of permissiveness and inhibition. J Neurosci 23:9276–9288.

Kozlova EN, Seiger A, Aldskogius H (1997) Human dorsal root ganglion neurons from embryonic donors extend axons into the host rat spinal cord along laminin-rich peripheral surroundings of the dorsal root transitional zone. J Neurocytol 26:811–822.

Kozlova EN (2003) Differentiation and migration of astrocytes in the spinal cord following dorsal root injury in the adult rat. Eur J Neurosci 17:782–790.

Landolt RM, Vaughan L, Winterhalter KH, Zimmermann DR (1995) Versican is selectively expressed in embryonic tissues that act as barriers to neural crest cell migration and axon outgrowth. Development 121:2303–2312.

Levine JM (1994) Increased expression of the NG2 chondroitin-sulfate proteoglycan after brain injury. J Neurosci 14:4716–4730.

Levine JM, Nishiyama A (1996) The NG2 chondroitin sulfate proteoglycan: a multifunctional proteoglycan associated with immature cells. Perspect Dev Neurobiol 3:245–259.

Lin RC, Matesic DF, Marvin M, McKay RD, Brustle O (1995) Re-expression of the intermediate filament nestin in reactive astrocytes. Neurobiol Dis 2:79–85.

Liu L, Rudin M, Kozlova EN (2000) Glial cell proliferation in the spinal cord after dorsal rhizotomy or sciatic nerve transection in the adult rat. Exp Brain Res 131:64–73.

Margolis RK, Rauch U, Maurel P, Margolis RU (1996) Neurocan and phosphacan: two major nervous tissue-specific chondroitin sulfate proteoglycans. Perspect Dev Neurobiol 3:273–290.

Matsui F, Nishizuka M, Yasuda Y, Aono S, Watanabe E, Oohira A (1998) Occurrence of a N-terminal proteolytic fragment of neurocan, not a C-terminal half, in a perineuronal net in the adult rat cerebrum. Brain Res 790:45–51.

McKeon RJ, Jurynec MJ, Buck CR (1999) The chondroitin sulfate proteoglycans neurocan and phosphacan are expressed by reactive astrocytes in the chronic CNS glial scar. J Neurosci 19: 10778–10788.

McKeon RJ, Schreiber RC, Rudge JS, Silver J (1991) Reduction of neurite outgrowth in a model of glial scarring following CNS injury is correlated with the expression of inhibitory molecules on reactive astrocytes. J Neurosci 11:3398–3411.

Morgenstern DA, Asher RA, Naidu M, Carlstedt T, Levine JM, Fawcett JW (2003) Expression and glycanation of the NG2 proteoglycan in developing, adult, and damaged peripheral nerve. Mol Cell Neurosci 24:787–802.

Murray M, Wang SD, Goldberger ME, Levitt P (1990) Modification of astrocytes in the spinal cord following dorsal root or peripheral nerve lesions. Exp Neurol 110:248–257.

Niederöst BP, Zimmermann DR, Schwab ME, Bandtlow CE (1999) Bovine CNS myelin contains neurite growth-inhibitory activity associated with chondroitin sulfate proteoglycans. J Neurosci 19: 8979–8989.

Ogawa T, Hagihara K, Suzuki M, Yamaguchi Y (2001) Brevican in the developing hippocampal fimbria: differential expression in myelinating oligodendrocytes and adult astrocytes suggests a dual role for brevican in central nervous system fiber tract development. J Comp Neurol 432:285–295.

Oohashi T, Hirakawa S, Bekku Y, Rauch U, Zimmermann DR, Su WD, Ohtsuka A, Murakami T, Ninomiya Y (2002) Bral1, a brain-specific link protein, colocalizing with the versican V2 isoform at the nodes of Ranvier in developing and adult mouse central nervous systems. Mol Cell Neurosci 19:43–57.

Pindzola RR, Doller C, Silver J (1993) Putative inhibitory extracellular matrix molecules at the dorsal root entry zone of the spinal cord during development and after root and sciatic nerve lesions. Dev Biol 156:34–48.

Ramer MS, Priestley JV, McMahon SB (2000) Functional regeneration of sensory axons into the adult spinal cord. Nature 403:312–316.

Ramer MS, McMahon SB, Priestley JV (2001a) Axon regeneration across the dorsal root entry zone. Prog Brain Res 132:621–639.

Ramer MS, Duraisingam I, Priestley JV, McMahon SB (2001b) Two-tiered inhibition of axon regeneration at the dorsal root entry zone. J Neurosci 21:2651–2660.

Rauch U, Grimpe B, Kulbe G, Arnold-Ammer I, Beier DR, Fassler R (1995) Structure and chromosomal localization of the mouse neurocan gene. Genomics 28:405–410.

Rauch U, Meyer H, Brakebusch C, Seidenbecher C, Gundelfinger ED, Beier DR, Fassler R (1997) Sequence and chromosomal localization of the mouse brevican gene. Genomics 44:15–21.

Rauch U, Feng K, Zhou XH (2001) Neurocan: a brain chondroitin sulfate proteoglycan. Cell Mol Life Sci 58:1842–1856.

Rudge JS, Silver J (1990) Inhibition of neurite outgrowth on astroglial scars in vitro. J Neurosci 10:3594–3603.

Schaeren-Wiemers N, Gerfin-Moser A (1993) A single protocol to detect transcripts of various types and expression levels in neural tissue and cultured cells: in situ hybridization using digoxigenin-labelled cRNA probes. Histochemistry 100:431–440.

Schmalfeldt M, Dours-Zimmermann MT, Winterhalter KH, Zimmermann DR (1998) Versican V2 is a major extracellular matrix component of the mature bovine brain. J Biol Chem 273:15758–15764.

Schmalfeldt M, Bandtlow CE, Dours-Zimmermann MT, Winterhalter KH, Zimmermann DR (2000) Brain derived versican V2 is a potent inhibitor of axonal growth. J Cell Sci:807–816.

Seidenbecher CI, Richter K, Rauch U, Fassler R, Garner CC, Gundelfinger ED (1995) Brevican, a chondroitin sulfate proteoglycan of rat brain, occurs as secreted and cell surface glycosylphosphatidylinositol-anchored isoforms. J Biol Chem 270:27206–27212.

Seidenbecher CI, Gundelfinger ED, Bockers TM, Trotter J, Kreutz MR (1998) Transcripts for secreted and GPI-anchored brevican are differentially distributed in rat brain. Eur J Neurosci 10:1621–1630.

Sroga JM, Jones TB, Kigerl KA, McGaughy VM, Popovich PG (2003) Rats and mice exhibit distinct inflammatory reactions after spinal cord injury. J Comp Neurol 462:223–240.

Suzuki M, Raisman G (1992) The glial framework of central white matter tracts: segmented rows of contiguous interfascicular oligodendrocytes and solitary astrocytes give rise to a continuous meshwork of transverse and longitudinal processes in the adult rat fimbria. Glia 6:222–235.

Tang X, Davies JE, Davies SJ (2003) Changes in distribution, cell associations, and protein expression levels of NG2, neurocan, phosphacan, brevican, versican V2, and tenascin-C during acute to chronic maturation of spinal cord scar tissue. J Neurosci Res 71:427–444.

Thon N, Haas CA, Rauch U, Merten T, Fassler R, Frotscher M, Deller T (2000) The chondroitin sulphate proteoglycan brevican is upregulated by astrocytes after entorhinal cortex lesions in adult rats. Eur J Neurosci 12:2547–2558.

Watanabe M, Toyama Y, Nishiyama A (2002) Differentiation of proliferated NG2-positive glial progenitor cells in a remyelinating lesion. J Neurosci Res 69:826–836.

Wu Y, Chen L, Zheng PS, Yang BB (2002) Beta 1-Integrin-mediated glioma cell adhesion and free radical-induced apoptosis are regulated by binding to a C-terminal domain of PG-M/versican. J Biol Chem 277:12294–12301.

Wujek JR, Lasek RJ (1983) Correlation of axonal regeneration and slow component B in two branches of a single axon. J Neurosci 3:243–251.

Yamada H, Fredette B, Shitara K, Hagihara K, Miura R, Ranscht B, Stallcup WB, Yamaguchi Y (1997) The brain chondroitin sulfate proteoglycan brevican associates with astrocytes ensheathing cerebellar glomeruli and inhibits neurite outgrowth from granule neurons. J Neurosci 17:7784–7795.

Yamaguchi Y (1996) Brevican: a major proteoglycan in adult brain. Perspect Dev Neurobiol 3:307–317.

Yamaguchi Y (2000) Lecticans: organizers of the brain extracellular matrix. Cell Mol Life Sci 57:276–289.

Yao LY, Moody C, Schonherr E, Wight TN, Sandell LJ (1994) Identification of the proteoglycan versican in aorta and smooth muscle cells by DNA sequence analysis, in situ hybridization and immunohistochemistry. Matrix Biol 14:213–225.

Zhang Y, Tohyama K, Winterbottom JK, Haque NS, Schachner M, Lieberman AR, Anderson PN (2001) Correlation between putative inhibitory molecules at the dorsal root entry zone and failure of dorsal root axonal regeneration. Mol Cell Neurosci 17:444–459.

(Accepted 1 March 2005)

4.2.1. Supplementary Methods and Results Part II: Spinal Cord Contusion-Lesions – Preliminary Studies

For a preliminary analysis of the distribution of different lecticans in spinal cord injuries, a limited series of animals were lesioned (suppl. fig. 5) in collaboration with Dr. Lisa Schnell from the group of Prof. Martin Schwab at the Brain Research Institute, University/ETH Zurich.

For this purpose, three to four months old wildtype mice were deeply anesthetized by a subcutaneous injection of Hypnorm® (fentanyl citrate plus fluanisone, Janssen-Cilag Ltd.) and Dormicum® (midazolam, Roche). The spinal cord was exposed by a narrow dorsal laminectomy at thoracic level T8. A contusion lesion on the spine at this level was then performed using a NYU (New York University) weight drop device that can control and calculate the impact. A 12 g weight for 3 sec was applied onto the spinal cord provoking a mild lesion. The wound was closed and sutured. Control animals underwent only a laminectomy ("sham" lesion) (Frei et al., 2000). Four and seven days post lesion, the mice were sacrificed by pentobarbital injection and perfusion through the left ventricle with Ringer's solution containing heparin (Liquemin, Roche) and sodium nitrite, followed by 4% PFA in PBS. Whole spines and brains were dissected and post-fixed overnight in the same fixative. Bone included in the biopsies was decalcified by an EDTA-based ultrasonic procedure (Reineke et al., 2006) and then the entire spines were paraffin embedded according to routine protocols. Immunohistochemistry, preceded when needed by an antigen retrieval treatment, was performed on sagittal sections applying the ABC method.

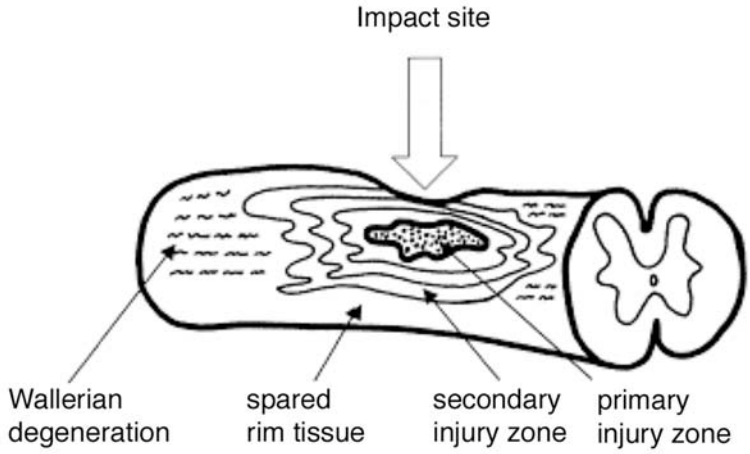

Supplementary figure 5: Cartoon showing the contusion lesion areas of interest around the site of impact. The secondary injury zone surrounds the most affected part, but some tissue remains spared. Wallerian degeneration is seen both above and below the impact site (from (Kostyk et al., 2003)).

Currently, only stainings for versicans and NG2 have been performed. NG2, a transmembrane CSPG with axonal growth inhibitory properties is associated with oligodendrocyte precursor cells. As markers we used in these experiments MBP for myelin, neurofilament-200 for axonal fibers and GFAP for astrocytes. Immunostainings (suppl. fig. 6 to 8) show that the versican isoform V2 (antibodies against versican GAG-α), normally present along myelinated fibers, is rapidly degraded

within the lesion site, whereas NG2 and versican V1 (versican GAG-β) are up-regulated in this area. The staining for these CSPGs is more prominent at the outher edge of the lesion. NG2 accumulation seems to precede the versican V1 deposition (suppl. fig. 7 and 8).

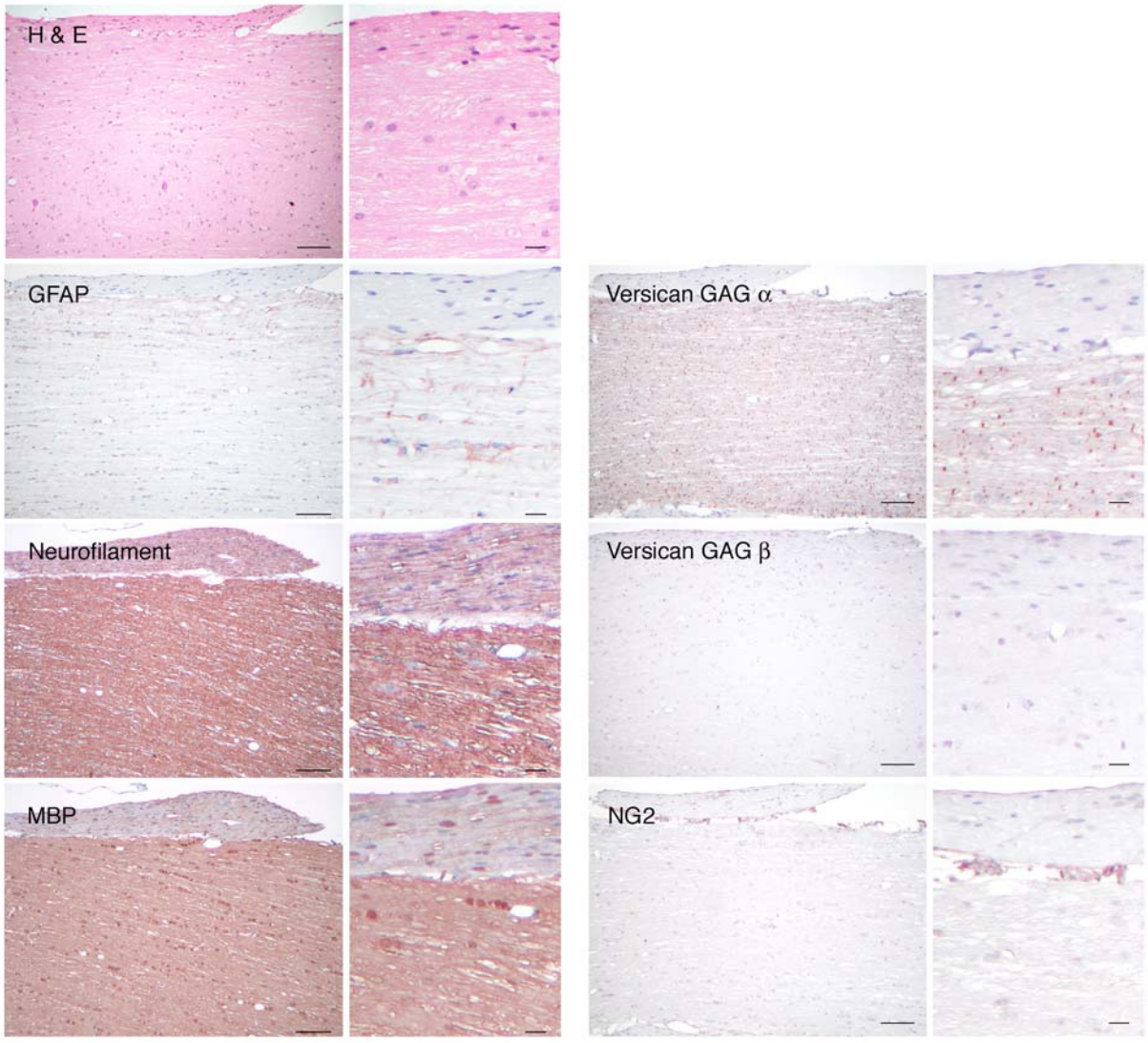

Supplementary figure 6: Hematoxylin/ Eosin and immunohistochemistry of spinal cords from **sham** lesioned animals, 4 days post lesion. Bars: 100 μm (overviews; left) and 20 μm (close-up pictures; right).

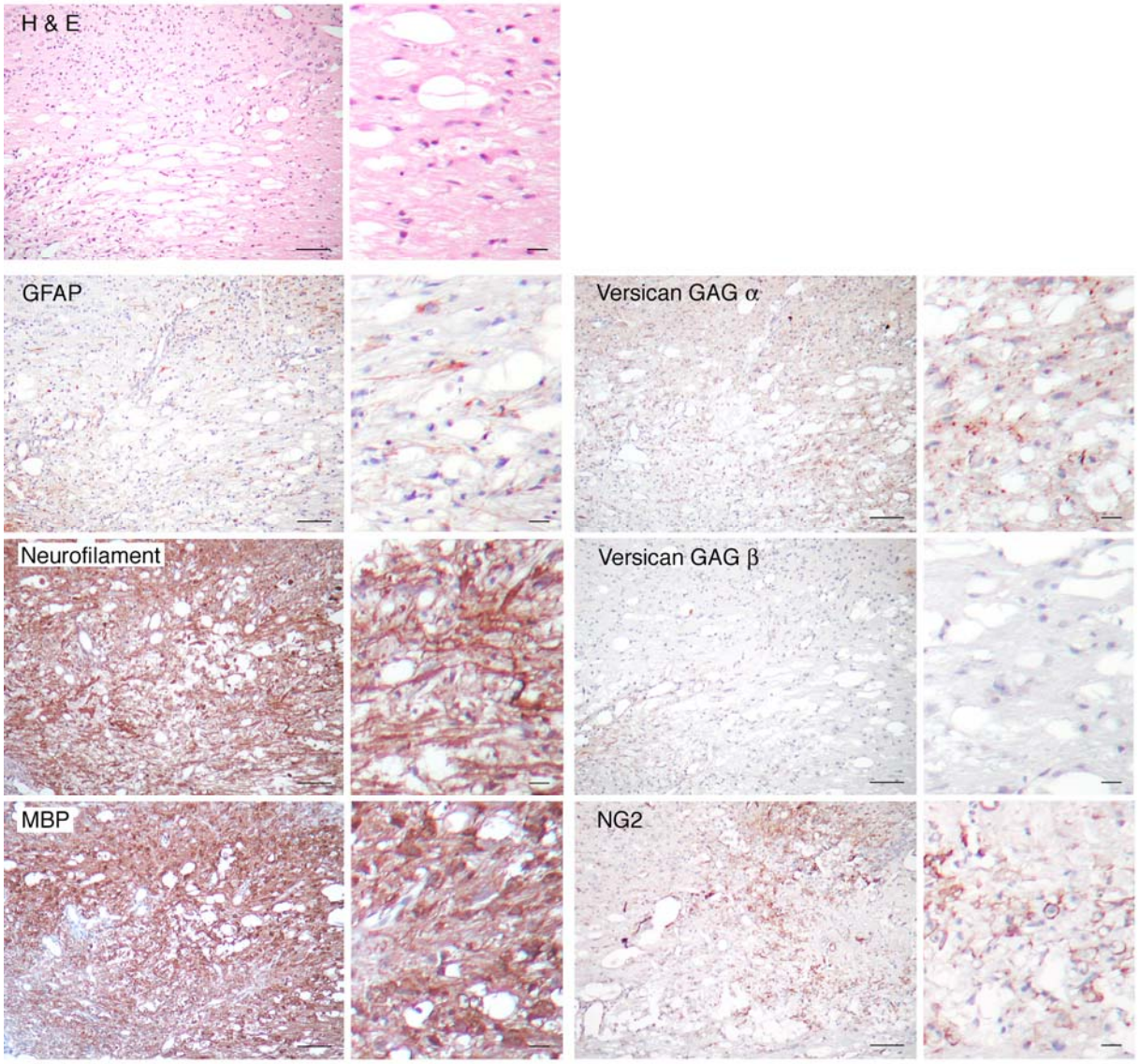

Supplementary figure 7: Hematoxylin/ Eosin and immunohistochemistry on spinal cords **4** days post contusion lesion. Bars: 100 μm (overviews; left) and 20 μm (close-up pictures; right).

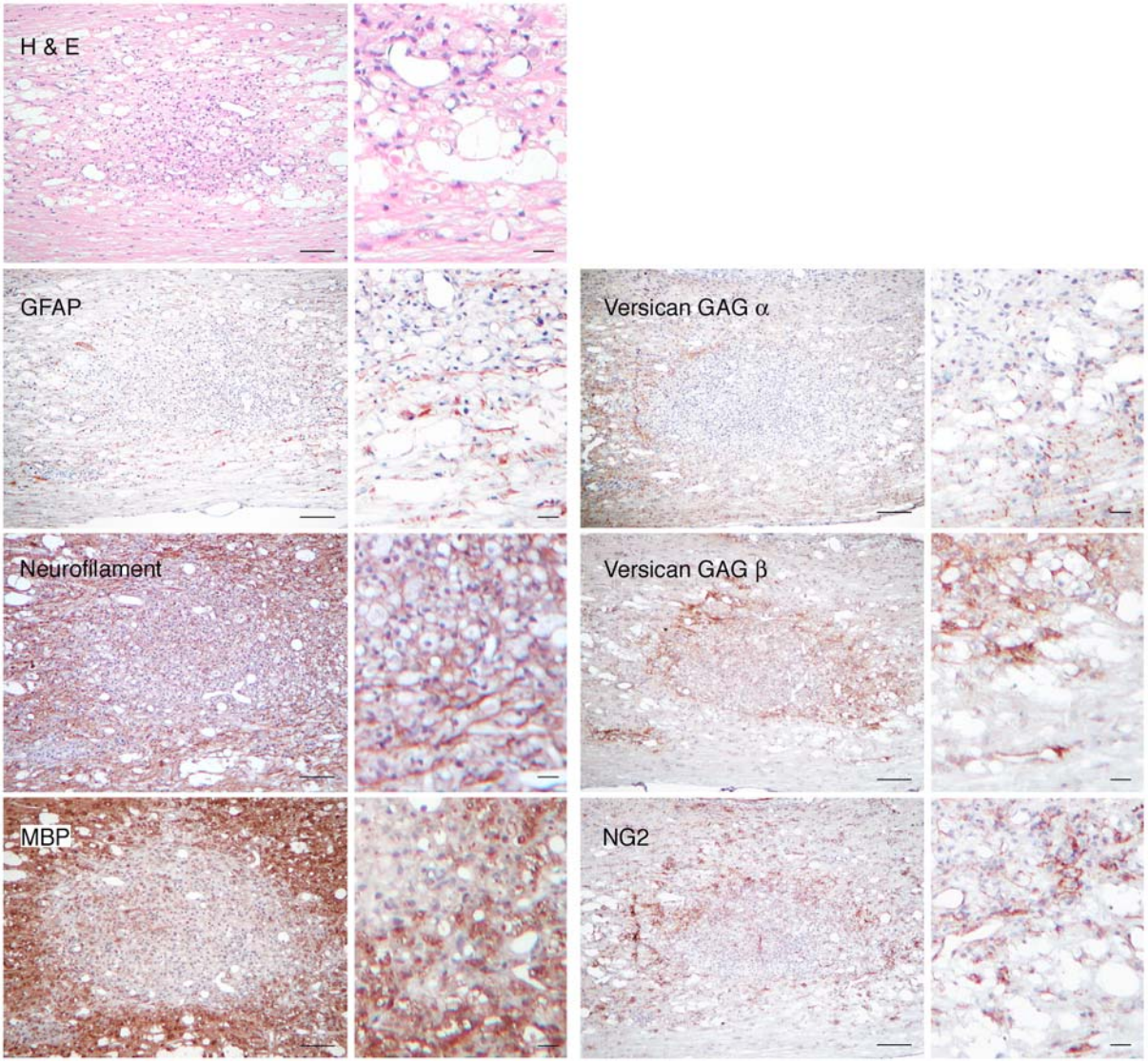

Supplementary figure 8**:** Hematoxylin/ Eosin and immunohistochemistry on spinal cords **7** days post contusion lesion.

Bars: 100 μm (overviews; left) and 20 μm (close-up pictures; right).

4.2.2. References

Frei E, Klusman I, Schnell L, Schwab ME (2000) Reactions of oligodendrocytes to spinal cord injury: cell survival and myelin repair. Exp Neurol 163:373-380.

Kostyk S, Popovich P, Stokes B (2003) Recent Advances in Spinal Cord Research. In: Spinal Cord Medicine: Principles and Practice. (Lin VW, ed). New York: Demos Medical Publishing, Inc.

Reineke T, Jenni B, Abdou MT, Frigerio S, Zubler P, Moch H, Tinguely M (2006) Ultrasonic decalcification offers new perspectives for rapid FISH, DNA, and RT-PCR analysis in bone marrow trephines. Am J Surg Pathol 30:892-896.

5. Conclusion and outlook

The primary goal of this thesis to generate an isoform-specific versican V0/V2 knockout mouse strain has been accomplished, and the early embryonic lethality associated with the constitutive inactivation of all versicans could be effectively circumvented by our new targeting strategy. This fact implies that the fatal defect in the heart development of hdf-mice (Mjaatvedt et al., 1998) is mainly caused by the absence of the V1 isoform and less likely the V3 splice-variant. In our previous immunohistochemical analysis of wildtype mice and chicken, we had regularly observed a co-expression of versican V1 and its larger relative V0. Both display a wide expression during embryonic development and are particularly associated with forming mesenchymal tissues, including those in the heart. Since our mouse strain lacks the V0 isoform apart from the adult CNS-specific versican V2, we can assume that the remaining versican V1 substitutes in most tissues the missing V0 and hereby guarantees normal survival and life span in our knockout strain.

From the technical viewpoint, we could demonstrate that our targeting approach introducing an ER-retention signal and a translational stop codon in exon VII of the versican gene is highly effective in abolishing versican V2 deposition in the CNS. Albeit we intended to leave this way the mRNA levels untouched and to ablate truncated versican core proteins via ER and lysosomes, we observed an unexpected reduction of the target-transcripts. The basis for this phenomenon is probably an activation of nonsense mediated decay (NMD) mechanisms in the knockout animals, which trigger degradation of aberrant messages. Indeed, the premature termination codon introduced in exon VII is located more than 55 nucleotides upstream of the next exon-exon junction and consequently complies with the rule that most cells obey to remove 'nonsense' mRNAs. Nevertheless, this NMD-mediated removal is in general not complete, leaving about 5-25% of the altered mRNA behind (Kuzmiak and Maquat, 2006). Our real-time RT-PCR experiments are fully in line with these observations. Despite some leftover of the V2 and V0 mRNAs, no truncated protein can be detected in our mutant mice, suggesting that the elimination on protein level functions as well. Although we have no final confirmation for this mechanism, our novel procedure has been suitable to suppress the deposition of artificial core protein fragments and to evade compensation through other alternative splice-variants or related proteins.

In contrast to our initial hopes, the absence of the axonal growth inhibiting versican V2 does not destabilize the fiber tract formation or cause excessive axonal sprouting and/or provoke myelination defects. In retrospect, this is however, not particularly surprising as also the elimination of other prominent myelin-derived inhibitors of axonal growth such as Nogo, myelin-associated glycoprotein (MAG) and oligodendrocyte myelin glycoprotein (OMgp) did not result in gross anatomical changes in the CNS of single mutants (Li et al., 1994; Kim et al., 2003; Simonen et al., 2003; Zheng et al., 2003; Huang et al., 2005; Zurn and Bandtlow, 2006). Similarly, mouse brains lacking the CNS-restricted lecticans neurocan or brevican presented no alterations upon histological examination (Zhou et al., 2001; Brakebusch et al., 2002). Co-expression and functional redundancy of different myelin inhibitors or ECM molecules may explain, why single mutants often

do not show striking phenotypes. Therefore, simultaneous eliminating of the partly co-localizing versican V2 and brevican, may provide more conclusive answers about their functions in fiber tract organization and stabilization. Nevertheless, based on our observations, we can exclude a rescue of a potential versican V2-null phenotype by compensatory up-regulation of other lecticans.

From our analysis of versican V0/V2 null mutants, we have obtained so far clear evidence that versican is the key organizer of the extracellular matrix surrounding the CNS nodes of Ranvier. The mechanisms of nodal assembly and stabilization of intracellular and extracellular contacts and the recruitment of ion channels is of great importance for electrical conductance and has, also in the context of regeneration and neurological diseases, gained increasing attention in recent years (Poliak and Peles, 2003; Salzer, 2003; Sherman and Brophy, 2005; Hedstrom and Rasband, 2006; Schafer and Rasband, 2006).

In regard to the assembly of nodal structures, we could confirm in vivo some of the interactions that had been previously postulated on the basis of in vitro assays. This includes the binding of versican and tenascin-R (Tn-R) (Aspberg et al., 1997) as well as of Tn-R and phosphacan (Xiao et al., 1997; Milev et al., 1998; Weber et al., 1999). Moreover, we show that Tn-R strictly requires versican V2 to maintain its association with the nodes of Ranvier, while it seems not to be held at this site by the binding to contactin and/or the β-subunits of sodium channels as formerly suggested from in vitro data (Srinivasan et al., 1998; Xiao et al., 1999; Ratcliffe et al., 2000; Isom, 2002).

While versican V2 deposition is crucial for the ECM assembly, our experiments also clearly demonstrate that the absence of versican V2 and even of the entire perinodal matrix does not affect the clustering of voltage-gated ion channels and the formation of paranodal and juxtaparanodal structures, as previously suspected by other groups. From our data, we can also conclude that neither versican V2, Tn-R, phosphacan nor other lecticans are related to the oligodendrocyte-derived soluble factors reported to induce node-like Na_v-clustering in vitro (Kaplan et al., 1997).

The way the perinodal matrix and versican V2 itself is anchored is currently not clear. The versican interaction seems to depend on binding partners other than hyaluronan or sulfatide and probably occurs via distinct axonal cell surface proteins. In the adult CNS, potential membrane receptors of versican are voltage-gated sodium channels (mainly Na_v 1.6) and in particular also the Ig-CAM neurofascin-186 (Nfasc-186). Especially the in vivo-assessment of the putative interaction with the latter will be difficult, as Nfasc-null mice die early after birth being not able to switch to saltatory conduction (Sherman et al., 2005). Since versican V2 is first detected at the nodal area in the second postnatal week, the hypothesis that Nfasc-186 recruits V2 will have to be tested in vitro. For this purpose, we could perform similar experiments to those of Hedstrom et al. (Hedstrom et al., 2007), who showed cell surface binding of recombinant brevican after addition to Nfasc-186-transfected COS cell cultures. Alternatively, we might try to establish embryonic neuron-glial co-cultures (Svenningsen et al., 2003) from $Nfasc^{-/-}$ animals and analyze the deposition of versican V2, in case that cells survive long enough to proceed to myelination.

Apart from the search for the nodal binding partner(s) of versican V2, investigations of its functions in vivo need also to be extended to other levels. For instance, the ultrastructure of the axoglial junctions should be examined in our knockout strain in detail, paying special attention to the space around the nodes, including the contacting perinodal astrocytes. In a very preliminary attempt we have already looked at axoglial junctions in electron microscopy. So far, we have neither noticed everted paranodal loops or abnormal branching of neurites at the CNS nodes of Ranvier. To draw a final conclusion more versican V0/V2 knockout animals should be studied, however.

Versican V2 aggregates around the node provide a strongly negatively charged matrix. It has been hypothesized that this ECM, which is able to bind cations, potentially acts as reservoir and/or diffusion barrier for sodium and potassium ions. If this extracellular metal ion pool is missing, reduced ion flux and slower conduction in the CNS may result. In fact, optic nerve-compound action potentials (CAP) measured with suction electrodes followed slightly slower kinetics in Tn-R null mice (Weber et al., 1999). Similar recordings of CAP in optic nerves of mice deficient in all three isoforms of RPTPβ were mostly normal (Harroch et al., 2000). Since versican V2 carries among the nodal ECM components the highest proportion of negative charges one would expect, that the conduction velocity would be lowest in our knockout strain, if these former CAP measurements were indeed representative. It is conceivable that such a change would potentially also translate into slower reaction times in a sensitive behavioral test.

To learn about versican V2 functions in the CNS, challenging the mutants with more aggressive means may be another option. This could include analyses of demyelination and remyelination in experimental autoimmune encephalomyelitis (EAE), a model of multiple sclerosis, or studies of the CNS response to injuries.

In the second part of this thesis project, done in collaboration with the laboratory of Anne Zurn in Lausanne, we therefore analyzed the putative roles of versicans in the dorsal root lesion model. The initial experiments were done in wildtype mice to explore first the differential distribution of all lecticans in the dorsal root entry zone (DREZ), the transition border between PNS and CNS. In this comparative study, we found that after rhizotomy, there is an up-regulation of versican V1 and neurocan, even in the absence of a glial scar, which is considered the major source of CSPGs in other types of lesions. Conversely, the normal constituents of the CNS white matter, brevican and versican V2, remained virtually unchanged. As a continuation of this project, we plan to analyze now the consequences of such lesions in knockout strains that lack versican V2. In fact, our collaborators could already show that some sensory axons of neurocan/brevican double deficient mice can grow across the DREZ, if an additional conditioning lesion is performed (Quaglia et al., 2008). From the experiments with versican V2 single and/or brevican/versican V2 double knockout strain we expect an even more pronounced regenerative effect after rhizotomy and delayed growth stimulation, as the up-regulation of neurocan and versican V1 isoform is only transient, and the resident inhibitory lecticans would be absent in this strain.

Finally, spinal cord contusion lesions could provide a new view into the role of versicans in glial scar-forming injuries. Our preliminary experiments done in wildtype animals could, for instance, be extended to versican V0/V2 knockout mice. Nevertheless, according to our recent observation, versican V1 seems to be the main isoform in glial scar tissues and not V2, as previously suggested (Asher et al., 2002). Hence, a yet to be generated conditional knockout strain, eliminating all versican splice-variants in central nervous tissues, may be more suitable for these experiments. Moreover, it would be interesting to cross versican-deficient strains with other null mice, in particular with the $NgR^{-/-}$ animals (Zheng et al., 2005), since the $NgR/p75^{NTR}$ complex apparently transmits the signals of the white matter inhibitors Nogo, MAG and OMgp, but not of CSPGs.

Summing-up all the data from this thesis work, one can assume that our new mouse strain not only provides a model to gain new insights into the establishment of specialized matrices at the CNS-nodes of Ranvier, but will also be of use to explore the roles of CSPGs in suppressing axonal regeneration in the mature CNS.

5.1. References

Asher RA, Morgenstern DA, Shearer MC, Adcock KH, Pesheva P, Fawcett JW (2002) Versican is upregulated in CNS injury and is a product of oligodendrocyte lineage cells. J Neurosci 22:2225-2236.

Aspberg A, Miura R, Bourdoulous S, Shimonaka M, Heinegård D, Schachner M, Ruoslahti E, Yamaguchi Y (1997) The C-type lectin domains of lecticans, a family of aggregating chondroitin sulfate proteoglycans, bind tenascin-R by protein-protein interactions independent of carbohydrate moiety. Proc Natl Acad Sci USA 94:10116-10121.

Brakebusch C, Seidenbecher CI, Asztely F, Rauch U, Matthies H, Meyer H, Krug M, Bockers TM, Zhou X, Kreutz MR, Montag D, Gundelfinger ED, Fassler R (2002) Brevican-deficient mice display impaired hippocampal CA1 long-term potentiation but show no obvious deficits in learning and memory. Mol Cell Biol 22:7417-7427.

Harroch S, Palmeri M, Rosenbluth J, Custer A, Okigaki M, Shrager P, Blum M, Buxbaum JD, Schlessinger J (2000) No obvious abnormality in mice deficient in receptor protein tyrosine phosphatase beta. Mol Cell Biol 20:7706-7715.

Hedstrom KL, Rasband MN (2006) Intrinsic and extrinsic determinants of ion channel localization in neurons. J Neurochem 98:1345-1352.

Hedstrom KL, Xu X, Ogawa Y, Frischknecht R, Seidenbecher CI, Shrager P, Rasband MN (2007) Neurofascin assembles a specialized extracellular matrix at the axon initial segment. J Cell Biol 178:875-886.

Huang JK, Phillips GR, Roth AD, Pedraza L, Shan W, Belkaid W, Mi S, Fex-Svenningsen A, Florens L, Yates JR, 3rd, Colman DR (2005) Glial membranes at the node of Ranvier prevent neurite outgrowth. Science 310:1813-1817.

Isom LL (2002) The role of sodium channels in cell adhesion. Front Biosci 7:12-23.

Kaplan MR, Meyer-Franke A, Lambert S, Bennett V, Duncan ID, Levinson SR, Barres BA (1997) Induction of sodium channel clustering by oligodendrocytes. Nature 386:724-728.

Kim JE, Li S, GrandPre T, Qiu D, Strittmatter SM (2003) Axon regeneration in young adult mice lacking Nogo-A/B. Neuron 38:187-199.

Kuzmiak HA, Maquat LE (2006) Applying nonsense-mediated mRNA decay research to the clinic: progress and challenges. Trends Mol Med 12:306-316.

Li C, Tropak MB, Gerlai R, Clapoff S, Abramow-Newerly W, Trapp B, Peterson A, Roder J (1994) Myelination in the absence of myelin-associated glycoprotein. Nature 369:747-750.

Milev P, Chiba A, Haring M, Rauvala H, Schachner M, Ranscht B, Margolis RK, Margolis RU (1998) High affinity binding and overlapping localization of neurocan and phosphacan protein-tyrosine phosphatase-zeta/beta with tenascin-R, amphoterin, and the heparin-binding growth-associated molecule. J Biol Chem 273:6998-7005.

Mjaatvedt C, Yamamura H, Capehart A, Turner D, Markwald R (1998) The *cspg2* gene, disrupted in the *hdf* mutant, is required for right cardiac chamber and endocardial cushion formation. Dev Biol 202:56-66.

Poliak S, Peles E (2003) The local differentiation of myelinated axons at nodes of Ranvier. Nat Rev Neurosci 4:968-980.

Quaglia X, Beggah AT, Seidenbecher C, Zurn AD (2008) Delayed priming promotes CNS regeneration post-rhizotomy in Neurocan and Brevican-deficient mice. Brain 131:240-249.

Ratcliffe CF, Qu Y, McCormick KA, Tibbs VC, Dixon JE, Scheuer T, Catterall WA (2000) A sodium channel signaling complex: modulation by associated receptor protein tyrosine phosphatase beta. Nat Neurosci 3:437-444.

Salzer JL (2003) Polarized domains of myelinated axons. Neuron 40:297-318.

Schafer DP, Rasband MN (2006) Glial regulation of the axonal membrane at nodes of Ranvier. Curr Opin Neurobiol 16:508-514.

Sherman DL, Brophy PJ (2005) Mechanisms of axon ensheathment and myelin growth. Nat Rev Neurosci 6:683-690.

Sherman DL, Tait S, Melrose S, Johnson R, Zonta B, Court FA, Macklin WB, Meek S, Smith AJ, Cottrell DF, Brophy PJ (2005) Neurofascins are required to establish axonal domains for saltatory conduction. Neuron 48:737-742.

Simonen M, Pedersen V, Weinmann O, Schnell L, Buss A, Ledermann B, Christ F, Sansig G, van der Putten H, Schwab ME (2003) Systemic deletion of the myelin-associated outgrowth inhibitor Nogo-A improves regenerative and plastic responses after spinal cord injury. Neuron 38:201-211.

Srinivasan J, Schachner M, Catterall WA (1998) Interaction of voltage-gated sodium channels with the extracellular matrix molecules tenascin-C and tenascin-R. Proc Natl Acad Sci U S A 95:15753-15757.

Svenningsen AF, Shan WS, Colman DR, Pedraza L (2003) Rapid method for culturing embryonic neuron-glial cell cocultures. J Neurosci Res 72:565-573.

Weber P, Bartsch U, Rasband MN, Czaniera R, Lang Y, Bluethmann H, Margolis RU, Levinson SR, Shrager P, Montag D, Schachner M (1999) Mice deficient for tenascin-R display alterations of the extracellular matrix and decreased axonal conduction velocities in the CNS. J Neurosci 19:4245-4262.

Xiao ZC, Bartsch U, Margolis RK, Rougon G, Montag D, Schachner M (1997) Isolation of a tenascin-R binding protein from mouse brain membranes - a phosphacan-related chondroitin sulfate proteoglycan. J Biol Chem 272:32092-32101.

Xiao ZC, Ragsdale DS, Malhotra JD, Mattei LN, Braun PE, Schachner M, Isom LL (1999) Tenascin-R is a functional modulator of sodium channel beta subunits. J Biol Chem 274:26511-26517.

Zheng B, Ho C, Li S, Keirstead H, Steward O, Tessier-Lavigne M (2003) Lack of enhanced spinal regeneration in Nogo-deficient mice. Neuron 38:213-224.

Zheng B, Atwal J, Ho C, Case L, He XL, Garcia KC, Steward O, Tessier-Lavigne M (2005) Genetic deletion of the Nogo receptor does not reduce neurite inhibition in vitro or promote corticospinal tract regeneration in vivo. Proc Natl Acad Sci U S A 102:1205-1210.

Zhou XH, Brakebusch C, Matthies H, Oohashi T, Hirsch E, Moser M, Krug M, Seidenbecher CI, Boeckers TM, Rauch U, Buettner R, Gundelfinger ED, Fassler R (2001) Neurocan is dispensable for brain development. Mol Cell Biol 21:5970-5978.

Zurn AD, Bandtlow CE (2006) Regeneration failure in the CNs: cellular and molecular mechanisms. Adv Exp Med Biol 557:54-76.

6. Acknowledgements

When facing such an enterprise at a slightly more advanced age, one has many more people to thank than a younger PhD student! With the danger that the list may be incomplete, I am especially grateful to following persons:

Peter Sonderegger, my doctor father, for adopting a PhD student almost matching his age and for being patient with my long-term dissertation. Esther Stöckli and Alex Hajnal, for accepting to be members of my thesis committee. Thank you all for investing your valuable time!

Although not directly involved in this thesis work, I would like to thank José Luis Millán for giving me the opportunity to enter the world of basic research and Barbara Ranscht for greatly motivating me to pursue this fascinating journey.

Many thanks go to Reinhard Fässler, who spent much of his precious time to introduce us into gene targeting strategies and practical work with embryonic stem cells and to Uwe Rauch and Cord Brakebusch (both at that time in Reinhard's lab) for stimulating discussions, technical advice and a lot of fun while learning.

Without Anne Zurn and Lisa Schnell, the studies of the role of lecticans in lesioned animals would have never been possible. Big thanks, Anne and Lisa, for your kind friendship and for having me on board in these interesting joint ventures!

I also express my deep gratitude to Bernhard Odermatt, who has always been ready to help and has given us so many good hints; and to Parvin Saremaslani, who taught me the very first steps in immunohistochemistry, while pushing me to practice my beginners' German.

Along this time, many former and present members of the lab have contributed with their refreshing and intelligent way to the great team spirit. The ones who helped me particularly in this thesis work, either by DNA sequencing or by preparing perfect tissue sections are Marie-Therese Abdou, Malek Ajmo, Regula Städeli, Belinda Senn and Karin Hansen. By taking over the bigger share of the diagnostic work, Simona Frigerio and Kirsten Struckmann made my research possible. Thanks to all of you!€

I am especially indebted to Phillipp Heitz and Holger Moch, for giving me the opportunity to work on this thesis aside of my diagnostic tasks and my lab-organization duties.

While risking to be a little biased, I want to thank Dieter, who extended my knowledge of biochemistry and molecular biology, taught me to critically look at the results of my experiments and to maintain my neural plasticity by keeping on thinking, thinking, thinking...

And finally, I am very grateful to my parents and my long-time friends from Argentina, who seem not to be directly linked to my activities here, but strongly encouraged me to accept this challenge.

7. Curriculum Vitae

Name	María Teresa Zimmermann-Dours
Title	Dipl. natw. (Master of Science, National University of Buenos Aires)
Date of Birth	February 19, 1951 (Azul, BsAs, Argentina)
Citizenship	Döttingen (AG), Switzerland and Argentina
Marital status	married
Private Address	Langgrütstrasse 192, 8047 Zurich, Switzerland
Business Address	Laboratory of Molecular Diagnostics, Department of Pathology, University Hospital, Schmelzbergstrasse 12, 8091 Zürich, Switzerland
Email	m.t.zimmermann-dours@access.uzh.ch

Basic Education

1957 - 1963	Primary and secondary school, Azul, BsAs, Argentina
1964 - 1968	High School. Bachiller (Matura), Azul, BsAs, Argentina

University Education and Academical Titles

1969 - 1976	Education in biochemistry and clinical chemistry at the National University of Buenos Aires, Argentina
1975	Licenciatura (Bachelor) in Clinical Chemistry, National University of Buenos Aires, Argentina
1976	Dipl. natw. (Diploma in Biochemistry; M.Sc. equivalent), National University of Buenos Aires, Argentina

Honors

1976	Fellowship of the Clinical Analysis Department, Buenos Aires University Hospital, Buenos Aires, Argentina

Professional Record

1973 – 1975	Assistant, Hematological Research Institute of the National Academy of Medicine, Buenos Aires, Argentina
1975 - 1986	Staff Biochemist, Department of Haemostasis, Hematological Research Institute of the National Academy of Medicine, Buenos Aires, Argentina
1979 - 1986	Staff Biochemist, Department of Haemostasis, Pavlovsky Hematological Center, Buenos Aires, Argentina
1986 - 1989	Research Assistant, La Jolla Cancer Research Foundation, La Jolla, CA, USA
since 1990	Biochemist, Laboratory of Molecular Biology, Department of Pathology, University of Zürich

List of Publications

Research Articles (peer reviewed)

1. Bergna, L.J., **Dours, M.T.**, Mondini, N. & Martinez Canaveri, A. (1981) Deficiencia congénita de Factor VII- Presentación de cuatro casos [Congenital factor VII deficiency. Report of 4 cases]. Medicina, **41** (Suppl.), 242-248.
   Impact factor ^{1993}: 0.235

2. Ranscht, B. with technical assistance from **Dours, M.T.** (1988) Sequence of contactin, a 130-kD glycoprotein concentrated in areas of interneuronal contact, defines a new member of the immunoglobulin supergene family in the nervous system. J. Cell Biol., **107**,1561-1573.
   Impact factor ^{1993}: 11.700 Times cited*: 224 (*until November 19th, 2008)

3. Ranscht, B. & **Dours-Zimmermann, M.T.** (1991) T-cadherin, a novel cadherin cell adhesion molecule in the nervous system lacks the conserved cytoplasmic region. Neuron, **7**, 391-402.
   Impact factor ^{1993}: 17.256 Times cited*: 181

4. Sacristan, M.P., Vestal, D.J., **Dours-Zimmermann, M.T.** & Ranscht, B. (1993) T-cadherin 2: molecular characterization, function in cell adhesion, and coexpression with T-cadherin and N-cadherin. J. Neurosci. Res., **34**, 664-680.
   Impact factor ^{1993}: 3.005 Times cited*: 21

5. Zimmermann, D.R., **Dours-Zimmermann, M.T.**, Schubert, M. & Bruckner-Tuderman, L. (1994) Versican is expressed in the proliferating zone in the epidermis and in association with the elastic network of the dermis. J. Cell Biol., **124**, 817-825.
   Impact factor ^{1993}: 12.149 Times cited*: 148

6. **Dours-Zimmermann, M.T.** & Zimmermann, D.R. (1994) A novel glycosaminoglycan attachment domain identified in two alternative splice-variants of human versican. J. Biol. Chem., **269**, 32992-32998.
   Impact factor ^{1994}: 7.716 Times cited*: 118

7. Dommann-Scherrer, C., Baumann Kurer, S. Zimmermann, D.R., Odermatt, B.F., **Dours-Zimmermann, M.T.**, Briner, J. & Heitz, Ph.U. (1995) Occult hepatosplenic T-γ/δ lymphoma: value of genotypic analysis in the differential diagnosis. Virchows Arch., **426**, 629-634.
   Impact factor ^{1994}: 1.815 Times cited*: 30

8. Wyss, M., Dummer, R., Dommann, S.N., Joller-Jemelka, H.I., **Dours-Zimmermann, M.T.**, Gilliet, F. & Burg, G. (1995) Lymphomatoid papulosis--treatment with recombinant interferon alfa-2a and etretinate. Dermatology, **190**, 288-291.
   Impact factor ^{1994}: 0.929 Times cited*: 10

9. Bruckner-Tuderman, L., Nilssen, Ø., Zimmermann, D.R., **Dours-Zimmermann, M.T.**, Kalinke, U., Gedde-Dahl T.Jr. & Winberg, J.O. (1995) Immunohistochemical and mutation analysis demonstrate that procollagen VII is processed to collagen VII through removal of the NC-2 domain. J. Cell Biol., **131**, 551-559.
   Impact factor ^{1994}: 12.149 Times cited*: 76

10. Dommann, S.N.W., Dommann-Scherrer, C.C., Zimmermann, D.R., **Dours-Zimmermann, M.T.**, Hassam, S. & Burg, G. (1995) Primary cutaneous T-cell rich B-cell lymphoma. A case report with a 13-year follow-up. Am. J. Dermatopathol. **17**, 618-624.
    Impact factor ^{1994}: 0.921 Times cited*: 12

11. Bode-Lesniewska, B., **Dours-Zimmermann, M. T.**, Odermatt, B.F., Briner, J., Heitz, Ph. U. & Zimmermann, D.R. (1996) Distribution of the large aggregating proteoglycan versican in adult human tissues. J. Histochem. Cytochem. **44**, 303-312.
    Impact factor ^{1997}: 2.776 Times cited*: 90

12. Dommann, S.N.W., Dommann-Scherrer, C.C., **Dours-Zimmermann, M.T.**, Zimmermann, D.R., Kural-Serbes B. & Burg, G. (1996) Clonal disease in extracutaneous compartments in cutaneous T-cell lymphomas - a comparative study between cutaneous T-cell lymphomas and pseudo-lymphomas. Arch. Dermatol. Res. **288**, 163-167.
    Impact factor ^{1997}: 1.234 Times cited*: 22

13. Dommann, S.N.W., Dommann-Scherrer, C.C., **Dours-Zimmermann, M.T.**, Zimmermann, D.R., Kural-Serbes B. & Burg, G. (1996) Cutaneous pleomorphic T-cell lymphoma showing lineage cross-over of antigen receptor gene rearrangement. Eur. J. Dermatol. **6**, 196-199.
    Impact factor ^{1997}: 0.464 Times cited*: 0

14. Paulus, W., Baur, l., **Dours-Zimmermann, M. T.** & Zimmermann, D.R. (1996) Differential expression of versican isoforms in brain tumors. J. Neuropathol. Exp. Neurol. **55**, 528-533.
    Impact factor ^{1997}: 4.253 Times cited*: 53

15. Schmalfeldt, M., **Dours-Zimmermann, M. T.**, Winterhalter, K.H. & Zimmermann, D.R. (1998) Versican V2 is a major extracellular matrix component of the mature bovine brain. J. Biol. Chem., **273**, 15758-15764.
    Impact factor ^{1998}: 7.199 Times cited*: 58

16. Schmalfeldt, M., Bandtlow, C. E., **Dours-Zimmermann, M.T.**, Winterhalter, K.H. & Zimmermann, D.R. (2000) Brain derived versican V2 is a potent inhibitor of axonal growth. J. Cell Sci., **113**, 807-816.
    Impact factor ^{2000}: 5.996 Times cited*: 83

17. Albinger-Hegyi, A., Hochreutener, B., Abdou, M.T., Hegyi, I., **Dours-Zimmermann, M.T.**, Kurrer, M.O., Heitz, Ph.U. & Zimmermann, D.R. (2002) High frequency of t(14;18)-translocation breakpoints outside of major breakpoint and minor cluster regions in follicular lymphomas – improved PCR protocols for their detection. Am. J. Pathol., **160**, 823-832.
    Impact factor ^{2002}: 6.750 Times cited*: 43

18. Beggah, A.T., **Dours-Zimmermann, M.T.**, Barras, F.M., Brosius, A., Zimmermann, D.R. & Zurn, A.D. (2005) Lesion-induced differential expression and cell association of Neurocan, Brevican, Versican V1 and V2 in the mouse dorsal root entry zone. Neuroscience, **133**, 749-62.
    Impact factor ^{2005}: 3.410 Times cited*: 16

19. Wong, C.E., Paratore, C., **Dours-Zimmermann, M.T.**, Rochat, A., Pietri, T., Suter, U., Zimmermann, D.R., Dufour, S., Thiery, J.P., Meijer, D., Beermann, F., Barrandon, Y. & Sommer, L. (2006) Neural crest-derived cells with stem cell features can be traced back to multiple lineages in the adult skin. J. Cell Biol., **175**, 1005-1015.
    Impact factor ^{2006}: 10.152 Times cited*: 22

20. Sakko, A.J., Ricciardelli, C., Mayne, K., **Dours-Zimmermann, M.T.**, Zimmermann, D.R., Neufing, P., Tilley, W.D., Marshall, V.R., & Horsfall, D.J. (2007) Changes in Steroid Receptors and Proteoglycan Expression in the Guinea Pig Prostate Stroma During Puberty and Hormone Manipulation. Prostate, **67**, 288-300.
    Impact factor ^{2007}: 3.674 Times cited*: -

Research Articles (not peer reviewed)

21. Zimmermann, D.R., **Dours-Zimmermann, M.T.**, Schubert, M., Bruckner-Tuderman, L. & Heitz, Ph. U. (1994) Expression of the extracellular matrix proteoglycan, versican, in human skin. Verh. Dtsch. Ges. Pathol. **78**, 481-484.
    Impact factor: - Times cited*: 1

22. Zimmermann, D.R., Städeli-Brodbeck, R., Ajmo, M., **Dours-Zimmermann, M.T.**, Pfyffer, G. E. & Heitz, Ph. U. (1997) Detection of Mycobacteria - A Molecular Pathology Approach. Verh. Dtsch. Ges. Pathol. **81**, 273-280.
    Impact factor: - Times cited*: 7

Review Articles (peer reviewed)

23. Zimmermann, D.R. & **Dours-Zimmermann, M.T.** (2008) Extracellular matrix of the central nervous system: from neglect to challenge. Histochem Cell Biol **130**, 635-653.
    Impact factor ^{2007}: 2.893 Times cited*: -

Book Chapters

24. Zimmermann, D.R. & **Dours-Zimmermann, M.T.** (1995) Versican, in "Human Protein Data". 3rd Installment. Haeberli, A. (ed.). VCH, Weinheim.

25. Zimmermann, D.R. & **Dours-Zimmermann, M.T.** (2002) Versican, in "The Encyclopedia of Molecular Medicine". Creighton, T.E. (ed.), John Wiley & Sons, New York, 5, 3353-3355. (peer reviewed)